Topics in chiral perturbation theory for charmed mesons

Dissertation
zur
Erlangung des Doktorgrades (Dr. rer. nat.)
der
Mathematisch-Naturwissenschaftlichen Fakultät
der
Rheinischen Friedrich-Wilhelms-Universität Bonn

von
Menglin Du
aus
Shanxi, China

Bonn 2017

Dieser Forschungsbericht wurde als Dissertation von der Mathematisch-Naturwissenschaftlichen Fakultät der Universität Bonn angenommen und ist auf dem Hochschulschriftenserver der ULB Bonn http://hss.ulb.uni-bonn.de/diss_online elektronisch publiziert.

Erstgutachter:	Prof. Dr. Ulf-G. Meißner
Zweitgutachter:	Prof. Dr. Feng-Kun Guo
Tag der Promotion:	03.08.2017
Erscheinungsjahr:	2017

Abstract

This thesis is concerned with topics in chiral perturbation theory for pseudoscalar charmed mesons in a manifestly Lorentz-invariant way. After constructing the chiral effective Lagrangian describing spinless matter fields living in the fundamental representation of $SU(N)$, we systematically study the effective generating functional using the background field method up to leading one-loop order, i.e. $O(p^3)$, where p denotes a small momentum or Goldstone boson mass. In general, when matter fields are included, loop diagrams are both UV divergent and spoil the power counting rules. To obtain a well defined effective generating functional, both free of UV divergences and power counting breaking (PCB) terms, we renormalize it within the extended-on-mass-shell (EOMS) scheme on the Lagrangian level. Using heat kernel expansion techniques, the divergences of the one-loop effective generating functional are extracted. The divergences are absorbed by counterterms not only from the third order but also from the second order chiral Lagrangian. Likewise, PCB terms are polynomials in chiral quantities, and thus can be absorbed by conterterms. The PCB terms and the counterterms are calculated using the external field expansion. The theory can be applied to any theory with a spontaneous symmetry breaking of $SU(N)_L \times SU(N)_R$ to $SU(N)_V$ and spinless matter fields in the fundamental representation.

The theory is then applied to the scattering of the Goldstone bosons of chiral symmetry off the pseudoscalar charmed mesons. To investigate the nonperturbative effects and describe the scattering lengths at unphysically high pion masses, we unitarize the scattering amplitudes to fit the available lattice data of the S-wave scattering lengths. The lattice data are well described. However, most of the low-energy constants (LECs) determined from the fit bear large uncertainties. Lattice simulations in more channels are necessary to pin down these values which can then be used to make predictions in other processes related by chiral and heavy quark symmetries. Furthermore, we search for dynamically generated open-charm states with $J^P = 0^+$ as poles of the S-matrix on various Riemann sheets. The trajectories of those poles for varying pion masses are presented as well.

To assess the contribution from the heavy quark spin partner, vector charmed mesons are included explicitly in order to quantify their influences on the S-wave scattering lengths. The obtained results are compared to the ones without an explicit contribution of the vector charmed mesons. It is found that the difference is negligible for S-wave scattering in the threshold region. This validates the use of D^*-less one-loop potentials in the study of the pertinent scattering lengths.

At last, we investigate the numerical values of the LECs of ChPT for charmed mesons. This thesis is tackled from two sides: estimates using the resonance exchange model, and positivity constraints from the general properties of the S-matrix including analyticity, crossing symmetry and unitarity. These estimates and constraints are compared with the values of the scattering length determined by fitting to lattice datas. Tensions are found, and possible reasons are discussed. We conclude that more data from lattice calculations and experiments are necessary to fix these constants better. As a by-product, we also estimate the coupling constant g_{DDa_2}, with a_2 the light tensor meson, via the QCD sum rule approach.

The original results obtained in this thesis have been published in the following series of papers

- M. L. Du, F. K. Guo and U.-G. Meißner, *"One-loop renormalization of the chiral Lagrangian for spinless matter fields in the SU(N) fundamental representation",* J. Phys. G **44**, 014001 (2017) [arXiv:1607.00822 [hep-ph]], Chapter 4.
- M. L. Du, F. K. Guo and U.-G. Meißner, *"Subtraction of power counting breaking terms in chiral perturbation theory: spinless matter fields",* JHEP **1610**, 122 (2016) [arXiv:1609.06134 [hep-ph]], Chapter 4.
- D. L. Yao, M. L. Du, F. K. Guo and U.-G. Meißner, *"One-loop analysis of the interactions between charmed mesons and Goldstone bosons",* JHEP **1511**, 058 (2015) [arXiv:1502.05981 [hep-ph]], Chaper 5.
- M. L. Du, F. K. Guo, U.-G. Meißner and D. L. Yao, *"Study of open-charm 0^+ states in unitarized chiral effective theory with one-loop potentials",* arXiv:1703.10836 [hep-ph], Chapers 5, 6.
- M. L. Du, F. K. Guo, U.-G. Meißner and D. L. Yao, *"Aspects of the low-energy constants in the chiral Lagrangian for charmed mesons",* Phys. Rev. D **94**, no. 9, 094037 (2016) [arXiv:1610.02963 [hep-ph]], Chapter 7.

Contents

CHAPTER 1

Introduction

The Standard Model (SM) Lagrangian encodes our knowledge of the fundamental interactions besides gravity. In SM all interactions are governed by the gauge symmetries. Gauge invariance is first proposed by Weyl to describe the electromagnetic interaction in quantum mechanics. It was extended to the non-abelian case by C. N. Yang and Mills in 1954 [1], the Yang-Mills theory.[1] However, the gauge symmetry asks for exact massless gauge bosons, which lead to long-range interactions. It seems impossible to describe the strong or weak interaction at that time. A landmark in constructing the SM is the introduction of the Higgs mechanism,[2] which is essential to explain the generation mechanism of the mass of gauge bosons. The mechanism was incorporated into the SM by Weinberg and Salam. The unification of the electromagnetism and weak interaction is accomplished under an $SU(2)_L \times U(1)_Y$ gauge group, where $SU(2)_L$ and $U(1)_Y$ represent weak isospin and hypercharge, respectively. In the SM, the $W^{\pm}$, Z^0 bosons acquire masses by the spontaneous gauge symmetry breaking (Higgs mechanism) of the electroweak symmetry from $SU(2)_L \times U(1)_Y$ to $U(1)_{\mathrm{em}}$, and the photon remains massless due to the unbroken $U(1)_{\mathrm{em}}$ symmetry which is different from $U(1)_Y$. The theory also predicts the existence of at least a scalar Higgs boson, which was observed in 2013 [5, 6]. Earlier, 't Hooft had proven that Yang-Mills theories are renormalizable [7, 8] in 1971.

Another crucial breakthrough in the SM is the discovery that the non-abelian gauge theories may reproduce a feature called asymptotic freedom, which is believed to be an important characteristic of the strong interaction. Asymptotic freedom was independently discovered by Gross and Wilczek [9, 10], and Politzer [11] in 1973.[3] Based on the quark model, the local $SU(3)_C$ symmetry gives rise to Quantum Chromodynamics (QCD), where the subscript C indicates the color space. Besides asymptotic freedom, QCD enjoys another peculiar property that color charged particles cannot be isolated singularly, the so-called color confinement. The incorporation of electroweak theory and QCD is recognized as the SM. The theory describes the interaction of the fundamental particles: the leptons, quarks, gauge bosons and Higgs boson, by the gauge symmetry of $SU(3)_C \times SU(2)_L \times U(1)_Y$. It has shown huge and continuous successes in experimental tests and predictions.

Different from Quantum Electrodynamics (QED), QCD has an ultraviolet (UV) fixed point at $\alpha_s = 0$ instead of an infrared fixed point, where α_s denotes the strong coupling constant. This means that perturbation theory works well in UV regions. According to the property of asymptotic freedom, quarks and gluons interact very weakly in high-energy regions. One could employ perturbation theory safely to

[1] R. Shaw introduced the same notion independently.

[2] The Higgs mechanism is independently proposed almost simultaneously in 1964 by Brout and Englert [2]; by Higgs [3]; and by Guralnik, Hagen, and Kibble [4].

[3] 't Hooft had found this result and announced it at a conference in 1972 [12, 13].

study the short-distance interactions, referred to as perturbative QCD. The earliest application of QCD is made in deep inelastic scattering, in which the operator product expansion (OPE) provides a very powerful tool in extracting the short-range information to which perturbative calculations are safely applied. However, with the decrease of the energy, due to the self-interaction of gluons, the coupling constant α_s grows, which would weaken the applicability of the perturbation theory. At energy, of the order of 1 GeV, the coupling constant becomes so large that the perturbation theory fails totally. The failure of the perturbative expansion in α_s requires other approaches to study the low-energy behavior of the strong interactions. However, up to today, an analytical solution from first principles of QCD is not available. In the meantime, vast amounts of hadronic data which require theoretical interpretation have been collected. Therefore, various methods and techniques have been developed to work with QCD at low energies, e.g. various dynamical models (potential, MIT bag and Skyrme), effective field theories, QCD sum rules, lattice QCD, $1/N_c$ expansions, and etc. Among them, effective field theories provides a simple and systematic way to study the specific physics or physics in specific energy region, and therefore become popular and paradigmatic tools in various fields of physics.

Chiral perturbation theory (ChPT) [14–16], as the low-energy effective theory of QCD, provides a successful and systematical framework to study hadronic physics at low energies. The Goldstone bosons are treated as the degrees of freedom explicitly instead of quarks and gluons. The hard modes are integrated out and encoded into the coupling constants, the so-called low energy constants (LECs). The effective Lagrangian is constructed with the same symmetries as QCD and is arranged in powers of external momenta and light quark masses. Under a proper power counting scheme, a relation between the momentum expansion and the loop expansion is well established. The systematic studies of the ChPT for pure Goldstone bosons to $O(p^4)$ have been done by Gasser and Leutwyler [15, 16]. Matter fields having nonvanishing masses in the chiral limit can be included in ChPT as well. ChPT including light baryons is known as baryon ChPT. However, the occurrence of the new mass scale (baryon mass) leads to the notable power counting breaking issue in baryon ChPT [17]. Various approaches were proposed to address the PCB issue, e.g. the heavy baryon ChPT [18–20], the infrared reularization [21], and the extended-on-mass-shell (EOMS) scheme [22]. Recently, the EOMS scheme was successfully applied to the study of πN scattering up to $O(p^4)$ [23] and in the presence of Δ-resonance [24]. Likewise, ChPT including other matter fields has the same powering counting breaking issue. The approaches used for baryon ChPT can be employed to ChPT including other matter fields.

Since the standard ChPT is organized in a double expansion in terms of small external momenta and light quark masses, the convergence of the chiral series would be in a question at relatively high energies, especially at the energies where the resonances appear. The perturbative scattering potentials to any finite chiral order can never reproduce the resonances in the relevant channels, and start to violate the unitarity largely and can not be trusted anymore. One way to restore the situation is to unitarize the perturbative potentials, however, usually with the price of losing the crossing symmetry.

In the hadronic world, many excited charmed/bottomed states and charmonia/bottomonia have been observed experimentally, see Refs. [25, 26] and the references therein. This leads to considerable theoretical works attempting to investigate properties of the new states and trying to assign them into the hadronic spectrum. According to the conventional quark model, hadrons consist of a quark-antiquark pair or three quarks. However, numerous exotic candidates which cannot fit into the conventional quark model have been observed. Studies on these exotic candidates do not only shed light on their nature, but also allow us to further understand the underlying QCD. The quark potential model is a powerful tool in studying the low lying excited states and assigning them in the hadronic spectrum. However, some states with quantum numbers allowed in conventional quark model are in disagreement with the expectations from quark potential models, e.g. $D_{s0}^*(2317)$ and $D_{s1}^*(2460)$. A number of possible explanations have been proposed to unravel their nature. More and more evidence suggests that the $D_{s0}^*(2317)$ is dominantly

a DK hadronic molecule [27–30]. Employing ChPT for D mesons, the scattering of charmed and Goldstone mesons provides a systematical tool to probe the inner structure of the $D_{s0}^{*}(2317)$.

In this work, we will systematically investigate the ChPT for spinless matter fields living in the $SU(N)$ fundamental representation to $O(p^3)$, i.e. one-loop level, and its application to the interactions between charmed mesons and Goldstone bosons. The work is organized as follow: In Chapter 2, we present an introduction to ChPT with special focus on the inclusion of matter fields and the accompanying power counting breaking issue. In Chapter 3, I give a brief introduction to the unitarization of two-body interaction. In Chapter 4, we will calculate the effective generating functional to $O(p^3)$, i.e. leading one-loop order, and then systematically renormalize it using the background field method and heat kernel techniques. In addition, the EOMS scheme will be performed to obtain a generating functional with a consistent power counting. From the effective generating functional, one can read off the two-body scattering amplitudes directly. Chapter 5 is devoted to the application of unitarized ChPT to charmed meson(D)- Goldstone boson(ϕ) scattering. By fitting to the available lattice data, we determine the LECs of the relevant chiral Lagrangian. Moreover, we will investigate the pole structures of the scattering potentials in various channels. In Chapter 6, the charmed vector mesons are included explicitly to the chiral Lagrangian and a full ChPT calculation is performed to investigate the importance of charmed vector resonances in $D\phi$ scattering. Due to the large number of LECs and the scarcity of the available lattice data, the LECs are poorly determined by the fit. The resonance exchange model is employed to investigate the numerical values of LECs in the chiral effective $D\phi$ Lagrangian in Chapter 7. In addition, positivity constraints derived from the general properties of the S-matrix will be also discussed.

CHAPTER 2

Chiral effective theories

QCD, responsible for the strong interaction and the hadronic spectrum, has not been analytically solved from first principles due to the high nonlinearity and the related nonperturbative property at low energies. Various effective field theories (EFTs), phenomenological approaches and numerical simulations are introduced to describe the strong processes at low energies and the hadronic properties.

In past years, EFTs have become valuable and practical tools in many branches of physics, in particular in condensed matter physics and particle physics. EFTs can avoid complicated calculations and unknown knowledge on details of the distinct scales. In this chapter, we will give a brief review on the EFTs of QCD and demonstrate how to construct ChPT and including matter fields.

2.1 Effective field theories

One of the most astonishing features about the world is that we can understand the physics at a given scale without knowing everything at other scales. In particle physics, a process may involve a large range of scales, from the sub-eV region to the TeV region. A detailed calculation involving the large energy range may be very complicated and impossibly achieved. Fortunately, we do not need to know everything to describe the phenomena at given (low) energies. EFTs provide us a valuable tool to simplify the calculation and allow us to focus on the physics or phenomena at the given energy without worrying about the poor knowledge of the underlying physics and the consequent complications. More details on the discussion of EFTs can be found in Refs. [31–36].

2.1.1 The principles of effective field theories

For a quantum system, the physics is encoded into the S-matrix, or amplitudes, which in general depends on the momenta of external particles in a complicated way. By analytic continuation, the amplitudes can be regarded as a complex function on the external momenta. It may exhibits complicated nonanalytic structures, e.g. branch cuts and poles, which arise when the internal particles can be on-shell. If the kinematic region that a given internal particle could be on-shell is far from the region concerned, the contribution of that internal particle can be well approximated by the first few terms in a Taylor expansion in some proper parameters (for a very heavy particle, the external momenta would be a nice expansion parameter). The procedure can be more simply achieved at the Lagrangian level, since the nonanalytic behavior that is due to the on-shellness of relevant light degrees of freedom in the low energy region are untouched in this Taylor expansion. In the language of the path integral, the irrelevant particle fields (or degrees of freedom) are integrated out. The expanded Lagrangian is usually called an effective

Lagrangian. In general, it consists of an infinite sum of local operators which are organized according to decreasing importance with increasing order of the proper parameters. In practice, one only needs to consider the first few terms of the Lagrangian according to the accuracy desired for the process in question. Like above, the EFTs obtained by integrating out the heavy fields from a more fundamental underlying theory are called top-down EFTs. In fact, EFTs can also be constructed when the underlying theory is unknown. The construction of the effective Lagrangian is guided by the symmetries, the so-called bottom-up EFTs.

Top-down and bottom-up approaches

In the top-down approach to EFTs, the underlying theory is known and we are interested in the low-energy sector. The basic principle of the top-down approach is removing heavy fields (or heavy components) from the Lagrangian by integrating them out. The role of the heavy fields (UV physics) in the infrared (IR) behavior of the theory was first discussed by Appelquist and Carazzone in Ref. [37]. It led to the decoupling theorem [37, 38], which states that if the low energy Lagrangian is renormalizable, then all effects of the heavy particles appear either as a renormalization of the coupling constants or else are suppressed by powers of the heavy particle masses. It is in accord with physical expectations since the influence of the heavy particles to low energy observables would disappear in the limit of infinite mass of the heavy particle. The virtual exchange of the heavy particle leads to powers of heavy particle mass at low energies by a proper Taylor expansion. The effective Lagrangian can be derived via

$$e^{iZ_{\rm eff}[\ell]} = \frac{\int [dh] e^{iZ[\ell,h]}}{\int [dh] e^{iZ[0,h]}}, \tag{2.1}$$

where ℓ and h represents the light and heavy fields respectively, $Z[\ell, h]$ is the underlying action, $Z_{\rm eff}[\ell]$ is the resulting effective action. In detail, considering a linear coupling of h to some combination of fields $J(\ell)$, with the Lagrangian

$$\mathcal{L} = \mathcal{L}_\ell + \frac{1}{2}(\partial_\mu h \partial^\mu h - m^2 h^2) + Jh, \tag{2.2}$$

where $\mathcal{L}_\ell$ is the pure light field Lagrangian. Then the effective Lagrangian is obtained at tree level by

$$\begin{aligned} e^{iZ_{\rm eff}[\ell]} &= e^{i\int d^4x \mathcal{L}_{\rm eff}(x)} \\ &= \frac{\int [dh] e^{i\int d^4x \mathcal{L}(h,\ell)}}{\int [dh] e^{i\int d^4x \mathcal{L}(h,0)}} \\ &= \frac{\int [dh] \exp\left\{i\int d^4x [-\frac{1}{2}(h-\mathcal{D}^{-1}J)\mathcal{D}(h-\mathcal{D}^{-1}J) + \frac{1}{2}J\mathcal{D}^{-1}J + \mathcal{L}_\ell\right\}]}{\int [dh] \exp\left\{i\int d^4x [-\frac{1}{2}h\mathcal{D}h]\right\}} \\ &= e^{i\int d^4x (\mathcal{L}_\ell + \frac{1}{2}J\mathcal{D}^{-1}J)}, \end{aligned} \tag{2.3}$$

where $\mathcal{D} = \partial^2 + m^2$. From Eq. (2.3) we obtain

$$\mathcal{L}_{\rm eff} = \mathcal{L}_\ell + \frac{1}{2}J\mathcal{D}^{-1}J. \tag{2.4}$$

Noting that the heavy particle propagator is far from on-shell in the low-energy sector concerning, one may obtain a local effective Lagrangian using Taylor expansion

$$(\partial^2 + m^2)^{-1} = \frac{1}{m^2}(1 - \frac{\partial^2}{m^2} + \frac{\partial^4}{m^4} - \dots). \tag{2.5}$$

Then we obtain an effective local Lagrangian series organized in powers of inverse of the heavy field mass

$$\mathcal{L}_{\text{eff}}(x) = \mathcal{L}_\ell + \frac{1}{2m^2}J(x)J(x) - \frac{1}{2m^4}J(x)\partial^2 J(x) + \frac{1}{2m^6}J(x)\partial^4 J(x) + \dots. \tag{2.6}$$

From the above procedure, the contribution of heavy field is expanded in a tower of increasing power of the inverse heavy field mass. At low energies, the series can be amputated according to the desired accuracy. The pure light sector Lagrangian $\mathcal{L}_\ell$ is untouched, thus the symmetries of the light fields in the underlying theory are still symmetries of the effective Lagrangian. The procedure can be extended to the loop level and a theory having several different heavy mass scales consecutively.

In the bottom-up approach to the EFTs, the underlying theory is either unknown or known but impossible to solve at low energies. QCD is one of the later cases, where the degrees of freedom at high energies (quarks and gluons) are different from those at low energies (hadrons). Due to the lack of the knowledge of underlying theory, no constraint is imposed on the construction of the effective Lagrangian except for the consideration of symmetries. The standard procedure to construct EFTs in the bottom-up approach is first specifying the degrees of freedom at the given energy scale, then writing down the most general possible local operators that satisfying the symmetries we are imposing. The coefficients of the operators, called Wilson coefficients or low energy constants (LECs), can be determined by comparing with experimental and/or lattice data. Similar with the top-down EFTs where the series of operators in Lagrangian is ordered in a systematic expansion in the power of inverse of heavy field mass, the most general operators in bottom-up EFTs also need a consistent power counting rule to organize the infinite number of operators and evaluate their importance.

Power counting scheme

A power counting scheme is to assess the importance of each local operator in the Lagrangian and the generated Feynman diagrams. It plays an essential role in the construction of EFTs. In the top-down low-energy EFTs, the Lagrangian is Taylor expanded in the power of $1/m_h$, with m_h the mass of the integrated out heavy field. In general, an effective Lagrangian can be expressed in the form

$$\mathcal{L}_{\text{eff}} = \mathcal{L}^{(0)}_{\text{eff}} + \frac{1}{\Lambda}\mathcal{L}^{(1)}_{\text{eff}} + \frac{1}{\Lambda^2}\mathcal{L}^{(2)}_{\text{eff}} + \dots, \tag{2.7}$$

where Λ represents a large energy scale of emerging new physics, including underlying theory with heavy fields. Since the energy scale $\Lambda \gg E$, with E the energy we are considering, the terms with higher dimension (denoted by the superscripts) can be neglected or taken into account perturbatively. As a result, counting the power of $1/\Lambda$ serves a natural and proper rule to assess the importance of each term in Lagrangian. At tree level, the amplitudes generated by $\mathcal{L}^{(n)}$ is suppressed by p^n/Λ^n, where p (e.g. external momenta, mass of light fields, peculiar components of momenta or fields, and etc.) collectively denotes the small expansion parameter compared with Λ. Therefore, the power counting rule for organizing the effective Lagrangian is straightforward. A systematic rule of assessing the importance of diagrams generated by the various terms of Lagrangian is subtle and needs our attention. The power D

of a given diagram with amplitude $\mathcal{M}(p)$ can be evaluated by analysing the behavior of the amplitude under a linear rescaling of all small parameters $p \to tp$ by [14]

$$\mathcal{M}(tp) = t^D \mathcal{M}(p). \tag{2.8}$$

Considering a diagram with N_V vertices, letting N_n be the number of vertices arising from the effective Lagrangian $\mathcal{L}^{(n)}_{\text{eff}}$, we have $N_V = \sum_n N_n$. Under the rescaling $p \to tp$ and $M \to tM$ with M the mass of light field, each internal propagator rescales as

$$\begin{aligned}\int \frac{d^4k}{(2\pi)^4}\frac{i}{k^2 - M^2 + i\epsilon} &\to \int \frac{d^4k}{(2\pi)^4}\frac{i}{k^2 - t^2M^2 + i\epsilon} \\ &= t^{-2}\int \frac{d^4k}{(2\pi)^4}\frac{i}{t^{-2}k^2 - M^2 + i\epsilon} \\ &= t^2 \int \frac{d^4l}{(2\pi)^4}\frac{i}{l^2 - M^2 + i\epsilon}.\end{aligned} \tag{2.9}$$

For each vertex generated from $\mathcal{L}^{(n)}_{\text{eff}}$, we obtain symbolically a factor p^n and a four-momentum conservation delta function, which lead to rescaling as t^n and t^{-4}, respectively. Therefore, the corresponding S-matrix rescales as $t^{2N_I + \sum_n N_n(n-4)}$, where N_I denotes the number of internal lines. Recalling that

$$S \sim i\mathcal{M}\delta^4(p_f - p_i) \tag{2.10}$$

and $\delta^4(tp_f - tp_i) \to t^{-4}\delta^4(p_f - p_i)$, one finds

$$D = 4 + 2N_I + \sum_n N_n(n-4). \tag{2.11}$$

For a diagram with N_V vertices, it needs $N_V - 1$ internal lines to connect all vertices at tree level, then the number of independent loops N_L increases each time when an extra internal line is added. So we have a relation

$$N_L = (N_I - N_V) + 1. \tag{2.12}$$

Inserting Eq. (2.12) into Eq. (2.11) and using $N_V = \sum_n N_n$, we finally obtain the Weinberg's power counting scheme [14]

$$D = 2 + \sum_n N_n(n-2) + 2N_L. \tag{2.13}$$

It is easy to conclude that a diagram with N_L loops are suppressed by a power $(p/\Lambda)^{2N_L}$ compared with the tree diagrams.[1] A relation between the p/Λ expansion on Lagrangian level and the loop expansion is well established allowing us to systematically applying EFTs with loops. Loops contain the important analytical structures for the analysis of S-matrix, the nonanalytical properties and the imaginary parts cannot originate from the tree level amplitudes. Not surprisingly, the loops usually have divergences. It means the EFTs need to be renormalized to remove the divergences in order to get physical quantities.

[1] Note that we have imposed that the particle mass scales same as the external momenta, which is valid for the pure Goldstone ChPT. One has no such relation in general.

2.1.2 Renormalization in effective field theories

In the normal sense, EFTs are nonrenormalizable. All terms allowed by the assumed symmetries of the theory are included in the effective Lagrangian. Only the operators with dimension 4 and less are renormalizable according to dimensional analysis. Since the effective Lagrangian is obtained by the Taylor expansion of the underlying full theory, it contains an infinite number of terms. Any truncation of the series destroys the UV structure of the full theory. As a result, the truncated effective theory turns out to be nonrenormalizable even if the full theory is renormalizable. However, the physical quantities are free of divergences. The renormalization of a general EFT is analogous to the full theory. The only difference is that one needs to deal with as many couplings as in the corresponding effective Lagrangian. In a mass-independent subtraction scheme, the number of couplings to be renromalized is finite to a given accuracy [32]. The divergences of loops are cancelled by the counter terms, i.e. the divergences of the low-energy constants, at the corresponding order.

It is well known that different renormalization schemes lead to equivalent results for the physical observables. In a mass-dependent subtraction scheme such as large momentum cutoff, the expansion of an EFT breaks down since all the higher order operators in the effective Lagrangian are equally important [33]. To guarantee the correct dimension, the loop contribution from the interaction $\mathcal{L}_{\text{eff}}^{(n)}$ is suppressed by

$$\frac{1}{\Lambda^{n'}} \int^{\Lambda} \frac{d^{4N_L}k}{k^{4N_L-n'}} \sim O(1), \tag{2.14}$$

where N_L represents the number of independent loops, n' depends on N_L and the topology of the diagram. The factor $\frac{1}{\Lambda^{n'}}$ comes from the low-energy constants of the Lagrangians which generate the diagram, and the denominator is the combination of momenta from derivative couplings and propagators.[2] Here we assume the momentum cutoff is of order Λ. All loops are of order 1 which breaks down the expansion and makes the calculations impossible. However, this problem can be cured if one uses a mass-independent subtraction scheme, e.g. dimensional regularization and minimal subtraction. In dimensional regularization, one finds

$$\frac{1}{\Lambda^{n'}} \int \frac{d^{4N_L}k}{k^{4N_L-n'}} \sim (\frac{m}{\Lambda})^{n'} \log \mu, \tag{2.15}$$

where m is some dimensional parameter appearing in the effective Lagrangian and μ is the renormalization scale. From Eq. (2.15), the loop contribution are suppressed compared with the tree level contributions. Mass-independent subtraction scheme shares many advantages in the practical calculations. However, it obscures the decoupling of heavy particles. The mass-independent subtraction gives rise to an incorrect behavior at low energies. The decoupling can be implemented by integrating out the heavy particles [39]. Effects of the heavy particles in EFTs are included via higher dimension operators, which are suppressed.

If $\mathcal{L}^{(0)}$ is renormalizable in the traditional sense, one cannot learn any information about the energy scale Λ from just looking at $\mathcal{L}^{(0)}$. At low energies much less than Λ, $\mathcal{L}^{(0)}$ can be regarded as a fundamental theory. Reversely, a fundamental theory can in turn become an effective theory of some other fundamental theory at higher energies. The EFTs can be categorised to two different types depending on the structure of the transition between the fundamental and the effective theories.

[2] Here we only focus on the influence of modes of order Λ to the low energy sector, i.e. $E \ll \Lambda$. Hence we can ignore the masses of the effective fields for a while.

2.1.3 Decoupling and non-decoupling EFTs

The decoupling EFTs are derived from the renormalizable fundamental theory by integrating out the heavy degrees of freedom leaving the light degrees of freedom. No light particles are generated in the transition from the fundamental to effective theory. The remaining operators in Lagrangian contains renormalizable and nonrenormalizable parts suppressed by inverse powers of Λ. It has the form of

$$\mathcal{L}_{\text{eff}} = \mathcal{L}_{d\leq 4} + \sum_{d>4} \frac{\mathcal{L}_d}{\Lambda^{d-4}}, \tag{2.16}$$

where $\mathcal{L}_{d\leq 4}$ is the renormailzable part, and the second part is nonrenormalizable. At low energies, corrections from the nonrenormalizable operators are suppressed by inverse powers of Λ. The famous Fermi theory of weak interactions is one example of decoupling EFTs. Even the Standard Model itself can be regarded as an effective theory of some underlying and more fundamental theory. Up to today, there is no experimental evidence for terms with $d > 4$ appearing in the Standard Model. It indicates that the Standard Model is sufficiently fundamental at the energies we can reach nowsday.

In the case that the explicit degrees of freedom of an EFT are different from those of the fundamental theory due to some mechanism, e.g. phase transitions, we have a non-decoupling EFT. When the light Goldstone bosons are generated by the spontaneously breaking of symmetries, these explicit light degrees of freedom are absent in the fundamental theory. The broken symmetry relates processes with different numbers Goldstone bosons, resulting in operators with different dimensions, the distinction between renormalizable and nonrenormalizable parts are not meaningful anymore. One of examples of non-decoupling EFTs is the Chiral Perturbation Theory, which will be introduced in the next section.

Usually, a fundamental theory can be translated to EFTs with different structures at a given energy, which lead to the equivalent results. It can be stated formally as Representation Independent Theorem [40, 41] that if two fields are related nonlinearly, e.g. $\phi = \chi F[\chi]$ with $F[0] = 1$, then the equivalent physical quantities result no matter whether they are calculated with the field ϕ using $\mathcal{L}(\phi)$ or with χ using $\mathcal{L}'(\chi) = \mathcal{L}(\chi F[\chi])$. The condition $F[0] = 1$ is to guarantee that the two fields have the same free field behavior and single particle singularities. This result is quite physically expected since experiments cannot distinguish the free particle ϕ from χ due to the same single-particle properties which is guaranteed by $F[0] = 1$. The theorem allows us to employ various realisations or representations of EFTs. It is very useful as it can simplify the calculations for some situations, especially for Chiral Perturbation Theory.

2.1.4 Examples of EFTs

Fermi Theory

A well-known EFT is the Fermi Theory of weak interactions. It was first proposed to explain the beta decay in 1933. Nowdays, it is regarded as an EFT of the SM at low energies. In the SM, the weak interactions between fermions are mediated through the $W^{\pm}$ bosons. At low energies, the momentum transferred by the propagator W is small compared to the mass of the W, M_W. Therefore, the interaction reduces to a contact interaction via

$$\frac{-g_{\mu\nu} + q_\mu q_\nu / M_W^2}{q^2 - M_W^2} \to \frac{g_{\mu\nu}}{M_W^2}. \tag{2.17}$$

The Fermi theory of the weak interactions then can be obtained from the SM via

$$\mathcal{L}_{\text{eff}} = -(\frac{g}{\sqrt{8}})^2 \frac{g_{\mu\nu}}{M_W^2} J^\mu J^\nu = -\frac{G_F}{\sqrt{2}} J_\mu J^\mu, \tag{2.18}$$

where $J_\mu = \sum_{ij} \bar{u}_i \gamma_\mu (1-\gamma_5) V_{ij} d_j + \sum_k \bar{\nu}_k \gamma_\mu (1-\gamma_5) l$, with V_{ij} the Cabibbo-Kobayashi-Maskawa mixing matrix and $G_F = \frac{\sqrt{2}g^2}{8M_W^2}$ the Fermi coupling constant.

Heavy quark effective theory (HQET)

Heavy quark systems provide a nice platform for applications of the EFT technology. The mass of heavy quarks $m_Q \gg \Lambda_{QCD}$ provides a natural separation of scales. The low energy ($\sim \Lambda_{QCD}$) effective Lagrangian is obtained by integrating out the heavy-components of heavy quarks. It provides a simplified description of the interactions of a single heavy quark with soft quarks and gluons. The heavy quark is nearly on-shell because of the soft interactions. And the velocity of the heavy quark v is almost unchanged since the change of v is suppressed as $\Delta v = \Delta p/m_Q$, with $\Delta p \sim \Lambda_{QCD}$. As an important consequence, the momentum of the heavy quark can be decomposed as $p_Q = m_Q v + k$, where v is usually setup as the velocity of the hadron containing the heavy quark with $v^2 = 1$, and k is the residual momentum, order of Λ_{QCD}. The nearly on-shell spinor is decomposed into two parts

$$Q(x) = e^{-im_Q v\cdot x}(h_v(x) + H_v(x)), \tag{2.19}$$

where $h_v(x) = e^{im_Q v\cdot x}\frac{1+\not{v}}{2}Q(x)$ and $H_v(x) = e^{im_Q\cdot x}\frac{1-\not{v}}{2}Q(x)$ are the large and small components, respectively. Inserting Eq. (2.19) into the QCD Lagrangian $\mathcal{L}_Q = \bar{Q}(x)(i\not{D} - m_Q)Q(x)$ yields

$$\mathcal{L}_Q = \bar{h}_v iv\cdot D h_v + \bar{H}(-iv\cdot D - 2m_Q)H_v + \bar{h}_v i\not{D}_\perp H_v + \bar{H}_v i\not{D}_\perp h_v, \tag{2.20}$$

where $D_\perp^\mu = D^\mu - v^\mu v\cdot D$. It shows that the field h_v describes a massless fermion and H_v describes a fermion with mass $2m_Q$. Soft interactions cannot excite the heavy fermion, so we integrate it out. At the tree level, it can be achieved by inserting the classical equation of motion for H_v

$$H_v = \frac{1}{2m_Q + iv\cdot D} i\not{D}_\perp h_v = \frac{1}{2m_Q}\sum_{n=0}^{\infty}\Big(-\frac{iv\cdot D}{2m_Q}\Big)^n i\not{D}_\perp h_v \tag{2.21}$$

into Eq. (2.20). To the subleading order in $1/m_Q$, one finds the

$$\mathcal{L}_{HQET} = \bar{h}_v iv\cdot D h_v + \frac{1}{2m_Q}\Big(\bar{h}_v (iD_\perp)^2 h_v + C_{\text{mag}}(\mu)\frac{g}{2}\bar{h}_v \sigma\cdot G h_v\Big) + \ldots. \tag{2.22}$$

It is worth mentioning that the covariant derivative $D_\mu = \partial_\mu + igA_{s\mu}$ and the field strength $G_{\mu\nu}$ contain only soft gluons. The hard gluons are integrated out and their effects are encoded into the Wilson coefficients, e.g. $C_{\text{mag}}(\mu)$. The second term are referred to as the non-relativistic kinetic energy and chromo-magnetic interaction, respectively. Lorentz invariance ensures that the Wilson coefficient of the kinetic term is not renormalized, i.e. exactly equal to unity. However, the coefficient of the chromo-magnetic term, $C_{\text{mag}}(\mu)$, receives corrections at loop levels.

The heavy quark effective Lagrangian Eq. (2.22) reveals many crucial features of heavy quark QCD. The leading order exhibits a global spin-flavor symmetry, which leads to many important relations between the properties of hadrons containing a single heavy quark. For more reviews on HQET, see

Refs. [42–49] and references therein.

Soft-collinear effective theory (SCET)

As a young member of the EFTs of SM, SCET provides a new and useful tool for the QCD factorization and the resummation of large logarithms using renormalization group evolution [50–52]. It describes the interactions of soft and collinear degrees of freedom in the presence of hard interactions, with the large momentum scale $Q \gg \Lambda_{QCD}$. In a process involving hard interactions and energetic light states (invariant mass $m \ll Q$) or the production of energetic jets, the highly energetic states scale in the light-cone frame as

$$(p_n^-, p_n^+, p_n^\perp) \sim (Q, m^2/Q, m) = Q(1, \lambda^2, \lambda), \tag{2.23}$$

where n denotes a light-like 4-vector with $n \cdot p_\perp = 0$ along which the energetic state moves, and $\lambda = m/Q$ is the expansion parameter of SCET. The scaling of such a collinear field remains unchanged if it interacts with an energetic particle in the same direction n, or with a soft particle with uniform scaling as

$$(p_s^-, p_s^+, p_s^\perp) \sim Q(\lambda^2, \lambda^2, \lambda^2). \tag{2.24}$$

The effective theory describing the interactions of collinear, Eq. (2.23), and soft, Eq. (2.24), degrees of freedom is called SCET_I. The scaling Eq. (2.24) applies to the energetic states with invariant mass $m^2 \gg \Lambda^2_{\text{QCD}}$, e.g. a jet with jet-mass $m_J^2 \gg \Lambda^2_{\text{QCD}}$. However, if the invariant mass is of order Λ_{QCD}, e.g. M_π, the scaling Eq. (2.24) is no longer applicable. To describe such a system, a modified version, SCET_II, is introduced, in which the scaling of soft modes is $Q(\lambda, \lambda, \lambda)$. In this section, only the SCET_I is considered, and from now on the subscript will be omitted for brevity.

Having the power counting of the relevant degrees of freedom Eqs. (2.23) and (2.24), we are able to derive the SCET Lagrangian from QCD. Since the collinear and soft degrees of freedom are treated explicitly, one splits the quark and gluon fields into a collinear and soft part

$$\begin{aligned} A^\mu(x) &\to A_c^\mu(x) + A_s^\mu(x), \\ \psi(x) &\to \psi_c(x) + \psi_s(x). \end{aligned} \tag{2.25}$$

The effective Lagrangian for the soft part is the same as the original QCD Lagrangian due to the unique scaling for the components of soft momenta. To derive the effective Lagrangian for the collinear fields and soft-collinear interactions, introducing an auxiliary light-cone vector $\bar{n}$ satisfying $\bar{n}^2 = 0$ and $n \cdot \bar{n} = 2$, one then splits the collinear fields into $\xi_n(x)$ and $\Xi_n(x)$

$$\psi_n(x) = \xi_n(x) + \Xi_n(x) \tag{2.26}$$

with $\xi_n(x) = \frac{\not{n}\not{\bar{n}}}{4}\psi_n(x)$ and $\Xi_n(x) = \frac{\not{\bar{n}}\not{n}}{4}\psi_n(x)$. The $\Xi_n(x)$ describes the degrees of freedom far off-shell and can be integrated out. Likewise to HQET, one finds

$$\mathcal{L}_c = \bar{\xi}_n \frac{\not{\bar{n}}}{2} in \cdot D \xi_n + \bar{\xi}_n i\not{D}_\perp \frac{1}{i\bar{n} \cdot D} i\not{D}_\perp \frac{\not{\bar{n}}}{2} \xi_n, \tag{2.27}$$

where

$$D_\perp^\mu = D^\mu - \frac{n^\mu}{2}\bar{n} \cdot D - \frac{\bar{n}^\mu}{2} n \cdot D.$$

Employing the power counting rule in Eqs. (2.23) and (2.24), the leading order SCET Lagrangian can be

written as

$$\begin{aligned}\mathcal{L}_{\rm SCET} &= \bar{\psi}_s i\not{D}_s \psi_s - \frac{1}{4}(F^{s,a}_{\mu\nu})^2 \\ &+ \bar{\xi}_n \frac{\not{n}}{2}\Big(in\cdot D_n + i\not{D}_{n\perp}\frac{1}{i\bar{n}\cdot D_n} i\not{D}_{n\perp}\Big)\xi_n - \frac{1}{4}(F^{n,a}_{\mu\nu})^2 \\ &+ g\bar{\xi}_n n\cdot A_s \frac{\not{n}}{2}\xi_n, \end{aligned} \tag{2.28}$$

where $F^{n,a}_{\mu\nu} = \frac{i}{g}[D_\mu, D_\nu]$. An important difference between SCET and HQET is that the SCET Lagrangian is not corrected by hard modes. The effect of hard modes are incorporated in the Wilson coefficients of the external source operators. The most important feature of SCET is the decoupling of soft gluons. Defining new fields $\xi^{(0)}_n$ and $A^{(0)}_n$ via

$$\xi_n(x) = S_n(x)\xi^{(0)}_n(x), \quad A^\mu_n(x) = S_n(x)A^{(0)\mu}_n(x)S^\dagger_n(x), \tag{2.29}$$

where $S_n(x)$ denotes a time-like soft Wilson line along the direction n,

$$S_n(x) = \mathbf{P}\exp\Big[ig\int_{-\infty}^0 ds n\cdot A_s(x+sn)\Big], \tag{2.30}$$

where $\mathbf{P}$ indicates the path ordering of the color matrices, the interaction between collinear and soft modes in SCET $\mathcal{L}_{c-s} = \bar{\xi}_n \frac{\not{n}}{2} in\cdot D\xi_n$ changes to

$$\mathcal{L}_{c-s} \to \bar{\xi}^{(0)}_n \frac{\not{n}}{2} in\cdot D^{(0)}_n \xi^{(0)}_n, \tag{2.31}$$

so that the soft gluon no longer appears in the collinear Lagrangian at leading order, which is the so-called decoupling transformation. It can also be proven that the soft and collinear gluons decouple at the leading order as well. The decoupling of soft and collinear modes at leading order is an important element in factorization. A crucial aspect of the full QCD is the gauge symmetry, which can be preserved in SCET by regarding the collinear fields and soft fields as quantum fields and background fields under soft and/or collinear gauge transformation, respectively. Another important characteristic of the SCET is the non-locality of operators in position space, due to the non-power suppressed derivatives along the light-cone directions corresponding to large energies. It is also manifested as the dependence of the Wilson coefficients on the large energy scales.

The SM as an EFT

The EFTs we introduced above belong to the top-down ones. In those cases, we integrate out the heavy or far off-shell degrees of freedom. In general, one writes down the most general structures of Lagrangian satisfying the underlying symmetries, then determine each Wilson coefficient by matching to the full theory. This procedure not only applies to top-down EFTs, but also applies to bottom-up ones. In the latter case, the Wilson coefficients can only be determined by matching to the experimental and/or lattice data. A well known bottom-up EFT is chiral perturbation theory, which is the main topic of this work and will be described in detail in the following sections. As mentioned before, the SM itself is widely regarded as an EFT of some unknown and more fundamental theory. In this case, the SM serves as a bottom-up EFT of some unknown underlying theory at leading order.

If we associate a large new scale of new physics Λ, then the SM can be regarded as the leading order

of an EFT of the new physics at low energies $\mathcal{L}^{(0)} = \mathcal{L}_{\rm SM}$. We can do a power counting in this $1/\Lambda$. The first order SM correction $\mathcal{L}^{(1)}$ has the form of

$$\mathcal{L}^{(1)} = \frac{C}{\Lambda} O_5, \tag{2.32}$$

where O_5 denotes the dimension 5 operators and the Wilson coefficient C is dimensionless. Likewise, one can construct higher order corrections with higher dimensional operators respecting the SM symmetries. One can calculate the corrections from high orders to the SM and compare them with the experiments. So far, no unambiguous evidence for the existence of such higher order corrections has been found.

2.2 Symmetries of QCD and chiral perturbation theory

2.2.1 Local symmetry of the QCD Lagrangian

The gauge principle has been proven to be very successful in physics to generate interactions between matter fields through the exchange of gauge bosons. The color degree of freedom was introduced into the quark model by Greenberg in 1964 [53], and independently by Han and Nambu in 1965 [54]. Here the matter fields are quarks, with six different flavors. The QCD Lagrangian can be obtained from the Lagrangian for free quarks by localizing the $SU(3)_C$ symmetry. The gauge bosons are called gluons. The QCD Lagrangian reads

$$\mathcal{L}_{\rm QCD} = \sum_f \bar{q}_f (i\not{D} - m_f) q_f - \frac{1}{2} {\rm Tr}_C (G_{\mu\nu} G^{\mu\nu}), \tag{2.33}$$

where the subscript f denotes the flavor, $D_\mu = \partial_\mu + igA_\mu$ with $A_\mu = \frac{\lambda^a}{2} A^a_\mu$ the gluon fields, $G_{\mu\nu} = \frac{1}{ig}[D_\mu, D_\nu]$ is the field strength tensor with g the $SU(3)_C$ gauge coupling constant. Here, the color index is suppressed and λ^a are Gell-Mann matrices. For each quark flavor f, the quark field q_f consists of a color triplet

$$q_f = \begin{pmatrix} q_{f,r} \\ q_{f,g} \\ g_{f,b} \end{pmatrix}, \tag{2.34}$$

with r =red, g =green and b =blue denoting the color. And the QCD Lagrangian (2.33) should be understood as in a matrix form. Under a $SU_C(3)$ gauge transformation, the quark fields transform as

$$q_f(x) \to q'_f(x) = U(x) q_f(x) = \exp\Big[- i\theta_a(x) \frac{\lambda^a}{2} \Big] q_f(x). \tag{2.35}$$

In order to keep the invariance of the Lagrangian under the local transformations $U(x)$, the gauge potential A_μ transforms as

$$A_\mu = A^a_\mu \frac{\lambda^a}{2} \to A'_\mu = U A_\mu U^\dagger + \frac{i}{g} \partial_\mu U U^\dagger. \tag{2.36}$$

Under the transformation (2.35) and (2.36), it is easy to show that the covariant derivative $D_\mu q_f$ transfroms as q_f, i.e. $D_\mu q_f(x) \to U(x) D_\mu q_f(x)$, and the field strength tensor $G_{\mu\nu}$ transforms as $G_{\mu\nu}(x) \to U(x) G_{\mu\nu}(x) U^\dagger(x)$. As the result, the QCD Lagrangian (2.33) is invariant under the local $SU_C(3)$ transformations with the field transformation (2.35) and (2.36).

From the point of gauge invariance, the operator

$$\mathcal{L}_\theta = \frac{g^2\theta}{32\pi^2}\epsilon_{\mu\nu\rho\sigma}\mathrm{Tr}_C(G^{\mu\nu}G^{\rho\sigma}), \tag{2.37}$$

can appear in the QCD Lagrangian as well, where $\epsilon_{\mu\nu\rho\sigma}$ denotes the totally antisymmetric Levi-Civita tensor, and θ is considered as a coupling constant. $\mathcal{L}_\theta$ is called the θ-term, which implies an P and CP violation of the strong interactions. It is worth mentioning that different values of θ correspond to different theories. This is different from the case of spontaneously breaking of symmetry, in which the different values of the vacuum expectation value label different states in the same theory [35]. The θ-term induces a neutron electric dipole moment (nEDM) of order [55, 56]

$$d_n \simeq \frac{e|\theta|m_\pi^2}{m_N^3} \simeq 10^{-16}|\theta|\text{e cm}, \tag{2.38}$$

and the experimental bound on the nEDM $d_n \lesssim 3\cdot 10^{-26}$ e cm [57] implies $\theta \lesssim 10^{-10}$. More details on the θ-term can be found in Refs. [35].

2.2.2 Global symmetries of QCD Lagrangian

In addition to the $SU_C(3)$ local symmetry, the QCD Lagrangian (2.33) exhibits global symmetries. It is invariant under a global $U(1)$ transformation

$$q_f(x) \to e^{-i\alpha}q_f(x), \tag{2.39}$$

where α is independent of x. According to Noether's theorem, every differentiable symmetry of the action of a physical system has a corresponding conservation law, the $U(1)$ symmetry leads to the conserved vector current

$$V_\mu = \bar{q}_f\gamma_\mu q_f, \tag{2.40}$$

where the sum in the color index is suppressed. For a conserved current, $\partial_\mu J^\mu = 0$, the charge

$$Q(t) = \int d^3x V_0(\vec{x},t) \tag{2.41}$$

is time independent, and thus a conserved quantity. The conserved vector current leads to the conservation of baryon number.

Besides the exact symmetries discussed above, the QCD Lagrangian also exhibits approximate global symmetries. Sometimes a Lagrangian would have a symmetry if certain of the parameters were set to zero. In that limit, the symmetry would lead to a set of interesting physical consequences. If the parameters are 'small' in some sense, the consequences may be still approximately valid. If a symmetry is not exact, the associated current and charge would be not conserved. The current divergence has the form of

$$\partial^\mu J_\mu^{\text{approx}} = f(\alpha), \tag{2.42}$$

where α is the 'small' parameter and $f(0) = 0$. In practice, the utility of an approximate symmetry is rarely known from the Lagrangian itself, it is only evident after its predictions are checked by experiments.

Thus far, the discussions are at the classical level. After the quantization, symmetries on the classical level may no longer be symmetries at loop levels, which leads to the so-called anomalies. We will come back to this topic on the next section.

The six flavors of quark are commonly classified into light and heavy quarks according to their masses compared with the mass of typical hadrons containing only light quarks or Λ_{QCD}. If we only consider the light quark systems, the masses of the light quarks can be regarded as small parameters. It leads to the approximate symmetry $SU_L(N_f) \times SU_R(N_f) \times U_V(1)$, where N_f denotes the number of light quarks under consideration. Starting from the massless QCD Lagrangian

$$\begin{aligned}\mathcal{L}^0_{\rm QCD} &= \sum_f \bar{q}_f i\not{D} q_f - \frac{1}{2}\mathrm{Tr}_C(G_{\mu\nu}G^{\mu\nu}), \\ &= \sum_f (\bar{q}_{f,R} i\not{D} q_{f,R} + \bar{q}_{f,L} i\not{D} q_{f,L}) - \frac{1}{2}\mathrm{Tr}_C(G_{\mu\nu}G^{\mu\nu}),\end{aligned} \tag{2.43}$$

where $q_{f,L}$ and $q_{f,R}$ represent the left- and right-handed chiral components, respectively, i.e. $q_{f,L} = P_L q_f$ and $q_{f,R} = P_R q_f$, with $P_{L,R}$ the projection operators $P_L = \frac{1}{2}(1-\gamma_5)$ and $P_R = \frac{1}{2}(1+\gamma_5)$. Due to the flavor independence of the covariant derivatives, $\mathcal{L}^0_{\rm QCD}$ is invariant under the transformations

$$\begin{aligned}\begin{pmatrix} u_L \\ d_L \\ \vdots \end{pmatrix} &\to U_L \begin{pmatrix} u_L \\ d_L \\ \vdots \end{pmatrix} = \exp\Big(-i\sum_a^{N_f^2-1} \alpha_L^a t^a\Big) e^{-i\theta_L} \begin{pmatrix} u_L \\ d_L \\ \vdots \end{pmatrix}, \\ \begin{pmatrix} u_R \\ d_R \\ \vdots \end{pmatrix} &\to U_R \begin{pmatrix} u_R \\ d_R \\ \vdots \end{pmatrix} = \exp\Big(-i\sum_a^{N_f^2-1} \alpha_R^a t^a\Big) e^{-i\theta_R} \begin{pmatrix} u_R \\ d_R \\ \vdots \end{pmatrix},\end{aligned} \tag{2.44}$$

where U_L and U_R are independent unitary $N_f \times N_f$ matrices, t^a are the corresponding generators of the groups. It is said that $\mathcal{L}^0_{\rm QCD}$ has a classical global $U_L(3) \times U_R(3)$ symmetry, or in other words, $SU_L(N_f) \times SU_R(N_f) \times U_V(1) \times U_A(1)$ symmetry. The associated conserved currents are

$$\begin{aligned} L^a_\mu &= \bar{q}_L \gamma_\mu t^a q_L, \quad \partial^\mu L^a_\mu = 0, \\ R^a_\mu &= \bar{q}_R \gamma_\mu t^a q_R, \quad \partial^\mu R^a_\mu = 0, \\ L^0_\mu &= \bar{q}_L \gamma_\mu q_L, \quad \partial^\mu L^0_\mu = 0, \\ R^0_\mu &= \bar{q}_R \gamma_\mu q_R, \quad \partial^\mu R^0_\mu = 0. \end{aligned} \tag{2.45}$$

Instead of these chiral currents, it is sometimes more convenient to use the linear combinations

$$\begin{aligned} V^a_\mu &= R^a_\mu + L^a_\mu = \bar{q}\gamma_\mu t^a q, \\ A^a_\mu &= R^a_\mu - L^a_\mu = \bar{q}\gamma_\mu\gamma_5 t^a q, \\ V_\mu &= R^0_\mu + L^0_\mu = \bar{q}\gamma_\mu q, \\ A_\mu &= R^0_\mu - L^0_\mu = \bar{q}\gamma_\mu\gamma_5 q. \end{aligned} \tag{2.46}$$

The nonzero masses of the light quarks in the QCD Lagrangian result in explicit non-vanishing divergences of the currents V^a_μ, A^a_μ and A_μ. As a consequence, the corresponding charges are no longer

time-independent in general. The quark mass term in $\mathcal{L}_{\rm QCD}$ is $\bar{q}M_q q = \bar{q}_R M_q q_L + \bar{q}_L M_q q_R$, where the quark mass matrix can be written as

$$M_q = \begin{pmatrix} m_u & 0 & 0 \\ 0 & m_d & 0 \\ 0 & 0 & \ddots \end{pmatrix}. \tag{2.47}$$

The existence of the mass term spoils the conservation of the charges, applying the equation of motion of QCD, the corresponding divergences read

$$\begin{aligned} \partial^\mu V^a_\mu &= i\bar{q}[M_q, t^a]q, \\ \partial^\mu A^a_\mu &= i\bar{q}\{t^a, M_q\}\gamma_5 q, \\ \partial^\mu V_\mu &= 0, \\ \partial^\mu A_\mu &= 2i\bar{q}M_q\gamma_5 q. \end{aligned} \tag{2.48}$$

The axial anomaly has not been taken into account in this section.

2.2.3 The fate of symmetries

Depending on the dynamics of the theory, symmetries of the Lagrangian can be manifested physically in different ways. Since the $U_A(1)$ symmetry is spoiled at the quantum level, the so-called $U_A(1)$ anomaly, the QCD Lagrangian possesses a $SU_L(N_f) \times SU_R(N_f) \times U_V(1)$ symmetry in the chiral limit in which the masses of light quarks are set to zero. From the symmetry consideration, one would naively expect that the hadrons consisted of light quarks organize themselves in approximately degenerate multiplets of irreducible representations of the symmetry group. The $U_V(1)$ symmetry results in the conservation of baryon number and provides a classification of hadrons into mesons and baryons. The conserved charge operators Q^a_V and Q^a_A have opposite parity, and they commute with the Hamiltonian $H^0_{\rm QCD}$. For each state of positive parity, one might expect the existence of a degenerated state of negative parity. Let $|+\rangle$ be an eigenstate of $H^0_{\rm QCD}$ with eigenvalue E and having positive parity,

$$H^0_{\rm QCD}|+\rangle = E|+\rangle, \quad P|+\rangle = +|+\rangle. \tag{2.49}$$

Defining $|\psi\rangle = Q^a_A|+\rangle$, one has[3]

$$H^0_{\rm QCD}|\psi\rangle = H^0_{\rm QCD}Q^a_A|+\rangle = Q^a_A H^0_{\rm QCD}|+\rangle = EQ^a_A|+\rangle = E|\psi\rangle. \tag{2.50}$$

As a consequence, the state $|\psi\rangle$ is also an eigenstate of $H^0_{\rm QCD}$ with eigenvalue E but with opposite parity,

$$P|\psi\rangle = PQ^a_A P^{-1}P|+\rangle = -|\psi\rangle. \tag{2.51}$$

However, such a parity doubling is not realized at the low-energy spectrum of baryons. The above discussions are based on an assumption that the ground state of QCD is annihilated by Q^a_A. Only in this case,

$$Q^a_A|+\rangle = Q^a_A a^\dagger|0\rangle = ([Q^a_A, a^\dagger] + a^\dagger Q^a_A)|0\rangle = |\psi\rangle, \tag{2.52}$$

[3] Of course, such a state is strictly speaking, not defined. One has to work in a finite volume and then let $V \to \infty$. We ignore this complication here.

where we have used the relation $[Q_A^a, a^\dagger] = -t^a b^\dagger$, which acting on $|0\rangle$ would produce $|\psi\rangle$. If the ground state is not annihilated by Q_A^a, the last equality Eq. (2.52) breaks down and the parity doubling would not show up. In fact, the $SU_A(N_f)$ symmetry exhibits itself as the emergence of the Goldstone bosons through spontaneous breaking of symmetry. And the $SU_V(N_f)$ expresses itself through the approximate degeneracy of multiplets of irreducible representations.

Due to the absence of the parity doubling for the low-lying states, it is assumed that the Q_A^a do not annihilate the QCD ground state, i.e. $Q_A^a|0\rangle \neq 0$, which means the ground state is not invariant under axial transformations. The symmetry is called 'hidden' if it is an invariance of the Lagrangian but not of the ground state. And thus one does not see the symmetry in the spectrum of states. This can be achieved by two different mechanisms. The first one is by acquiring vacuum expectation values for scalar fields, e.g. the Higgs fields for the breaking of $SU_L^{EW}(2)$ symmetry in the electroweak interactions. The second one is caused by a dynamical mechanism, e.g. acquiring vacuum expectation values of the quark condensate in QCD. The broken symmetries are not really broken, they are rather realized in a special way, generating Nambu-Goldstone bosons or generating masses for the Higgs particles. This can be stated formally by the Nambu-Goldstone theorem: when a generic continuous symmetry is spontaneously broken, i.e. its currents are conserved but the ground state is not invariant under the action of the corresponding charges, then new massless scalar particles appear in the spectrum of possible excitations, the so-called Nambu-Goldstone bosons or just Goldstone bosons for simplicity. It is physically intuitive since one can relate two different states by an energy costless 'dynamical' action, corresponding to a long-wavelength fluctuation or massless mediation boson. If, instead, the symmetry is not exact, i.e. if it is explicitly broken as well as spontaneously broken, then the Goldstone bosons are not exactly massless, though they typically remain relatively light. They are sometimes called pseudo-Goldstone bosons. In general we do not distinguish the Goldstone bosons and pseudo-Goldstone bosons.

The fact is that in the chiral limit, the QCD Lagrangian possesses the symmetry $SU_L(N_f) \times SU_R(N_f) \times U_V(1)$, while the physical QCD vacuum has symmetry $SU_V(N_f) \times U_V(1)$. The $U_V(1)$ leads to the baryon number conservation, while the $SU_L(N_f) \times SU_V(N_f)$ is spontaneously broken to the subgroup $SU_V(N_f)$, and $N_f^2 - 1$ Goldstone bosons emerge.

2.2.4 The CCWZ formalism

The general formalism for effective Lagrangians with spontaneously broken symmetries has been worked out by Callan, Coleman, Wess, and Zumino [40, 41], the CCWZ formalism. Consider a theory in which the Lagrangian possesses a global symmetry G, while the vacuum has the symmetry H which is a subgroup of G, i.e. the symmetry G is spontaneously broken down to its subgroup H. Then the vacuum manifold is the coset space G/H.

Let G be a compact, connected, semisimple Lie group with n dimensions and H be a continuous subgroup of G. We denote with T_a the generators of H and with X_b the remaining generators chosen such that T_a and X_b form a complete basis of generators of G, orthonormal to each other. In some neighborhood of the identity of G, the group elements $g \in G$ can be decomposed uniquely into

$$g = e^{iX_b\xi_b} e^{iT_a\theta_a}, \tag{2.53}$$

where ξ_b and θ_a are real parameters. For any element $g \in G$ one has

$$g e^{iX_b\xi_b} = g' = e^{iX_b\xi'_b} e^{iT_a\theta'_a}, \tag{2.54}$$

where $\xi' = \xi'(\xi, g)$ and $\theta' = \theta'(\theta, g)$. Furthermore, let

$$h: \quad \psi \to D(h)\psi, \tag{2.55}$$

with $h \in H$, be a linear representation of the subgroup H, the transformations

$$g: \quad \xi \to \xi', \quad \psi \to D(e^{iT_a\theta'_a})\psi \tag{2.56}$$

give a nonlinear realization of the group G. It worth mentioning that there is a special case in which the transformation of ξ can be much simplified. Introducing an automorphism $R: g \to R(g)$ such that

$$\begin{aligned} T_a &\to T_a, \\ X_b &\to -X_b. \end{aligned} \tag{2.57}$$

Applying R to Eq. (2.54), one obtains

$$R(g)e^{-iX_b\xi_b} = e^{-iX'_b\xi'_b}e^{iT_a\theta'_a}. \tag{2.58}$$

Then the $e^{iT_a\theta'_a}$ can be eliminated by Eqs. (2.54) and (2.58) with a simplified result

$$ge^{2iX_b\xi_b}R(g^{-1}) = e^{2iX_b\xi'_b}. \tag{2.59}$$

The result is very useful for the chiral group since the parity operator induces an automorphism which changes the sign of the axial generators.

Let $\Xi(x) \in G$ be the transformation that transforms the standard vacuum to the local field configuration

$$\phi(x) = \Xi(x)|0\rangle.$$

where $|0\rangle$ is the vacuum state. The transformation $\Xi(x)$ is not unique: $\Xi(x)h(x)$, with $h \in H$, gives the same field configuration $\phi(x)$. The CCWZ formalism is to pick up the broken generators X_b and choose

$$\Xi(x) = e^{iX_b\xi_b(x)}. \tag{2.60}$$

Under a global symmetry transformation $g \in G$, the field configuration $\phi(x)$ is transformed to $g\phi(x)$, which induces the transformation of Ξ: $\Xi(x) \to g\Xi(x)$. The new transformation $g\Xi(x)$ is no longer in the form of Eq. (2.60), rather has the form of (2.54)

$$g\Xi(x) = \Xi'(x)h(x), \tag{2.61}$$

where $g\Xi$ and Ξ' describe the same field configuration differ by an $h \in H$ transformation. The transformation h is non-trivial since it depends on the both g and $\Xi(x)$, see Eq. (2.54). The transformation law of the Goldstone boson field Eq. (2.61) can be written as

$$\Xi(x) \to g\Xi(x)h^{-1}(g, \Xi(x)). \tag{2.62}$$

Any other choice of the realization gives the same results for physical observables, with different off-shell Green functions.

2.2.5 Chiral effective theory

The QCD Lagrangian with external sources can be written as

$$\mathcal{L}_{QCD} = \mathcal{L}^0_{QCD} + \bar{q}\gamma^\mu(v_\mu + a_\mu)q - \bar{q}(s - ip\gamma_5)q, \tag{2.63}$$

where the external sources $v_\mu(x)$, $a_\mu(x)$, $s(x)$, and $p(x)$ are hermitian, color neutral matrices in flavor space. Note that the quark mass term is included in $s(x)$, the QCD Lagrangian Eq. (2.33) can be recovered by setting $s(x) = M_q$ with the other sources vanishing. With the external sources, the global chiral symmetry $SU_L(N_f) \times SU_R(N_f)$ can be extended to a local chiral symmetry. The Lagrangian QCD (2.63) is invariant under independent local transformations

$$q_L(x) \to g_L(x)q_L(x), \quad q_R(x) \to g_R(x)q_R(x), \tag{2.64}$$

which leads to the transformations of the external sources:

$$\begin{aligned} \mathcal{M} \equiv (s + ip) &\to g_R(s + ip)g_L, \\ r_\mu \equiv v_\mu + a_\mu &\to g_R r_\mu g_R^\dagger - i\partial_\mu g_R g_R^\dagger, \\ \ell_\mu \equiv v_\mu - a_\mu &\to g_L \ell_\mu g_L^\dagger - i\partial_\mu g_L g_L^\dagger. \end{aligned} \tag{2.65}$$

For $N_f = 3$, the couplings of photons to quarks are described by the term

$$eA_\mu \bar{q} Q \gamma^\mu q = eA_\mu(\bar{q}_L Q_L \gamma^\mu q_L + \bar{q}_R Q_R \gamma^\mu q_R), \tag{2.66}$$

where A_μ is the photon field and

$$Q_L = Q_R = Q = \begin{pmatrix} 2/3 & 0 & 0 \\ 0 & 1/3 & 0 \\ 0 & 0 & 1/3 \end{pmatrix}.$$

Therefore, the interaction Eq. (2.66) can be included by setting

$$\ell_\mu = eA_\mu Q, \quad r_\mu = eA_\mu Q. \tag{2.67}$$

Likewise, the couplings of quarks to $W^\pm_\mu$ bosons can be included in a similar way by changing

$$\ell_\mu \to -\frac{e}{\sqrt{2} sin\theta_W}(W^+_\mu T_+ + \text{h.c.}), \tag{2.68}$$

where θ_W is the Weiberg angle, V_{ij} are Kobayashi-Maskawa mixing matrix elements and

$$T_+ = \begin{pmatrix} 0 & V_{ud} & V_{us} \\ 0 & 0 & 0 \\ 0 & 0 & 0 \end{pmatrix}. \tag{2.69}$$

It has already been argued that the chiral symmetry of QCD is not realized in the hadronic spectrum. We thus expect that the symmetry to be realized through the spontaneous breaking and the emergence of Goldstone modes. If we look at the low-lying hadronic spectrum, there exist natural candidates for this, or exactly pseudo-Goldstone bosons. The three pions correspond to the three Goldstone bosons for $N_f = 2$, and with four kaons and one eta correspond to the case of $N_f = 3$. The breaking of the chiral

symmetry is rather an empirical result which has not been proven analytically though lattice results exist.

The chiral symmetry of QCD $SU_L(N_f) \times SU_R(N_f)$ is spontaneously broken to the vector subgroup $SU_V(N_f)$ by the quark condensate $\langle \bar{q}q \rangle$. The Goldstone boson manifold is the coset space $SU_L(N_f) \times SU_N(N_f)/SU_V(N_f)$, which is isomorphic to $SU(N_f)$. There are two commonly used bases to realize the broken chiral symmetry of QCD, the u-basis and the U-basis.

The U-basis

The unbroken generators of H and the broken generators X span the space of the generators of G. Let T_L^a and T_R^a be the generators of G and act only on left- and right-handed quarks respectively. Then the unbroken generators are $T^a = T_L^a + T_R^a$, and the broken generators are $X^a = T_L^a - T_R^a$. We write the elements $g \in G$ in the form of

$$g = \begin{pmatrix} g_L & 0 \\ 0 & g_R \end{pmatrix}. \tag{2.70}$$

The automorphism R in Eq. (2.59) maps g^{-1} as

$$R(g^{-1}) = \begin{pmatrix} g_R^{-1} & 0 \\ 0 & g_L^{-1} \end{pmatrix}. \tag{2.71}$$

The nonlinear realization $e^{2iX_b\xi_b}$ is chosen to have the form

$$\exp 2i \begin{pmatrix} T_a\xi_a & 0 \\ 0 & -T_a\xi_a \end{pmatrix} = \begin{pmatrix} U(x) & 0 \\ 0 & U^{-1}(x) \end{pmatrix}. \tag{2.72}$$

The transformation Eq. (2.59) gives

$$U(x) \to g_L U(x) g_R^{-1}. \tag{2.73}$$

The u-basis

The unbroken transformation have the form of Eq. (2.70) with $g_L = g_R = h$

$$\begin{pmatrix} h & 0 \\ 0 & h \end{pmatrix}. \tag{2.74}$$

The nonlinear realization $e^{iX_b\xi_b}$ in Eq. (2.54), i.e. $\xi(x)$ in Eq. (2.62), has the form of

$$\xi(x) = \begin{pmatrix} u(x) & 0 \\ 0 & u^{-1}(x) \end{pmatrix}. \tag{2.75}$$

Then the Eq. (2.54) (or 2.62) gives the transformation law for $u(x)$,

$$u(x) \to g_L u(x) h^{-1}(x) = h(x) u(x) g_R^{-1}, \tag{2.76}$$

where $h(x)$ is dependent on g_L, g_R and $u(x)$.

Comparing Eq. (2.54) with Eq. (2.59), one sees that

$$U(x) = u^2(x). \tag{2.77}$$

Power counting

To construct an effective theory, the next step is to specify the power counting rules. At sufficiently low energies, it follows from the dimensional analysis that the coefficient of an operator with n derivatives behaves as $(p/\Lambda_\chi)^n$, where p denotes the momenta of Goldstone fields and Λ_χ is the mass scale of the chiral symmetry breaking. As a consequences, each derivative acting on Goldstone fields are counted as $O(p)$. The inclusion of external sources and their transformation properties require the derivative on $U(x)$ to be replaced by a covariant derivative

$$\partial_\mu U \to D_\mu U = \partial_\mu U - i r_\mu U + i U \ell_\mu, \tag{2.78}$$

such that the transformation of $D_\mu U$ under a $g \in G$ is

$$D_\mu U \to g_L D_\mu U g_R^{-1}. \tag{2.79}$$

The associated field strength tensors read

$$\begin{aligned} F_L^{\mu\nu} &= \partial^\mu r^\nu - \partial^\nu r^\mu - i[r^\mu, r^\nu], \\ F_R^{\mu\nu} &= \partial^\mu \ell^\nu - \partial^\nu \ell^\mu - i[\ell^\mu, \ell^\nu]. \end{aligned} \tag{2.80}$$

The covariant derivate D_μ requires that the external sources r^μ and ℓ^μ are counted as ∂^μ, i.e. $O(p)$.

In QCD Lagrangian Eq. (2.33), the quark mass term breaks the $SU_L(N_f) \times SU_R(N_f)$ explicitly, which leads to the 'small' masses of the Goldstone bosons. It is easy to incorporate the quark mass term into the theory by setting the scalar source $s = M_q$. However, M_q is a constant matrix and does not transform under $SU_L(N_f) \times SU_R(N_f)$, so the quark mass term breaks the symmetry explicitly. In principle, one can organize the effective Lagrangian in an independent expansion in both derivatives and quark masses. It is convenient to combine these two expansion in a single one by using the relations between meson and quark masses. The standard ChPT is defined by a simple choice of the counting rule for scalar and pseudoscalar sources, $s, p \sim O(p^2)$. The chiral counting rules read

$$\begin{aligned} U &\sim O(p^0), \\ D_\mu U, r_\mu, \ell_\mu &\sim O(p), \\ F_{L,R}^{\mu\nu}, s, p &\sim O(p^2). \end{aligned} \tag{2.81}$$

Chiral effective Lagrangian

Note also that the QCD Lagrangian is invariant under a parity transformation, under which the fields take the form

$$\begin{aligned} U &\leftrightarrow U^\dagger, \\ \ell^\mu &\leftrightarrow r^\mu, \\ s &\leftrightarrow s, \\ p &\leftrightarrow -p. \end{aligned} \tag{2.82}$$

The invariance should be considered in the construction of the effective Lagrangians.

It is expected that the leading effective Lagrangian should be free of derivatives, order of 1. However, according to the transformation law for $U(x)$, i.e. Eq. (2.73), the only possible operator which is invariant

under the transformation g is $\langle U^\dagger U\rangle$, which is only an irrelevant constant, with $\langle \dots \rangle$ denoting the trace in flavor space. There are no odd-power terms due to the Lorentz invariance. The nontrivial leading order Lagrangian then has the form

$$\begin{aligned}\mathcal{L}_2 &= \alpha_1\langle D_\mu U D^\mu U^\dagger\rangle + \alpha_2\langle (s+ip)U^\dagger + U(s+ip)^\dagger\rangle \\ &\quad + i\alpha_3\langle (s-ip)U^\dagger - U(s+ip)^\dagger\rangle,\end{aligned} \tag{2.83}$$

where the term proportional to α_3 violates parity and thus can be dropped.

Now we consider the chiral effective Lagrangian of QCD in detail. The nonlinear realization $U(x)$ of the Goldstone fields is commonly written in the form

$$U(x) = \exp\Big(i\frac{\phi(x)}{F_0}\Big), \tag{2.84}$$

where

$$\phi(x) = \sum_{i=1}^{3}\tau_i\phi_i(x) = \begin{pmatrix}\phi_3 & \phi_1 - i\phi_2\\ \phi_1 + i\phi_2 & -\phi_3\end{pmatrix} = \begin{pmatrix}\pi^0 & \sqrt{2}\pi^+\\ \sqrt{2}\pi^- & -\pi^0\end{pmatrix}, \tag{2.85}$$

and

$$\begin{aligned}\phi(x) = \sum_{a=1}^{8}\lambda_a\phi_a(x) &= \begin{pmatrix}\phi_3 + \frac{1}{\sqrt{3}}\phi_8 & \phi_1 - i\phi_2 & \phi_4 - i\phi_5\\ \phi_1 + i\phi_2 & -\phi_3 + \frac{1}{\sqrt{3}}\phi_8 & \phi_6 - i\phi_7\\ \phi_4 + i\phi_5 & \phi_6 + i\phi_7 & -\frac{2}{\sqrt{3}}\phi_8\end{pmatrix} \\ &= \begin{pmatrix}\pi^0 + \frac{1}{\sqrt{3}}\eta & \sqrt{2}\pi^+ & \sqrt{2}K^+\\ \sqrt{2}\pi^- & -\pi^0 + \frac{1}{\sqrt{3}}\eta & \sqrt{2}K^0\\ \sqrt{2}K^- & \sqrt{2}\bar{K}^0 & -\frac{2}{\sqrt{3}}\eta\end{pmatrix},\end{aligned} \tag{2.86}$$

for $N_f = 2$ and $N_f = 3$, respectively. Here, the τ_i and λ_a are the usual Pauli and Gell-Mann matrices, F_0 is a constant and turns out to be the meson decay constant in the chiral limit. The Lagrangian Eq. (2.83) is usually written in the form

$$\mathcal{L}_2 = \frac{F_0^2}{4}\langle D_\mu U D^\mu U^\dagger\rangle + \frac{F_0^2}{4}\langle \chi U^\dagger + U\chi^\dagger\rangle, \tag{2.87}$$

where

$$\chi = 2B_0 M_q, \tag{2.88}$$

with B_0 a constant related to the quark condensate. The second term corresponds to the explicit symmetry breaking term due to the nonvanishing quark masses. To determine the constant F_0, we recall that the pion decay constant is defined by

$$\langle 0|\bar{d}\gamma_\mu\gamma_5 u|\pi^+(p)\rangle = i\frac{F_\pi}{\sqrt{2}}p_\mu. \tag{2.89}$$

We can calculate the matrix-element Eq. (2.89) by taking a functional derivative with respect to a_μ. At

the lowest order ($O(p^2)$), one gets

$$F_0 = F_\pi. \tag{2.90}$$

To determine the constant B_0, we calculate the vacuum expectation value of $\mathcal{L}_2$, i.e. $U = U^\dagger = 1$,

$$\langle \mathcal{L}_2 \rangle = B_0 F_0^2 \sum_{f=1}^{N_f} m_f. \tag{2.91}$$

Comparing with in QCD,

$$\frac{\partial \langle \mathcal{L}_{QCD} \rangle}{\partial m_f} = -\frac{1}{N_f} \langle \bar{q} q \rangle \tag{2.92}$$

with $\langle \bar{q} q \rangle = \sum_{f=1}^{N_f} \langle \bar{q}_f q_f \rangle$, one finds

$$B_0 = -\frac{1}{N_f F_0^2} \langle \bar{q} q \rangle. \tag{2.93}$$

In chiral limit, the flavor symmetry implies that $\langle \bar{q}_f q_f \rangle$ is independent of flavor and thus $B_0 = -\frac{1}{F_0^2} \langle \bar{q}_f q_f \rangle$.

For the sake of simplicity, we will consider the $N_f = 3$ case from now on. Inserting Eq. (2.86) into the Lagrangian $\mathcal{L}_2$, one has the mass term

$$\begin{aligned} \mathcal{L}_{2,\text{mass}} &= -B_0(m_u + m_d)\pi^+\pi^- - B_0(m_u + m_s)K^+K^- + B_0(m_d + m_s)K^0\bar{K}^0 \\ &- \frac{1}{2}B_0\pi^0\pi^0 + \frac{1}{\sqrt{3}}B_0(m_u - m_d)\pi^0\eta + \frac{1}{6}B_0(m_u + m_d + 4m_s)\eta\eta. \end{aligned} \tag{2.94}$$

In the isospin-symmetric limit $m_u = m_d = \hat{m}$, the $\pi^0\eta$ mixing term vanishes and we obtain the masses of the Goldstone bosons (to $O(p^2)$),

$$\begin{aligned} M_\pi^2 &= 2B_0\hat{m}, \\ M_K^2 &= B_0(\hat{m} + m_s), \\ M_\eta^2 &= \frac{2}{3}B_0(\hat{m} + 2m_s). \end{aligned} \tag{2.95}$$

The Eqs. (2.95) satisfy the well-known Gell-Mann-Okubo relation

$$4M_K^2 = 3M_\eta^2 + M_\pi^2. \tag{2.96}$$

The construction of the higher order Lagrangians is similar to the $\mathcal{L}_2$, one writes down the most general structure of the local operators satisfying the full symmetry of QCD at the given order. However, this procedure tends to end up with far too many terms, which are usually dependent on each other. One needs to eliminate the non independent operators and finds a minimal but still complete set of operators. The equations of emotion of lower orders and some identities, like e.g. Cayley-Hamilton theorem, are usually used to eliminate the redundant operators. The operators having the form of $O_{\text{EOM}} \times O'$ can be eliminated by redefinition of the fields, and thus can be dropped. Here, O_{EOM} is the equation of emotion derived at lower orders. The Cayley-Hamilton theorem states that every square matrix over a commutative ring

satisfies its own characteristic equation. The details in constructing higher order Lagrangians can be found in Refs. [15, 36, 58, 59]. The Lagrangian for $SU(N_f)$ at $O(p^4)$ has the form of

$$\begin{aligned}
\mathcal{L}_4 &= L_0\langle D^\mu U^\dagger D^\nu U D_\mu U^\dagger D_\nu U\rangle \\
&\quad + L_1\langle D_\mu U^\dagger D^\mu U\rangle^2 + L_2\langle D_\mu U^\dagger D_\nu U\rangle\langle D^\mu U^\dagger D^\nu U\rangle \\
&\quad + L_3\langle D_\mu U^\dagger D^\mu U D_\nu U^\dagger D^\nu U\rangle + L_4\langle D_\mu U^\dagger D^\mu U^\dagger\rangle\langle\chi^\dagger U + \chi U^\dagger\rangle \\
&\quad + L_5\langle D_\mu U^\dagger D^\mu U(\chi^\dagger U + U^\dagger\chi)\rangle \\
&\quad + L_6\langle\chi^\dagger U + \chi U^\dagger\rangle^2 + L_7\langle\chi^\dagger U - \chi U^\dagger\rangle \\
&\quad + L_8\langle\chi^\dagger U\chi^\dagger U + \chi U^\dagger\chi U^\dagger\rangle \\
&\quad - iL_9\langle F_R^{\mu\nu} D_\mu U D_\nu U^\dagger + F_{\mu\nu}^L D_\mu U^\dagger D_\nu U\rangle + L_{10}\langle U^\dagger F_R^{\mu\nu} U F_{L\mu\nu}\rangle \\
&\quad + H_1\langle F_{R\mu\nu}F_R^{\mu\nu} + F_{L\mu\nu}F_L^{\mu\nu}\rangle + H_2\langle\chi^\dagger\chi\rangle,
\end{aligned} \tag{2.97}$$

where the coefficients L_i are called low-energy constants (LECs) in ChPT. The terms proportional to H_i are contact terms which contain external fields only. They are not relevant for low-energy phenomenology, but they are necessary for the computation of operator expectation values.

At above the chiral effective Lagrangians are constructed on the U-basis. The Lagrangians can also be constructed in the u-basis. One defines

$$u_\mu = i\{u^\dagger(\partial_\mu - ir_\mu)u - u(\partial_\mu - i\ell_\mu)u^\dagger\}, \tag{2.98}$$

which transforms under $SU_L(N_f)\times SU_R(N_f)$ as

$$u_\mu \to h u_\mu h^\dagger. \tag{2.99}$$

The external sources χ and field strength tensor $F_{L,R}^{\mu\nu}$ are combined with the Goldstone field u to form the new quantities

$$\begin{aligned}
\chi_\pm &= u^\dagger\chi u^\dagger \pm u\chi^\dagger u, \\
f_\pm^{\mu\nu} &= uF_L^{\mu\nu}u^\dagger \pm u^\dagger F_R^{\mu\nu}u,
\end{aligned} \tag{2.100}$$

such that their transformation laws satisfy

$$\begin{aligned}
\chi_\pm &\to h\chi_\pm h^\dagger, \\
f_\pm^{\mu\nu} &\to h f_\pm^{\mu\nu} h^\dagger.
\end{aligned} \tag{2.101}$$

For the objects transforming as $u_\mu, \chi_\pm$, and $f_\pm^{\mu\nu}$, collectively denoted as X, a covariant derivative can be defined as

$$\nabla_\mu X = \partial_\mu X + [\Gamma_\mu, X], \tag{2.102}$$

where the connection Γ_μ is defined as

$$\Gamma_\mu = \frac{i}{2}\{u^\dagger(\partial_\mu - ir_\mu)u + u(\partial_\mu - i\ell_\mu)u^\dagger\}. \tag{2.103}$$

It is easy to show that $\nabla_\mu X$ transforms as X as well. One useful relation which can be derived from the

Operator	P	C	h.c.	Chiral order
ϕ	$-\phi$	ϕ^T	ϕ	1
U	$U^\dagger$	U^T	$U^\dagger$	1
$D_\mu U$	$(D^\mu U)^\dagger$	$(D_\mu U)^T$	$(D_\mu U)^\dagger$	p
r_μ	ℓ^μ	$-\ell_\mu^T$	r_μ	p
ℓ_μ	r^μ	$-r_\mu^T$	ℓ_μ	p
χ	$\chi^\dagger$	χ^T	$\chi^\dagger$	p^2
$F_{L,R}^{\mu\nu}$	$F_{L,R\mu\nu}$	$-F_{L,R}^{\mu\nu T}$	$F_{R,L}^{\mu\nu}$	p^2

Table 2.1: The transformations and chiral orders of the building blocks in the U-basis

definition of the covariant derivative and u_μ is

$$f_-^{\mu\nu} = -(\nabla^\mu u^\nu - \nabla^\nu u^\mu). \tag{2.104}$$

In the u-basis, the leading and next-to-leading order Lagrangian can be written as

$$\begin{aligned}
\mathcal{L}_2 &= \frac{F_0^2}{2}\langle u_\mu u^\mu + \chi_+\rangle, \\
\mathcal{L}_4 &= L_0\langle u^\mu u^\nu u_\mu u_\nu\rangle + L_1\langle u_\mu u^\mu\rangle^2 + L_2\langle u_\mu u^\nu\rangle\langle u^\mu u_\nu\rangle \\
&\quad + L_3\langle u_\mu u^\mu u_\nu u^\nu\rangle + L_4\langle u_\mu u^\mu\rangle\langle\chi_+\rangle \\
&\quad + L_5\langle u_\mu u^\mu\chi_+\rangle + L_6\langle\chi_+\rangle^2 + L_7\langle\chi_-\rangle^2 \\
&\quad + \frac{L_8}{2}\langle\chi_+^2 + \chi_-^2\rangle - iL_9\langle f_+^{\mu\nu}u_\mu u_\nu\rangle \\
&\quad + \frac{L_{10}}{4}\langle f_{+\mu\nu}f_+^{\mu\nu} - f_{-\mu\nu}f_-^{\mu\nu}\rangle \\
&\quad + \frac{H_1}{2}\langle f_{+\mu\nu}f_+^{\mu\nu} + f_{-\mu\nu}f_-^{\mu\nu}\rangle + \frac{H_2}{4}\langle\chi_+^2 - \chi_-^2\rangle.
\end{aligned} \tag{2.105}$$

At the next-to-next-to-leading order, the number of operators increases rapidly, e.g. over 100 in the $SU(3)$ case. However, the construction of them are the same. For convenience, we list the transformation law of the building blocks in the U- and u- bases under chiral symmetry and C, P parity, as well as their chiral orders in Table. 2.1 and 2.2.

Finally, the power counting $\chi \sim O(p^2)$ leads to the counting of the masses of Goldstone bosons M_ϕ as $M_\phi^2 \sim p^2$, which ensures that the Weinberg's power counting scheme in Sec. 2.1.1 can be applied to ChPT perfectly. Weinberg's power counting scheme makes a systematic expansion in the chiral order/dimension and loops possible.

2.3 Anomalies

2.3.1 The $U_A(1)$ anomaly

Thus far, we have ignored the $U_A(1)$ anomaly at the quantum level. The massless QCD Lagrangian has a chiral symmetry $SU_L(N_f) \times SU_R(N_f) \times U_V(1) \times U_A(1)$ at the classical level. The classically conserved

Operator	P	C	h.c.	Chiral order
u	$u^\dagger$	u^T	$u^\dagger$	1
Γ_μ	Γ^μ	$-\Gamma_\mu^T$	$-\Gamma_\mu$	p
u_μ	$-u^\mu$	u_μ^T	u_μ	p
$\chi_\pm$	$\pm\chi_\pm$	$\chi_\pm^T$	$\pm\chi_\pm$	p^2
$f_{\pm\mu\nu}$	$\pm f_\pm^{\mu\nu}$	$\mp f_{\pm\mu\nu}^T$	$f_{\pm\mu\nu}$	p^2
$h_{\mu\nu}$	$-h^{\mu\nu}$	$h_{\mu\nu}^T$	$h_{\mu\nu}$	p^2

Table 2.2: The transformations and chiral orders of the building blocks in the u-basis

axial current is

$$A_\mu = \bar{q}\gamma_\mu\gamma_5 q, \quad \partial^\mu A_\mu = 0. \tag{2.106}$$

However, we will see that the $U_A(1)$ is no longer a symmetry for the full quantum theory such that the divergence has an anomaly

$$\partial^\mu A_\mu = \frac{N_f}{8\pi}\alpha_s \epsilon^{\mu\nu\alpha\beta} F^a_{\mu\nu} F^a_{\alpha\beta}. \tag{2.107}$$

In a path integral treatment [60], the symmetries of a theory can be investigated by considering the generating functional. Considering an infinitesimal symmetry transformation

$$\varphi \to \varphi' = \varphi + \epsilon f(\varphi), \tag{2.108}$$

one has

$$\mathcal{L}(\varphi') = \mathcal{L}(\varphi) + J^\mu \partial_\mu \epsilon. \tag{2.109}$$

If ϵ is a constant, the Lagrangian is invariant under the transformation. Considering a generating functional

$$W[v_\mu] = \int [d\varphi] \exp\Big[i \int d^4x (\mathcal{L} - v_\mu J^\mu)\Big], \tag{2.110}$$

the matrix elements involving J_μ can be obtained by the functional derivative with respect to v^μ,

$$J_\mu(x) = i\frac{\delta}{\delta v_\mu(x)} \ln W[v_\nu]. \tag{2.111}$$

Rewriting Eq. (2.111) as

$$\delta \ln W[v_\mu] = \ln W[v_\mu + \delta v_\mu] - \ln W[v_\mu] = -i \int d^4x J^\mu \delta v_\mu, \tag{2.112}$$

let $\delta v_\mu = -\partial_\mu \epsilon$ one has

$$\delta \ln W[v_\mu] = \ln W[v_\mu - \partial_\mu \epsilon] - \ln W[v_\mu] = -i \int d^4x \epsilon(x) \partial^\mu J_\mu. \tag{2.113}$$

Considering

$$W[v_\mu - \partial_\mu \epsilon] = \int [d\varphi] \exp i \int d^4x (\mathcal{L}(\varphi) - (v_\mu - \partial_\mu \epsilon) J^\mu), \tag{2.114}$$

if we change the integration variables,

$$\int [d\varphi] = \int [d\varphi'] \mathcal{J}, \tag{2.115}$$

with $\mathcal{J}$ the Jacobian, combining with Eq. (2.109), one obtains

$$W[v_\mu - \partial_\mu \epsilon] = \int [d\varphi'] \mathcal{J} \exp i \int d^4x (\mathcal{L}(\varphi') + v_\mu J^\mu) = W[v_\mu] \mathcal{J}. \tag{2.116}$$

In the last equality we assume that the Jacobian $\mathcal{J}$ is independent of the integrated fields. If the path integral measure is invariant under the transformation (2.108), one has $\mathcal{J} = 1$ and thus

$$\partial_\mu J^\mu = 0. \tag{2.117}$$

What happens in the $U_A(1)$ anomaly is that the $U_A(1)$ transformation changes the path integral measure. For a function of Grassmann variables (z_1, z_2), the Jacobian is defined via

$$\int dz_1 dz_2 f(z) = \mathcal{J} \int dz_1' dz_2' f(\mathbf{C} z'), \tag{2.118}$$

where $\mathcal{J} = [\det \mathbf{C}]^{-1}$. The accompanying Jacobian $\mathcal{J}$ with the transformation $\psi \to \psi' = e^{-i\epsilon\gamma_5}\psi$ and $\bar{\psi} \to \bar{\psi}' = e^{-i\epsilon\gamma_5}\bar{\psi}$ is

$$\mathcal{J} = [\det(e^{i\epsilon\gamma_5})]^{-1} [\det(e^{i\epsilon\gamma_5})]^{-1}, \tag{2.119}$$

where the determinant runs over the spinor, flavor, color and spacetime indices. Making use of $\det \mathbf{C} = e^{\mathrm{tr} \ln \mathbf{C}}$ with tr denoting the trace over the full spanned space, we write

$$\mathcal{J} = e^{-2i\mathrm{tr}(\epsilon\gamma_5)}. \tag{2.120}$$

The Jacobian is ill-defined and can be regularized via

$$\mathcal{J} = \lim_{M\to\infty} \exp\Big[-2i\mathrm{tr}\epsilon(x)\gamma_5 e^{-(\not{D}/M)^2} \Big], \tag{2.121}$$

with D_μ the QCD covariant derivative. It can be evaluated via

$$\begin{aligned} & \lim_{M\to\infty} \mathrm{tr}\gamma_5 e^{-(\not{D}/M)^2} \\ = & \lim_{M\to\infty} \lim_{y\to x} \int \frac{d^4k}{(2\pi)^4} \mathrm{tr}'\Big(\gamma_5 e^{-(\not{D}/M)^2}\Big) e^{ik(x-y)} \\ = & \lim_{M\to\infty} \lim_{y\to x} \int \frac{d^4k}{(2\pi)^4} e^{ik(x-y)} \mathrm{tr}'\Big(\gamma_5 e^{-(i\not{k}+\not{D})^2/M^2}\Big). \end{aligned}$$

It can be further evaluated via

$$\begin{aligned}
&\lim_{M\to\infty}\int\frac{d^4k}{(2\pi)^4}\mathrm{tr}'\left(\gamma_5 e^{-(i\not{k}+\not{D})^2/M^2}\right)\\
=&\lim_{M\to\infty}M^4\int\frac{d^4l}{(2\pi)^4}\mathrm{tr}'\left(\gamma_5 e^{-(i\not{l}+\frac{\not{D}}{M})^2}\right)\\
=&\lim_{M\to\infty}M^4\int\frac{d^4l}{(2\pi)^4}\mathrm{tr}'\left(\gamma_5 e^{l^2-2il\cdot D/M-\not{D}^2/M^2}\right)\\
=&\frac{1}{2}\int\frac{d^4l}{(2\pi)^4}e^{l^2}\mathrm{tr}'(\gamma_5\not{D}^4)\\
=&\frac{g_s^2}{64\pi^2}N_f\epsilon^{\mu\nu\alpha\beta}F^a_{\mu\nu}F^a_{\alpha\beta},
\end{aligned}\tag{2.122}$$

where tr' denotes the full trace excluding the spacetime indices, and the following formulas are used

$$\int\frac{d^4l}{(2\pi)^4}e^{l^2}=i\int\frac{d^4l_E}{(2\pi)^4}e^{-l_E^2}=\frac{i}{16\pi^2},\tag{2.123}$$

and

$$\not{D}^2=D^2+\frac{1}{4}[\gamma_\mu,\gamma_\nu]ig_sF_{\mu\nu}.\tag{2.124}$$

Applying Eqs. (2.113) and (2.116), plus the explicit symmetry breaking quark mass term, it is easy to read off

$$\partial^\mu A_\mu=2i\bar{q}M_q\gamma_5 q+\frac{N_f}{8\pi}\alpha_s\epsilon^{\mu\nu\alpha\beta}F^a_{\mu\nu}F^a_{\alpha\beta}.\tag{2.125}$$

Quarks do not only carry color charges, but also electromagnetic charges. The anomaly function Eq. (2.125) is replaced by

$$\partial^\mu A_\mu=2i\bar{q}M_q\gamma_5 q+\frac{\alpha}{4\pi}N_c\epsilon^{\mu\nu\alpha\beta}F_{\mu\nu}F^{\alpha\beta}\langle Q^2t\rangle,\tag{2.126}$$

where $Q=\mathrm{diag}(2/3,-1/3,\dots)$ is the quark charge matrix, N_c is the number of colors, $t=\lambda^3$ or λ^8, depending on the number of flavors.

2.3.2 The Wess-Zumino-Witten action

It is easy to see that the Lagrangian $\mathcal{L}_2$ and $\mathcal{L}_4$ exhibit a larger symmetry than QCD. It is found that the chiral anomalies cannot be expressed as local effective Lagrangians. The two Lagrangians are invariant under the transformation $\phi(x)\leftrightarrow-\phi(x)$. They only contain the interactions involving an even number of Goldstone bosons, and it is impossible to be used to describe the reaction like $K^+K^-\to\pi^+\pi^-\pi^0$. Furthermore, the process $\pi^0\to\gamma\gamma$ cannot be described by $\mathcal{L}_2$ and $\mathcal{L}_4$.

Wess and Zumino worked out the consistency conditions which have to be satisfied in the presence of the anomalies in 1971 [61]. In case of spontaneous symmetry breaking $SU_L(N_f)\times SU_R(N_f)\to SU_V(N_f)$, the homotopy group is trivial and a smooth interpolating field between the 4-dimensional Minkowski

spacetime and a 5-dimensional sphere, B_5, can be established. The WZW action is written as

$$S = \int_{B_5} d^4x d\alpha \mathcal{L}(x,\alpha), \tag{2.127}$$

where the Lagrangian is G invariant and restricted by integrability conditions. Employing Poincaré's lemma, the action can be cast into a closed 5-form on G/H. The terms which cannot be reduced to 4-dimensional integrals can be obtained by the generators of the fifth de Rham cohomology group $H^5(G/H;\mathbf{R})$. The coset subgroup is a simple Lie group and H^5 has a single generator

$$\Omega = -\frac{i}{240\pi^2}\langle (U^{-1}dU)^5\rangle, \tag{2.128}$$

which is the Wess-Zumino-Witten term. In order to describe physical processes, external sources are included and the full action can be written in a compact n-forms as [62, 63]

$$S[U,\ell,r]_{WZW} = -\frac{i}{240\pi^2}N_c\int_{B_5}\langle\Sigma_L^5\rangle - \frac{i}{48\pi^2}N_c\int_{M_4}[W(U,\ell,r) - W(1,\ell,r)], \tag{2.129}$$

where

$$\begin{aligned} W(U,\ell,r) &= \langle U\ell^3U^\dagger r + \frac{1}{4}U\ell U^\dagger rU\ell U^\dagger r + iUd\ell\ell U^\dagger r + idrU\ell U^\dagger r \\ &\quad -i\Sigma_L\ell U^\dagger rU\ell + \Sigma U^\dagger drU\ell - \Sigma^2U^\dagger rU\ell + \Sigma\ell d\ell + \Sigma d\ell\ell \\ &\quad -i\Sigma\ell^3 + \frac{1}{2}\Sigma\ell\Sigma\ell - i\Sigma^3\ell\rangle - (R\leftrightarrow L), \end{aligned} \tag{2.130}$$

where $\Sigma_L = U^\dagger dU$, $\ell = dx^\mu\ell_\mu$, $r = dx^\mu r_\mu$ and $d = dx^\mu\partial_\mu$. The first term is an integral over the field $U(x,\alpha)$ that smoothly interpolates between $U(x,0) = 1$ and $U(x,1) = U(x)$. The integral in the second term is over the Minkowski space only.

2.4 Chiral perturbation theory for matter fields

So far we have considered the purely mesonic sector involving the self-interactions of Goldstone bosons and their interaction with external currents. ChPT can be extended to include matter fields, e.g. baryons, heavy mesons and etc., which transform as irreducible representation of $SU_V(N_f)$ instead of $SU_L(N_f)\times SU_R(N_f)$. Different from the Goldstone bosons, the matter fields have nonvanshing masses in the chiral limit, i.e. as $m_q \to 0$. While the matter fields are realized by a linear representation of the $SU_V(N_f)$, the transformation law under $SU_L(N_f)\times SU_R(N_f)$ is not fixed and can be described by the CCWZ formalism Eq. (2.56).

Since the masses of matter fields do not vanish in the chiral limit, denoted as $\mathring{m}$, the temporal component of the momenta of the matter fields do not correspond to a 'small' quantity. Therefore one has to assign a new power counting for the matter field sectors. At low energies when the three-momentum is small, one may count $k^2 - \mathring{m}^2$, with k the four-momentum, as $O(p)$. Expressed in the Lagrangian level, the chiral counting scheme for the elements of matter fields is

$$\psi \sim O(p^0), \quad \partial_\mu\psi \sim O(p^0), \quad (\partial_\mu\partial^\mu + \mathring{m}^2)\psi \sim O(p). \tag{2.131}$$

2.4.1 Chiral perturbation theory for baryons

The construction of ChPT for matter fields is straightforward by applying the CCWZ formalism. The transformation laws for the Goldstone fields and baryon fields (Ψ) read

$$u(x) \to g_L u(x) h^{-1}(x), \quad \Psi(x) \to h(x)\Psi(x), \tag{2.132}$$

for the $N_f = 2$ case, where the proton and neutron fields are collected in a doublet

$$\Psi(x) = \begin{pmatrix} p(x) \\ n(x) \end{pmatrix}. \tag{2.133}$$

The local character of the transformations implies that a connection Γ_μ needs to be introduced to compensate the transformation of $\partial_\mu h(x)$:

$$D_\mu \Psi(x) = (\partial_\mu + \Gamma_\mu)\Psi(x) \to h(x) D_\mu \Psi(x). \tag{2.134}$$

Here the connection is $\Gamma_\mu = \frac{1}{2}[u^\dagger(\partial_\mu - ir_\mu)u + u(\partial_\mu - i\ell_\mu)u^\dagger]$, as already introduced in Sec. 2.2.5.

For the spinor fields, the power counting scheme is a little subtle due to the bilinear $\bar{\Psi}\Gamma\Psi$, which can be understood by investigating the matrix elements of a positive energy plane-wave

$$\psi_p^+(x) = e^{-ip\cdot x}\sqrt{E_N + m_N}\begin{pmatrix} \chi \\ \frac{\vec{\sigma}\cdot\vec{p}}{E_N + m_N}\chi \end{pmatrix}, \tag{2.135}$$

where χ is a two-component Pauli spinor. In the low energy limit, the lower component is suppressed with respect to the upper component. The matrices γ_5, $\gamma_5\gamma_0$, γ_i and σ_{i0} couple large and small components but not large with large, while the matrices $\mathbf{1}$, γ_0, $\gamma_5\gamma_i$ and σ_{ij} do not. As a consequence, the chiral counting scheme for the baryon sector are [64]

$$\begin{aligned} \Psi \sim O(p^0), \quad D_\mu \Psi \sim O(p^0), \quad (i\not{D} - \mathring{m}_N)\Psi \sim O(p), \\ 1, \gamma_\mu, \gamma_\mu\gamma_5, \sigma_{\mu\nu} \sim O(p^0), \quad \gamma_5 = O(p). \end{aligned} \tag{2.136}$$

The counting for the Goldstone bosonic fields and external fields remains the same as in purely Goldstone bosonic ChPT.

Then the most general effective Lagrangian for πN with a single nucleon in the initial and final states has the form of $\bar{\Psi}O\Psi$, where O is an operator acting on the spinor and transforming under $SU_L(2) \times SU_R(2)$ as $h(x)Oh(x)^{-1}$. Taking the discrete symmetries C, P and T into account, the most general effective πN Lagrangian at leading order has the form

$$\mathcal{L}_{\pi N}^{(1)} = \bar{\Psi}\Big(i\not{D} - \mathring{m}_N + \frac{1}{2}\mathring{g}_A\gamma_\mu\gamma_5 u^\mu\Big)\Psi, \tag{2.137}$$

where $\mathring{g}_A$ is the axial-vector coupling constant in the chiral limit.

To proceed to the $N_f = 3$ case, we consider the octet of the $J^P = \frac{1}{2}^+$ baryons. In the $N_f = 2$ case, the nucleons are living in a fundamental representation. However, the octet of $\frac{1}{2}^+$ form a baryons adjoint

representation of $SU_V(3)$. They are collected in a traceless 3×3 matrix B,

$$B = \sum_{a=1}^{8} \lambda^a B^a = \begin{pmatrix} \frac{1}{\sqrt{2}}\Sigma^0 + \frac{1}{\sqrt{6}}\Lambda & \Sigma^+ & p \\ \Sigma^- & -\frac{1}{\sqrt{2}}\Sigma^0 + \frac{1}{\sqrt{6}}\Lambda & n \\ \Xi^- & \Xi^0 & -\frac{2}{\sqrt{6}}\Lambda \end{pmatrix}. \tag{2.138}$$

The baryon fields transform as

$$B(x) \to h(x)B(x)h(x)^{-1}. \tag{2.139}$$

The covariant derivative acting on baryons is replaced by

$$D_\mu B = \partial_\mu + [\Gamma_\mu, B]. \tag{2.140}$$

The leading order Goldstone boson (ϕ)-baryon Lagrangian reads

$$\mathcal{L}^{(1)}_{\phi B} = \langle \bar{B}(i\not{D} - \mathring{m}_B)B\rangle - \frac{\mathring{D}}{2}\langle \bar{B}\gamma^\mu\gamma_5\{u_\mu, B\}\rangle - \frac{\mathring{F}}{2}\langle \bar{B}\gamma^\mu\gamma_5[u_\mu, B]\rangle, \tag{2.141}$$

where the low energy constants $\mathring{D}$ and $\mathring{F}$ determine the axial-vector coupling of baryons to the Goldstone bosons. They are related to the axial-vector coupling constant $\mathring{g}_A$ via $\mathring{D} + \mathring{F} = \mathring{g}_A$.

Like in purely Goldstone bosonic ChPT, a power counting rule can be assigned to each Feynman diagram. In baryon ChPT, the scaling of Goldstone bosons is the same as the purely Goldstone bosonic case. The Goldstone boson propagator is counted as $O(p^{-2})$. However, since the the off-shellness of the baryon field $\not{k} - m_N$ is counted as $O(p)$, the baryon propagator then scales as $O(p^{-1})$. Considering the measure of the loop integral, one can derive a chiral dimension n for a given Feynman diagram

$$n = 4L + \sum_k V_k - 2I_\phi - I_N, \tag{2.142}$$

where L, V_k, I_ϕ and I_N are the numbers of loops, k^{th} order vertices, Goldstone boson propagators and nucleon propagators, respectively. Eq. (2.142) is the naive power counting rule for a Feynman diagram. However, in practice, a Feynman diagram may produce terms whose chiral order is lower than that given by the naive power counting. Those terms are called power counting breaking terms. It only happens in the ChPT for matter fields. Many regularizations are proposed to address this issue. We will come back to this issue in the next section.

2.4.2 Chiral perturbation theory for spinless matter fields

The construction of ChPT for spinless matter fields is similar with that for baryons. In this work, we focus on the matter fields living in an anti-fundamental representation of $SU_V(N_f)$. Applying the CCWZ formalism, the transformation law under the $SU_L(N_f) \times SU_R(N_f)$ for the Goldstone boson fields and spinless matter fields, denoted by $P = (P_1, P_2, \dots)$, are

$$\begin{aligned} U &\to g_L U g_R^{-1}, \qquad & u &\to g_L u h(x)^{-1} = h(x) u g_R^{-1}, \\ P &\to P h(x)^{-1}, \qquad & P^\dagger &\to h(x) P^\dagger. \end{aligned} \tag{2.143}$$

The chiral covariant derivative acting on matter fields is defined as

$$D_\mu P^\dagger = \partial_\mu P^\dagger + \Gamma_\mu P^\dagger, \quad D_\mu P = \partial_\mu P + P\Gamma_\mu^\dagger. \tag{2.144}$$

On the Goldstone bosonic side, one has three building blocks $u_\mu, \chi_\pm$, as well as the covariant derivatives on them such as $\nabla_\mu u_\nu$. They transform under $SU_L(N_f) \times SU_R(N_f)$ as

$$\begin{aligned} u_\mu \to h u_\mu h^{-1}, \quad \chi_\pm \to h\chi_\pm h^{-1}, \quad \nabla_\mu u_\nu \to h\nabla_\mu u_\nu h^{-1}, \ldots \\ P^\dagger \to hP^\dagger, \quad D_\mu P^\dagger \to hD_\mu P^\dagger, \quad D_\mu D_\nu P^\dagger \to hD_\mu D_\nu P^\dagger, \ldots \end{aligned} \tag{2.145}$$

The power counting rule for these building blocks is

$$\begin{aligned} D_\mu P^{(\dagger)} \sim O(p^0), \qquad D_\mu D_\nu P^{(\dagger)} \sim O(p^0), \qquad (D_\mu D^\mu + m^2)P^{(\dagger)} \sim O(p), \\ u_\mu \sim O(p), \qquad \chi_\pm \sim O(p^2), \qquad \nabla_\mu u_\nu \sim O(p^2), \quad \ldots, \end{aligned} \tag{2.146}$$

where m is the mass of the P field in chiral limit. Based on the transformation properties and power counting of the blocks, it is easy to construct the effective Lagrangian to any finite order. Up to next-to-next-to leading order, the Lagrangians describing ϕP interactions read [28, 65–67]

$$\begin{aligned} \mathcal{L}^{(1)}_{\phi P} &= D_\mu P D^\mu P^\dagger - m^2 P P^\dagger, \\ \mathcal{L}^{(2)}_{\phi P} &= P\Big[-h_0\langle\chi_+\rangle - h_1\chi_+ + h_2\langle u_\mu u^\mu\rangle - h_3 u_\mu u^\mu\Big]P^\dagger \\ &\quad + D_\mu P\Big[h_4\langle u_\mu u^\nu\rangle - h_5\{u^\mu, u^\nu\}\Big]D_\nu P^\dagger\,, \\ \mathcal{L}^{(3)}_{\phi P} &= \Big[i\,g_1 P[\chi_-, u_\nu]D^\nu P^\dagger + g_2 P[u^\mu, \nabla_\mu u_\nu + \nabla_\nu u_\mu]D^\nu P^\dagger \\ &\quad + g_3 P\Big[u_\mu, \nabla_\nu u_\rho\Big]D^{\mu\nu\rho}P^\dagger + g_4 P\nabla_\nu\chi_+ D^\nu P^\dagger + g_5 P\langle\nabla_\nu\chi_+\rangle D^\nu P^\dagger + h.c.\Big] \\ &\quad + i\,\gamma_1 D^\mu P f^+_{\mu\nu} D^\nu P^\dagger + \gamma_2 P[u^\mu, f^-_{\mu\nu}]D^\nu P^\dagger\,, \end{aligned} \tag{2.147}$$

where $D^{\mu\nu\rho} = \{D_\mu, \{D_\nu, D_\rho\}\}$. The h_6 term in Ref. [28] is of order $O(p^3)$ instead of $O(p^2)$, thus can be absorbed into the terms of $O(p^3)$,

$$\begin{aligned} & D_\mu P[u^\mu, u^\nu]D_\nu P^\dagger \\ =\ & -P[\nabla_\mu u^\mu, u^\nu]D_\nu P^\dagger - P[u^\mu, \nabla_\mu u^\nu]D_\nu P^\dagger - P[u^\mu, u^\nu]D_\mu D_\nu P^\dagger \\ =\ & -\frac{1}{2}(P[u^\mu, \nabla_\mu u^\nu + \nabla_\nu u^\mu]D_\nu P^\dagger + P[u^\mu, \nabla_\mu u^\nu - \nabla_\nu u^\mu]D_\nu P^\dagger \\ & + P[u^\mu, u^\nu][D_\mu, D_\nu]P^\dagger + 2P[\nabla_\mu u^\mu, u^\nu]D_\nu P^\dagger) \\ =\ & -\frac{1}{2}\Big(P[u^\mu, \nabla_\mu u_\nu + \nabla_\nu u_\mu]D^\nu P^\dagger - P[u^\mu, f^-_{\mu\nu}]D^\nu P^\dagger \\ & + iP[\chi_-, u_\nu]D^\nu P^\dagger + \frac{1}{4}P[u^\mu, u^\nu][u_\mu, u_\nu]P^\dagger - \frac{i}{2}P[u^\mu, u^\nu]f^+_{\mu\nu}P^\dagger\Big) \\ =\ & -\frac{1}{2}\Big(P[u^\mu, \nabla_\mu u_\nu + \nabla_\nu u_\mu]D^\nu P^\dagger - P[u^\mu, f^-_{\mu\nu}]D^\nu P^\dagger + iP[\chi_-, u_\nu]D^\nu P^\dagger\Big) \\ & + O(p^4). \end{aligned} \tag{2.148}$$

In particular, for the two-flavor case $N_f = 2$, the Cayley-Hamilton relation, i.e. $\{A, B\} = A\langle B\rangle + B\langle A\rangle +$

$\langle AB\rangle - \langle A\rangle\langle B\rangle$ for any arbitrary 2×2 matrices A and B, can be used to reduce the number of operators. The Lagrangian for $N_f = 2$ has been constructed in Ref. [68] in the context of $SU(2)$ ChPT for kaons. For completeness, the relevant terms are listed,

$$\begin{aligned}
\mathcal{L}^{(1)}_{\pi K} &= D_\mu K^\dagger D^\mu K - M_K^2 K^\dagger K\,,\\
\mathcal{L}^{(2)}_{\pi K} &= A_1\langle\Delta_\mu\Delta^\mu\rangle K^\dagger K + A_2\langle\Delta^\mu\Delta^\nu\rangle D_\mu K^\dagger D^\nu K + A_3 K^\dagger\chi_+ K + A_4\langle\chi_+\rangle K^\dagger K\\
\mathcal{L}^{(3)}_{\pi K} &= B_1\Big(K^\dagger[\Delta^{\nu\mu},\,\Delta_\nu]D_\mu K - D_\mu K^\dagger[\Delta^{\nu\mu},\,\Delta_\nu]K\Big)\\
&\quad + B_2\langle\Delta^{\mu\nu}\Delta^\rho\rangle\Big(D_{\mu\nu}K^\dagger D_\rho K + D_\rho K^\dagger D_{\mu\nu}K\Big)\\
&\quad + B_3\Big(K^\dagger[\Delta_\mu,\,\chi_-]D^\mu K - D_\mu K^\dagger[\Delta^\mu,\,\chi_-]K\Big)\,,\\
\mathcal{L}^{(4)}_{\pi K} &= C_3\Big[\langle\Delta^{\mu\nu}\Delta^\rho\rangle(D_{\mu\nu}K^\dagger D_\rho K + D_\rho K^\dagger D_{\mu\nu}K)\\
&\qquad -2(D^{\mu\nu}K^\dagger\Delta_\mu\Delta_{\nu\rho}D^\rho K + D^\rho K^\dagger\Delta_{\nu\rho}\Delta_\mu D^{\mu\nu}K)\Big]\\
&\quad + C_5\Big(D_\mu K^\dagger\chi_+ D^\mu K - M_K^2 K^\dagger\chi_+ K\Big) + C_6\langle\chi_+\rangle\Big(D_\mu K^\dagger D^\mu K - M_K^2 K^\dagger K\Big)\\
&\quad + \dots\,,
\end{aligned}\tag{2.149}$$

with the notations

$$\begin{aligned}
\Delta_\mu = -\frac{i}{2}u_\mu \quad \Delta_{\mu\nu} = -\frac{i}{4}\left(\nabla_\mu u_\nu + \nabla_\nu u_\mu\right)\,,\\
K^\dagger = P\,,\quad K = P^\dagger\,,\quad D_{\mu\nu} = \left\{D_\mu, D_\nu\right\}.
\end{aligned}\tag{2.150}$$

By comparing the Lagrangians, one has a relation between the two sets of LECs,

$$\begin{aligned}
&A_1 = 2h_3 - 4h_2\,,\quad A_2 = 4(h_5 - h_4)\,,\quad A_3 = -h_1\,,\quad A_4 = -h_0\,,\\
&B_1 = 8g_2\,,\quad B_3 = -2g_1\,,\\
&C_3 = 8g_3,\quad C_5 = -2g_4\,,\quad C_6 = -2g_5\,.
\end{aligned}\tag{2.151}$$

Notice that the B_2 term therein is actually $O(p^4)$, which can be seen by partial integration. Instead, the C_3 term of Eq. (2.150) is in fact of $O(p^3)$. The corrected assignment can be checked from the explicit expression of the scattering amplitudes in Ref. [69].

2.5 Power counting breaking and regularizations

In the presence of matter fields with generic masses $m \gtrsim \Lambda_\chi$, the navie power counting analysis Eq. (2.142) is no longer valid because the loop integrals also yield terms of the form m/Λ_χ which spoil the power counting [17], the so-called power counting breaking terms. Loop corrections contribute to the πN scattering amplitude at $O(p^2)$ instead of $O(p^3)$ according to the naive power counting. To see the power counting breaking (PCB) issue, let us consider the one-loop correction to the nucleon mass. Employing the Lagrangian Eq. (2.137), the $\overline{\text{MS}}$-renormalized self-energy contribution to the nucleon mass reads [17, 58]

$$\delta_m = -\frac{3\mathring{g}_A^2}{4F_0^2}2mM^2\Delta,\tag{2.152}$$

where

$$\Delta = \frac{1}{16\pi^2}\Big[-1+\log\frac{m^2}{\mu^2}-\frac{M^2}{2m^2}\log\frac{M^2}{m^2}+\frac{2M}{m}\sqrt{1-\frac{M^2}{4m^2}}\arccos\Big(\frac{M}{2m}\Big)\Big],$$

with M the pion mass. Expanding it around the small M/m, up to $O(p^3)$, one has

$$\delta_m = \frac{3\mathring{g}_A^2 M^2}{32\pi^2 F_0^2}(1-\log\frac{m^2}{\mu^2})-\frac{3\mathring{g}_A^2 M^3}{32\pi F_0^2}. \tag{2.153}$$

It shows that the loop correction contributes from $O(p^2)$, instead of $O(p^3)$ obtained by naive power counting. In Eq. (2.152), the power counting breaking term, i.e. $\frac{3\mathring{g}_A^2 M^2}{32\pi^2 F_0^2}(1-\log\frac{m^2}{\mu^2}) \sim O(p^2)$, is analytical to the chiral quantity, i.e. M, and the nonanalytic part satisfies the naive power counting. It is a general feature for the loop correction and will be the key to the covariant solutions to the PCB issue.

There have been several solutions to the PCB issue, e.g. the most well-known heavy baryon ChPT (HBChPT) [18–20], the infrared regularization (IR) [21], and the extended-on-mass-shell (EOMS) scheme [22]. In HBChPT, the heavy components of the anti-baryon fields are integrated out. The new Lagrangian is organized in inverse powers of m, and the dependence of the baryon mass is removed from the propagators. As a consequence, the only mass scale appearing in the loops is the Goldstone boson mass and thus the PCB issue is avoided. However, the $1/m$ expansion sometimes leads to incorrect low-energy analytic properties [20]. The expansion series near the anomalous threshold fails to converge and an infinite number of terms are needed.[4] A manifestly Lorentz covariant regularization scheme which preserves the analytic structure and the power counting can also be formulated. The crucial step was made by Ellis and Tang [71, 72]. They noted that the soft-momentum part of a loop diagram is infrared singular and the PCB terms, coming from the hard-momentum modes only, are a local polynomial in chiral quantities and thus can be absorbed into the LECs of the most general chiral Lagrangian. Based on their work, Becher and Leutwyler proposed the IR scheme which isolates the infrared singular parts of the loops by extending the Feynman parameter integration upper bound from unity to infinity [21]. Due to the fact that the infrared regular parts of loops can be obtained by expanding the integrand in small quantities and then integrating each term [73], the EOMS scheme was proposed, in which additional subtractions beyond the $\overline{\text{MS}}$ scheme are performed to get rid of the PCB terms.

2.5.1 Heavy baryon ChPT

The first solution to the power counting problem is brought by Jenkins and Manohar [18] following methods from heavy quark effective theory. The basic idea of HBChPT is to consider the nucleon as extremely heavy, only the baryon momenta relative to the rest mass is small and concerned. The 4-momentum of baryon is decomposed as (similar with in HQET)

$$p_\mu = m v_\mu + k_\mu, \tag{2.154}$$

with $k_\mu \ll v\cdot p$ and v_μ the baryon 4-velocity satisfying $v^2 = 1$. The baryon field is split into 'heavy' and 'light' components

$$N_v(x) = e^{imv\cdot x}P_v^+\Psi(x), \quad H_v(x) = e^{imv\cdot x}P_v^-\Psi(x), \tag{2.155}$$

[4] This can be overcome by using the extended propagator $i/(v\cdot k + k^2/2m)$ instead of the strict HB propagator $i/v\cdot k$, see e.g. Ref. [70].

where $P_v^{\pm} = \frac{1\pm\not{v}}{2}$ is the projection operator. Integrating out the 'heavy' component, to tree-level one has

$$\mathcal{L}_{\text{HBChPT}} = \bar{N}_v(iv\cdot D + \frac{\mathring{g}_A}{2}\not{u}_\perp\gamma_5)N_v + \sum_{n=1}^{\infty}\frac{1}{(2m)^n}\mathcal{L}^{(n)}_{\text{HBChPT}}, \tag{2.156}$$

where $u_\perp^\mu = h^\mu - v\cdot u v^\mu$. The first term, up to the leading order can be reduced to

$$\mathcal{L}^{(1)}_{\text{HBChPT}} = \bar{N}_v(iv\cdot D + \mathring{g}_A u\cdot S_v)N_v, \tag{2.157}$$

where $S_v^\mu = \frac{i}{2}\gamma_5\sigma^{\mu\nu}v_\nu = -\frac{1}{2}\gamma_5(\gamma^\mu\not{v} - v^\mu)$ obeys the following relations

$$S_c\cdot v = 0, \quad S_v^2 = \frac{1-d}{4}, \quad \{S_v^\mu, S_v^\nu\} = \frac{1}{2}(v^\mu v^\nu - g^{\mu\nu}), \quad [S_v^\mu, S_v^\nu] = i\epsilon^{\mu\nu\alpha\beta}v_\alpha S_{v\beta}.$$

Expressions for higher order operators can be found in Ref. [19]. HBChPT is thus a double expansion in q/Λ_χ and q/m. From the Lagrangian Eq. (2.157), one can read off the baryon propagator $\frac{i}{v\cdot k}$. The absence of the mass scale m in the integrals makes sure that only soft modes contribute to the loops and thus the naive power counting Eq. (2.142) is satisfied, which can be easily checked by dimensional analysis. To examine the convergence of this $1/m$ expansion, we follow Becher and Leutwyler [21] and consider the scalar form factor of the nucleon in the isospin limit,

$$\langle N(p')|\hat{m}(\bar{u}u + \bar{d}d)|N(p)\rangle = \bar{u}'u\sigma(t), \quad t = (p'-p)^2. \tag{2.158}$$

The leading one-loop correction of this form was worked out in Ref. [17] in a Lorentz invariant formulation,

$$\sigma(t) = \frac{3\mathring{g}_A^2M^2m}{4F_0^2}\Big[(t-2M^2)\gamma(t) - \frac{M}{8\pi m}\Big], \tag{2.159}$$

where

$$\gamma(t) = -i\int\frac{d^4k}{(2\pi)^4}\frac{1}{(M^2-k^2)(M^2-(k-q)^2)(m^2-(p-k)^2)}, \tag{2.160}$$

here we denote $q_\mu = p_\mu - p'_\mu$. This function is analytic in t except for a cut along the positive real axis from $4M^2$ to infinity. The function $\gamma(t)$ represents a triangle graph Fig. 2.1 with one nucleon propagator and two pion propagators, and it shows up in the πN scattering amplitude to one loop. The imaginary part of $\gamma(t)$ can be expressed as [17]

$$\text{Im}\gamma(t) = \frac{\theta(t-4M^2)}{8\pi\sqrt{t(4m^2-t)}}\arctan\frac{(t-4M^2)(4m^2-t)}{t-2M^2}. \tag{2.161}$$

The analytic continuation of $\gamma(t)$ to the second sheet contains a brach cut point $t_c = 4M^2 - M^4/m^2$, coming from the arctan and lying just below the threshold $4M^2$. This is called anomalous threshold, and turns out to be very important in the calculations for the specific physical observables. And it implies that the form factor does not admit an expansion in powers of chiral quantities in the region near threshold.

Since the HBChPT series corresponds to the inverse power of m expansion of the relativistic result

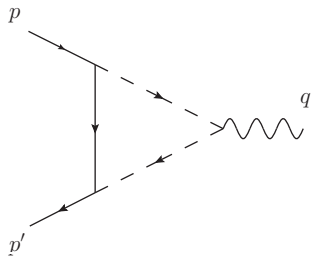

Figure 2.1: Triangle graph. The solid, dashed and wiggly lines represent the nucleons, pions and an external scalar source, respectively.

[19], within HBChPT,

$$\mathrm{Im}\gamma(t)_{\mathrm{HBChPT}} = \frac{t-4M^2}{32\pi m\sqrt{t}}\Big(\pi - \frac{t-2M^2}{m\sqrt{t-4M^2}}\Big), \tag{2.162}$$

provides a decent representation if t is not close to the threshold. An infinite series of internal insertions must be taken into account to properly describe the form factor near threshold. One way to solve this problem of HBChPT is to use the extended propagator $\frac{i}{v\cdot k+k^2/2m}$ instead of $\frac{i}{v\cdot k}$, it gives the proper analytic behavior near threshold, see Ref. [70].

2.5.2 Analytic structures of loop integrals

A consistent and ideal way to dealing with the problem of HBChPT is to formulate a theory which has a proper power counting and proper analytic structures as well. The first attempt in this direction was made by Tang and Eills [71, 72]. While the anti-nucleon field are integrated out to recover the proper power counting, Tang [71] noted that their contributions are hard-mode effect, and that the proper low-energy expansion makes sense only if all hard-momentum effects are absorbed into the LECs. Tang noticed that the PCB terms come from the hard-momentum modes only, and they turn out to be local polynomial in chiral quantities and thus could be absorbed by the redefinition of the LECs. He proposed a prescription to extract the soft part of a Feynman diagram in the following way:

- take the loop momenta to be of order p,
- make a covariant p/m expansion of the integrand,
- exchange the order of the integration and summation of the resulting power series.

Let q be the loop momentum and consider the integration over the time component q_0. Closing the contour by a semicircle at infinity, one finds that the q_0 integration of a loop is given by the sum of three contributions: (1) the semicircle; (2) the soft poles, of order p, and (3) the hard poles, of order m. The contribution from the semicircle only produce divergences and will be removed by the usual renormalization. A p/m expansion of the soft-pole structures, e.g. pion propagators, is not allowed since the expansion would destroy the nonanalytic structures of the low-energy behavior. However, a p/m expansion of the hard-pole structures is allowed because the pole is located much higher than the loop momentum, which is of order p. This expansion destroys the hard-pole structures and removes these poles once we truncate the expansion. However this is harmless since the low-energy EFTs only concerns the low-energy bahavior, and the truncation of the effective Lagrangian have already spoiled

the hard-pole structures. In step 3, even without truncating the series, the exchange of the integration and summation also removes the hard poles. In a proper low-energy EFT, the hard-mode effects are all encoded into the LECs.

For a closed baryon loop, the only energy scale appearing in the loop is the mass of nucleon. In dimensional regularization, it is easy to conclude that the loop contains hard parts and no soft part due to the absence of soft scale. A more detailed discussion can be found in Ref. [71]. Once the baryon loops are excluded, any baryon lines are connected to external baryons by baryon number conservation. Thus the baryon propagators are nearly on-shell and are of order p^{-1}. For a loop containing m nearly on-shell nucleon and n pion propagators, symbolically written as

$$\int \frac{d^4q}{(2\pi)^4} \frac{1}{[(k+q)^2 - m^2]^m [q^2 - M^2]^n}, \tag{2.163}$$

if we only consider the soft part, i.e. the integration momentum is of order p, then the loop integral Eq. (2.163) scales under $p \to tp$, $M \to tM$ and $(k^2 - m^2) \to t(k^2 - m^2)$ as

$$\begin{aligned} & \int \frac{d^4q}{(2\pi)^4} \frac{1}{[(k+q)^2 - m^2]^m [q^2 - M^2]^n}, \\ \to & \int \frac{d^4q}{(2\pi)^4} \frac{1}{[t(k^2 - m^2) + 2k\cdot q + q^2]^m [q^2 - t^2M^2]^n}, \\ = & \int \frac{d^4l}{(2\pi)^2} \frac{t^{4-m-2n}}{[(k^2 - m^2) + 2k\cdot l + tl^2]^m [l^2 - M^2]^n}. \end{aligned} \tag{2.164}$$

Due to the presence of the t factor in the nucleon propagator on the last line, the loop integral turns out to that it does not scale uniformly like in purely Goldstone bosons case, e.g. Eq. (2.9). t is an arbitrary number, in the chiral limit (vanishing pion mass and external external 3-momenta), it tends to be zero. Counted in chiral dimensions, one can see that the at leading order, the loop integral is of order p^{4-m-2n}, consistent with the naive power counting. It is worth mentioning that the soft parts of the loop integral not only contains the leading order p^{4-m-2n}, but also contains higher orders. For the soft part, q^2 is small, and can be regarded as a higher order perturbation in the nucleon propagator, thus can be expanded in a series. However, for the hard part, the hard pole lies around $2k\cdot q + q^2 = 0$, i.e. $q = -2k$. When q^2 becomes large, the expansion breaks down. As a result, the power counting breaks down as well. Since the soft part of loop integrals satisfies the power counting, the PCB terms can only come from the hard part of loops. The most important step made by Tang and Ellis is to realize that the PCB terms, from the hard parts, are just polynomials of chiral quantities.

Let us consider a loop H with I scalar internal lines,

$$H_G = \mu^{L(4-d)} \int \prod_{l=1}^{L} \frac{d^dk_l}{(2\pi)^d} \prod_{i=1}^{I} \frac{i}{q_i^2 - m_i^2 + i\epsilon}, \tag{2.165}$$

where the momentum q_i^μ is a linear combination of the loop momentum k_i^μ and the external momenta. Using Feynman parameters, one obtains

$$H_G = i^I \Gamma(I) \mu^{L(4-d)} \int_\infty^\infty \prod_{k=1}^{I} [d\alpha_k \theta(\alpha_k)] \prod_{l=1}^{L} \frac{d^dk_l}{(2\pi)^d} \frac{\delta(1 - \sum_{j=1}^I \alpha_j)}{[\sum_{i=1}^I \alpha_i (q_i^2 - m_i^2) + i\epsilon]^I}. \tag{2.166}$$

Singularities of H arise when the contour of integration gets pinched between two or more poles of the integrand (pinch singularities) or between poles of the integrand and endpoints of the integration contour (endpoint singularities). Landau equations provide a useful tool for investigating the analytic properties of a Feynman graph. The Landau equations for H are given by

$$\begin{aligned} &\text{for each i}: \quad \text{either} \quad \alpha_i = 0 \quad \text{or} \quad q_i^2 = m_i^2, \\ &\text{for each i}, \mu: \quad \sum_{i=1}^{I} \alpha_i \frac{\partial q_i^2}{\partial k_l^\mu} = 0, \end{aligned} \tag{2.167}$$

which means that either an internal line i of H is on-shell or the Feynman parameter α_i vanishes. If $\alpha_i = 0$, line i does not contribute to the remaining Landau equations, and the Landau equations for H is identical to the Landau equations for the sub-graph h of H which is obtained by shrinking line i into a point. A solution to the Landau equations where all α_is are nonzero is called the leading singularity of H; singularities with n internal lines off shell are called (sub)^n-leading singularities. It follows that every (sub)^n-leading singularity of H can be represented by a leading singularity of a subgraph where the corresponding n internal lines have been shrunk. The complete set of singularities of a graph H is given by the leading singularities of each subgraphs.

For a graph containing both nucleon and pion internal lines, the loop integral can be split into two parts,

$$H_G = I_G + R_G, \tag{2.168}$$

where the entire low-energy analytic structure of H is collected into I, while the terms multiplied by factors of the form m_N^{ld-n} with l and n integers, are collected in R, the regular part. I and H have identical low-energy analytic structure, and R can be accounted for through a renormalization of the low-energy constants. This separation can be achieved by separating out the subgraphs that lie outside of the low-energy region. These subgraphs are referred to as regular subgraphs. The factor m_N^{ld-n} will be singular at $m_N = 0$ for appropriate d, thus separating out the $m_N = 0$ singularities will ensure that the terms multiplied by fractional powers of m_N are separated out. A more detailed discussion on the separation of irregular and regular parts Eq. (2.168) can be found in Ref. [74]. It is easy to see that the regular parts correspond to the hard-mode effects in the loops.

2.5.3 Infrared regularization

Tang's method indeed extracts the soft part of a Feynman graph which fulfils the power counting. However, it relies on the chiral expansion of the loop integrals which is not always convergent. Based on Tang's work, Becher and Leutwyler proposed a more formal scheme to extract the soft-momentum parts, or infrared singular parts, of a Feynman graph, which is called Infrared Regularization (IR). It relies on the fact that the infrared singular parts of the loops can be separated from the remainder uniquely as Eq. (2.168). Let us look at the simplest case, the self-energy. The corresponding scalar loop integral is

$$H(p^2) = \frac{\mu^{(4-d)}}{i} \int \frac{d^d k}{(2\pi)^d} \frac{1}{(k^2 - M^2)((p-k)^2 - m^2)}. \tag{2.169}$$

This integral develops an infrared singularity for vanishing M due to the infrared mode of integration. The high momentum one is free of infrared singularities and thus leads to a contribution that can be expanded in a Taylor expansion [75]. In order to separate out the infrared parts, one uses the Feynman

parameterization

$$\frac{1}{ab} = \int_0^1 dz \frac{1}{[(1-z)a + zb]^2},$$

Performing the integration over k, one obtains

$$H(p^2) = \frac{\Gamma(2-d/2)}{(4\pi)^{d/2}} m^{d-4} \int_0^1 dz C^{d/2-2}, \tag{2.170}$$

where $C = z^2 - 2\alpha\Omega z(1-z) + \alpha^2(1-z)^2$ with $\alpha = \frac{M}{m}$ and $\Omega = \frac{p^2-m^2-M^2}{2mM}$. The infrared singularity arises from small values of z. Performing a change of variable $z = \alpha u$, the upper limit of integration becomes infinity as M goes to zero. One thus extract the infrared singular parts by extending the integration to ∞ and define the infrared singular part by

$$I = \frac{\Gamma(2-d/2)}{(4\pi)^{d/2}} m^{d-4} \int_0^\infty dz C^{d/2-2} = \frac{\Gamma(2-d/2)}{(4\pi)^{d/2}} m^{d-4} \alpha^{d-3} \int_0^\infty du D^{d/2-2},$$

with $D = 1 - 2\Omega u + u^2 + 2\alpha u(\Omega u - 1) + \alpha^2 u^2$. The difference between H and I is the infrared regular part R,

$$R = -\frac{\Gamma(2-d/2)}{(4\pi)^{d/2}} m^{d-4} \int_1^\infty dz C^{d/2-2}, \tag{2.171}$$

so that

$$H = I + R. \tag{2.172}$$

The infrared singularity comes from the small values of z and is excluded in the expression of R. Both I and R are chirally symmetric by themselves, so that R can be absorbed into the low-energy constants of the effective Lagrangian. The infrared singular part contains an overall factor α^3, so that the chiral expansion of I only consist of noninteger powers of the chiral expansion,

$$I = O(p^{d-3}) + O(p^{d-2}) + O(p^{d-1}) + \ldots, \tag{2.173}$$

while the infrared regular part only contains nonnegative integer powers,

$$R = O(p^0) + O(p) + O(p^2) + \ldots. \tag{2.174}$$

It is instructive to interpret the decomposition of H to I and R in terms of Eq. (2.170). The infrared part is obtained by taking the integration upper limit from 1 to ∞

$$\int_0^\infty \frac{z}{[(1-z)a + zb]^2} = \frac{1}{a(b-a)}. \tag{2.175}$$

It shows that the decomposition Eq. (2.172) corresponds to the decomposition

$$\frac{1}{ab} = \frac{1}{a(b-a)} - \frac{1}{b(b-a)}. \tag{2.176}$$

As a result, the infrared singular part reads

$$I = \frac{\mu^{d-4}}{i}\int\frac{d^dk}{(2\pi)^d}\frac{1}{(M^2-k^2)(m^2-p^2+2p\cdot k-M^2)}. \tag{2.177}$$

It differs from H in that the term k^2 in the nucleon propagator is replaced by M^2. And the regular part is given by

$$R = -\frac{\mu^{d-4}}{i}\int\frac{d^dk}{(2\pi)^d}\frac{1}{(m^2-(p-k)^2)(m^2-p^2+2p\cdot k-M^2)}. \tag{2.178}$$

It is easy to see that the I part fulfils the power counting, as discussed in the last subsection, and the regular part involves two nucleon propagators, therefore it is a hard effect.

The method can be extended to general one-loop integrals. It suffices to consider the scalar integrals,

$$H_{mn} = \frac{\mu^{d-4}}{i}\int\frac{d^dk}{(2\pi)^d}\frac{1}{a_1a_2\dots a_mb_1\dots b_n}, \tag{2.179}$$

where $a_i = (q_i+k)^2 - M^2$ and $b_j = (p_j-k)^2 - m^2$ are inverse of the pion and nucleon propagators, respectively. Using the formula [21]

$$\frac{1}{a_1a_2\dots a_m} = \Big(-\frac{\partial}{\partial M^2}\Big)^{m-1}\int_0^1 dx_1\cdots\int_0^1 dx_{m-1}\frac{X}{A}, \tag{2.180}$$

where

$$X = x_2(x_3)^2\dots(x_m)^{m-1}, \tag{2.181}$$

for $m>2$ and $X=1$ for $m=2$. The denominator A can be obtained with the recursion relation

$$A = A_m,\quad A_1 = a_1,\quad A_{l+1} = x_lA_l + (1-x_l)a_{l+1},\quad (l=1,\dots,l-1).$$

The result for A is quadratic in k, $A = \bar{A} - (k-\bar{q})^2$, where $\bar{A}$ is a constant of order p^2, and $\bar{q}$ represents a linear combination of external momenta and is of order p. Likewise, the nucleon dominator B has the same form $B = \bar{B} - (\bar{P}-k)^2$ with $\bar{P} = m^2 + O(p)$ and $\bar{B} = m^2 + O(p)$. The integral H_{mn} then can be evaluated via

$$H_{mn} = \Big(-\frac{\partial}{\partial M^2}\Big)^{m-1}\Big(-\frac{\partial}{\partial m^2}\Big)\int_0^1 dxdyXY\frac{\mu^{d-4}}{i}\int\frac{d^dk}{(2\pi)^d}\frac{1}{AB}, \tag{2.182}$$

with

$$\int_0^1 dxdy = \int_0^1 dx_1\cdots\int_0^1 dx_{m-1}\int_0^1 dy_1\cdots\int_0^1 dy_{n-1}.$$

As a result,

$$H_{mn} = \int_0^1 dxdyXY\Big(-\frac{\partial}{\partial\bar{A}}\Big)^{m-1}\Big(-\frac{\partial}{\partial\bar{B}}\Big)^{n-1}H_{p\to\bar{P}-\bar{q},M^2\to\bar{A},m^2\to\bar{B}}. \tag{2.183}$$

Splitting H_{mn} into regular and infrared singular parts R_{mn} and I_{mn}, respectively, and comparing with the

self-energy case, the representation for I_{mn} reads

$$I_{mn} = \int_0^1 dxdyXY\Big(-\frac{\partial}{\partial\bar{A}}\Big)^{m-1}\Big(-\frac{\partial}{\partial\bar{B}}\Big)^{n-1} I_{p\to\bar{P}-\bar{q},M^2\to\bar{A},m^2\to\bar{B}}. \tag{2.184}$$

The chiral expansion of the singular part I_{mn} only contains noninteger powers for noninteger d, while the regular part R_{mn} can be expanded in a Taylor expansion and can therefore be absorbed into the low-energy constants of the Lagrangian. Therefore, H_{mn} can be replaced by its singular part I_{mn} in the loop integrals, which is the infrared renormalization condition,

$$H_{mn}^{IR} = I_{mn}. \tag{2.185}$$

2.5.4 Extended On-Mass-Shell scheme

The most important step made by Tang was to realize that the power counting breaking violating terms are just polynomials of chiral quantities. In IR, only the infrared singularities which obey the power counting are calculated. Contrary to IR, one can evaluate the regular parts instead and subtract them from the full loop integral to obtain a subtracted result that fulfils the power counting. The subtracted regular parts representing the hard effects are absorbed into the LECs. One of these schemes is the extended on-mass shell (EOMS) scheme [22, 76]. The central idea consists in performing additional subtractions beyond the $\overline{\text{MS}}$ scheme. Since the regular parts are polynomials of chiral quantities, one can expand the integrand in small quantities and then exchanging the integration and summation without change the regular parts, see Ref. [73]. However, this procedure would destroy the infrared singular parts. Considering a two-point loop, the integrand is expanded in small chiral quantities as

$$\begin{aligned}
&\frac{1}{[(k-p)^2-m^2][k^2-M^2]}\\
=&\sum_{i,j=0}^{\infty}\frac{(p^2-m^2)^i(M^2)^j}{i!j!}\Big[\Big(\frac{1}{2p^2}p_\mu\frac{\partial}{\partial p_\mu}\Big)^i\Big(\frac{\partial}{\partial M^2}\Big)^j\frac{1}{[(k-p)^2-m^2][k^2-M^2]}\Big]_{p^2-m^2=0,M^2=0}\\
=&\frac{1}{(k^2-2k\cdot p)(k^2)}\Big|_{p^2-m^2=0}+M^2\frac{1}{(k^2-2k\cdot p)(k^2)}\Big|_{p^2-m^2=0}\\
&+(p^2-m^2)\Big[\frac{1}{2m^2}\frac{1}{(k^2-2k\cdot p)^2}-\frac{1}{2m^2}\frac{1}{(k^2-2k\cdot p)(k^2)}\\
&-\frac{1}{(k^2-2k\cdot p)^2k^2}\Big]_{p^2-m^2=0}+\dots,
\end{aligned} \tag{2.186}$$

where $[\dots]_{p^2-m^2=0}$ means that we consider the coefficients of chiral quantities only for p^μ satisfying the on-mass-shell condition, which gives rise the name EOMS. Although the coefficients depend on p^μ, after integration of the series and evaluating each term at on-mass-shell condition $p^2 = m^2$, these coefficients turns out to be only the functions of m^2. It confirms that the regular part encodes the hard effects of loops only. Integrating each term in Eq. (2.186), one obtains the regular part [77]

$$R = -\frac{m^{d-4}\Gamma(2-d/2)}{(4\pi)^{d/2}(d-3)}\Big[1-\frac{p^2-m^2}{2m^2}+\frac{(d-6)(p^2-m^2)^2}{4m^4(d-5)}+\frac{(d-3)M^2}{2m^2(d-5)}+\dots\Big].$$

It coincides with the result from the expansion of R in Ref. [21]. In this example, only the first term violates the power counting and is thus the only term which needs to be subtracted from H in order to get

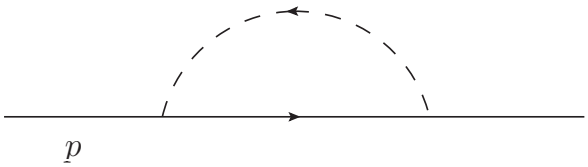

Figure 2.2: Self-energy graph. The solid and dashed represent the nucleons and pions, respectively.

a renormalized expression $H^r_{\rm EOMS}$ which fulfils the power counting: $H^r_{\rm EOMS} = H - H_{\rm subtr}$ with

$$H_{\rm subtr} = \frac{\mu^{d-4}}{i}\int\frac{d^dk}{(2\pi)^d}\frac{1}{k^2(k^2-2k\cdot p)}\Big|_{p^2-m^2} = -\frac{m^{d-4}\Gamma(2-d/2)}{(4\pi)^{d/2}(d-3)\mu^{4-d}}. \tag{2.187}$$

In general, the regular part R proportional to fractional powers of the heavy mass m and thus responsible for the breaking of power counting of the loop integral Eq. (2.165) is derived in Ref. [74]. According to the Landau equations, it is easy to see that subgraphs containing only heavy propagators and low-energy momentum insertions are regular subgraphs which give rise to fractional powers of m [74]. These subgraphs can not produce singularities in the low-energy region and thus belong to R_G. Any subgraph of a regular subgraph is also regular. This gives rise to the notion of a minimally contracted regular (MCR) subgraph, i.e. a regular subgraph $\mathfrak{g}$ that is not a subgraph of any other regular subgraph with more lines than $\mathfrak{g}$. To one-loop, there are at most two different MCR subgraphs for a given graph and every internal heavy particle line belongs to exactly one of them, the proof of this can be found in Ref. [74]. Since different MCR subgraphs have no common lines, they do not have common subgraphs. As a consequence, the regular part of H_G is given by a sum on the MCR as follows [74]:

$$\begin{aligned} R_G &= i^I\Gamma(I)\mu^{4-d}\sum_{\mathfrak{g}}\int_0^\infty\prod_{i\in\mathfrak{g}}d\alpha_i\int_{-\infty}^0\prod_{j\notin\mathfrak{g}}(-d\alpha_j)\delta(1-\sum_{k=1}^I\alpha_k) \\ &\quad\times\int\frac{d^dk}{(2\pi)^d}\frac{1}{(\sum_{i=1}^I\alpha_i(q_i^2-m_i^2)+i\epsilon)^I}. \end{aligned} \tag{2.188}$$

The integral can be carried out yielding

$$\begin{aligned} R_G &= -\kappa_I\sum_{\mathfrak{g}}\int_1^\infty d\lambda\lambda^{|\mathfrak{g}|-1}(1-\lambda)^{I-|\mathfrak{g}|-1}\int_0^1\Big(\prod_{i\in\mathfrak{g}}dz_i\Big)\delta\Big(1-\sum_{k\in\mathfrak{g}}z_k\Big) \\ &\quad\times\int_0^1\Big(\prod_{j\notin\mathfrak{g}}dz_j\Big)\delta(1-\sum_{k\notin\mathfrak{g}}z_k)\Big[(1-\lambda)^2\sum_{i,j\notin\mathfrak{g}}z_i\Omega_{ij}z_j+\lambda^2\sum_{i,j\in\mathfrak{g}}z_i\Omega_{ij}z_j \\ &\quad+2\lambda(1-\lambda)\sum_{i\in\mathfrak{g},j\notin\mathfrak{g}}z_i\Omega_{ij}z_j-i\epsilon\Big]^{d/2-I}, \end{aligned} \tag{2.189}$$

where $|\mathfrak{g}|$ denotes the number of internal lines belonging to the MCR subgraphs $\mathfrak{g}$ and

$$\kappa_I = (-1)^I\frac{i^{I+1}}{16\pi^2}\frac{\Gamma(I-d/2)}{(4\pi\mu^2)^{d/2-2}},\quad \Omega_{ij} = \frac{m_i^2+m_j^2-(q_i-q_j)^2}{2}. \tag{2.190}$$

As an example let us look at the self-energy graph of a heavy particle shown in Fig. 2.2. It has two subgraphs shown in Fig. 2.3 obtained by contracting 1 internal lines. They correspond to the sub-leading

Figure 2.3: Self-energy graph. The solid and dashed represent the nucleons and pions, respectively. The left corresponds to the regular part.

singularities at $m = 0$ and $M = 0$, respectively. The first tadpole lying outside the low-energy region is the MCR subgraph and thus gives rise to the regular part

$$R_G = -\kappa \int_1^\infty d\lambda \Big[(1-\lambda)^2 M^2 + \lambda^2 m^2 + 2\lambda(1-\lambda)\frac{(m^2 + M^2 - p^2)}{2}\Big]^{d/2-2},$$

which coincides with the result obtained by Becher and Leutwyler in Ref. [21]. It is straightforward to prove that R_G is analytic in the low-energy region, e.g. see Ref. [74]. Therefore, R_G can be Taylor expanded in the small chiral quantities. One can truncate the chiral expansion of R_G to the order of EFT Lagrangian, yielding the so-called PCB terms $R_G^{\rm subtr}$, and subtract them from the original integral H_G to obtain a EOMS renormalized loop integral

$$H^r_{\rm EOMS} = H - R_G^{\rm subtr}. \tag{2.191}$$

To see how the IR and EOMS are related to each other, let us consider an arbitrary loop integral. After combining the propagators using the Feynman parameterization and some change of variables, performing the loop momentum integration, the loop integral has the form

$$H = \int_0^1 dz f(z), \tag{2.192}$$

where $f(z)$ is a function depending on the external momenta, masses and the space-time dimension d. The IR splits H into infrared singular and regular part by

$$\int_0^1 dz \cdots = \int_0^\infty dz \cdots - \int_1^\infty dz \ldots. \tag{2.193}$$

In the regular part, one can expand the integrand in chiral quantities and interchange summation and integration. It leads to

$$\begin{aligned} R_{\rm IR} &= -\int_1^\infty dz \sum_{i=0}^\infty \frac{f^{(n)}(0)}{n!} z^n \\ &= \sum_{i=0}^\infty \frac{f^{(0)}(0)}{(n+1)!}. \end{aligned} \tag{2.194}$$

On the other hand, in EOMS, the regular part is extracted order by order by expanding the integrand of

the original loop in chiral quantities and interchange the summation and integration,

$$\begin{aligned} R_{\text{EOMS}} &= \int_0^1 dz \sum_{i=0}^{\infty} \frac{f^{(n)}(0)}{n!} z^n \\ &= \sum_{i=0}^{\infty} \frac{f^{(0)}(0)}{(n+1)!}. \end{aligned} \tag{2.195}$$

Although the domain of Eq. (2.194) is $\mathrm{Re}(n) < -1$, which is totally different from in Eq. (2.195), they are equivalent by analytic continuation.

CHAPTER 3

Unitarization

As already discussed in the last chapter, the applicability of ChPT is restricted to the regions of low energies where excited states in the hadronic spectrum have been integrated out. In the case of $\pi\pi$ scattering this boundary is given by the mass of the lightest vector mesons, i.e. $\rho(770)$, which appears as a resonance in the $L = 1$, $I = 1$ channel, and the $f_0(500)$ in the $I = L = 0$ channel. It cannot be reproduced by the perturbative calculation at any finite order. One also encounters low lying excitations such as $\Delta(1232)$ in πN scattering or $\Lambda(1405)$ in the strangeness $S = -1$ channels. There have been many attempts to construct various methods which allows for an extension of ChPT to the regions where resonances appear. In this chapter, we first study the elementary elements of the S-matrix of strong interactions. Then various unitarization schemes are introduced subsequently.

3.1 Elements of S-matrix theory of strong interactions

In a scattering experiment, particles move toward each other and later on move apart. If the observations of incoming and outgoing particles are made sufficiently early and sufficiently late, respectively, i.e. the particles are sufficiently far apart, the interactions among the particles are sufficiently weak. The particles behave as free particles during the observations, and thus can be described by the asymptotic states $|m, \text{in}\rangle$ or $|n, \text{out}\rangle$ for the incoming or outgoing states far away, respectively. The S-matrix can be defined as an operator mapping incoming states to outgoing states,

$$\langle n, \text{out}| = \langle n, \text{in}|S, \quad \text{and} \quad S^\dagger|m, \text{in}\rangle = |m, \text{out}\rangle. \tag{3.1}$$

Since the set of incoming states or outgoing states is complete, the S-matrix can be formally written as

$$S = \sum_m |m, \text{in}\rangle\langle m, \text{out}|. \tag{3.2}$$

The orthonormality and completeness conditions imply that S is unitary

$$SS^\dagger = 1, \quad \text{and} \quad S^\dagger S = 1. \tag{3.3}$$

This is a result of the conservation of probability. We are concerned with matrix elements

$$\langle p_{f_1}, p_{f_2} \ldots, \text{out}|p_{i_1}, p_{i_2} \ldots, \text{in}\rangle = \langle p_{f_1}, p_{f_2} \ldots, \text{in}|S\,|p_{i_1}, p_{i_2} \ldots, \text{in}\rangle \tag{3.4}$$

that describe transitions of a configuration of particles moving with momenta $p_{i_1}, p_{i_2}, \ldots$ into another configuration with $p_{f_1}, p_{f_2} \ldots$. The states in Eq. (3.4) may be either of 'in' type or 'out' type, so henceforth we do not write these labels for brevity. If the particles do not interact at all in the processes, S is simply the identity operator. To isolate the interaction part of the S-matrix, one defines the T-matrix by

$$S = 1 + iT. \tag{3.5}$$

The unitarity condition Eq. (3.3) implies

$$-i(T - T^\dagger) = T^\dagger T. \tag{3.6}$$

Inserting a complete set of intermediate states into the right-hand-side (R.H.S.) of Eq. (3.6), we have

$$2\mathrm{Im}\langle f|T|i\rangle = \sum_n \int \Big[\prod_{i=1}^{i_n} \frac{d^3 p_i}{2p_i^0 (2\pi)^3}\Big] \langle f|T^\dagger|n\rangle\langle n|T|i\rangle, \tag{3.7}$$

where i_n is the number of particles in the intermediate state $|n\rangle$. When $i = f$ is a configuration of two particles with momenta p_1 and p_2, it gives the optical theorem

$$\mathrm{Im}T(p_1 p_2 \to p_1 p_2) = 2k_{\mathrm{cm}}\sqrt{s}\sigma_{\mathrm{total}}(p_1 p_2 \to \text{anything}), \tag{3.8}$$

where k_{cm} is the momentum of the particles in the center-of-mass (c.m.) frame and $\sqrt{s}$ is the total energy in the c.m. frame.

In this work, we only consider the scattering of two particles, both in the initial and final states,

$$a(p_1) + b(p_2) \to c(p_3) + d(p_4) \tag{3.9}$$

with p_i the four-momentum for the i^{th} particle. Given the three-momenta of the initial particles, there would be six degrees of freedom for the finial states, $\vec{p}_3$ and $\vec{p}_4$. However, due to the conservation of the four-momenta, the number of the degrees of freedom reduces to two, e.g. the polar angles (θ, ϕ) of the particle c in the c.m. Moreover, in the c.m. frame, taking the z-axis along the initial momentum of the particle a, then rotation invariance with respect to the z-axis requires that the elements of the T-matrix are independent on ϕ, i.e. $T(s, \theta)$. Here we have taken the explicit dependence of T on the total energy into account. Spanning the $T(s, \theta)$ in the θ-space in terms of the Legendre polynomials $P_\ell(\theta)$, we have

$$T(s, \theta) = \sum_{\ell=0}^{\infty} (2\ell + 1) P_\ell(\cos\theta) T_\ell(s), \tag{3.10}$$

where $T_\ell(s)$ is called the partial wave amplitude with angular momentum ℓ. The inverse of Eq. (3.10) can be obtained by making use of the orthonormality and completeness conditions of the Legendre polynomials,

$$T_\ell(s) = \frac{1}{2}\int_{-1}^{1} d\cos\theta P_\ell(\cos\theta) T(s, \theta). \tag{3.11}$$

Performing the partial wave decomposition on both sides of the unitarity condition Eq. (3.7), below the

threshold of intermediate states with more than two particles one has

$$-i(T_\ell(s)_{if} - T_\ell^*(s)_{if}) = \sum_n T_\ell(s)_{in} T_\ell^*(s)_{fn} \frac{|\vec{p}_n|^2}{4\pi\sqrt{s}} \theta(\sqrt{s} - m_{\text{thr,n}}), \tag{3.12}$$

where T_{if} represents $\langle f|T|i\rangle$, $|\vec{p}_n|$ is the modulus of the c.m. three-momentum for the intermediate state $|n\rangle$, and $m_{\text{thr,n}}$ is the threshold of the n-th channel. Due to time invariance, one has

$$\text{Im}T_\ell(s) = \sum_n T_\ell(s)_{in} T_\ell^*(s)_{nf} \frac{|\vec{p}_n|^2}{8\pi\sqrt{s}} \theta(\sqrt{s} - m_{\text{thr,n}}). \tag{3.13}$$

It can be written in a matrix form as

$$\text{Im}T_\ell(s) = T_\ell^\dagger(s)\rho(s)T_\ell(s), \tag{3.14}$$

with $\rho(s)$ a diagonal matrix with

$$\rho(s)_{ij} = \frac{|\vec{p}_n|^2}{8\pi\sqrt{s}} \delta_{ij} \theta(\sqrt{s} - m_{\text{thr,n}}). \tag{3.15}$$

In general, Eq. (3.14) is valid at higher energies, and $\rho(s)$ is the generalized phase space factor. It is related to the T-matrix via

$$\begin{aligned} \rho(s) &= (T_\ell^\dagger)^{-1} . \frac{T_\ell - T_\ell^\dagger}{2i} . (T_\ell)^{-1} \\ &= \frac{1}{2i}\left[(T_\ell^\dagger)^{-1} - (T_\ell)^{-1}\right] \\ &= -\text{Im}T_\ell^{-1}(s). \end{aligned} \tag{3.16}$$

The Eq. (3.16) is the basis for the K-matrix approach, which is defined as

$$T_\ell = (K^{-1} + i\rho)^{-1}, \tag{3.17}$$

hence $K^{-1} = \text{Re}(T_\ell^{-1})$.

The partial wave S-matrix is defined as

$$S_\ell = 1 + 2i\rho^{1/2} T_\ell \rho^{1/2}. \tag{3.18}$$

The unitarity condition Eq. (3.14) implies

$$S_\ell^\dagger S_\ell = 1. \tag{3.19}$$

Therefore, S_ℓ can be parameterized as

$$S_\ell(s) = e^{2i\delta_\ell(s)}. \tag{3.20}$$

For a multi-channel case, the matrix element $(S_\ell^\dagger S_\ell)_{ij} = \delta_{ij}$ means

$$|(S_\ell)_{i1}|^2 + |(S_\ell)_{i2}|^2 + \cdots + |(S_\ell)_{in}|^2 = 1. \tag{3.21}$$

Then one has $|(S_\ell)_{ii}|^2 \leq 1$, and it can be written as

$$(S_\ell)_{ii} = \eta_{\ell i} e^{2i\delta_{\ell i}}, \tag{3.22}$$

where $\eta_{\ell i}$ is called the inelasticity. For the elastic case, one has $\eta = 1$. For a two-channel process, the matrix S_ℓ can be written as

$$S_\ell = \begin{pmatrix} \eta_\ell e^{2i\delta_{\ell 1}} & i(1-\eta^2)^{1/2} e^{i(\delta_{\ell 1}+\delta_{\ell 2})} \\ i(1-\eta^2)^{1/2} e^{i(\delta_{\ell 1}+\delta_{\ell 2})} & \eta e^{2i\delta_{\ell 2}} \end{pmatrix}. \tag{3.23}$$

For elastic scattering one has $\eta = 1$ and unitarity of S-matrix is evident.

On the other hand, for the total energy below the inelastic threshold, the unitarity condition is

$$\begin{aligned} 2\mathrm{Im}\langle p_3 p_4|T|p_1 p_2\rangle &= \int \frac{d^4k_1 d^4k_2}{(2\pi)^2} \delta^{(+)}(k_1^2 - m_1^2)\delta^{(+)}(k_2^2 - m_2^2) \\ &\quad \times \delta^{(4)}(p_1 + p_2 - p_3 - p_4)\langle p_3 p_4|T|k_1 k_2\rangle \langle p_1 p_2|T|k_1 k_2\rangle^*. \end{aligned} \tag{3.24}$$

Above the threshold for inelastic scattering, a new term must be added to the R.H.S. of the Eq. (3.24) to include the extra intermediate states allowed by the energy conservation. It requires a corresponding change in the L.H.S., which implies that the elastic scattering matrix element has a singularity at each energy threshold for a new allowed intermediate state. This is a very valuable result of the unitarity of S-matrix.

Considering the scattering given by (3.9) once again, the conservation of four-momentum and the on-shell condition $p_i^2 = m_i^2$ implies that only three Lorentz scalars can be formed by the momenta p_i. They are the well known Mandelstam variables s, t and u, given by

$$\begin{aligned} s &= (p_1 + p_2)^2 = (p_3 + p_4)^2, \\ t &= (p_1 - p_3)^2 = (p_2 - p_4)^2, \\ u &= (p_1 - p_4)^2 = (p_2 - p_3)^2. \end{aligned} \tag{3.25}$$

Making use of the CPT theorem, we find that the following three processes share a common scattering amplitude,

$$\begin{aligned} a(p_1) + b(p_2) &\to c(p_3) + d(p_4), && (s-\text{channel}), \\ a(p_1) + \bar{c}(-p_3) &\to \bar{b}(-p_2) + d(p_4), && (t-\text{channel}), \\ a(p_1) + \bar{d}(-p_4) &\to c(p_3) + \bar{b}(-p_2), && (u-\text{channel}), \end{aligned} \tag{3.26}$$

where the bar over a particle represents the corresponding anti-particle. Expressed in terms of Mandelstam variables, we have the relation

$$\mathcal{M}_{ab\to cd}(s,t,u) = \mathcal{M}_{a\bar{d}\to c\bar{b}}(u,t,s) = \mathcal{M}_{a\bar{c}\to \bar{b}d}(t,s,u), \tag{3.27}$$

where $\mathcal{M}_{a_1a_2\to a_3a_4}(s,t,u)$ is the scattering amplitude for the process $a_1(p_1)a_2(p_2) \to a_3(p_3)a_4(p_4)$. The analysis of the number of degrees of freedom shows that the three Mandelstam variables are not independent, it follows that

$$s + t + u = \sum_{i=1}^{4} m_i^2.$$

In the c.m. frame, the three-momentum of incoming particles is

$$|\vec{p}_{1,2}|^2 = \frac{1}{4s}\Big(s-(m_1+m_2)^2\Big)\Big(s-(m_1-m_2)^2\Big). \tag{3.28}$$

The momentum transferred t is related to the scattering angle by

$$t = m_1^2 + m_3^2 - \frac{(s+m_1^2-m_2^2)(s+m_3^2-m_4^2)}{2s} - \frac{\cos\theta}{2s}\sqrt{\lambda(s,m_1^2,m_2^2)\lambda(s,m_3^2,m_4^2)}, \tag{3.29}$$

where $\lambda(a,b,c) = a^2+b^2+c^2-2ab-2ac-2bc$ is the Källén function. In order to define a single-valued t (and u) on the complex s plane, one has to introduce branch cuts with branch points $(m_1 \pm m_2)^2$ and $(m_3 \pm m_4)^2$. Usually, we set the brach cut from $-\infty$ to $\max\{(m_1-m_2)^2,(m_3-m_4)^2\}$ and from $\min\{(m_1+m_2)^2,(m_3+m_4)^2\}$ to $+\infty$ along the real axis. If there exist discrete intermediate states, i.e. stable single states, they will exhibit themselves as poles on the complex s plane. The continuous spectra, intermediate multi-particle states, would contribute to the S-matrix elements with branch cuts.

With branch cuts in the s plane, it is necessary to decide which limit on approaching to the branch cut gives the physical quantities. The perturbation theory shows that the physical amplitudes are given by the limit on the right-hand cut from the upper-half s plane

$$T_\ell(s)_{\text{physical}} = \lim_{\epsilon\to 0+} T_\ell(s+i\epsilon). \tag{3.30}$$

Considering a single-channel process, below the inelastic threshold, we have

$$S_\ell = 1 + 2i\rho(s)T_\ell(s), \tag{3.31}$$

where

$$\rho(s) = \sqrt{1-\frac{(m_1+m_2)^2}{s}}.$$

In the region $(m_1-m_2)^2 < s < (m_1+m_2)^2$, the T_ℓ are real. One then can define a complex function $T_\ell(s)$ on the whole s-plane with analytic continuation. The unitarity condition requires that $T_\ell(s)$ has an imaginary part for $s > (m_1+m_2)^2$ along the real axis, i.e. a branch cut from $(m_1+m_2)^2$ to $+\infty$. It is the result of the unitarity of S-matrix and the cut is usually called the unitary cut, or right-hand cut. From the partial wave decomposition

$$T_\ell(s) = \frac{1}{s-(m_1+m_2)^2}\int_{(m_1+m_2)^2-s}^{0} dt P_\ell\Big(1+\frac{2t}{s-(m_1+m_2)^2}\Big)T(s,t), \tag{3.32}$$

we see that when $t > (m_1+m_2)^2$, that is $s < (m_1-m_2)^2$, $T(s,t)$ has imaginary parts. It leads to a branch cut $s < (m_1-m_2)^2$ for the $T_\ell(s)$, called the left-hand cut. As a result, the left-hand cut is regarded as 'unphysical cut' compared with the 'physical cut', right-hand cut. We make the analytic continuation from the unitary cut, which is caused by the phase space factor $\rho(s)$, $\rho(s^*) = -\rho^*(s)$. We specify the physical sheet as the first Riemann sheet, starting from the upper half of the physical sheet to the lower half by crossing over the real axis where $T_\ell(s)$ has only real parts. Denoting the number of Riemann sheets with the superscripts, the analytic continuation requires

$$T_\ell^I(s-i\epsilon) = T_\ell^{II}(s+i\epsilon) \tag{3.33}$$

across the unitary cut. Then the Schwartz reflection principle implies that the unitarity condition reads

$$T_\ell^I(s+i\epsilon) - T_\ell^{II}(s+i\epsilon) = 2iT_\ell^I(s+i\epsilon)\rho(s+i\epsilon)T_\ell^{II}(s+i\epsilon), \tag{3.34}$$

from which one can obtain

$$T_\ell^{II}(s) = \frac{T_\ell^I(s)}{S_\ell^I(s)}, \tag{3.35}$$

and

$$\begin{aligned} \frac{T_\ell^{II}(s)}{T_\ell^I(s)} &= \frac{T_\ell^I(s) - T_\ell^I(s) + T_\ell^{II}(s)}{T_\ell^I(s)} = 1 + 2i\rho(s)T_\ell^{II}(s) \\ = \quad S_\ell^{II}(s) &= \frac{1}{S_\ell^I(s)}. \end{aligned} \tag{3.36}$$

The zeros of the S-matrix on the first Riemann sheet correspond to poles on the second sheet, and vice versa.

The above discussion can be generalized to multi-channel processes. Taking a double-channel system with channel 1 ab and channel 2 cd for example, one has

$$\begin{aligned} S_{11} &= 1 + 2i\rho_1 T_{11}, \\ S_{22} &= 1 + 2i\rho_2 T_{22}, \\ S_{12} &= 2i\sqrt{\rho_1\rho_2}T_{12}. \end{aligned} \tag{3.37}$$

Let us assume that opening the channel 2 needs more energy, i.e. $m_c+m_d > m_a+m_b$. When $s > (m_a+m_b)^2$, the intermediate states $|a,b\rangle$ could be on-shell, and thus leads to imaginary part for T-matrix elements. $s > (m_a + m_b)^2$ corresponds to a right-hand cut.For the same reason, there is an extra right-hand cut for $s > (m_c + m_d)^2$.Each time one crosses over the right-hand cut one 'walks' from a Riemann sheet to the next one. As a consequence, one gets four Riemann sheets, which can be labelled by the sign of the $\rho_i(s)$ along the right hand cuts, e.g.

$$\begin{aligned} &\rho_1 > 0, \quad \rho_2 > 0, \qquad T^I(s), \\ &\rho_1 < 0, \quad \rho_2 > 0, \qquad T^{II}(s), \\ &\rho_1 < 0, \quad \rho_2 < 0, \qquad T^{III}(s), \\ &\rho_1 > 0, \quad \rho_2 < 0, \qquad T^{IV}(s). \end{aligned} \tag{3.38}$$

So far we have extended the amplitude $T(s,t,u)$, initially defined on three disjoint physical regions, to the whole complex plane by making using of analytic continuation. To accomplish it, one needs the knowledge of the singularities of $T(s,t,u)$ as a function of two of complex variables, e.g. s and t. The singularities are always caused by on-shell intermediate states. The singularity will be a branch cut if the intermediate state is a multi-particle state or a simply pole is the intermediate state is a single-particle state. That unstable particles (resonances) should be represented by complex poles was first suggested by Møller in 1946 [78]. It is worth mentioning that due to the Schwartz reflection principle, $T_\ell^*(s) = T_\ell(s^*)$, poles in the complex plane occur in complex conjugate positions.

Experimental data frequently show peaks, bumps or dips when the cross sections are displayed as functions of invariant energy. The most familiar way to interpreting these situations is to suppose that

each peak is due to a resonance and that the phase shift δ_ℓ increases rapidly through around $\pi/2$ at the resonance energy.

In the physical Riemann sheet, there can exist only poles on the real axis below the lowest threshold, the bound state. Note that a pole on the real axis above the first threshold violates the unitarity condition, Eq. (3.14), since it would imply $\infty = \infty^2$ which makes no sense. However, on the unphysical sheets, there can be poles on the whole complex plane. If a pole is located above the threshold, it would be unstable and with an imaginary part describing its width due to the allowed decay phase space. A simple picture [79] of why poles off the real axis only can be located on the unphysical sheets can be demonstrated from the propagator of a resonance in Breit-Wigner representation,

$$\frac{1}{s - M_R^2 + iM_R\Gamma_R(s)}, \tag{3.39}$$

with $\Gamma_R(s)$ the width of the resonance for $s = M_R^2$, and note that $\Gamma_R(s) \propto p^{2\ell+1}$ with ℓ the spin of the resonance. If $s \to M_R^2 \pm i\epsilon$, the term $iM_R\Gamma_R$ develops an imaginary part in the physical sheet which goes as $\pm iM_R\Gamma_R(M_R^2)$ so that it cannot be cancelled by the imaginary part of s since they both have the same sign. Only if it is on the unphysical sheet, the sign is opposite and the cancellation is possible. The existence of pole off the real axis spoils causality.

Considering a pair of poles P and P', e.g. $s_P = s_0 \pm i\gamma$ with $\gamma > 0$, on the second sheet. Since below the inelastic threshold we have $T_\ell^{II}(s - i\epsilon) = T_\ell^I(s + i\epsilon)$, the pole $s_0 - i\gamma$ is closer to the physical region. At the region near s_P, the $T_\ell(s)$ has the form of

$$T_\ell(s) \approx \frac{T_P}{s - s_0 + i\gamma}, \tag{3.40}$$

which has the same form as the Breit-Wigner formula. From Eq. (3.40) it is clear that δ_ℓ,

$$\delta_\ell = \arctan \frac{\mathrm{Im}T_\ell}{\mathrm{Re}T_\ell} \tag{3.41}$$

changes $\pi/2$ as s passes through s_P.

3.2 Lippmann-Schwinger equation

Chiral perturbation theory has been proven to be very successful in describing the static properties and the low-energy behavior of the light pseudoscalar meson octet. The standard ChPT is organized in a double expansion in terms of small momenta and light quark masses, it is expected to work only well at the low energies. It is clear that the standard chiral series, keeping a finite order, can not give an analytical structure for the possible resonances, which is absolutely a nonperturbative effect. One way to overcome this problem is to iterate the lowest order potential in the Lippman-Schwinger equation. For simplicity, we consider the scattering of two spinless particle masses m_1, m_2 and initial (final) momenta p, q (p', q'). The lowest interacting potential is denoted by $V(p, p', P)$, with P the total momentum $P = p + q = p' + q'$. Then the Lippmann-Schwinger equation for the full scattering amplitude $T(p, p', P)$ reads

$$T(p, p', P) = V(p, p', P) + \int \frac{d^4l}{(2\pi)^4} V(p, l, P)G(l, P)T(l, p', P), \tag{3.42}$$

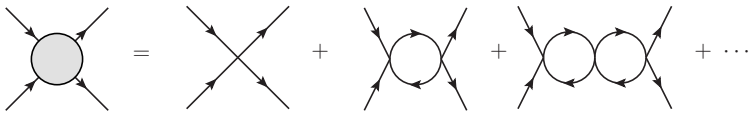

Figure 3.1: Diagrammatic illustration for the Lippmann-Schwinger equation.

where

$$G(l,P) = i\frac{1}{l^2 - m_1^2 + i\epsilon}\frac{1}{(P-l)^2 - m_2^2 + i\epsilon}$$

is the two-particle propagator. For coupled-channel cases, it should be understood in the matrix form, for which $G(l,P) = \mathrm{diag}\{G_i(l,P)\}$ with i the channel index. It is always written in a shorthand notation

$$T = V + VGT$$

for brevity. Clearly, Eq. (3.42) is an iterative integral equation and can be expanded in powers of V,

$$T = V + VGV + VGVGV + \ldots, \tag{3.43}$$

which is diagrammatically shown in Fig. 3.1. The solution for T is nothing else than the infinite summation of a bubble chain in the s-channel. It is clear that this method does not generate all the diagrams. Loops in the t- or u-channel are not taken into account. However, the scheme has proven very successful, which indicates that the relevant infinite series needed to reproduce the structure of the T-matrix is taken into account in Eq. (3.43). This can be explained by that the singularities associated to t-(or u)channel are sufficiently far away from the physical region.

In principle, one has to solve the integrals in Eq. (3.43) by taking V off shell. However, at least when dealing with an S-wave, we only need the on-shell information for approximation. The interaction kernel $V(p,p',P)$ has the form of

$$\begin{aligned} V(p,p',P) &= V_{\rm on}(s) + (p^2 - m_1^2)V_{\rm off}^{(1)}(s) + (q^2 - m_2^2)V_{\rm off}^{(2)}(s) \\ &\quad + (p'^2 - m_1^2)V_{\rm off}^{(3)}(s) + (q'^2 - m_2^2)V_{\rm off}^{(4)}(s). \end{aligned} \tag{3.44}$$

Here the interaction kernel is restricted to purely linear off-shell terms. The same decomposition applies to T. Making use of Eq. (3.42), one has

$$\begin{aligned} T_{\rm on} &= V_{\rm on} + i\int\frac{d^4l}{(2\pi)^4}\frac{V_{\rm on}T_{\rm on}}{(l^2 - m_1^2 + i\epsilon)((P-l)^2 - m_2^2 + i\epsilon)} \\ &\quad + i\int\frac{d^4l}{(2\pi)^4}\frac{T_{\rm on}V_{\rm off}^{(3)} + T_{\rm off}^{(1)}V_{\rm on} + (l^2 - m_1^2)T_{\rm off}^{(1)}V_{\rm off}^{(3)}}{(P-l)^2 - m_2^2 + i\epsilon} \\ &\quad + i\int\frac{d^4l}{(2\pi)^4}\frac{T_{\rm on}V_{\rm off}^{(4)} + T_{\rm off}^{(2)}V_{\rm on} + ((P-l)^2 - m_2^2)T_{\rm off}^{(2)}V_{\rm off}^{(4)}}{l^2 - m_1^2 + i\epsilon} \\ &\quad + i\int\frac{d^4l}{(2\pi)^4}\Big(T_{\rm off}^{(1)}V_{\rm off}^{(4)} + T_{\rm off}^{(2)}V_{\rm off}^{(3)}\Big). \end{aligned} \tag{3.45}$$

In dimensional regularization, it can be evaluated as

$$\begin{aligned} T_{\rm on} &= V_{\rm on} + V_{\rm on} G(s) T_{\rm on} \\ &+ (s - m_1^2 + m_2^2) T_{\rm off}^{(1)} V_{\rm off}^{(3)} \Delta(m_2^2) + (s + m_1^2 - m_2^2) T_{\rm off}^{(2)} V_{\rm off}^{(4)} \Delta(m_1^2), \end{aligned} \tag{3.46}$$

where $\Delta(m^2) = \int \frac{d^4l}{(2\pi)^4} \frac{i}{l^2 - m^2 + i\epsilon}$. The chiral logarithms ($\Delta(m^2)$) reflects that the expansion in powers of small quark masses is not an ordinary Taylor series, which cannot be absorbed into the redefinition of the low energy constants of the most general Lagrangian at tree level in principle. But if we are not interested in the Goldstone mass dependence of the amplitudes, the logarithms can be absorbed into the redefinition of coupling constants. And when it comes to the phenomenology of scattering in a nonperturbative region one is not interested in the behavior of the amplitudes when approaching the chiral limit, so the contribution from the chiral logarithms are usually numerically small. One may argue that the off-shell effects are compensated numerically by adjusting the low-energy constants. Dropping the off-shell terms, the second line terms in Eq. (3.46), we are left with the algebraic form of the Lippmann-Schwinger equation, the so-called one-shell approximation,

$$T_{\rm on}(s) = V_{\rm on}(s) + V_{\rm on}(s) G(s) T_{\rm on}(s), \tag{3.47}$$

or

$$T_{\rm on}(s) = \frac{1}{1 - V_{\rm on}(s) G(s)} V_{\rm on}(s), \tag{3.48}$$

with $G(s)$ the scalar loop integral

$$G(s) = \int \frac{d^4l}{(2\pi)^4} \frac{i}{(l^2 - m_1^2 + i\epsilon)((P-l)^2 - m_2^2 + i\epsilon)}, \quad s = P^2. \tag{3.49}$$

So far we have not considered the renormalization of Eq. (3.48). The loop integrals in Eq. (3.46) are divergent. In principle, the divergence will be absorbed by the suitable counter terms. However, summing bubble loops in s-channel violates the crossing symmetry and so that the renormalization of the Lippmann-Schwinger equation cannot be accomplished by local effective Lagrangians which can only produce counter terms that fulfil crossing symmetry [80]. However, the divergences of loops can be removed by redefining the interaction kernel V properly. Let λ_G denote the infinite part of G, i.e. $G = G^r + \lambda_G$, decomposing the V as

$$V_{\rm on} = V_{\rm on}^r + \lambda_V, \tag{3.50}$$

with

$$\lambda_V = V_{\rm on} \lambda_G V_{\rm on} (1 + \lambda_G V_{\rm on})^{-1}, \tag{3.51}$$

it is easy to obtain

$$T_{\rm on}^r(s) = V_{\rm on}^r(s) + V_{\rm on}^r G^r(s) T_{\rm on}^r. \tag{3.52}$$

Instead of being absorbed by local counter terms, the divergences of loops is cancelled by an appropriate redefinition of interaction kernel V.

3.3 The Inverse Amplitude Method

Another attempt to extend the chiral potentials to the nonperturbative regime is the Inverse Amplitude Method (IAM) [81–83]. The approach is successful in reproducing low-energy behavior and poles in the amplitudes associated to the ρ and K^* in the vector channels and the σ in the scalar channel. Chiral partial wave amplitudes are obtained as an expansion $t(s) = t_2(s) + t_4(s) + t_6(s) + \ldots$, where $t_n \sim O(p^{2n})$. It satisfies elastic unitarity perturbatively:

$$\mathrm{Im}\, t_2(s) = 0, \quad \mathrm{Im}\, t_4(s) = \rho(s) t_2(s)^2, \quad \mathrm{Im}\, t_6(s) = 2\rho(s) t_2(s) \mathrm{Re}\, t_4(s), \ldots \tag{3.53}$$

To one-loop order, one has

$$\begin{aligned} t_2(s) &= a_0 + a_1 s, \\ t_4(s) &= b_0 + b_1 s + b_2 s^2 \\ &+ \frac{s^3}{\pi} \int_{RC} ds' \frac{\mathrm{Im}\, t_4(s')}{s'^3 (s' - s - i\epsilon)} + LC, \end{aligned} \tag{3.54}$$

where RC and LC represent the right-hand cut and left-hand cut, respectively. Since $t_2(s)$ is real, $g(s) = t_2(s)^2/t(s)$ has the same cuts. A dispersion relation for $g(s)$ reads

$$\begin{aligned} g(s) &= g(0) + g'(0)s + \frac{1}{2} g''(0) s^2 \\ &+ \frac{s^3}{\pi} \int_{RC} ds' \frac{\mathrm{Im}\, g(s')}{s'^3 (s' - s - i\epsilon)} + LC(G) + PC(s), \end{aligned} \tag{3.55}$$

where PC is the pole contribution due to the possible zeros of $t(s)$. In the elastic approximation, since

$$\mathrm{Im} \frac{1}{t(s)} = \mathrm{Im} \frac{t(s)^*}{|t(s)|^2} = -\frac{\mathrm{Im}\, t(s)}{|t(s)|^2} = -\rho(s), \tag{3.56}$$

one has

$$\mathrm{Im}\, g(s) = -\rho(s) t_2(s)^2 = -\mathrm{Im}\, t_4(s) \tag{3.57}$$

on the right-hand cut. In addition, in the low energy region,

$$g(s) = \frac{t_2^2}{t_2 + t_4 + \ldots} \simeq t_2 - t_4 + \ldots, \tag{3.58}$$

one can approximate

$$\mathrm{Im}\, g(s) \simeq -\mathrm{Im}\, t_4(s) \tag{3.59}$$

on the left cut. Making use of Eq. (3.58), one finds that $g(s)$ can be recast as:

$$\begin{aligned} g(s) &\simeq t_2(0) + t_2'(0)s - t_4(0) - t_4'(0)s - t_4''(0)\frac{s^2}{2} - \frac{s^3}{\pi} \int_{RC} ds' \frac{\mathrm{Im}\, t_4(s')}{s'^3 (s' - s)} - LC(t_4) \\ &= t_2(s) - t_4(s), \end{aligned} \tag{3.60}$$

here we have neglected the pole contribution which is of higher order and only numerically relevant below threshold. Therefore, we arrive at the elastic formula for the IAM

$$t(s) \simeq \frac{t_2^2(s)}{t_2(s) - t_4(s)}. \tag{3.61}$$

It can be extended to higher orders of ChPT [84], e.g. to NNLO,

$$t(s) \simeq \frac{t_2^2(s)}{t_2(s) - t_4(s) + t_4^2(s)/t_2(s) - t_6(s)}. \tag{3.62}$$

The generalization of the IAM to coupled channels was given in Ref. [85]. We denote the coupled-channel amplitude by a matrix T. Expanding T^{-1} in powers of p^2, one has

$$\begin{aligned} T &\simeq T_2 + T_2 + \ldots, \\ T^{-1} &\simeq T_2^{-1} \cdot (1 + T_4 \cdot T_2^{-1})^{-1} \simeq T_2^{-1} \cdot (1 - T_4 \cdot T_2^{-1}). \end{aligned} \tag{3.63}$$

The inversion of T_2 may not be invertible. In order to avoid T^{-1}, we start from Eq. (3.17) by formally multiplying by $T_2 \cdot T_2^{-1}$ on the right and $T_2^{-1} \cdot T_2$ on the left,

$$T = T_2 \cdot (T_2 \cdot \mathrm{Re}\, T^{-1} \cdot T_2 + i T_2 \cdot \rho \cdot T_2)^{-1} \cdot T_2. \tag{3.64}$$

Using Eq. (3.63), we find

$$T_2 \cdot \mathrm{Re}\, T^{-1} \cdot T_2 \simeq T_2 - \mathrm{Re}\, T_4, \tag{3.65}$$

and recalling that $\mathrm{Im}\, T_4 = -T_2 \cdot \rho \cdot T_2$ we finally obtain the IAM formula for coupled-channels

$$T = T_2 \cdot (T_2 - T_4)^{-1} \cdot T_2. \tag{3.66}$$

3.4 The N/D method

After some intuitive discussions, a more thorough investigation of loop effects to generate imaginary parts will be given in this section. Making use of the N/D method [86], we will derive the most general structure of an arbitrary partial-wave amplitude when unphysical cuts are neglected. It is expected that the unphysical cuts can be considered small for the amplitudes where resonances in the s- channel appear, e.g. the case of the ρ and K^* resonances in the P-wave $\pi\pi$ and $K\pi$ scattering, respectively.

For simplicity, we first consider the elastic case. In general, a partial-wave amplitude $T_\ell^I(s)$, with I the isospin, has two kinds of cuts, the right-hand cut and an unphysical cut. The right-hand cuts are required by the unitarity and the unphysical cuts are caused by the crossing symmetry. We already have derived (see Eq. (3.56)),

$$\mathrm{Im}\, T^{-1} = -\rho(s) \tag{3.67}$$

for $s > s_{\mathrm{thr}} = (m_1 + m_2)^2$ and

$$\rho(s) = \frac{p}{8\pi\sqrt{s}}, \quad \text{with} \quad p = \frac{\lambda^{1/2}(s, m_1^2, m_2^2)}{2\sqrt{s}} \tag{3.68}$$

the c.m. three momentum, and the isospin and angular momentum indices are suppressed. For the process of type $a + a \to a + a$, there is only a left-hand cut for $s < 0$. However, for the process of type $a + b \to a + b$, apart from the left-hand cut $s < (m_a - m_b)^2$ there also exists a circular cut for $|s| = |m_a^2 - m_b^2|$. In this work, we only consider the left-hand cuts. If we work in the complex p^2-plane, all cuts will be linear cuts and only the left- and right-hand cuts appear. In the N/D method, a partial wave amplitude $T_\ell(s)$ is expressed as a quotient of two functions,

$$T_\ell(s) = \frac{N_\ell(s)}{D_\ell(s)}, \tag{3.69}$$

where the denominator $D_\ell(s)$ collects the right-hand cuts and the numerator $N_\ell(s)$ encodes the unphysical cuts. The partial wave amplitude $T_\ell(s)$ near the threshold behaves as $p^{2\ell} \equiv \nu^\ell$. Define a new quantity

$$T'_\ell(s) = \frac{T_\ell(s)}{\nu^\ell}, \tag{3.70}$$

and it can be written in the form of

$$T'_\ell(s) = \frac{N'_\ell(s)}{D'_\ell(s)}. \tag{3.71}$$

It is easy to find that

$$\begin{aligned}
&\operatorname{Im} D'_\ell = \operatorname{Im} T'^{-1}_\ell N'_\ell = -\rho(s) N'_\ell \nu', && s > s_{\text{thr}},\\
&\operatorname{Im} D'_\ell = 0, && s < s_{\text{thr}},\\
&\operatorname{Im} N'_\ell = \operatorname{Im} T'_\ell D'_\ell, && s < s_{\text{left}},\\
&\operatorname{Im} N'_\ell = 0, && s > s_{\text{left}}.
\end{aligned} \tag{3.72}$$

Employing a dispersion relation, one has

$$\begin{aligned}
D'_\ell(s) &= \sum_{m=0}^{n-1} \bar{a}_m s^m - \frac{(s-s_0)^n}{\pi} \int_{s_{\text{thr}}}^{\infty} ds' \frac{\nu(s')^\ell \rho(s') N'_\ell(s')}{(s'-s)(s'-s_0)^n},\\
N'_\ell(s) &= \sum_{m=0}^{n-\ell-1} \bar{a}'_m s^m + \frac{(s-s_0)^{n-\ell}}{\pi} \int_{-\infty}^{s_{\text{left}}} ds' \frac{\operatorname{Im} T_\ell(s') D'_\ell(s')}{\nu(s')^\ell (s'-s_0)^{n-\ell}(s'-s)},
\end{aligned} \tag{3.73}$$

where n is the number of subtractions needed so that

$$\lim_{s\to\infty} \frac{N'_\ell}{s^{n-\ell}} = 0. \tag{3.74}$$

Eqs. (3.73) constitutes a system of integral equations, in which the input is given by $\operatorname{Im} T_\ell(s)$ along the left hand cut. However, they are not the most general solutions of Eqs. (3.72) since we have not considered the possible zeros of T_ℓ, which can be included through poles in D'_ℓ (CDD poles). Following Ref. [87], we write along the real axis

$$\operatorname{Im} D'_\ell(s) = \frac{d\lambda(s)}{ds}. \tag{3.75}$$

Then one has the solution

$$\lambda(s) = \sum_i \lambda(s_i)\theta(s - s_i) - \int_{s_{\rm thr}}^{s} \nu(s')^\ell \rho(s') N'_\ell(s') ds', \tag{3.76}$$

with $\theta(s)$ the usual Heaviside function and s_i the points along the real axis where $T'_\ell(s_i) = 0$.

It follows that

$$\begin{aligned}
D'_\ell(s) &= \sum_{m=0}^{n-1} \bar{a}_m s^m - \frac{(s-s_0)^n}{\pi} \int_{s_{\rm thr}}^{\infty} ds' \frac{\nu(s')^\ell \rho(s') N'_\ell(s')}{(s'-s)(s'-s_0)^n} \\
&\quad + \frac{(s-s_0)^n}{\pi} \int_{s_{\rm thr}}^{\infty} ds' \frac{\sum_i \lambda(s_i)\delta(s'-s_i)}{s'-s)(s'-s_0)^n} \\
&= \sum_{m=0}^{n-1} \bar{a}_m s^m - \frac{(s-s_0)^n}{\pi} \int_{s_{\rm thr}}^{\infty} ds' \frac{\nu(s')^\ell \rho(s') N'_\ell(s')}{(s'-s)(s'-s_0)^n} \\
&\quad + \sum_i \frac{\lambda(s_i)}{\pi(s_i-s_0)^n} \frac{(s-s_0)^n}{s_i - s} \\
&= -\frac{(s-s_0)^n}{\pi} \int_{s_{\rm thr}}^{\infty} ds' \frac{\nu(s')^\ell \rho(s') N'_\ell(s')}{(s'-s)(s'-s_0)^n} \\
&\quad + \sum_{m=0}^{n-1} \tilde{a}_m s^m + \sum_i \frac{\tilde{\gamma}_i}{s - s_i}.
\end{aligned} \tag{3.77}$$

Eq. (3.77) can also be obtained by making use of Cauchy theorem for complex integration and allowing for the presence of poles D'_ℓ inside and along the integration contour. At the moment, we neglect the left-hand cut. Then one has:

$$N'_\ell(s) = \sum_{m=0}^{n-\ell-1} \tilde{a}'_m s^m = C \prod_{i=1}^{n-\ell-1} (s - s_i). \tag{3.78}$$

Dividing N'_ℓ and D'_ℓ by Eq. (3.78), one arrives at that

$$\begin{aligned}
T'_\ell(s) &= \frac{1}{D'_\ell(s)}, \\
N'_\ell(s) &= 1, \\
D'_\ell(s) &= -\frac{(s-s_0)^{\ell+1}}{\pi} \int_{s_{\rm thr}}^{\infty} ds' \frac{\nu(s')^\ell \rho(s')}{(s'-s)(s'-s_0)^{\ell+1}} + \sum_{m=0}^{\ell} a_m s^m + \sum_i \frac{R_i}{s - s_i}.
\end{aligned} \tag{3.79}$$

The CDD poles are associated to the possibility of elementary particles not originating from a given potential or forces between the scattering states [88]. An advantage of the N/D method is that we have a dispersive representation where the right cut of the inverse amplitude is treated exactly within the elastic approximation. It is free of the $s = 0$ singularities of the K-matrix, since the right cut structure is that of the dispersive relation, whose imaginary part coincides with $\rho(s)$ on the real axis above threshold. If the left hand cut is taken into account, it can be introduced perturbatively through $N_\ell(s)$.

In QCD, we split the subtraction constants a_m of Eq. (3.79) into two pieces [89]

$$a_m = a_m^L + a_m^{SL}(s_0), \tag{3.80}$$

where the term a_m^L will go as N_c and a_m^{SL} is $O(1)$ in the QCD $1/N_c$ expansion, due to that the meson-meson scattering amplitudes go as N_c^{-1}. In addition, the integral in Eq. (3.79) is $O(1)$, same order of a_m^{SL}. It follows that in $N_c \to \infty$ limit,

$$D_\ell'^{\infty}(s) = \sum_{m=0}^{\ell} a_m^L s^m + \sum_i \frac{R_i^\infty}{s - s_i}, \tag{3.81}$$

where R_i^∞ is the leading part of R_i. It is clear that Eq. (3.81) represents tree level structures, contact and pole terms, which have nothing to do with potential scattering which is large N_c suppressed.

Introducing the notation

$$T_\ell^\infty(s) = \nu^\ell \Big(\sum_{m=0}^{\ell} a_m^\ell s^m + \sum_i \frac{R_i^\infty}{s - s_i} \Big), \tag{3.82}$$

and defining $g_\ell(s)$ by

$$g_\ell(s)\nu^\ell = \sum_{m=0}^{\ell} a_m^{SL}(s_0) s^m - \frac{(s - s_0)^{\ell+1}}{\pi} \int_{s_{\rm thr}}^{\infty} ds' \frac{\nu(s')^\ell \rho(s')}{(s' - s)(s' - s_0)^{\ell+1}}. \tag{3.83}$$

We arrive at

$$T_\ell(s) = \left(1/T_\ell^\infty(s) + g_\ell(s)\right)^{-1}. \tag{3.84}$$

The T_ℓ^∞ corresponds to the tree-level structures before unitarization. The unitarization is accomplished through the function $g_\ell(s)$. The formalism can be easily generalized to scattering processes with coupled-channel cases by employing the usual matrix notation [89].

In Ref. [90], a general scheme which can be applied to any order in the chiral calculations was represented. It is started from the the fact that unitarity implies that the inverse of a partial wave amplitude satisfies

$$\mathrm{Im}\, T^{-1}(s)_{ij} = -\rho(s)_i \delta_{ij} \tag{3.85}$$

with the subscripts i and j referring to the physical channels. Hence one can write a once-subtracted dispersion relation for the $\mathrm{Im}\, T_\ell^{-1}(s)$, which is

$$\begin{aligned} T^{-1}(s)_{ij} &= \mathcal{T}^{-1}(s)_{ij} + \Big(-\tilde{a}_i(s_0)\delta_{ij} + \frac{s - s_0}{\pi} \int_{s_{\rm thr}}^{\infty} ds' \frac{\mathrm{Im}\, T^{-1}(s')_{ij}}{(s' - s)(s' - s_0)} \Big) \\ &= \mathcal{T}^{-1}(s)_{ij} - \delta_{ij} \Big(\tilde{a}_i(s_0) + \frac{s - s_0}{\pi} \int_{s_{\rm thr}}^{\infty} ds' \frac{\rho(s')_i}{(s' - s)(s' - s_0)} \Big) \\ &= \mathcal{T}^{-1}(s)_{ij} + g(s)_i \delta_{ij}. \end{aligned} \tag{3.86}$$

Here $\mathcal{T}^{-1}(s)_{ij}$ represents the contributions from local and pole terms as well as crossed channel dynamics

but without the right-hand cut and $g(s)_i$ is the familiar scalar loop integral:

$$\begin{aligned} g(s)_i &= \int \frac{d^4 l}{(2\pi)^4} \frac{i}{(l^2 - M_i^2 + i\epsilon)((P-l)^2 - m_i^2 + i\epsilon)} \\ &= \frac{1}{16\pi^2}\Big\{a_i(\mu) + \ln\frac{m_i^2}{\mu^2} + \frac{M_i^2 - m_i^2 + s}{2s}\ln\frac{M_i^2}{m_i^2} + \frac{q_i}{\sqrt{s}}\ln\frac{m_i^2 + M_i^2 - s - 2\sqrt{s}q_i}{m_i^2 + M_i^2 - s + 2\sqrt{s}q_i}\Big\}, \end{aligned} \tag{3.87}$$

where M_i and m_i are the masses of the two particles in the state i and q_i is the modulus of the c.m. three-momentum. From Eq. (3.86) one gets the T-matrix in matrix form as:

$$T(s) = \left(\mathcal{T}^{-1} + g(s)\right)^{-1} = \left(1 + \mathcal{T}\cdot g(s)\right)^{-1}\cdot\mathcal{T}. \tag{3.88}$$

CHAPTER 4

Effective generating functional to next-to-next-to leading order

In Chapter 2 we have constructed the leading terms of the chiral Lagrangians for Goldstone bosons and spinless matter fields, which are obtained by organizing the underlying Lagrangian in a chiral series at the classical level. As we know, the classical field theory associated with a given Lagrangian is equivalent to the set of tree-level diagrams of the corresponding quantum field theory. Disregarding the loop graphs would violate unitarity. General power counting [14] and Sec. 2.1.1 show that graphs containing n loops (each of loop containing Goldstone propagators) are suppressed by p^{2n} in comparison to tree graphs. The loop graphs therefore do not modify the low energy behavior at classical level. However, to a specific order, one may need to consider the loop graphs generated by the Lagrangian of lower orders, e.g. at order p^4 one needs to take into account both tree-level graphs generated by Lagrangian of order p^4 and the one-loop graphs generated by the leading order Lagrangian, i.e. of order p^2. In terms of the Feynman path integral the above prescription can be written in the form

$$e^{iZ} = e^{i\int dx\mathcal{L}_4}\int [dU]e^{i\int dx\mathcal{L}_2}, \tag{4.1}$$

where the integral over the field $U(x)$ is calculated in one-loop approximation. The explicit forms of the Lagrangians $\mathcal{L}_2$ and $\mathcal{L}_4$ are given in Eqs. (2.87), (2.97) or (2.105).

In this chapter, we will employ the background field method to study the effective generating functional of ChPT for spinless matter fields living in the $SU(N)$ fundamental representation up to leading one-loop order, i.e. $O(p^3)$. In general, loop graphs are associated with UV divergences, which need to be renormalized. The divergences can be calculated using dimensional regularization which preserves the relevant symmetries. For purely Goldstone bosonic ChPT, one finds that counterterms which absorb the divergences and renormalize the theory are of order $O(p^4)$. However, in relativistic ChPT for matter fields (e.g. baryonic ChPT), the one-loop diagrams need to be renormalized by LECs from different orders. It is associated with the power counting breaking issue of the ChPT for matter fields due to the presence of the new energy scale provided by the matter field mass in chiral limit. Apart from the UV divergences, the finite parts of loop graphs contribute to various chiral orders. The terms violating the power counting, that is power counting breaking terms, are proven to be polynomials of chiral quantities and therefore can be absorbed by the redefinition of the LECs. With the renormalized one-loop effective generating functional, we will provide a systematic subtraction of the power counting breaking terms at the Lagrangian level in Sec. 4.3.

4.1 One-loop effective generating functional of ChPT for spinless matter fields

We will consider the case of the interaction between Goldstone bosons with a single matter field. The generating functional for the correlation functions of quark currents between single matter fields is defined via

$$e^{iZ[j,J,J^\dagger]} = \int [d\phi][dP][dP^\dagger] \exp i\left\{S_\phi + S_{\phi P} + \int d^4x \left(PJ^\dagger + JP^\dagger\right)\right\}, \tag{4.2}$$

where $S_\phi = \int d^4x\, \mathcal{L}_\phi$ and $S_{\phi P} = \int d^4x\, \mathcal{L}_{\phi P}$ denote the Goldstone boson and the ϕP chiral actions, respectively, J and $J^\dagger$ are the sources coupled to the spinless matter fields, and j denotes various external fields (vector v_μ, axial a_μ, scalar s and pseudoscalar p). As usual, the quark mass terms will be included in the external scalar source s. The effective chiral Lagrangians can be expanded as

$$\mathcal{L}_\phi = \sum_{n=1}^{\infty} \mathcal{L}_\phi^{(2n)}, \qquad \mathcal{L}_{\phi P} = \sum_{n=1}^{\infty} \mathcal{L}_{\phi P}^{(n)}, \tag{4.3}$$

where the superscripts denote the chiral dimension.

With the power counting scheme given in Sec. 2.1.1, up to order $O(p^3)$ the effective generating functional of ChPT for spinless matter fields contains three different classes of contributions [1]: (a) the purely Goldstone bosonic Lagrangian to $O(p^4)$, i.e. Eqs. (2.87), (2.97) or (2.105)[2]; (b) the Lagrangian for spinless matter fields to $O(p^3)$, i.e. Eqs. (2.147); (c) the one-loop effective generating functional associated with the lowest order Lagrangian Eq. (2.87) and the first line in Eq. (2.147). The sum of these contributions

$$Z = Z_{\phi\phi} + Z_{\phi P} + Z_{\text{one-loop}} \tag{4.4}$$

generates the general solution of the Ward identities at $O(p^3)$ in the low-energy expansion. Since we encode the quantum correction, i.e. one-loop contribution, into the effective generating functional $Z_{\text{one-loop}}$, up to one-loop level all quantities are evaluated effectively at the 'classical' level.

For a given Lagrangian $\mathcal{L}(\varphi)$, the evaluation of the Feynman path integral in the one-loop approximation can be done in a standard way [91, 92]. One expands the action

$$Z = \int d^4x \mathcal{L}(\varphi) \tag{4.5}$$

in the vicinity of the classical solution $\bar{\varphi}$, which is determined by the external fields through the classical

[1] One reason to include the purely Goldstone boson part to $O(p^4)$ is due to the power counting rule that the Goldstone boson propagator $i/(q^2 - m_\phi^2)$ is counted as $O(p^{-2})$, while the matter field propagator $i/(q^2 - m^2)$ is counted as $O(p^{-1})$. As a result, the $O(p^4)$ Goldstone boson Lagrangian could enter the calculation of the amplitudes for single matter fields of $O(p^3)$. One example is given by the contribution of the wave function renormalization of the Goldstone bosons to the ϕ-P scattering amplitudes at $O(p^3)$ [65].

[2] Here we are not considering the WZW action.

equations of motion. The effective one-loop generating functional is evaluated via

$$\begin{aligned} e^{iZ_{\text{eff}}} &= \int [d\varphi] e^{i\left(\overline{Z}+\overline{\frac{\partial Z}{\partial\varphi}}\varphi+\frac{1}{2}\overline{\frac{\partial^2 Z}{\partial\varphi^2}}\varphi^2\right)}, \\ &= N e^{i\overline{Z}} \det\left(\overline{\frac{\partial^2 Z}{\partial\varphi^2}}\right)^{-\frac{1}{2}}, \end{aligned} \tag{4.6}$$

with N an irrelevant number. It can be written in a more explicit form

$$Z_{\text{eff}} = \overline{Z} + \frac{i}{2} \ln \det \overline{\frac{\partial^2 Z}{\partial\varphi^2}}, \tag{4.7}$$

where a "bar" means that all quantities are to be evaluated at the classical solution $\bar{\varphi}$. The second term corresponds to the one-loop effective generating functional.

In this section, we evaluate the generating functional for ChPT for spinless matter fields to the leading one-loop order using the background field method. To leading order one-loop generating functional, the relevant Lagrangian is

$$\mathcal{L}_{LO} = \mathcal{L}_2 + \mathcal{L}^{(1)}_{\phi P}. \tag{4.8}$$

The basic idea of the background field method is to split the fields into classical background fields and quantum fluctuations. After integrating out the fluctuations, the resulting effective action actually describes the one-loop contribution of the original action. If only the divergent parts of the loops are considered, one could employ the heat kernel techniques to extract the UV divergence of the effective action, which contains all the possible one-loop divergences and needs to be renormalized by various counter terms provided by the LECs of the higher order Lagrangians. To this end, we perturb the fields $u(x)$ and $P(x)$ around the solutions of the classical equations of motion $\bar{u}(x)$ and $\bar{P}(x)$,

$$\begin{aligned} u^2 &= \bar{u}\, e^{-i\eta}\, \bar{u}, \\ P &= \bar{P} + h, \end{aligned} \tag{4.9}$$

where η is a traceless Hermitian matrix, $\eta = \eta^a \lambda^a$ ($a = 1, \ldots, N^2 - 1$). Then we substitute the decompositions in Eq. (4.9) into the generating functional given by Eq. (4.2). Since we work up to the leading one-loop order, we retain only the quadratic terms in η and h from $\mathcal{L}^{(2)}_{\phi}$ and $\mathcal{L}^{(1)}_{\phi P}$ while the terms linear in the fluctuations give the equations of motion. The equations of motion of the classical fields are

$$\begin{aligned} \nabla_\mu u^\mu &= \frac{i}{2}(\chi_- - \frac{1}{N}\langle\chi_-\rangle), \\ D_\mu D^\mu P^\dagger + m^2 P^\dagger &= 0. \end{aligned} \tag{4.10}$$

For convenience, we collect the fluctuations in the following vectors

$$\xi_A = \left(\eta^a, \frac{\sqrt{2}}{F_0} h_i\right), \quad \xi^\dagger_B = \left(\eta^b, \frac{\sqrt{2}}{F_0} h^\dagger_j\right)^T, \tag{4.11}$$

where $i, j = 1, \ldots, N$ while A and B run from 1 to $(N^2-1)+N$ for N^2-1 Goldstone boson fluctuations and N matter field fluctuations. To second order in the fluctuations, the chiral connection Γ_μ, the axial-vector

vielbein u_μ and χ_+ read

$$\begin{aligned}
\Gamma_\mu &= \bar{\Gamma}_\mu + \frac{1}{4}\Big[\bar{u}_\mu, \eta\Big] + \frac{1}{8}\Big[\eta, \nabla_\mu \eta\Big] + O(\eta^3), \\
\nabla_\mu \eta &= \partial_\mu \eta + \Big[\bar{\Gamma}_\mu, \eta\Big], \\
u_\mu &= \bar{u}_\mu - \nabla_\mu \eta + \frac{1}{8}[\eta, [\bar{u}_\mu, \eta]] + O(\eta^3), \\
\chi_+ &= \bar{\chi}_+ - \frac{i}{2}\{\bar{\chi}_-, \eta\} - \frac{1}{8}\{\eta, \{\bar{\chi}_+, \eta\}\} + O(\eta^3)\,.
\end{aligned} \tag{4.12}$$

From now on, we will neglect the bars over the classical field configurations for brevity. Using the expressions in Eq. (4.12), the terms in the action quadratic in ξ take the form of

$$S^{\text{quad}} = -\frac{F_0^2}{2}\int dx\, \xi_A \left(\mathbb{D}_\mu \mathbb{D}^\mu + \sigma\right)^{AB} \xi_B^\dagger\,. \tag{4.13}$$

Here, the covariant derivative $\mathbb{D}_\mu^{AB}$ is given in matrix form by

$$\mathbb{D}_\mu^{AB} = \begin{pmatrix} d_\mu^{ab} & \frac{1}{4\sqrt{2}F_0}(P[u_\mu, \lambda^a])_j \\ \frac{1}{4\sqrt{2}F_0}([u_\mu, \lambda^b]P^\dagger)_i & D_\mu^{ij} \end{pmatrix}, \tag{4.14}$$

where

$$\begin{aligned}
d_\mu^{ab} &= \delta^{ab}\partial_\mu - \frac{1}{2}\langle [\lambda^a, \lambda^b]\Gamma_\mu\rangle - \frac{1}{8F_0^2}\left(D_\mu P[\lambda^a, \lambda^b]P^\dagger - P[\lambda^a, \lambda^b]D_\mu P^\dagger\right), \\
D_\mu^{ij} &= \delta^{ij}\partial_\mu + (\Gamma_\mu)^{ij}\,,
\end{aligned} \tag{4.15}$$

and the non-derivative term σ^{AB} stands for

$$\sigma^{AB} = \begin{pmatrix} \sigma_{11}^{ab} & \sigma_{12}^{aj} \\ \sigma_{21}^{ib} & \sigma_{22}^{ij} \end{pmatrix}, \tag{4.16}$$

with

$$\begin{aligned}
\sigma_{11}^{ab} &= -\frac{1}{8}\langle u_\mu \left[\lambda^a, [u^\mu, \lambda^b]\right]\rangle + \frac{1}{16}\langle\left\{\lambda^a, \{\chi_+, \lambda^b\}\right\}\rangle + \frac{3}{32F_0^2}P[u_\mu, \lambda^a][u^\mu, \lambda^b]P^\dagger \\
&\quad - \frac{1}{64F_0^4}\left(D_\mu P[\lambda^a, \lambda^c]P^\dagger - P[\lambda^a, \lambda^c]D_\mu P^\dagger\right)\left(D^\mu P[\lambda^c, \lambda^b]P^\dagger - P[\lambda^c, \lambda^b]D^\mu P^\dagger\right), \\
\sigma_{12}^{aj} &= -\frac{1}{4\sqrt{2}F_0}(P[\nabla_\mu u^\mu, \lambda^a])_j - \frac{3}{4\sqrt{2}F_0}(D_\mu P[u^\mu, \lambda^a])_j\,, \\
&\quad + \frac{1}{32\sqrt{2}F_0^3}\left(D_\mu P[\lambda^a, \lambda^c]P^\dagger - P[\lambda^a, \lambda^c]D_\mu P^\dagger\right)(P[u_\mu, \lambda^c])_j, \\
\sigma_{21}^{ib} &= \frac{1}{4\sqrt{2}F_0}\left([\nabla_\mu u^\mu, \lambda^b]P^\dagger\right)_i + \frac{3}{4\sqrt{2}F_0}\left([u^\mu, \lambda^b]D_\mu P^\dagger\right)_i\,, \\
&\quad + \frac{1}{32\sqrt{2}F_0^3}\left([u_\mu, \lambda^c]P^\dagger\right)_i\left(D_\mu P[\lambda^c, \lambda^b]P^\dagger - P[\lambda^c, \lambda^b]D_\mu P^\dagger\right),
\end{aligned}$$

and

$$\sigma_{22}^{ij} = m^2\delta^{ij} - \frac{1}{32F_0^2}\left([u_\mu, \lambda^c]P^\dagger\right)_i \left(P[u^\mu, \lambda^c]\right)_j . \tag{4.17}$$

In each of the $\sigma_{11,12,21}$, the last term contains more than two matter fields, and thus does not contribute to the correlation function of operators sandwiched between single matter fields. The one-loop term in the generating functional is a Gaussian integral over the fluctuations ξ, which can be evaluated with standard methods [35, 91]:

$$\begin{aligned} e^{iZ_{\text{one-loop}}} &= \int [d\xi] \exp\left\{-i\frac{F_0^2}{2}\xi_A \left(\mathbb{D}_\mu\mathbb{D}^\mu + \sigma\right)^{AB} \xi_B^\dagger\right\} \\ &= \mathcal{N}\left(\det\left[\mathbb{D}_\mu\mathbb{D}^\mu + \sigma\right]\right)^{-1/2} \\ &= \mathcal{N}\exp\left\{-\frac{1}{2}\text{tr}\,\log\left(\mathbb{D}_\mu\mathbb{D}^\mu + \sigma\right)\right\} , \end{aligned} \tag{4.18}$$

where $\mathcal{N}$ is an irrelevant normalization, "tr" stands for the trace over the space-time as well as the flavor space spanned by the basis of the ξ_A. The UV divergences in the generating functional $Z_{\text{one-loop}}$ can be extracted by using the heat kernel expansion, and they only show up in the first few expansion coefficients.

Together with the tree level generating functional, up to leading one-loop order, the effecitve generating functional is

$$Z_{\text{eff}} = Z_{\text{eff}}^{\phi\phi} + Z_{\text{eff}}^{\phi P} + Z_{\text{one-loop}}, \tag{4.19}$$

with

$$\begin{aligned} Z_{\text{eff}}^{\phi\phi} &= \int d^4x(\mathcal{L}_2 + \mathcal{L}_4), \\ Z_{\text{eff}}^{\phi P} &= \int d^4x(\mathcal{L}_{\phi P}^{(1)} + \mathcal{L}_{\phi P}^{(2)} + \mathcal{L}_{\phi P}^{(3)}), \\ Z_{\text{one-loop}} &= \frac{i}{2}\text{tr}\,\log\left(\mathbb{D}_\mu\mathbb{D}^\mu + \sigma\right), \end{aligned} \tag{4.20}$$

Notice that all quantities are to be evaluated at the classical solution. What remains to be done is to evaluate the determinant of $\log\left(\mathbb{D}_\mu\mathbb{D}^\mu + \sigma\right)$. This determinant is a formal object which contains UV divergences and requires to be renormalized. In the following section we determine the UV divergences which can be given in a closed form. The finite part of the determinant cannot be given in a closed form. However it may be expanded in powers of the external fields. We will work it out and extract the power counting breaking terms based on this expansion later on.

4.2 Renormalization

The UV divergences of the generating functional $Z_{\text{one-loo}}$ can be extracted by making use of the heat kernel expansion since they only show up in the first few expansion coefficients. The short-distance properties of the operator $\mathcal{D}^{AB} = (D_\mu D^\mu + \sigma)^{AB}$ are governed by the d'Alembertian $\Box$. In d-dimensional

Minkowski space the exponential kernel associated with $\Box$ is given by

$$\langle x|e^{-\lambda\Box}|y\rangle = i(4\pi\lambda)^{-d/2}e^{z^2/4\lambda}, \tag{4.21}$$

where λ is taken on the positive imaginary axis and $z = x - y$. To extract the leading short-distance behavior we write the kernel $e^{-\lambda\mathcal{D}}$ in the form [93]

$$\langle x|e^{-\lambda\mathcal{D}}|y\rangle = i(4\pi\lambda)^{d/2}e^{z^2/4\lambda}H(x|\lambda|y), \tag{4.22}$$

where the kernel $H(x|\lambda|y)$ satisfies the differential equation

$$\frac{\partial}{\partial\lambda}H + \frac{1}{\lambda}z_\mu D^\mu H - D_\mu D^\mu + \sigma H = 0 \tag{4.23}$$

and the boundary condition

$$H(x|0|x) = 1. \tag{4.24}$$

The d-dimensional determinant of $\mathcal{D}$ can then by defined as [15]

$$\begin{aligned}\ln\det\mathcal{D} &= -\int_0^{i\infty}\frac{d\lambda}{\lambda}\mathrm{tr}\,e^{-\lambda\mathcal{D}} \\ &= -i(4\pi)^{-d/2}\int_0^{i\infty}d\lambda\lambda^{-1-d/2}\int dx\mathrm{Tr}\,H(x|\lambda|x),\end{aligned} \tag{4.25}$$

where "Tr" is defined via $\mathrm{tr} = \int dx\mathrm{Tr}$. The UV divergences produced by the loops show up at the lower end of the integration over λ: $\det\mathcal{D}$ has poles at $d = 0, 2, 4, \ldots$. Using the Taylor expansion

$$H(x|\lambda|y) = H_0(x|y) + \lambda H_1(x|y) + \lambda^2 H_2(x|y) + \ldots \tag{4.26}$$

we find

$$\begin{aligned}\frac{i}{2}\ln\det\mathcal{D} &= -\int dx\Big[\frac{1}{d}\mathrm{Tr}\,H_0(x|x) + \frac{1}{4\pi(d-2)}\mathrm{Tr}\,H_1(x|x) \\ &\quad + \frac{1}{(4\pi)^2(d-4)}\mathrm{Tr}\,H_2(x|x) + \ldots\Big].\end{aligned} \tag{4.27}$$

The differential equation (4.23) implies the recursion relations:

$$\begin{aligned}(z_\mu D^\mu + n + 1)H_{n+1}(x|y) + D_\mu D^\mu H_n(x|y) + \sigma H_n(x|y) = 0, \\ z_\mu D^\mu H_0(x|y) = 0,\end{aligned} \tag{4.28}$$

which can be used to determine $H_n(x|x)$. Putting $n = 1$, $x = y$ we get

$$H_2(x|x) = \frac{1}{2}D_\mu D^\mu H_1(x|x) - \frac{1}{2}\sigma(x)H_1(x|x). \tag{4.29}$$

The value of $D_\mu D^\mu H_1(x|x)$ can be obtained by first applying $D_\mu D^\mu$ to the recursion relation with $n = 0$

$$\begin{aligned} & D_\mu D^\mu (1 + z_\nu D^\nu) H_1(x|y) + D_\mu D^\mu (-D_\nu D^\nu + \sigma(x)) H_0(x|y) \\ = \; & (D_\mu D^\mu + D_\mu g^{\mu\nu} D_\nu + D_\mu z_\nu D^\mu D^\nu) H_1(x|y) - (D_\mu D^\mu)^2 H_0(x|y) + D_\mu D^\mu \sigma H_0(x|y) \\ = \; & (3 D_\mu D^\mu + z_\nu D_\mu D^\mu D^\nu) H_1(x|y) - (D_\mu D^\mu)^2 H_0(x|y) + D_\mu D^\mu \sigma H_0(x|y) \end{aligned} \tag{4.30}$$

and then taking $x = y$ we have:

$$\begin{aligned} 3 D_\mu D^\mu H_1(x|x) = & (D_\mu D^\mu)^2 H_0(x|x) - [D_\mu, [D^\mu, \sigma]] H_0(x|x) \\ & - 2 [D_\mu, \sigma] D^\mu H_0(x|x) - \sigma D_\mu D^\mu H_0(x|x). \end{aligned} \tag{4.31}$$

Likewise, the derivatives of H_0 can be obtained by repeatedly applying the differential opterator D_μ to the differential equation and using the definition

$$D_\mu D_\nu - D_\nu D_\mu = \Gamma_{\mu\nu}. \tag{4.32}$$

In this manner one easily finds

$$\begin{aligned} H_0(x|x) &= 1, \\ D_\mu H_0(x|x) &= 0, \\ D_\mu D_\nu H_0(x|x) &= \frac{1}{2} \Gamma_{\mu\nu}, \\ (D_\mu D^\mu)^2 H_0(x|x) &= \frac{1}{2} \Gamma_{\mu\nu} \Gamma^{\mu\nu}, \\ H_1(x|x) &= -\sigma(x) H_0(x|x). \end{aligned} \tag{4.33}$$

Putting them together we obtain

$$H_2(x|x) = \frac{1}{12} \Gamma_{\mu\nu} \Gamma^{\mu\nu} + \frac{1}{2} \sigma^2 - \frac{1}{6} [D_\mu, [D^\mu, \sigma]]. \tag{4.34}$$

The last term does not contribute to $\mathrm{tr} H_2$ since it gives rise to a total derivatives.

We use the ζ-function technique to specify the finite part of the determinant, which is defined by

$$\ln \det_\mu \mathcal{D} = -\frac{d}{ds}\Big|_{s=0} \frac{1}{2} \frac{\mu^{2s}}{\Gamma(s)} \int_0^\infty d\lambda \lambda^{s-1} \mathrm{tr}\, e^{-\lambda \mathcal{D}}. \tag{4.35}$$

The first three terms in the series expansion of H produce poles at $s = 2$, $s = 1$ and $= 0$, respectively. The pole at $s = 0$ is responsible for the scale dependence of the finite part:

$$\mu \frac{\partial}{\partial \mu} \ln \det_\mu \mathcal{D} = -(4\pi)^{-2} \int dx\, \mathrm{Tr} H_2(x|x). \tag{4.36}$$

Back to the case of ChPT for spinless matter fields, as we are only interested in the UV divergences, we only consider the terms having a $1/(d-4)$ pole. We have $\mathcal{D}^{AB} = (\mathbb{D}_\mu \mathbb{D}^\mu + \sigma)^{AB}$, and the associated "field strength" tensor $[\mathbb{D}_\mu, \mathbb{D}_\nu]$ is denoted as $\mathbb{F}_{\mu\nu}$:

$$\mathbb{F}^{AB}_{\mu\nu} = \begin{pmatrix} -\frac{1}{2} \langle [\lambda^a, \lambda^b] \mathrm{A}_{\mu\nu} \rangle + \Sigma_{11}^{ab} & \Sigma_{12}^{aj} \\ \Sigma_{21}^{ib} & \Gamma_{\mu\nu}^{ij} + \Sigma_{22}^{ij} \end{pmatrix}, \tag{4.37}$$

where [3]

$$
\begin{aligned}
\mathrm{A}_{\mu\nu} &= \Gamma_{\mu\nu} + \frac{1}{4F_0^2}\Big(2D_\mu P^\dagger D_\nu P - 2D_\nu P^\dagger D_\mu P + P^\dagger[D_\mu, D_\nu]P - [D_\mu, D_\nu]P^\dagger P\Big) \\
&\quad + \frac{1}{(4F_0^2)^2}[P^\dagger D_\mu P - D_\mu P^\dagger P, P^\dagger D_\nu P - D_\nu P^\dagger P], \\
\Sigma_{11}^{ab} &= \frac{1}{32F_0^2}(P[u_\mu, \lambda^a][u_\nu, \lambda^b]P^\dagger - P[u_\nu, \lambda^a][u_\mu, \lambda^b]P^\dagger), \\
\Sigma_{12}^{aj} &= \frac{1}{4\sqrt{2}F_0}(D_\mu P[u_\nu, \lambda^a] - D_\nu P[u_\mu, \lambda^a] + P[\nabla_\mu u_\nu - \nabla_\nu u_\mu, \lambda^a])_j \\
&\quad - \frac{1}{32\sqrt{2}F_0^3}\Big[(D_\mu P[\lambda^a, \lambda^c]P^\dagger - P[\lambda^a, \lambda^c]D_\mu P^\dagger)(P[u_\nu, \lambda^c])_j - (\mu \leftrightarrow \nu)\Big], \\
\Sigma_{21}^{ib} &= \frac{1}{4\sqrt{2}F_0}([u_\nu, \lambda^b]D_\mu P^\dagger - [u_\mu, \lambda^b]D_\nu P^\dagger + [\nabla_\mu u_\nu - \nabla_\nu u_\mu, \lambda^b]P^\dagger)_i \\
&\quad - \frac{1}{32\sqrt{2}F_0^3}\Big[([u_\mu, \lambda^c]P^\dagger)_i(D_\nu P[\lambda^c, \lambda^b]P^\dagger - P[\lambda^c, \lambda^b]D_\nu P^\dagger) - (\mu \leftrightarrow \nu)\Big], \\
\Sigma_{22}^{ij} &= \frac{1}{32F_0^2}\Big[([u_\mu, \lambda^c]P^\dagger)_i(P[u_\nu, \lambda^c])_j - ([u_\nu, \lambda^c]P^\dagger)_i(P[u_\mu, \lambda^c])_j\Big],
\end{aligned}
\tag{4.38}
$$

with

$$
\Gamma_{\mu\nu} = [D_\mu, D_\nu] = \partial_\mu\Gamma_\nu - \partial_\nu\Gamma_\mu + [\Gamma_\mu, \Gamma_\nu]\,. \tag{4.39}
$$

In dimensional regularization, the relevant term reads

$$
Z^{\mathrm{div}}_{\text{one-loop}} = \frac{1}{2(4\pi)^{d/2}}\mu^{d-4}\Gamma(2-\frac{d}{2})\int d^4x\,\mathrm{Tr}\Big(\frac{1}{12}\mathbb{F}_{\mu\nu}\mathbb{F}^{\mu\nu} + \frac{1}{2}\sigma^2\Big). \tag{4.40}
$$

To get the final result, we make use of the equations of motion for the classical fields and the identities:

$$
\begin{aligned}
\Gamma_{\mu\nu} = [D_\mu, D_\nu] &= \frac{1}{4}[u_\mu, u_\nu] - \frac{i}{2}f^+_{\mu\nu}, \\
\nabla_\mu u_\nu - \nabla_\nu u_\mu &= -f^-_{\mu\nu},
\end{aligned}
\tag{4.41}
$$

one obtains all possible one-loop divergences. Up to $O(p^3)$, those relevant for single matter fields read

$$
\begin{aligned}
Z^{\mathrm{div}}_{\phi P} = -\frac{\lambda}{F_0^2}\int d^dx\Big[&\frac{m^2}{24}P\langle u^\mu u_\mu\rangle P^\dagger + \frac{m^2}{24}N\,Pu^\mu u_\mu P^\dagger + \frac{7}{12}D_\mu P\langle u^\mu u^\nu\rangle D_\nu P^\dagger \\
&+ \frac{7}{24}N\,D_\mu P\{u^\mu, u^\nu\}D_\nu P^\dagger - \frac{3}{64}N(P[u^\mu, \nabla_\mu u_\nu + \nabla_\nu u_\mu]D^\nu P^\dagger + h.c.) \\
&+ \frac{N}{6}i\,D^\mu P f^+_{\mu\nu}D^\nu P^\dagger + \frac{11}{96}N\,P[u^\mu, f^-_{\mu\nu}]D^\nu P^\dagger\Big],
\end{aligned}
\tag{4.42}
$$

[3] Note that P is a $1\times N$ vector, and $P^\dagger$ is a $N\times 1$ vector. As a result, $P^\dagger P$ is a $N\times N$ matrix.

where $\lambda = \mu^{d-4}[(4\pi)^{d/2}(d-4)]^{-1}$. Two relations used in deriving Eq. (4.42) are

$$\begin{aligned} & D^\mu P\{u^\nu, \nabla_\mu u_\nu\}P^\dagger + P\{u^\nu, \nabla_\mu u_\nu\}D^\mu P^\dagger \\ &= D^\mu P\{u^\nu, \nabla_\mu u_\nu\}P^\dagger - D^\mu P\{u^\nu, \nabla_\mu u_\nu\}P^\dagger + O(p^4) \\ &= O(p^4), \end{aligned} \tag{4.43}$$

and

$$\begin{aligned} & D_\mu P[u^\mu, u^\nu]D_\nu P^\dagger \\ &= -P[\nabla_\mu u^\mu, u^\nu]D_\nu P^\dagger - P[u^\mu, \nabla_\mu u^\nu]D_\nu P^\dagger - P[u^\mu, u^\nu]D_\mu D_\nu P^\dagger \\ &= -\frac{1}{2}(P[u^\mu, \nabla_\mu u^\nu + \nabla_\nu u^\mu]D_\nu P^\dagger + P[u^\mu, \nabla_\mu u^\nu - \nabla_\nu u^\mu]D_\nu P^\dagger \\ &\quad + P[u^\mu, u^\nu][D_\mu, D_\nu]P^\dagger + 2P[\nabla_\mu u^\mu, u^\nu]D_\nu P^\dagger) \\ &= -\frac{1}{2}\Big(P[u^\mu, \nabla_\mu u_\nu + \nabla_\nu u_\mu]D^\nu P^\dagger - P[u^\mu, f^-_{\mu\nu}]D^\nu P^\dagger \\ &\quad + iP[\chi_-, u_\nu]D^\nu P^\dagger + \frac{1}{4}P[u^\mu, u^\nu][u_\mu, u_\nu]P^\dagger - \frac{i}{2}P[u^\mu, u^\nu]f^+_{\mu\nu}P^\dagger\Big) \\ &= -\frac{1}{2}\Big(P[u^\mu, \nabla_\mu u_\nu + \nabla_\nu u_\mu]D^\nu P^\dagger - P[u^\mu, f^-_{\mu\nu}]D^\nu P^\dagger + iP[\chi_-, u_\nu]D^\nu P^\dagger\Big) \\ &\quad + O(p^4). \end{aligned} \tag{4.44}$$

In order to obtain a finite one-loop effective action, the UV divergences in Eq. (4.42) need to be cancelled by those of the LECs

$$\mathcal{L} = \sum_i h_i O_i = \sum_i \left[h_i^r(\mu) + h_i^0 \lambda\right] O_i \,, \tag{4.45}$$

where $c_i^r(\mu)$ is the finite part of the c_i and is scale-dependent. From Eq. (4.42) and Eq. (2.147), it is easy to read off the divergent parts of the corresponding LECs, which up to $O(p^3)$ are given by

$$\begin{aligned} h_0^0 = h_1^0 = 0, \quad h_2^0 = \frac{m^2}{24}, \quad h_3^0 = -\frac{m^2}{24}N, \quad h_4^0 = \frac{7}{12}, \quad h_5^0 = -\frac{7}{24}N, \\ g_1^0 = 0, \quad g_2^0 = -\frac{3}{64}N, \quad g_{3,4,5}^0 = 0, \quad \gamma_1^0 = \frac{N}{6}, \quad \gamma_2^0 = \frac{11}{96}N \,. \end{aligned} \tag{4.46}$$

These coefficients determine the scale dependence of the corresponding renormalized LECs, and the pertinent renormalization group equations read

$$\frac{\partial h_i^r(\mu)}{\partial \mu} = -\frac{h_i^0}{16\pi^2} \,. \tag{4.47}$$

From Eq. (4.46), one clearly sees that the one-loop divergences also renormalize the LECs at a lower order (here, the h_i's). For $N = 3$, the values of h_i^0 and g_i^0 agree with those found in an explicit calculation of the scattering amplitudes [65].

We have checked that integrating out the Goldstone boson fluctuations leads to the divergence structure

of the purely Goldstone boson effective action for N flavors [94]:

$$\begin{aligned} Z_\phi^{\mathrm{div},\phi} = -\lambda \int d^d x \Big[& \frac{N}{48}\langle u_\mu u_\nu u^\mu u^\nu\rangle + \frac{1}{16}\langle u_\mu u^\mu\rangle^2 + \frac{1}{8}\langle u_\mu u_\nu\rangle\langle u^\mu u^\nu\rangle \\ & + \frac{N}{24}\langle u_\mu u^\mu u_\nu u^\nu\rangle + \frac{1}{8}\langle u_\mu u^\mu\rangle\langle\chi_+\rangle + \frac{N}{8}\langle u_\mu u^\mu \chi_+\rangle + \frac{N^2+2}{16N^2}\langle\chi_+\rangle^2 \\ & + \frac{N^2-4}{16N}\langle\chi_+^2\rangle - \frac{N}{12} i\langle f_{\mu\nu}^+ u^\mu u^\nu\rangle - \frac{N}{24}\langle f_{\mu\nu}^+ f^{+\mu\nu}\rangle \Big]. \end{aligned} \tag{4.48}$$

Yet, as can be expected, Z_ϕ^{div} also gets contributions due to the presence of the matter field loops. The matter fields are expected to be much heavier than the Goldstone bosons, and therefore their effects in loops on the properties of Goldstone bosons might be irrelevant, at least for the ChPT of QCD. Nevertheless, they contribute to the divergence of the generational functional, which is given here for completeness

$$Z_\phi^{\mathrm{div},P} = -\lambda \int d^d x \Big[\frac{1}{96}\langle u_\mu u_\nu u^\mu u^\nu\rangle - \frac{1}{96}\langle u_\mu u^\mu u_\nu u^\nu\rangle - \frac{i}{24}\langle f_{\mu\nu}^+ u^\mu u^\nu\rangle - \frac{1}{48}\langle f_{\mu\nu}^+ f^{+\mu\nu}\rangle \Big]. \tag{4.49}$$

For a specific number of light flavors, the additional relations, e.g. the Cayley-Hamilton theorem, could be used to remove the additional terms in Eqs. (4.48) and (4.49) (e.g. $\langle u_\mu u_\nu u^\mu u^\nu\rangle$ for $N = 2, 3$). The Cayley-Hamilton theorem states that every square matrix over a commutative ring satisfies its own characteristic equation. For the two-dimensional case, the theorem implies the relation

$$\{A, B\} = A\langle B\rangle + B\langle A\rangle + \langle AB\rangle - \langle A\rangle\langle B\rangle, \tag{4.50}$$

for arbitrary 2×2 matrices A and B. For the $SU(3)$ case, one has

$$\langle u^\mu u^\nu u_\mu u_\nu\rangle = -2\langle u^\mu u_\mu u^\nu u_\nu\rangle + \frac{1}{2}\langle u_\mu u^\mu\rangle^2 + \langle u^\mu u_\nu\rangle\langle u_\mu u^\nu\rangle. \tag{4.51}$$

For comparison, we list the divergences of LECs related to $\phi\phi$ interaction at $O(p^4)$ for purely Goldstone bosonic ChPT and ChPT for spinless matter fields for $N = 2$ and $N = 3$, respectively, in Table 4.1. Note that although the one-loop effective operators in Eqs. (4.48) and (4.49) are counted as $O(p^4)$, they could enter the ϕP interaction at $O(p^3)$.

4.3 Subtraction of power counting breaking terms

In last section, the one-loop effective generating functional is expanded in a series of poles at $d = 0, 2, 4, \ldots$, see Eq. (4.27). The UV divergences correspond to the term $d = 4$ in dimensional regularization. To obtain the finite part, one has to sum infinite terms. Alternatively, the determinant of the differential $\mathcal{D}$ can be calculated in a series expansion in powers of the external fields. One can calculate the finite part of the determinant by treating the external fields as perturbations. If the external fields are switched off ($v_\mu = a_\mu = p = 0$, $s = \mathcal{M}$), the differential operator $\mathcal{D}_0 = \Box + M^2$ [15].

To this end, we split $\mathcal{D}$ into a Klein-Gordon operator $\mathcal{D}_0$ for free fields and a remaining interaction part

c_i^0	O_i	purely Goldstone bosonic ChPT		Including spinless matter	
		$N_f = 2$	$N_f = 3$	$N_f = 2$	$N_f = 3$
L_1^0	$\langle u_\mu u^\mu \rangle^2$	$\frac{1}{12}$	$\frac{3}{32}$	$\frac{7}{96}$	$\frac{19}{192}$
L_2^0	$\langle u_\mu u^\nu \rangle^2$	$\frac{1}{6}$	$\frac{3}{16}$	$\frac{17}{96}$	$\frac{19}{96}$
L_3^0	$\langle (u_\mu u^\mu)^2 \rangle$	0	0	0	$-\frac{1}{32}$
L_4^0	$\langle u_\mu u^\mu \rangle \langle \chi_+ \rangle$	$\frac{1}{8}$	$\frac{1}{8}$	$\frac{1}{8}$	$\frac{1}{8}$
L_5^0	$\langle u_\mu u^\mu \chi_+ \rangle$	$\frac{1}{4}$	$\frac{3}{8}$	$\frac{1}{4}$	$\frac{3}{8}$
L_6^0	$\langle \chi_+ \rangle^2$	$\frac{3}{32}$	$\frac{11}{144}$	$\frac{3}{32}$	$\frac{11}{144}$
L_7^0	$\langle \chi_- \rangle^2$	0	0	0	0
L_8^0	$\langle \chi_+ \chi_+ \rangle$	0	$\frac{5}{48}$	0	$\frac{5}{48}$
L_9^0	$-i\langle f_{\mu\nu}^+ u^\mu u^\nu \rangle$	$\frac{1}{6}$	$\frac{1}{4}$	$\frac{5}{24}$	$\frac{7}{24}$
L_{10}^0	$\frac{1}{2}\langle f_{\mu\nu}^+ f^{+\mu\nu} \rangle$	$-\frac{1}{6}$	$-\frac{1}{4}$	$-\frac{5}{24}$	$-\frac{7}{24}$

Table 4.1: The renormalization of $O(p^4)$ LECs for purely Goldstone bosonic ChPT and ChPT for spinless matter fields.

δ_r: $\mathcal{D}^{AB} = \mathcal{D}_0^{AB} + \delta_r^{AB}$. Then the determinant can be calculated in an expansion of the interaction term:

$$\begin{aligned}\frac{i}{2}\mathrm{tr}\,\log\mathcal{D} &= \frac{i}{2}\mathrm{tr}\,\log(\mathcal{D}_0+\delta_r) = \frac{i}{2}\mathrm{tr}\{\log\mathcal{D}_0 + \log(\mathbf{1}-\delta_r\Delta)\}\\ &= \frac{i}{2}\mathrm{tr}\,\log\mathcal{D}_0 - \frac{i}{2}\mathrm{tr}(\delta_r\Delta) - \frac{i}{4}\mathrm{tr}(\delta_r\Delta\delta_r\Delta) - \frac{i}{6}\mathrm{tr}(\delta_r\Delta\delta_r\Delta\delta_r\Delta) + \ldots,\end{aligned} \tag{4.52}$$

where Δ is the inverse of $-\mathcal{D}_0$:

$$\Delta^{AB}(x-y) = \delta^{AB}\int\frac{d^dp}{(2\pi)^d}\frac{e^{-ip(x-y)}}{p^2-m_A^2+i\epsilon}, \tag{4.53}$$

and the remainder δ_r is

$$\delta_r = \{\hat\Gamma^\mu,\partial_\mu\} + \hat\Gamma^\mu\hat\Gamma_\mu + \hat\sigma\,, \tag{4.54}$$

with $\hat\sigma^{AB} = \sigma^{AB} - m_A^2\delta^{AB}$. Here $\hat\Gamma_\mu$ is defined via $\mathbb{D}_\mu^{AB} = \delta^{AB}\partial_\mu + \hat\Gamma_\mu^{AB}$ which means

$$\hat\Gamma_\mu^{AB} = \begin{pmatrix} -\frac{1}{2}\langle[\lambda^a,\lambda^b]\Gamma_\mu\rangle - \frac{1}{8F_0^2}\left(D_\mu P[\lambda^a,\lambda^b]P^\dagger - P[\lambda^a,\lambda^b]D_\mu P^\dagger\right), & \frac{1}{4\sqrt{2}F_0}(P[u_\mu,\lambda^a])_j \\ \frac{1}{4\sqrt{2}F_0}([u_\mu,\lambda^b]P^\dagger)_i, & \Gamma_\mu^{ij}\end{pmatrix}, \tag{4.55}$$

and the expression for σ^{AB} is listed in Eq. (4.16).

The first term $\frac{i}{2}\mathrm{tr}\,\log\mathcal{D}_0$ in Eq. (4.52) is an irrelevant constant. The second term $\mathrm{tr}\,\delta_r\Delta$ is the set of all tadpole graphs. The third term collects all the two-point loop graphs, etc. Since the external fields v_μ and s (a_μ and p) correspond to terms with an even (odd) number of boson fields, following the counting scheme used in Refs. [15, 16], we count v_μ and $s-\mathcal{M}$ as $O(\phi^2)$, where ϕ here should be understood as representing both the Goldstone boson and matter fields. Thus, $\hat\Gamma_\mu$ and $\hat\sigma$ are of $O(\phi^2)$. The the one-loop

functional up to $O(\phi^4)$, i.e. with at most four external meson fields, can be calculated as [95]

$$\begin{aligned}
Z^{\text{one-loop}} &= -\frac{i}{2}\mathrm{tr}\left[\hat{\sigma(x)}\Delta(0) + \hat{\Gamma}^{\mu}(x)\hat{\Gamma}_{\mu}(x)\Delta(0)\right] \\
&\quad -\frac{i}{4}\mathrm{tr}\Big[\left\{\hat{\Gamma}^{\mu}(x),\partial^{x}_{\mu}\right\}\Delta(x-y)\left\{\hat{\Gamma}^{\nu}(y),\partial^{y}_{\nu}\right\}\Delta(y-x) \\
&\quad +2\left\{\hat{\Gamma}^{\mu}(x),\partial^{x}_{\mu}\right\}\Delta(x-y)\hat{\sigma}(y)\Delta(y-x) \\
&\quad +2\hat{\Gamma}^{\mu}(x)\hat{\Gamma}_{\mu}(x)\Delta(x-y)\hat{\sigma}(y)\Delta(y-x)\Big] + O(\phi^6) \\
&= -\frac{i}{2}\mathrm{tr}\left[\hat{\sigma}(x)\Delta(0) + \hat{\Gamma}^{\mu}(x)\hat{\Gamma}_{\mu}(x)\Delta(0)\right] \\
&\quad -\frac{i}{4}\mathrm{tr}\Big[\hat{\Gamma}^{\mu}(x)\partial^{x}_{\mu}\Delta(x-y)\hat{\Gamma}^{\nu}(y)\partial^{y}_{\nu}\Delta(y-x) \\
&\quad +\hat{\Gamma}^{\mu}(x)\partial^{x}_{\nu}\Delta(x-y)\hat{\Gamma}^{\nu}(y)\partial^{y}_{\mu}\Delta(y-x) \\
&\quad +\hat{\Gamma}^{\mu}(x)\partial^{x}_{\mu}\partial^{x}_{\nu}\Delta(x-y)\hat{\Gamma}^{\nu}(y)\Delta(y-x) \\
&\quad +\hat{\Gamma}^{\mu}(x)\Delta(x-y)\hat{\Gamma}^{\nu}(y)\partial^{y}_{\mu}\partial^{y}_{\nu}\Delta(y-x) \\
&\quad +2\hat{\Gamma}^{\mu}(x)\partial^{x}_{\mu}\Delta(x-y)\hat{\sigma}(y)\Delta(y-x) \\
&\quad +2\hat{\Gamma}^{\mu}(x)\Delta(x-y)\hat{\sigma}(y)\partial^{y}_{\mu}\Delta(y-x) \\
&\quad +\hat{\sigma}(x)\Delta(x-y)\hat{\sigma}(y)\Delta(y-x)\Big] + O(\phi^6).
\end{aligned}$$

When the light quark masses are different, the free Klein-Gordon propagator is not diagonal in the cartesian basis spanned by $\lambda^1, \lambda^2, \ldots, \lambda^{N^2-1}$. It is more convenient to use the physical basis such as $\lambda^{\pi^+} = -\frac{1}{\sqrt{2}}(\lambda^1 + i\lambda^2)$ and so on, in which we have

$$\mathcal{D}_0^{PQ} = \delta^{PQ}(\Box + M_P^2). \tag{4.56}$$

In this notation, the one-loop functional to $O(\phi^4)$ can be written as [16]

$$\begin{aligned}
Z^{\text{one-loop}} &= \frac{i}{2}\sum_P \int d^4x \Delta_P(0)\hat{\sigma}_{PP}(x) + \frac{i}{4}\sum_{P,Q}[\Delta_P(0)+\Delta_Q(0)]\hat{\Gamma}_{\mu PQ}(x)\hat{\Gamma}^{\mu}_{QP}(x) \\
&\quad + \sum_{P,Q}\int d^4x d^4y \Big[M^{PQ}_{\mu\nu}(x-y)\hat{\Gamma}^{\mu}_{PQ}(x)\hat{\Gamma}^{\nu}_{QP}(y) + K^{PQ}_{\mu}(x-y)\hat{\Gamma}^{\mu}_{PQ}(x)\hat{\sigma}_{QP}(y) \\
&\quad + J^{PQ}(x-y)\hat{\sigma}_{PQ}(x)\hat{\sigma}_{QP}(y)\Big] + O(\phi^6),
\end{aligned} \tag{4.57}$$

where

$$\begin{aligned}
M^{PQ}_{\mu\nu}(z) &= \frac{i}{4}\left(\partial_\mu\Delta_P\partial_\nu\Delta_Q + \partial_\nu\Delta_P\partial_\mu\Delta_Q - \partial_{\mu\nu}\Delta_P\Delta_Q - \Delta_P\partial_{\mu\nu}\Delta_Q\right), \\
K^{PQ}_{\mu}(z) &= \frac{i}{2}(\partial_\mu\Delta_P\Delta_Q - \Delta_P\partial_\mu\Delta_Q), \\
J^{PQ}(z) &= -\frac{i}{4}\Delta_P\Delta_Q,
\end{aligned} \tag{4.58}$$

with $\Delta_P(z) = \Delta(z, M_P^2)$ defined as the free propagator for a spinless field of mass M_P in d-dimension. The

explicit expressions of various kernels in terms of loop integrals in momentum space have the form

$$\mathcal{K}_a^{PQ}(x-y) = \int \frac{d^4p}{(2\pi)^2} e^{-ip(x-y)} \mathcal{K}_a^{PQ}(p), \tag{4.59}$$

with

$$\begin{aligned} M_{\mu\nu}^{PQ}(p) &= -g_{\mu\nu} B_{00}(p^2, m_P^2, m_Q^2) \\ &\quad -\frac{1}{4} p_\mu p_\nu \left[B_0(p^2, m_P^2, m_Q^2) + 4B_1(p^2, m_P^2, m_Q^2) + 4B_{11}(p^2, m_P^2, m_Q^2) \right], \\ K_\mu^{PQ}(p) &= i p_\mu \left[\frac{1}{2} B_0(p^2, m_P^2, m_Q^2) + B_1(p^2, m_P^2, m_Q^2) \right], \\ J^{PQ}(p) &= \frac{1}{4} B_0(p^2, m_P^2, m_Q^2), \end{aligned} \tag{4.60}$$

where the loop functions B_0, B_1, B_{00} and B_{11} are defined in Appendix A.

With the expressions of the kernel Eq. (4.59), one may read off the one-loop graphs directly from the determinant Eq. (4.57) up to four external legs. This means that the amplitudes of $P\phi$ scattering can be read off straightforward up to $O(p^3)$. However, as mentioned in Sec. 2.1.1, the one-loop effective functional Eq. (4.57) contains power counting breaking terms, which should be absent in a well-defined low-energy effective theory. In the EOMS scheme, those terms are removed by shifting the LECs by finite parts. In the following we will calculate the power counting breaking terms with dimensional regularization with the $\overline{\text{MS}}$ scheme, in which any loop integral involving matter field propagators contains terms starting from $O(1)$.

The loops involving only matter field propagators do not play any dynamical role in the low-energy effective field theory, neither do they introduce non-analyticity in the quark masses, and thus can be absorbed into a redefinition of the LECs. As a result, the explicit closed matter field loops are not necessary to be included in the calculation. Thus, the Goldstone boson part of the one-loop functional is identical to that in the standard Goldstone boson ChPT, which can be found in Refs. [16]. The PCB terms of interest are from the loops containing both Goldstone boson and matter field internal propagators. They correspond to the terms of $M_{\mu\nu}^{PQ}$, K_μ^{PQ} and J^{PQ} in Eq. (4.57) with P and Q in different blocks (Goldstone bosons and matter fields). Since we are only interested in the single matter field sector, which is the sector relevant for processes with a single matter field in both initial and final states and can be studied using the effective Lagragians in Eq. (2.147), and the terms contributing at orders lower than that required by Eq. (2.142), we only need the following terms of $\hat{\Gamma}_\mu$ and $\hat{\sigma}$ for calculating the PCB part, which is of $O(p^2)$, of the one-loop generating functional

$$\begin{aligned} \hat{\Gamma}_\mu'^{AB} &= \frac{1}{4\sqrt{2}F_0} \begin{pmatrix} 0 & \left(P[u_\mu, \lambda^a]\right)_j \\ \left([u_\mu, \lambda^b]P^\dagger\right)_i & 0 \end{pmatrix}, \\ \hat{\sigma}'^{AB} &= \frac{3}{4\sqrt{2}F_0} \begin{pmatrix} 0 & -\left(D^\mu P[u_\mu, \lambda^a]\right)_j \\ \left([u_\mu, \lambda^b]D^\mu P^\dagger\right)_i & 0 \end{pmatrix}. \end{aligned} \tag{4.61}$$

Since the elements of Γ_μ' and σ' are of $O(p)$, the PCB terms of loops only refer to the $O(1)$ terms of the loop integrals. As a result, they are independent of the internal Goldstone boson masses. Therefore,

the relevant one-loop generating functional to $O(\phi^4)$ can be rewritten in the form

$$\begin{aligned}
Z'^{\text{one-loop}} &= \int d^4x d^4y \frac{d^4p}{(2\pi)^4} e^{-ip(x-y)} \\
&\times\Big\{\frac{1}{8}\left\langle \hat{\Gamma}'^{\mu\nu}(x)\hat{\Gamma}'_{\mu\nu}(y)\right\rangle \Big[B_0(p^2,m^2,0)+4B_1(p^2,m^2,0)+4B_{11}(p^2,m^2,0)\Big] \\
&-\left\langle \hat{\Gamma}'_{\mu}(x)\hat{\Gamma}'^{\mu}(y)\right\rangle \left[B_{00}(p^2,m^2,0)+\frac{p^2}{4}(B_0(p^2,m^2,0)+4B_1(p^2,m^2,0)+4B_1(p^2,m^2,0))\right] \\
&+\left\langle \partial_\mu\tilde{\Gamma}'^{\mu}(x)\hat{\sigma}(y)\right\rangle \left[\frac{B_0(p^2,m^2,0)}{2}+B_1(p^2,m^2,0)\right]+\frac{1}{4}B_0(p^2,m^2,0)\left\langle \hat{\sigma}'(x)\hat{\sigma}'(y)\right\rangle \Big\}, \\
&= \int d^4x d^4y \frac{d^4p}{(2\pi)^4} e^{-ip(x-y)}\Big\{-\left\langle \hat{\Gamma}'_{\mu}(x)\hat{\Gamma}'^{\mu}(y)\right\rangle B_{11}(p^2,m^2,0) \\
&-\frac{1}{4}\left\langle \partial_\mu\Gamma'_\nu\partial^\nu\Gamma'^{\mu}\right\rangle B_0(p^2,m^2,0)+4B_1(p^2,m^2,0)+4B_{11}(p^2,m^2,0) \\
&+\left\langle \partial_\mu\tilde{\Gamma}'^{\mu}(x)\hat{\sigma}(y)\right\rangle \left[\frac{B_0(p^2,m^2,0)}{2}+B_1(p^2,m^2,0)\right]+\frac{1}{4}B_0(p^2,m^2,0)\left\langle \hat{\sigma}'(x)\hat{\sigma}'(y)\right\rangle \Big\}, \qquad (4.62)
\end{aligned}$$

where we have defined $\hat{\Gamma}'_{\mu\nu}=\partial_\mu\hat{\Gamma}'_\nu-\partial_\nu\hat{\Gamma}'_\mu+[\hat{\Gamma}'_\mu,\hat{\Gamma}'_\nu]$, and

$$\tilde{\Gamma}'^{AB}_{\mu} = \frac{1}{4\sqrt{2}F_0}\begin{pmatrix} 0 & \left(P[u_\mu,\lambda^a]\right)_j \\ -\left([u_\mu,\lambda^b]P^\dagger\right)_i & 0\end{pmatrix}. \qquad (4.63)$$

Since all the operators in Eq. (4.62) are of $O(p^2)$, we can extract the PCB terms by keeping only the $O(p^0)$ part of these loop functions. In the EOMS scheme, the PCB terms come from the leading chiral expansion of one-loop functions $A_0(m^2)$ and $B_0(m^2,m^2,0)$. The closed matter loop $A_0(m^2)$ is infrared regular, and the regular part of the loop integral $B_0(p^2,m^2,M^2)$ can be expanded as [96]

$$\begin{aligned}
B_0^{\text{reg.}}(p^2,m^2,M^2) &= \frac{\Gamma(2-d/2)}{(4\pi)^{d/2}(d-3)}\left(\frac{m}{\mu}\right)^{d-4}\Big[1-\frac{p^2-m^2}{2m^2}+\frac{(d-6)(p^2-m^2)^2}{4m^4(d-5)} \\
&+\frac{(d-3)M^2}{2m^2(d-5)}+\cdots\Big]. \qquad (4.64)
\end{aligned}$$

More explicitly, using Eq. (A.4), the infrared regular PCB parts of the loop functions are

$$\begin{aligned}
A_0^{\text{PCB}}(m^2) &= -\frac{m^2}{16\pi^2}\log\frac{m^2}{\mu^2}, \\
B_0^{\text{PCB}}(p^2,m^2,0) &= \frac{1}{16\pi^2}\left(1-\log\frac{m^2}{\mu^2}\right), \\
B_1^{\text{PCB}}(p^2,m^2,0) &= -\frac{1}{16\pi^2}\left(1-\frac{1}{2}\log\frac{m^2}{\mu^2}\right), \\
B_{00}^{\text{PCB}}(p^2,m^2,0) &= \frac{m^2}{288\pi^2}\left(2-3\log\frac{m^2}{\mu^2}\right), \qquad (4.65)
\end{aligned}$$

and

$$B_{11}^{\mathrm{PCB}}(p^2,m^2,0)=\frac{1}{144\pi^2}\left(8-3\log\frac{m^2}{\mu^2}\right). \tag{4.66}$$

Applying the results of Eqs. (4.65), (4.66) and the equations of motion for the classical background fields, it is easy to obtain the PCB terms of interest:

$$\begin{aligned}
Z_{\text{one-loop}}^{\mathrm{PCB}} \;=\; & \frac{1}{16\pi^2F_0^2}\int d^4x\Bigg\{\frac{m^2}{144}\left[2-3\log\left(\frac{m^2}{\mu^2}\right)\right]\left\langle PP^\dagger\right\rangle\left\langle u_\mu u^\mu\right\rangle \\
& +\frac{m^2N}{144}\left[2-3\log\left(\frac{m^2}{\mu^2}\right)\right]\left\langle Pu_\mu u^\mu P^\dagger\right\rangle \\
& +\frac{7}{72}\left[5-3\log\left(\frac{m^2}{\mu^2}\right)\right]\left\langle D^\mu PD^\nu P^\dagger\right\rangle\left\langle u_\mu u_\nu\right\rangle \\
& +\frac{7N}{144}\left[5-3\log\left(\frac{m^2}{\mu^2}\right)\right]\left\langle D^\mu P\left\{u_\mu,u_\nu\right\}D^\nu P^\dagger\right\rangle\Bigg\}.
\end{aligned} \tag{4.67}$$

One can subtract these PCB terms in Eq. (4.67) to get a consistent power counting. Within the EOMS scheme, they are absorbed into the redefinition of the LECs of $O(p^2)$ as

$$\mathcal{L}_{\phi P}^{(2)}=\sum_{i=0}^{5}h_iO_i=\sum_{i=0}^{5}\left[h_i^r(\mu)+h_i^0\lambda+\frac{1}{16\pi^2F_0^2}h_i^{\mathrm{PCB}}\right]O_i\,, \tag{4.68}$$

where O_i represent local operators in the Lagrangian of $O(p^2)$, μ is the scale of dimensional regularization, $\lambda=\mu^{d-4}(4\pi)^{-d/2}/(d-4)$, $h_i^r(\mu)$ are the UV finite and scale-dependent part of the LECs h_i, the coefficients h_i^0 of the UV divergence $\sim\lambda$ have been given in Eq. (4.46), and h_i^{PCB} are the PCB parts. From Eq. (2.147) and Eq. (4.67), they can be easily read off as

$$\begin{aligned}
h_0^{\mathrm{PCB}} &= 0, \quad h_2^{\mathrm{PCB}}=-m^2\left(\frac{1}{72}-\frac{1}{48}\log\frac{m^2}{\mu^2}\right), \quad h_3^{\mathrm{PCB}}=m^2\left(\frac{N}{72}-\frac{N}{48}\log\frac{m^2}{\mu^2}\right), \\
h_1^{\mathrm{PCB}} &= 0, \quad h_4^{\mathrm{PCB}}=-\frac{7}{72}\left(5-3\log\frac{m^2}{\mu^2}\right), \qquad h_5^{\mathrm{PCB}}=\frac{7N}{144}\left(5-3\log\frac{m^2}{\mu^2}\right).
\end{aligned} \tag{4.69}$$

Note that we have dropped the tadpole loops with matter field propagators completely. For $N=3$, the expressions of h_i^{PCB} agree with those found in an explicit calculation of the charmed-meson–Goldstone-boson scattering amplitudes [65].

CHAPTER 5

One-loop analysis of interactions between D mesons and Goldstone bosons

In last chapter, we have systematically studied the effective generating functional of ChPT for spinless matter fields in the fundamental representation of $SU(N)$ up to $O(p^3)$. This kind of theory can be applied to the scattering between light pseudoscalar mesons and pseudoscalar heavy mesons, $SU(2)$ ChPT for kaons, three-flavor ChPT involving charmed mesons, and other relevant cases with the same pattern of spontaneous symmetry breaking and spinless matter fields.

The application of $SU(2)$ ChPT for spinless matter fields to kaon-pion scattering while treating the kaons as matter fields ensures a better convergence of chiral expansion than that of $SU(3)$ ChPT which treats the kaons as Goldstone bosons as well [68]. This theory is often used in the chiral extrapolation of lattice results at unphysical up and down quark masses to the physical values, see, e.g. Ref. [97]. While there are lots of data for the $K\pi$ scattering, no direct experimental data for $D\pi$ scattering exists. Nevertheless, there have been lattice calculations of the scattering lengths for the scattering of a light pseudoscalar meson off a charmed meson [29, 98–101]. The investigation of the S-wave scattering processes in the charmed D-meson sector is important for the understanding of the 0^+ strange and non-strange charmed mesons [28, 29, 102–108].

The hadronic interaction between charmed D mesons and the Goldstone bosons ϕ of the spontaneous breaking of chiral symmetry of the strong interaction (D-ϕ interaction for short hereafter) is important for the understanding of the chiral dynamics of QCD and the interpretation of the hadron spectrum in the heavy hadron sector. Many investigations have been devoted to study it in the last decade, partly triggered by the observation of the charm-strange meson $D_{s0}^*(2317)$ with $J^P = 0^+$ in 2003 [109, 110]. The $D_{s0}^*(2317)$ couples to the DK channel, and being below the DK threshold it decays into the isospin breaking channel $D_s\pi$. In order to unravel its nature, theorists study the D-ϕ interaction and intend to extract the information encoded in it. For instance, the $D_{s0}^*(2317)$ is interpreted as a DK molecule [27] by using a chiral unitary approach to the S-wave D-ϕ interaction [102, 104, 105]. In these works, the LO amplitudes from the heavy meson ChPT [111–113] are used as the kernels of resumed amplitudes. Extensions to the NLO can be found in Refs. [28, 103, 108, 114, 115].

In the meantime, significant progress has also been made in lattice QCD [116, 117]. Using the Lüscher formalism and its extension to coupled channels (for early works on this topic, see e.g. Refs. [118, 119]), scattering lengths and recently phase shifts for the $D\phi$ interaction have been calculated at unphysical quark masses [29, 98–101, 120]. The first calculation only concerns the channels free of disconnected Wick contractions [29, 98], i.e., $D\pi$ with isospin $I = 3/2$, $D\bar{K}$ with $I = 0, 1$, D_sK and $D_s\pi$. The channels with disconnected Wick contractions such as $D\pi$ with $I = 1/2$ and DK with $I = 0$ were calculated

later in Refs. [99–101]. On the one hand, the lattice results can be used to determine the low-energy constants (LECs) in the chiral Lagrangian [29, 65, 115, 121, 122]. On the other hand, with these lattice calculations more insights into the nature of the $D_{s0}^*(2317)$ and other positive-parity charmed mesons are obtained. In particular, in Ref. [29], it is concluded that the lattice calculation of other channels performed there supports the interpretation that $D_{s0}^*(2317)$ is dominantly a DK hadronic molecule. In addition, using the parameters fixed in that work, energy levels in the $I = 1/2$ channel were computed in Ref. [123], and a remarkable agreement with the lattice results reported in Ref. [120] was found. This agreement was taken to be as a strong evidence that the particle listed as $D_0^*(2400)$ in the Review of Particle Physics [50] in fact corresponds to two states with poles located at $\left(2105^{+6}_{-8} - i\,102^{+10}_{-12}\right)$ MeV and $\left(2451^{+36}_{-26} - i\,134^{+7}_{-8}\right)$ MeV, respectively [123], similar to the well-known two-pole scenario of the $\Lambda(1405)$ [90]. In this scenario, the puzzle that the non-strange $D_0^*(2400)$ has a mass larger than the strange partner $D_{s0}^*(2317)$ can be easily understood. The poles were searched for in unitarized ChPT with the interaction kernel computed at NLO. In view of the phenomenological importance of the $D_{s0}^*(2317)$ and $D_0^*(2400)$, it is crucial to check the stability of the NLO predictions by extending to the next-to-next-to-leading order (NNLO), which is one of the purposes of this chapter.

In Ref. [124], the D-ϕ scattering lengths were calculated in the framework of nonrelativistic heavy meson ChPT [111–113] to the leading one-loop order in the heavy quark limit. Nevertheless, as mentioned by the authors and confirmed by Ref. [125], this nonrelavistic formulation neglects sizeable recoil corrections.[1] The calculations in various unitarized versions of ChPT in Refs. [28, 29, 121, 122] are performed in a covariant formalism, but only up to NLO as mentioned above. The first NNLO calculation of the scattering lengths was given by Ref. [125] using the EOMS scheme. However, the calculation in that work is perturbative while the interactions in certain channels are definitely nonperturbative. For instance, in the channel with $(S, I) = (1, 0)$, where S and I represent strangeness and isospin, respectively, the existence of the $D_{s0}^*(2317)$ below the DK threshold calls for a nonperturbative treatment of the DK interaction or inclusion of an explicit field for the $D_{s0}^*(2317)$. In addition, all the NNLO counter term contributions are neglected in Ref. [125] due to the poorly known LECs. Here, we intend to present a detailed covariant description of the D-ϕ interaction up to NNLO in the framework of UChPT, and the EOMS approach which preserves the proper analytic structure of the amplitudes will be used in renormalization procedure.

In this chapter, we will discuss the D-ϕ scattering in general and give the scattering amplitude up to $O(p^3)$. To unitarize the one-loop potentials, the unitarization formulae obtained in Chapter 3 need to be modified to accommodate the one-loop potentials. Then we will fix the values of the LECs by fitting to the available lattice data of the S-wave D-ϕ scattering lengths. Then we search for poles in the unitarized amplitudes, and study their trajectories with varying pion mass.

5.1 D-ϕ scattering

5.1.1 Analyticity

We consider the two-body scattering $D_1(p_1)\phi_1(p_2) \to D_2(p_3)\phi_2(p_4)$. The matrix elements for a scattering are written in terms of an invariant amplitude $-i\mathcal{M}$. The S-matrix for $2 \to 2$ scattering is related to $\mathcal{M}$ by

$$\langle p_3 p_4|S|p_1 p_2\rangle = I - i(2\pi)^4\delta^4(p_1 + p_2 - p_3 - p_4)\frac{\mathcal{M}(p_1 p_2; p_3 p_4)}{(2E_1)^{1/2}(2E_2)^{1/2}(2E_3)^{1/2}(2E_4)^{1/2}}, \tag{5.1}$$

[1] It is, however, known since a long time that in the heavy baryon approach such recoil corrections can easily be incorporated by using as the propagator $i/(v\cdot l - l^2/2m)$ instead of simply $i/v\cdot l$ [70].

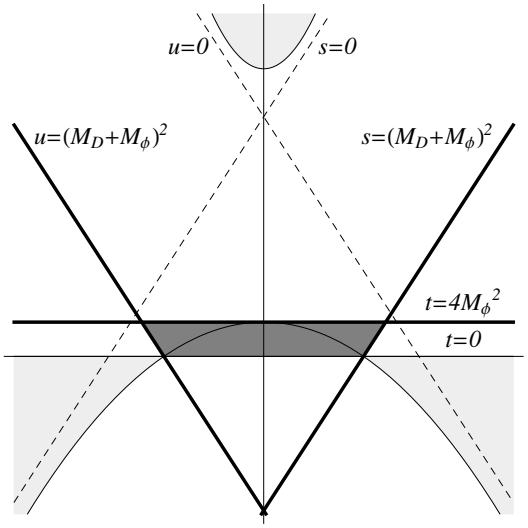

Figure 5.1: The Mandelstam plane. The Mandelstam triangle is the region bounded by the thick lines: $s = (M_D + M_\phi)^2$, $u = (M_D + M_\phi)^2$ and $t = 4M_\phi^2$. The upper part of the Mandelstam triangle is marked in dark gray, which is surrounded by the previous three lines and the one corresponding to $t = 0$. The physical regions are marked in light gray.

with the normalization

$$\langle p'|p\rangle = (2\pi)^3\delta^3(\mathbf{p}-\mathbf{p}').$$

The scattering process is on-shell, hence, $p_1^2 = M_{D_1}^2$, $p_2^2 = M_{\phi_1}^2$, $p_3^2 = M_{D_2}^2$ and $p_4^2 = M_{\phi_2}^2$, with M_{D_1} (M_{ϕ_1}) and M_{D_2} (M_{ϕ_2}) the masses of the incoming and outgoing D mesons (Goldstone bosons), respectively. In addition, the Mandelstam variables are defined as

$$s = (p_1 + p_2)^2\,, \quad t = (p_1 - p_3)^2\,, \quad u = (p_1 - p_4)^2\,, \tag{5.2}$$

which satisfy the relation $s + t + u = M_{D_1}^2 + M_{\phi_1}^2 + M_{D_2}^2 + M_{\phi_2}^2$. In the Mandelstam s-t plane, the kinematical region of the $D\phi$ scattering is defined as the domain where the Kibble function [126] $\Phi = t\left[su - (M_D^2 - M_\phi^2)^2\right]$ is non-negative. The plane is depicted in Fig. 5.1, where the bottom-right, bottom-left and top areas in light gray denote the s-, u- and t-channel physical regions, respectively. The interior of the triangle surrounded by lines of $s = (M_D + M_\phi)^2$, $u = (M_D + M_\phi)^2$ and $t = 4M_\phi^2$ is called the Mandelstam triangle, where the scattering amplitude is real and analytical.

Expressed in terms of Mandelstam variables, each of the amplitudes for a specific scattering can be denoted by $\mathcal{A}_{D_1\phi_1\to D_2\phi_2}(s,t)$. We are mostly interested in the partial wave physical amplitudes $\mathcal{A}_\ell(s)_{D_1\phi_1\to D_2\phi_2}(s)$, which are defined via (3.10)

$$\mathcal{A}_{D_1\phi_1\to D_2\phi_2}(s,t(s,\cos\theta)) = \sum_\ell (1+2\ell)P_\ell(\cos\theta)\mathcal{A}_\ell(s)_{D_1\phi_1\to D_2\phi_2}. \tag{5.3}$$

Here, the Mandelstam variable t is expressed in terms of s and the scattering angle θ,

$$\begin{aligned} t(s,\cos\theta) = {} & M_{D_1}^2 + M_{D_2}^2 - \frac{1}{2s}\left(s + M_{D_1}^2 - M_{\phi_1}^2\right)\left(s + M_{D_2}^2 - M_{\phi_2}^2\right) \\ & - \frac{\cos\theta}{2s}\sqrt{\lambda(s, M_{D_1}^2, M_{\phi_1}^2)\lambda(s, M_{D_2}^2, M_{\phi_2}^2)}\,. \end{aligned} \tag{5.4}$$

with $\lambda(a,b,c) = a^2 + b^2 + c^2 - 2ab - 2bc - 2ac$ the Källén function. Then the unitarity relation in terms of $\mathcal{A}_\ell(s)$ has the form

$$\mathcal{A}_\ell(s)_{D_1\phi_1\to D_2\phi_2} - \mathcal{A}_\ell(s)^*_{D_2\phi_2\to D_1\phi_1} = \sum_n 2ip_n \mathcal{A}_\ell(s)_{D_n\phi_n\to D_2\phi_2} \mathcal{A}_\ell(s)^*_{D_n\phi_n\to D_1\phi_1}, \tag{5.5}$$

with

$$p_n(s) = \frac{1}{2\sqrt{s}} \sqrt{(s-(M_{D_n}+M_{\phi_n})^2)(s-(M_{D_n}-M_{\phi_n})^2)} \tag{5.6}$$

the phase space of the two-particle intermediate states with the masses M_{D_n} and M_{ϕ_n}.

The partial wave amplitude $\mathcal{A}_\ell(s)_{D_1\phi_1\to D_2\phi_2}$ is a function of energy s, which is analytic everywhere except for poles and cuts connected to the kinetic and dynamic singularities (see e.g. [127–129]). The kinematic singularities are defined by the unitarity relation Eq. (5.5) and by explicit expressions of the helicity amplitudes for nonzero spins which is absent in our case. The singularities due to two-body unitarity, i.e. Eq. (5.5), are square-root branch points at each threshold. Usually the cuts are drawn from the branch points (threshold) to positive infinity in the s plane. The thresholds involved for $D\phi$ scattering as well as a possible resonance $D^*_{s0}(2317)$ are shown in Fig. 5.2.[2]

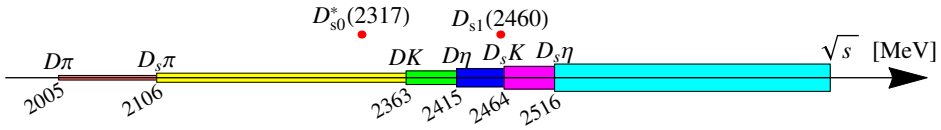

Figure 5.2: Involved thresholds, $D^*_{s0}(2317)$ and $D_{s1}(2460)$.

The dynamic singularities are associated with an interaction mechanism. The cuts from dynamic singularities are drawn to the left along the real axis from the lowest s-channel threshold. In some cases they may overlap with the unitarity cuts, thus occupying the whole real axis. The overlapping of the left-hand and right-hand cuts violates the real analyticity of amplitudes and need more consideration in detail. For a given matrix element $\mathcal{A}(s)$, which contains an infinite number of diagrams, the left-hand and right-hand cuts may overlap. However, each diagram has non-overlapping cuts. Therefore in each diagram there is a gap between the cuts, and the "amplitudes" corresponding to the diagram are real-analytic functions of s. Hence we may "conclude" that each matrix element is a real-analytic function. The standard way of taking both the unitarity and dynamic singularities into account is the N/D method in Sec. 3.4. In the framework of N/D method [129, 130] one can show that the overlapping of the left-hand and right-hand cuts does not jeopardize the usual analytic properties of the amplitudes under the condition that the cuts do not overlap in the matrix product $\hat{p}\hat{\xi}$, where $\hat{p}$ is the diagonal matrix of momenta and $\hat{\xi}$ is the matrix of left-hand discontinuities.

5.1.2 Relations between the isospin and physical amplitudes

In this work we do not consider the effect of isospin violation. It is more convenient to study the scattering amplitudes in the isospin basis instead of the particle basis. The scattering amplitudes in the isospin basis can be classified by two quantum numbers, the strangeness S and isospin I of the

[2] The $D_{s1}(2460)$, can be interpreted as a resonance of the D^*K as a heavy quark spin partner of $D^*_{s0}(2317)$, is also shown in the figure.

scattering system. Hereafter, the scattering amplitudes with the definite strangeness and isospin are called strangeness-isospin amplitudes for short. We will give the relations between the scattering amplitudes in isospin basis and in particle basis.

A direct product of two irreducible representations of the $SU(2)$ isospin group can be decomposed into a sum of irreducible representations. In what follows, the Clebsch-Gordan coefficients follows the Condon-Shortley convention, which assigns that $\langle I_1, I_1; I_2, I_2|I, I\rangle$ are real and $\langle I_1, I_1; I_2, I - I_1|I, I\rangle$ are positive for all I_1, I_2, I.

Before we give the relations between the scattering amplitudes in isospin basis and in particle basis, one needs to specify the phase convention for the isospin eigenstates. In principle, there is an arbitrariness of the overall phase between the physical states and isospin states. When an assignment is given, however, the charge conjugate relations are specified as a consequence since the G-parity of the physical states are definite. Taking the pion triplet for example, if the assignments reads

$$|\pi^+\rangle = -|1, +1\rangle, \quad |\pi^0\rangle = |1, 0\rangle, \quad |\pi^-\rangle = |1, -1\rangle, \tag{5.7}$$

then the charge conjugation must be

$$C|\pi^\pm\rangle = |\pi^\mp\rangle, \quad C|\pi^0\rangle = |\pi^0\rangle \tag{5.8}$$

in order to guarantee $G|\pi^{\pm,0}\rangle = -|\pi^{\pm,0}\rangle$. Since by definition,

$$G|I, I_3\rangle = Ce^{-i\pi I_2}|I, I_3\rangle = (-1)^{I-I_3}C|I, -I_3\rangle.$$

Acting on $|\pi^+\rangle$ for instance, $G|\pi^+\rangle = Ce^{-i\pi I_2}|\pi^+\rangle = -Ce^{-i\pi I_2}|1, +1\rangle = -C|1, -1\rangle = -C|\pi^-\rangle = -|\pi^+\rangle$, hence $C|\pi^-\rangle = |\pi^+\rangle$. The other charge conjugation relations can be derived in the same way.

Given the phase conventions

$$\begin{aligned}
|D^+\rangle &= -|\frac{1}{2}, +\frac{1}{2}\rangle\,, \qquad |D^0\rangle = |\frac{1}{2}, -\frac{1}{2}\rangle,\\
|\bar{D}^0\rangle &= +|\frac{1}{2}, +\frac{1}{2}\rangle\,, \qquad |D^-\rangle = |\frac{1}{2}, -\frac{1}{2}\rangle,\\
|K^+\rangle &= +|\frac{1}{2}, +\frac{1}{2}\rangle\,, \qquad |K^0\rangle = |\frac{1}{2}, -\frac{1}{2}\rangle,\\
|\bar{K}^0\rangle &= -|\frac{1}{2}, +\frac{1}{2}\rangle\,, \qquad |K^-\rangle = |\frac{1}{2}, -\frac{1}{2}\rangle,
\end{aligned} \tag{5.9}$$

the charge conjugate operation gives

$$\begin{aligned}
&C|D^\pm\rangle = |D^\mp\rangle\,, \quad C|D^0\rangle = |\bar{D}^0\rangle\,, \quad C|\bar{D}^0\rangle = |D^0\rangle\,.\\
&C|K^\pm\rangle = |K^\mp\rangle\,, \quad C|K^0\rangle = |\bar{K}^0\rangle\,, \quad C|\bar{K}^0\rangle = |K^0\rangle\,.
\end{aligned}$$

According to the conventions Eq. (5.9) and Clebsch-Gordan coefficients, the relations between isospin and physical amplitudes can be easily obtained. Taking the scattering $DK \to DK$ for example, the

physical states are related to the isospin states by

$$
\begin{aligned}
|D^+K^+\rangle &= -|\frac{1}{2},+\frac{1}{2}\rangle_D|\frac{1}{2},+\frac{1}{2}\rangle_\phi = -|1,+1\rangle_I,\\
|D^+K^0\rangle &= -|\frac{1}{2},+\frac{1}{2}\rangle_D|\frac{1}{2},-\frac{1}{2}\rangle_\phi = -\sqrt{\frac{1}{2}}|1,0\rangle_I - \sqrt{\frac{1}{2}}|0,0\rangle_I,\\
|D^0K^+\rangle &= +|\frac{1}{2},-\frac{1}{2}\rangle_D|\frac{1}{2},+\frac{1}{2}\rangle_\phi = \sqrt{\frac{1}{2}}|1,0\rangle_I - \sqrt{\frac{1}{2}}|0,0\rangle_I,\\
|D^0K^0\rangle &= +|\frac{1}{2},-\frac{1}{2}\rangle_D|\frac{1}{2},-\frac{1}{2}\rangle_\phi = |1,-1\rangle_I,
\end{aligned}
\tag{5.10}
$$

with the subscript I denoting the isospin of the scattering system. It follows that

$$
\begin{aligned}
\mathcal{A}_{D^+K^+\to D^+K^+} &= A^{I=1}_{DK\to DK},\\
\mathcal{A}_{D^+K^0\to D^+K^0} &= \frac{1}{2}\mathcal{A}^{I=1}_{DK\to DK} + \frac{1}{2}\mathcal{A}^{I=0}_{DK\to DK},\\
\mathcal{A}_{D^0K^+\to D^0K^+} &= \frac{1}{2}\mathcal{A}^{I=1}_{DK\to DK} + \frac{1}{2}\mathcal{A}^{I=0}_{DK\to DK},\\
\mathcal{A}_{D^0K^0\to D^0K^0} &= \mathcal{A}^{I=1}_{DK\to DK},\\
\mathcal{A}_{D^+K^0\to D^0K^+} &= -\frac{1}{2}\mathcal{A}^{I=1}_{DK\to DK} + \frac{1}{2}\mathcal{A}^{I=0}_{DK\to DK},\\
\mathcal{A}_{D^0K^+\to D^+K^0} &= -\frac{1}{2}\mathcal{A}^{I=1}_{DK\to DK} + \frac{1}{2}\mathcal{A}^{I=0}_{DK\to DK}.
\end{aligned}
\tag{5.11}
$$

Likewise, since

$$
\begin{aligned}
|D^+\bar{K}^0\rangle &= +|\frac{1}{2},+\frac{1}{2}\rangle_D|\frac{1}{2},+\frac{1}{2}\rangle_\phi = |1,+1\rangle_I,\\
|D^+K^-\rangle &= -|\frac{1}{2},+\frac{1}{2}\rangle_D|\frac{1}{2},-\frac{1}{2}\rangle_\phi = -\sqrt{\frac{1}{2}}|1,0\rangle_I - \sqrt{\frac{1}{2}}|0,0\rangle_I,\\
|D^0\bar{K}^0\rangle &= -|\frac{1}{2},-\frac{1}{2}\rangle_D|\frac{1}{2},+\frac{1}{2}\rangle_\phi = -\sqrt{\frac{1}{2}}|1,0\rangle_I + \sqrt{\frac{1}{2}}|0,0\rangle_I,\\
|D^0K^-\rangle &= |\frac{1}{2},-\frac{1}{2}\rangle_D|\frac{1}{2},-\frac{1}{2}\rangle_\phi = |1,-1\rangle_I,
\end{aligned}
\tag{5.12}
$$

one finds

$$
\begin{aligned}
\mathcal{A}_{D^+\bar{K}^0\to D^+\bar{K}^0} &= \mathcal{A}^{I=1}_{D\bar{K}\to D\bar{K}},\\
\mathcal{A}_{D^+K^-\to D^+K^-} &= \frac{1}{2}\mathcal{A}^{I=1}_{D\bar{K}\to D\bar{K}} + \frac{1}{2}\mathcal{A}^{I=0}_{D\bar{K}\to D\bar{K}},\\
\mathcal{A}_{D^0\bar{K}^0\to D^0\bar{K}^0} &= \frac{1}{2}\mathcal{A}^{I=1}_{D\bar{K}\to D\bar{K}} + \frac{1}{2}\mathcal{A}^{I=0}_{D\bar{K}\to D\bar{K}},\\
\mathcal{A}_{D^0K^-\to D^0K^-} &= \mathcal{A}^{I=1}_{D\bar{K}\to D\bar{K}},\\
\mathcal{A}_{D^+K^-\to D^0\bar{K}^0} &= \frac{1}{2}\mathcal{A}^{I=1}_{D\bar{K}\to D\bar{K}} - \frac{1}{2}\mathcal{A}^{I=0}_{D\bar{K}\to D\bar{K}},\\
\mathcal{A}_{D^0\bar{K}^0\to D^+K^-} &= \frac{1}{2}\mathcal{A}^{I=1}_{D\bar{K}\to D\bar{K}} - \frac{1}{2}\mathcal{A}^{I=0}_{D\bar{K}\to D\bar{K}}.
\end{aligned}
\tag{5.13}
$$

The relations for $D\pi \to D\pi$ scattering can be obtained in the same way. The isospin of the pions is $I = 1$, thus we have

$$
\begin{aligned}
|D^+\pi^+\rangle &= |1,+1\rangle|\frac{1}{2},+\frac{1}{2}\rangle = |\frac{3}{2},+\frac{3}{2}\rangle_I,\\
|D^0\pi^+\rangle &= -|1,+1\rangle|\frac{1}{2},-\frac{1}{2}\rangle = -\sqrt{\frac{1}{3}}|\frac{3}{2},+\frac{1}{2}\rangle - \sqrt{\frac{2}{3}}|\frac{1}{2},+\frac{1}{2}\rangle_I,\\
|D^+\pi^0\rangle &= -|1,0\rangle|\frac{1}{2},+\frac{1}{2}\rangle = -\sqrt{\frac{2}{3}}|\frac{3}{2},+\frac{1}{2}\rangle_I + \sqrt{\frac{1}{3}}|\frac{1}{2},+\frac{1}{2}\rangle_I,\\
|D^0\pi^0\rangle &= |1,0\rangle|\frac{1}{2},-\frac{1}{2}\rangle = \sqrt{\frac{2}{3}}|\frac{3}{2},-\frac{1}{2}\rangle_I + \sqrt{\frac{1}{3}}|\frac{1}{2},-\frac{1}{2}\rangle_I,\\
|D^+\pi^-\rangle &= -|1,-1\rangle|\frac{1}{2},+\frac{1}{2}\rangle = -\sqrt{\frac{1}{3}}|\frac{3}{2},-\frac{1}{2}\rangle_I + \sqrt{\frac{2}{3}}|\frac{1}{2},-\frac{1}{2}\rangle_I,\\
|D^0\pi^-\rangle &= |1,-1\rangle|\frac{1}{2},-\frac{1}{2}\rangle = |\frac{3}{2},-\frac{3}{2}\rangle_I.
\end{aligned}
\tag{5.14}
$$

It follows

$$
\begin{aligned}
\mathcal{A}_{D^+\pi^+\to D^+\pi^+} &= \mathcal{A}^{I=\frac{3}{2}}_{D\pi\to D\pi},\\
\mathcal{A}_{D^0\pi^+\to D^0\pi^+} &= \frac{1}{3}\mathcal{A}^{I=\frac{3}{2}}_{D\pi\to D\pi} + \frac{2}{3}\mathcal{A}^{I=\frac{1}{2}}_{D\pi\to D\pi},\\
\mathcal{A}_{D^+\pi^0\to D^+\pi^0} &= \frac{2}{3}\mathcal{A}^{I=\frac{3}{2}}_{D\pi\to D\pi} + \frac{1}{3}\mathcal{A}^{I=\frac{1}{2}}_{D\pi\to D\pi},\\
\mathcal{A}_{D^0\pi^0\to D^0\pi^0} &= \frac{2}{3}\mathcal{A}^{I=\frac{3}{2}}_{D\pi\to D\pi} + \frac{1}{3}\mathcal{A}^{I=\frac{1}{2}}_{D\pi\to D\pi},\\
\mathcal{A}_{D^+\pi^-\to D^+\pi^-} &= \frac{1}{3}\mathcal{A}^{I=\frac{3}{2}}_{D\pi\to D\pi} + \frac{2}{3}\mathcal{A}^{I=\frac{1}{2}}_{D\pi\to D\pi},\\
\mathcal{A}_{D^0\pi^-\to D^0\pi^-} &= \mathcal{A}^{I=\frac{3}{2}}_{D\pi\to D\pi},\\
\mathcal{A}_{D^0\pi^+\to D^+\pi^0} &= \frac{\sqrt{2}}{3}\mathcal{A}^{I=\frac{3}{2}}_{D\pi\to D\pi} - \frac{\sqrt{2}}{3}\mathcal{A}^{I=\frac{1}{2}}_{D\pi\to D\pi},\\
\mathcal{A}_{D^+\pi^+\to D^0\pi^+} &= \frac{\sqrt{2}}{3}\mathcal{A}^{I=\frac{3}{2}}_{D\pi\to D\pi} - \frac{\sqrt{2}}{3}\mathcal{A}^{I=\frac{1}{2}}_{D\pi\to D\pi},\\
\mathcal{A}_{D^0\pi^0\to D^+\pi^-} &= -\frac{\sqrt{2}}{3}\mathcal{A}^{I=\frac{3}{2}}_{D\pi\to D\pi} + \frac{\sqrt{2}}{3}\mathcal{A}^{I=\frac{1}{2}}_{D\pi\to D\pi},\\
\mathcal{A}_{D^+\pi^-\to D^0\pi^0} &= -\frac{\sqrt{2}}{3}\mathcal{A}^{I=\frac{3}{2}}_{D\pi\to D\pi} + \frac{\sqrt{2}}{3}\mathcal{A}^{I=\frac{1}{2}}_{D\pi\to D\pi}.
\end{aligned}
\tag{5.15}
$$

One of the particles in the processes $D\eta \to D\eta$, $D_s\eta \to D_s\eta$, $D_s\pi \to D_s\pi$, $D_sK \to D_sK$ and $D_s\bar{K} \to D_s\bar{K}$ is isospin zero, thus their amplitudes own definite total ispspin, which are equal to the isospin of the other particles. Straightforwardly we have

$$
\begin{aligned}
\mathcal{A}^{I=\frac{1}{2}}_{D\eta\to D\eta} &= \mathcal{A}_{D^+\eta\to D^+\eta} = \mathcal{A}_{D^0\eta\to D^0\eta},\\
\mathcal{A}^{I=0}_{D_s\eta\to D_s\eta} &= \mathcal{A}_{D_s^+\eta\to D_s^+\eta},
\end{aligned}
\tag{5.16}
$$

and

$$\begin{aligned}
\mathcal{A}^{I=1}_{D_s\pi\to D_s\pi} &= \mathcal{A}_{D_s^+\pi^+\to D_s^+\pi^+} = \mathcal{A}_{D_s^+\pi^0\to D_s^+\pi^0} = \mathcal{A}_{D_s^+\pi^-\to D_s^+\pi^-},\\
\mathcal{A}^{I=\frac{1}{2}}_{D_sK\to D_sK} &= \mathcal{A}_{D_s^+K^+\to D_s^+K^+} = \mathcal{A}_{D_s^+K^0\to D_s^+K^0},\\
\mathcal{A}_{D_s\bar{K}\to D_s\bar{K}} &= \mathcal{A}_{D_s^+K^-\to D_s^+K^-} = \mathcal{A}_{D_s^+\bar{K}^0\to D_s^+\bar{K}^0}.
\end{aligned} \tag{5.17}$$

In above equations, the Mandelstam variables s, t and u are dropped, they should be understood as $\mathcal{A}(s,t,u)$.

On the other hand, one can construct the amplitudes with definite isospin and strangeness in terms of physical amplitudes. Another interesting property of the amplitudes is the crossing symmetry, which states that the following processes:

$$\begin{aligned}
a+b &\to c+d, \quad (s-\text{channel})\\
\bar{c}+b &\to \bar{a}+d, \quad (t-\text{channel})\\
a+\bar{d} &\to c+\bar{b}, \quad (u-\text{channel})
\end{aligned} \tag{5.18}$$

share the same amplitude $\mathcal{A}$. In detail, it implies

$$\begin{aligned}
\mathcal{A}_{D^+K^+\to D^+K^+}(s,t,u) &= \mathcal{A}_{D^+K^-\to D^+K^-}(u,t,s),\\
\mathcal{A}_{D^+K^0\to D^+K^0}(s,t,u) &= \mathcal{A}_{D^+\bar{K}^0\to D^+\bar{K}^0}(u,t,s),\\
\mathcal{A}_{D^+K^0\to D^0K^+}(s,t,u) &= \mathcal{A}_{D^+K^-\to D^0\bar{D}\bar{K}^0}(u,t,s),\\
\mathcal{A}_{D^+\pi^+\to D^+\pi^+}(s,t,u) &= \mathcal{A}_{D^+\pi^-\to D^+\pi^-}(u,t,s),\\
\mathcal{A}_{D^0\pi^+\to D^0\pi^+}(s,t,u) &= \mathcal{A}_{D^0\pi^-\to D^0\pi^-}(u,t,s),\\
\mathcal{A}_{D^+\pi^0\to D^+\pi^0}(s,t,u) &= \mathcal{A}_{D^+\pi^0\to D^+\pi^0}(u,t,s),\\
\mathcal{A}_{D^0\pi^+\to D^+\pi^0}(s,t,u) &= \mathcal{A}_{D^0\pi^0\to D^+\pi^-}(u,t,s),\\
\mathcal{A}_{D^+\eta\to D^+\eta}(s,t,u) &= \mathcal{A}_{D^+\eta\to D^+\eta}(u,t,s),\\
\mathcal{A}_{D_s^+\eta\to D_s^+\eta}(s,t,u) &= \mathcal{A}_{D_s^+\eta\to D_s^+\eta}(u,t,s),\\
\mathcal{A}_{D_s^+\pi^+\to D_s^+\pi^+}(s,t,u) &= \mathcal{A}_{D_s^+\pi^-\to D_s^+\pi^-}(u,t,s),\\
\mathcal{A}_{D_s^+K^+\to D_s^+K^+}(s,t,u) &= \mathcal{A}_{D_s^+K^-\to D_s^+K^-}(u,t,s).
\end{aligned} \tag{5.19}$$

Making use of the crossing symmetry and isospin symmetry, all of the strangeness-isospin amplitudes can be related to ten amplitudes of the physical processes. We begin with the single-channel interactions. There are four single-channels in total. The corresponding quantum numbers of (S,I) are $(-1,0)$, $(-1,1)$, $(0,3/2)$ and $(2,1/2)$. Their strangeness-isospin amplitudes are related to the physical-process amplitudes by

$$\mathcal{A}^{(-1,0)}_{D\bar{K}\to D\bar{K}}(s,t,u) = 2\,\mathcal{A}_{D^+K^+\to D^+K^+}(u,t,s) - \mathcal{A}_{D^0K^-\to D^0K^-}(s,t,u)\,, \tag{5.20}$$

$$\mathcal{A}^{(-1,1)}_{D\bar{K}\to D\bar{K}}(s,t,u) = \mathcal{A}_{D^0K^-\to D^0K^-}(s,t,u)\,, \tag{5.21}$$

$$\mathcal{A}^{(0,3/2)}_{D\pi\to D\pi}(s,t,u) = \mathcal{A}_{D^+\pi^+\to D^+\pi^+}(s,t,u)\,, \tag{5.22}$$

$$\mathcal{A}^{(2,1/2)}_{D_sK\to D_sK}(s,t,u) = \mathcal{A}_{D_s^+K^+\to D_s^+K^+}(s,t,u)\,. \tag{5.23}$$

For the coupled channels with $(S, I) = (1, 0)$, the strangeness-isospin amplitudes read

$$\mathcal{A}^{(1,0)}_{DK\to DK}(s,t,u) = 2\,\mathcal{A}_{D^0K^-\to D^0K^-}(u,t,s) - \mathcal{A}_{D^+K^+\to D^+K^+}(s,t,u)\,, \tag{5.24}$$

$$\mathcal{A}^{(1,0)}_{D_s\eta\to D_s\eta}(s,t,u) = \mathcal{A}_{D_s^+\eta\to D_s^+\eta}(s,t,u)\,, \tag{5.25}$$

$$\mathcal{A}^{(1,0)}_{D_s\eta\to DK}(s,t,u) = -\sqrt{2}\,\mathcal{A}_{D_s^+K^-\to D^0\eta}(u,t,s)\,. \tag{5.26}$$

For the coupled channels with $(S, I) = (1, 1)$, one has

$$\mathcal{A}^{(1,1)}_{D_s\pi\to D_s\pi}(s,t,u) = \mathcal{A}_{D_s^+\pi^0\to D_s^+\pi^0}(s,t,u)\,, \tag{5.27}$$

$$\mathcal{A}^{(1,1)}_{DK\to DK}(s,t,u) = \mathcal{A}_{D^+K^+\to D^+K^+}(s,t,u)\,, \tag{5.28}$$

$$\mathcal{A}^{(1,1)}_{DK\to D_s\pi}(s,t,u) = \sqrt{2}\,\mathcal{A}_{D_s^+K^-\to D^0\pi^0}(u,t,s)\,. \tag{5.29}$$

For $(S, I) = (0, 1/2)$, there are three channels: $D\pi, D\eta$ and $D_s\bar{K}$. The isospin relations are given by

$$\mathcal{A}^{(0,1/2)}_{D\pi\to D\pi}(s,t,u) = \frac{3}{2}\mathcal{A}_{D^+\pi^+\to D^+\pi^+}(u,t,s) - \frac{1}{2}\mathcal{A}_{D^+\pi^+\to D^+\pi^+}(s,t,u)\,, \tag{5.30}$$

$$\mathcal{A}^{(0,1/2)}_{D\eta\to D\eta}(s,t,u) = \mathcal{A}_{D^+\eta\to D^+\eta}(s,t,u)\,, \tag{5.31}$$

$$\mathcal{A}^{(0,1/2)}_{D_s\bar{K}\to D_s\bar{K}}(s,t,u) = \mathcal{A}_{D_s^+K^+\to D_s^+K^+}(u,t,s)\,, \tag{5.32}$$

$$\mathcal{A}^{(0,1/2)}_{D\eta\to D\pi}(s,t,u) = \sqrt{3}\mathcal{A}_{D^0\eta\to D^0\pi^0}(s,t,u)\,, \tag{5.33}$$

$$\mathcal{A}^{(0,1/2)}_{D_s\bar{K}\to D\pi}(s,t,u) = \sqrt{3}\mathcal{A}_{D_s^+K^-\to D^0\pi^0}(s,t,u)\,, \tag{5.34}$$

$$\mathcal{A}^{(0,1/2)}_{D_s\bar{K}\to D\eta}(s,t,u) = \mathcal{A}_{D_s^+K^-\to D^0\eta}(s,t,u)\,. \tag{5.35}$$

5.2 D-ϕ interactions in ChPT for spinless matter fields

It is well-known that ChPT [14–16] has become an useful and standard tool in studying the hadron interaction at low energies. Based on Weinberg's power counting rules [14], great achievements have been obtained both in the pure mesonic sector and the one including matter fields such as baryons, the latter known as baryon ChPT. In this section, we study the interactions between charmed mesons and Goldstone bosons with ChPT in which the spinless charmed mesons are regarded as matter fields since they have nonvanishing masses in the chiral limit. We are interested in the $SU(3)$ case and the pseudoscalar charmed mesons can be collected in a fundamental representation $P:\ D = (D^0, D^+, D_s^+)$, and the light Goldstone bosons are in an octet,

$$\phi = \begin{pmatrix} \frac{1}{\sqrt{2}}\pi^0 + \frac{1}{\sqrt{6}}\eta & \pi^+ & K^+ \\ \pi^- & -\frac{1}{\sqrt{2}}\pi^0 + \frac{1}{\sqrt{6}}\eta & K^0 \\ K^- & \bar{K}^0 & -\frac{2}{\sqrt{6}}\eta \end{pmatrix}. \tag{5.36}$$

In Chaper 4, we have obtained the effective generating functional up to $O(p^3)$, i.e. leading one-loop order, which is free of UV divergences and fulfils the power counting. One can read off the scattering amplitudes for D-ϕ from the generating functional Eqs. (4.19) and (4.57), taking into account the redefinition of LECs Eqs. (4.45) and (4.68).

In this section we exhibit the complet sef of independent D-ϕ scattering amplitudes on the basis of the

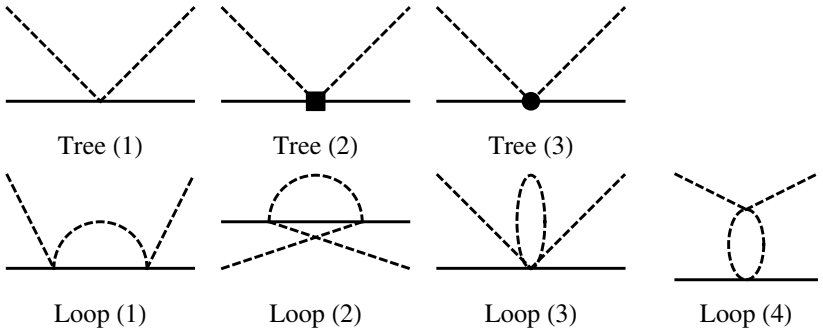

Figure 5.3: The 1-point irreducible (1PI) Feynman diagrams for D-ϕ scattering up to leading one-loop order. The solid (dashed) lines represent the D (Goldstone) mesons. The square stands for the contact vertex coming from Lagrangian $\mathcal{L}^{(2)}_{D\phi}$, while the filled circle denotes an insertion from $\mathcal{L}^{(3)}_{D\phi}$. All other vertices are generated either by $\mathcal{L}^{(1)}_{D\phi}$ or $\mathcal{L}^{(2)}_{\phi\phi}$.

phycial states. They correspond to the ten physical processes listed in the second column in Table 5.1. All the other amplitudes can be obtained by either crossing symmetry or time-reversal invariance. In what follows, we fill first give the tree-level amplitudes which can be reduced into a common structure but with different coefficients because of $SU(3)$ symmetry. Then the loop amplitudes will be given.

5.2.1 Tree-level amplitudes

The Feynman diagrams of the tree-level contribution to the scattering amplitudes are displayed in the first line of Fig. 5.3. Since we do not consider the exchange of resonances, such contributions are encoded in the contact terms for the D-ϕ scattering. When calculating the Feynman diagrams, all the bare parameters, such as the decay constant F_0 and the masses, are maintained. They will be replaced by the corresponding physical quantities when the renormalization is performed. The LO, i.e. $O(p)$, tree amplitude is the Weinberg–Tomozawa term [3], and has the following form,

$$\mathcal{A}^{(1)}(s,t,u) = C_{\rm LO}\frac{s-u}{4F_0^2}, \tag{5.37}$$

where the coefficients $C_{\rm LO}$ for different physical processes are listed in Table 5.1. The Weinberg-Tomozawa term depends only on the pion decay constant due to the fact that it originates from the kinetic term in $\mathcal{L}^{(1)}_{D\phi}$, which is a result of the spontaneous breaking of chiral symmetry in QCD.

The $O(p^2)$ Lagrangian $\mathcal{L}^{(2)}_{D\phi}$ generates the tree-level contribution at NLO as

$$\mathcal{A}^{(2)}(s,t,u) = \frac{1}{F_0^2}\left[-4h_0C_0^{(2)} + 2h_1C_1^{(2)} - 2C_{24}^{(2)}H_{24}(s,t,u) + 2C_{35}^{(2)}H_{35}(s,t,u)\right], \tag{5.38}$$

where the coefficients are shown in Table 5.1, and the functions $H_{24}(s,t,u)$ and $H_{35}(s,t,u)$ are defined by

$$H_{24}(s,t,u) = 2h_2\, p_2\cdot p_4 + h_4\,(p_1\cdot p_2 p_3\cdot p_4 + p_1\cdot p_4 p_2\cdot p_3)\,, \tag{5.39}$$
$$H_{35}(s,t,u) = h_3\, p_2\cdot p_4 + h_5\,(p_1\cdot p_2 p_3\cdot p_4 + p_1\cdot p_4 p_2\cdot p_3)\,. \tag{5.40}$$

[3] As the vector charmed mesons are not taken into account, there is no Born term due to the exchange of these mesons.

Table 5.1: The coefficients in the LO and NLO tree-level amplitudes of the 10 relevant physical processes. The Gell-Mann-Okubo mass relation, $3M_\eta^2 = 4M_K^2 - M_\pi^2$, is used to simplify the coefficients when necessary.

	Physical processes	$C_{\rm LO}$	$C_0^{(2)}$	$C_1^{(2)}$	$C_{24}^{(2)}$	$C_{35}^{(2)}$
1	$D^0K^- \to D^0K^-$	1	M_K^2	$-M_K^2$	1	1
2	$D^+K^+ \to D^+K^+$	0	M_K^2	0	1	0
3	$D^+\pi^+ \to D^+\pi^+$	1	M_π^2	$-M_\pi^2$	1	1
4	$D^+\eta \to D^+\eta$	0	M_η^2	$-\frac{1}{3}M_\pi^2$	1	$\frac{1}{3}$
5	$D_s^+K^+ \to D_s^+K^+$	1	M_K^2	$-M_K^2$	1	1
6	$D_s^+\eta \to D_s^+\eta$	0	M_η^2	$\frac{4}{3}\left(M_\pi^2 - 2M_K^2\right)$	1	$\frac{4}{3}$
7	$D_s^+\pi^0 \to D_s^+\pi^0$	0	M_π^2	0	1	0
8	$D^0\eta \to D^0\pi^0$	0	0	$-\frac{1}{\sqrt{3}}M_\pi^2$	0	$\frac{1}{\sqrt{3}}$
9	$D_s^+K^- \to D^0\pi^0$	$-\frac{1}{\sqrt{2}}$	0	$-\frac{1}{2\sqrt{2}}\left(M_K^2 + M_\pi^2\right)$	0	$\frac{1}{\sqrt{2}}$
10	$D_s^+K^- \to D^0\eta$	$-\sqrt{\frac{3}{2}}$	0	$\frac{1}{2\sqrt{6}}\left(5M_K^2 - 3M_\pi^2\right)$	0	$-\frac{1}{\sqrt{6}}$

Table 5.2: The coefficients in the NNLO tree-level amplitudes of the 10 relevant physical processes.

	physical process	$C_{1a}^{(3)}$	$C_{1b}^{(3)}$	$C_{23}^{(3)}$
1	$D^0K^- \to D^0K^-$	M_K^2	0	1
2	$D^+K^+ \to D^+K^+$	0	0	0
3	$D^+\pi^+ \to D^+\pi^+$	M_π^2	0	1
4	$D^+\eta \to D^+\eta$	0	0	0
5	$D_s^+K^+ \to D_s^+K^+$	M_K^2	0	1
6	$D_s^+\eta \to D_s^+\eta$	0	0	0
7	$D_s^+\pi^0 \to D_s^+\pi^0$	0	0	0
8	$D^0\eta \to D^0\pi^0$	0	0	0
9	$D_s^+K^- \to D^0\pi^0$	$-\frac{1}{\sqrt{2}}M_K^2$	$\frac{1}{\sqrt{2}}\left(M_K^2 - M_\pi^2\right)$	$-\frac{1}{\sqrt{2}}$
10	$D_s^+K^- \to D^0\eta$	$-\sqrt{\frac{3}{2}}M_K^2$	$\frac{1}{\sqrt{6}}\left(M_\pi^2 - M_K^2\right)$	$-\sqrt{\frac{3}{2}}$

Finally, the tree-level amplitude at $O(p^3)$ reads

$$\mathcal{A}^{(3)}(s,t,u) = \frac{1}{F_0^2}\left\{4g_1\Big[C_{1a}^{(3)}(p_1+p_3)\cdot(p_2+p_4) + C_{1b}^{(3)}(p_1+p_3)\cdot p_2\Big] + 4C_{23}^{(3)}G_{23}(s,t,u)\right\}, \tag{5.41}$$

with

$$\begin{aligned} G_{23}(s,t,u) = &-g_2\, p_2\cdot p_4(p_1+p_3)\cdot(p_2+p_4) \\ &+2g_3\left[(p_1\cdot p_2)(p_1\cdot p_4)p_1\cdot(p_2+p_4) + (p_1 \to p_3)\right]. \end{aligned} \tag{5.42}$$

The corresponding coefficients can be found in Table 5.2. The $C_{1b}^{(3)}$ term survives only for inelastic scattering processes.

5.2.2 One-loop contribution

The one-loop connected graphs for D-ϕ scattering are shown in the second line of Fig. 5.3. All the vertices in the loop graphs originate from the Lagrangians $\mathcal{L}^{(1)}_{D\phi}$ and $\mathcal{L}^{(2)}_{\phi\phi}$ which are free of unknown LECs. Similar to the tree-level amplitudes, it suffices to calculate the loop amplitudes for the 10 physical processes. They read

$$
\begin{aligned}
\mathcal{A}^{\text{loop}}_{D^0K^-\to D^0K^-}(s,t) &= \frac{1}{16F^4}\Big\{\mathcal{F}^{(DK)}_{DK}(s,t)+2\mathcal{F}^{(DK)}_{DK}(u,t)+\frac{3}{2}\mathcal{F}^{(D_s\eta)}_{DK}(u,t)\\
&\quad+\frac{1}{2}\mathcal{F}^{(D_s\pi)}_{DK}(u,t)+(s-u)\left(\mathcal{I}_\eta+2\mathcal{I}_K+\mathcal{I}_\pi\right)\\
&\quad-4(s-u)\left[\mathcal{J}^{00}_\pi(t)+2\mathcal{J}^{00}_K(t)\right]\Big\},\\
\mathcal{A}^{\text{loop}}_{D^+K^+\to D^+K^+}(s,t) &= \frac{1}{16F^4}\left\{\mathcal{F}^{(D_s\pi)}_{DK}(s,t)+\mathcal{F}^{(DK)}_{DK}(u,t)-4(s-u)\left[\mathcal{J}^{00}_\pi(t)-\mathcal{J}^{00}_K(t)\right]\right\},\\
\mathcal{A}^{\text{loop}}_{D^+\pi^+\to D^+\pi^+}(s,t) &= \frac{1}{16F^4}\Big\{\mathcal{F}^{(D\pi)}_{D\pi}(s,t)+3\mathcal{F}^{(D\pi)}_{D\pi}(u,t)+\mathcal{F}^{(D_sK)}_{D\pi}(u,t)\\
&\quad+\frac{4}{3}(s-u)\left(2\mathcal{I}_\pi+\mathcal{I}_K\right)-4(s-u)\left[2\mathcal{J}^{00}_\pi(t)+\mathcal{J}^{00}_K(t)\right]\Big\},\\
\mathcal{A}^{\text{loop}}_{D^+\eta\to D^+\eta}(s,t) &= \frac{1}{16F^4}\left[\frac{3}{2}\mathcal{F}^{(D_sK)}_{D\eta}(s,t)+\frac{3}{2}\mathcal{F}^{(D_sK)}_{D\eta}(u,t)\right],\\
\mathcal{A}^{\text{loop}}_{D_s^+K^+\to D_s^+K^+}(s,t) &= \frac{1}{16F^4}\Big[\mathcal{F}^{(D_sK)}_{D_sK}(s,t)+\mathcal{F}^{(D_sK)}_{D_sK}(u,t)+\frac{3}{2}\mathcal{F}^{(D\eta)}_{D_sK}(u,t)\\
&\quad+\frac{3}{2}\mathcal{F}^{(D\pi)}_{D_sK}(u,t)+(s-u)\left(\mathcal{I}_\eta+2\mathcal{I}+\mathcal{I}\pi\right)\\
&\quad-12(s-u)\mathcal{J}^{00}_K(t)\Big],
\end{aligned}
$$

$$
\begin{aligned}
\mathcal{A}^{\text{loop}}_{D_s^+\eta\to D_s^+\eta}(s,t) &= \frac{1}{16F^4}\left[3\,\mathcal{F}^{(DK)}_{D_s\eta}(s,t)+3\,\mathcal{F}^{(DK)}_{D_s\eta}(u,t)\right],\\
\mathcal{A}^{\text{loop}}_{D_s^+\pi^0\to D_s^+\pi^0}(s,t) &= \frac{1}{16F^4}\left[\mathcal{F}^{(DK)}_{D_s\pi}(s,t)+\mathcal{F}^{(DK)}_{D_s\pi}(u,t)\right],\\
\mathcal{A}^{\text{loop}}_{D^0\eta\to D^0\pi^0}(s,t) &= \frac{\sqrt{3}}{64F^4}\left[\mathcal{F}^{(D_sK)}_{D\eta}(s,t)+\mathcal{F}^{(D_sK)}_{D\pi}(s,t)+2\,\mathcal{G}^{(D_sK)}_{D\eta,D\pi}(s,t)+(s\leftrightarrow u)\right],
\end{aligned}
\tag{5.43}
$$

$$
\begin{aligned}
\mathcal{A}^{\text{loop}}_{D_s^+K^-\to D^0\pi^0}(s,t) &= \frac{\sqrt{2}}{16F^4}\Big\{\frac{1}{2}\left[\mathcal{F}^{(D\pi)}_{D_sK}(s,t)+\mathcal{F}^{(D\pi)}_{D\pi}(s,t)+2\,\mathcal{G}^{(D\pi)}_{D_sK,D\pi}(s,t)\right]\\
&\quad+\frac{1}{4}\left[\mathcal{F}^{(D_sK)}_{D_sK}(s,t)+\mathcal{F}^{(D_sK)}_{D\pi}(s,t)+2\,\mathcal{G}^{(D_sK)}_{D_sK,D\pi}(s,t)\right]\\
&\quad-\frac{s-u}{12}\left(3\mathcal{I}_\eta+11\mathcal{I}_\pi+10\mathcal{I}_K\right)+\frac{\Delta_{D_sD}}{24}\left(3\mathcal{I}_\eta-5\mathcal{I}_\pi+2\mathcal{I}_K\right)\\
&\quad-\left({}^1\mathcal{K}^{(\eta K)}_{D_sK,D\pi}(s,t)+{}^2\mathcal{K}^{(\eta K)}_{D_sK,D\pi}(s,t)\right)\\
&\quad-\left(\frac{5}{3}\,{}^1\mathcal{K}^{(K\pi)}_{D_sK,D\pi}(s,t)+{}^2\mathcal{K}^{(K\pi)}_{D_sK,D\pi}(s,t)\right)\Big\},
\end{aligned}
\tag{5.44}
$$

and

$$\begin{aligned}\mathcal{A}^{\rm loop}_{D_s^+K^-\to D^0\eta}(s,t) = \frac{\sqrt{6}}{16F^4}\Big\{&\frac{1}{4}\left(\mathcal{F}^{(D_sK)}_{D_sK}(s,t)+\mathcal{F}^{(D_sK)}_{D\eta}(s,t)+2\,\mathcal{G}^{(D_sK)}_{D_sK,D\eta}(s,t)\right)\\ &-\frac{1}{2}\left(\mathcal{F}^{(DK)}_{D_sK}(u,t)+\mathcal{F}^{(DK)}_{D\eta}(u,t)+\mathcal{G}^{(DK)}_{D_sK,D\eta}(u,t)+\mathcal{G}^{(DK)}_{D_s\eta,DK}(u,t)\right)\\ &+\left({}^1\mathcal{K}^{(K\pi)}_{D_sK,D\eta}(s,t)-{}^2\mathcal{K}^{(K\pi)}_{D_sK,D\eta}(s,t)\right)\\ &-\left({}^1\mathcal{K}^{(\eta K)}_{D_sK,D\eta}(s,t)+{}^2\mathcal{K}^{(\eta K)}_{D_sK,D\eta}(s,t)\right)\\ &+\frac{\Delta_{D_sD}}{6}(5M_\eta^2+8M_K^2-M_\pi^2)\left(2\mathcal{H}^1_{K\pi}(t)+\mathcal{H}_{K\pi}(t)\right)\\ &-\frac{\Delta_{D_sD}}{3}(M_\eta^2-4M_K^2+M_\pi^2)\left(2\mathcal{H}^1_{\eta K}(t)+\mathcal{H}_{\eta K}(t)\right)\\ &+\frac{\Delta_{D_sD}}{8}\left(\mathcal{I}_\eta+\mathcal{I}_\pi-2\mathcal{I}_K\right)-\frac{s-u}{4}\left(\mathcal{I}_\eta+\mathcal{I}_\pi+6\mathcal{I}_K\right)\Big\}\,,\end{aligned} \tag{5.45}$$

where we have defined $\Delta_{ab}=M_a^2-M_b^2$, $\Sigma_{ab}=M_a^2+M_b^2$,

$$\begin{aligned}\mathcal{F}^{(cd)}_{ab}(s,t) &= \left[3(s-M_a^2)+(s-M_c^2)\right]\mathcal{I}-(s-\Sigma_{bc})^2\,\mathcal{H}_{cd}(s)+2\left(t-2M_b^2\right)\mathcal{H}^{00}_{cd}(s)\\ &\quad+2\,(s-\Delta_{ab})\,(s-\Sigma_{bc})\,\mathcal{H}^1_{cd}(s)-(s-\Delta_{ab})^2\,\mathcal{H}^{11}_{cd}(s)\,,\end{aligned} \tag{5.46}$$

$$\begin{aligned}\mathcal{G}^{(ef)}_{ab,cd}(s,t) &= \frac{1}{2}\Delta_{bd}^2\mathcal{H}_{ef}(s)+\frac{1}{2}\,(\Delta_{ac}-\Delta_{bd})^2\,\mathcal{H}^{11}_{ef}(s)-\Delta_{bd}\,(\Delta_{ac}-\Delta_{bd})\,\mathcal{H}^1_{ef}(s),\\ {}^1\mathcal{K}^{(ef)}_{ab,cd}(s,t) &= \Delta_{ac}\left\{\frac{1}{2}\mathcal{I}_f+\frac{1}{2}t\left[\mathcal{H}_{ef}(t)+\mathcal{H}^1_{ef}(t)\right]-\mathcal{H}^{00}_{ef}(t)-t\mathcal{H}^{11}_{ef}(t)\right\},\\ {}^2\mathcal{K}^{(ef)}_{ab,cd}(s,t) &= -3(s-u)\mathcal{H}^{00}_{ef}(t)-\Delta_{ac}\Big[\frac{1}{6}(6\Sigma_{de}+6\Delta_{df}-13\Delta_{bd})\mathcal{H}^1_{ef}(t)\\ &\quad+\frac{1}{6}(3\Sigma_{de}+3\Delta_{df}-2\Delta_{bd})\mathcal{H}_{ef}(t)-3\Delta_{bd}\mathcal{H}^{11}_{ef}(t)\Big],\end{aligned} \tag{5.47}$$

and

$$\begin{aligned}\mathcal{I}_a &= \frac{1}{16\pi^2}A_0(M_a^2),\\ \mathcal{H}^{\rm tensor}_{ab}(s) &= \frac{1}{16\pi^2}B_{\rm tensor}(s,M_a^2,M_b^2),\\ \mathcal{J}^{\rm tensor}_{a}(s) &= \frac{1}{16\pi^2}B_{\rm tensor}(s,M_a^2,M_a^2),\end{aligned} \tag{5.48}$$

with $A_0(m^2)$ and $B_{\rm tensor}(s,m_1^2,m_2^2)$ the standard loop functions in Appendix A.

5.2.3 Renormalization

In the previous sections, the 1PI Feynman graphs are all calculated, which are related to the so-called amputated amplitudes. To derive the S-matrix elements, one should perform wave function renormalization. Moreover, in the end, all the bare parameters should be replaced by the corresponding physical ones.

Wave function renormalization

To perform the wave function renormalization, one multiplies the external lines with the square roots of the wave function renormalization constants of the corresponding fields and takes them on the mass shell. In perturbation theory, if the calculation is done up to a certain order (up to $O(p^3)$ in our case), the wave function renormalization is equivalent to taking the graphs in Fig. 5.4 into account. All the higher order contributions beyond the required accuracy are ignored.

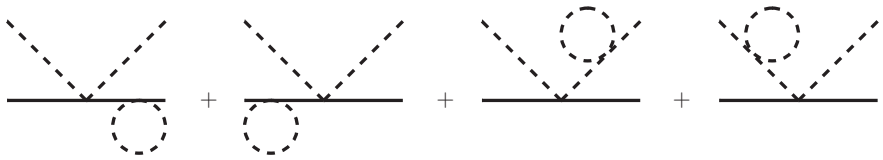

Figure 5.4: Feynman diagrams for the wave function renormalization at $O(p^3)$.

Hence, when taking wave function renormalization into consideration, the scattering amplitude becomes

$$\mathcal{A}(s,t) = \mathcal{A}^{(1)}_{\text{tree}}(s,t) + \mathcal{A}^{(2)}_{\text{tree}}(s,t) + \mathcal{A}^{(3)}_{\text{tree}}(s,t) + \mathcal{A}^{(3)}_{\text{loop}}(s,t) + \mathcal{A}^{(3)}_{\text{wf}}(s,t)\,. \tag{5.49}$$

The first three terms are tree contribution given in Section 5.2.1, while the fourth term is the loop contribution discussed in Section 5.2.2. The last term $\mathcal{A}_{\text{wf}}(s,t)$ corresponds to the contribution from the wave function renormalization. It can be obtained from the LO amplitude in combination with the wave function renormalization constants. For instance, considering the scattering process $D_1\phi_1 \to D_2\phi_2$, it is given by

$$\mathcal{A}^{(3)}_{\text{wf}}(s,t) = \frac{1}{2}(\delta\mathcal{Z}_{D_1} + \delta\mathcal{Z}_{\phi_1} + \delta\mathcal{Z}_{D_2} + \delta\mathcal{Z}_{\phi_2})\mathcal{A}^{(1)}_{\text{tree}}(s,t)\,, \tag{5.50}$$

with $\delta\mathcal{Z} = \mathcal{Z} - 1$ and $\mathcal{Z}$ is the wave function renormalization constant up to the order considered. To be explicit, the wave function renormalization constants for D and D_s are $\mathcal{Z}_D = \mathcal{Z}_{D_s} = 1$ and for the Goldstone bosons are

$$\begin{aligned}
\mathcal{Z}_\pi &= 1 - \frac{1}{F_0^2}\left[8L_4(2M_K^2 + M_\pi^2) + 8L_5M_\pi^2 + \frac{1}{3}\bar{I}_K + \frac{2}{3}\bar{I}_\pi\right],\\
\mathcal{Z}_K &= 1 - \frac{1}{F_0^2}\left[8L_4(2M_K^2 + M_\pi^2) + 8L_5M_K^2 + \frac{1}{2}\bar{I}_K + \frac{1}{4}\bar{I}_\pi + \frac{1}{4}\bar{I}_\eta\right],\\
\mathcal{Z}_\eta &= 1 - \frac{1}{F_0^2}\left[8L_4(2M_K^2 + M_\pi^2) + \frac{8}{3}L_5(4M_K^2 - M_\pi^2) + \bar{I}_K\right],
\end{aligned} \tag{5.51}$$

Note that in the above expressions, the UV divergence of the loop functions is not subtracted on purpose. This is due to the fact that the $\mathcal{Z}$'s are not physical observables such that they might be divergent, namely the LECs L_4 and L_5 are not sufficient to absorb the UV divergence in those expressions. The UV divergence cancellation as well as the PCB terms absorption will be discussed in the following section at the level of the S-matrix elements. As one will see, the S-matrix elements are free of any divergence.

Extended-On-Mass-Shell subtraction scheme

The loop integrals in the amplitude shown in Eq. (5.49) is UV divergent, and we need renormalization to absorb the divergences by counterterms. Moreover, PCB terms show up in the chiral expansion if we use dimensional regularization with the $\overline{\text{MS}}$ scheme. It is necessary to get rid of them to have a good power counting. We will use the EOMS subtraction scheme which has the proper analyticity and correct power counting for the amplitudes. The essence of the EOMS scheme is to perform two subsequent subtractions: the $\overline{\text{MS}}$ subtraction and the EOMS finite subtraction.

In the $\overline{\text{MS}}$ subtraction, the UV divergent parts are extracted and then cancelled by the divergences in the bare LECs, which are separated into finite and divergent parts as follows:

$$h_i = h_i^r(\mu) + \frac{\alpha_i}{16\pi^2 F_0^2} R\,, \qquad g_j = g_j^r(\mu) + \frac{\beta_j}{16\pi^2 F_0^2} R\,, \qquad L_k = L_k^r(\mu) + \frac{\Gamma_k}{32\pi^2} R\,, \tag{5.52}$$

where $R = \frac{2}{d-4} + \gamma_E - 1 - \ln(4\pi)$, with γ_E the Euler constant, and d is the number of space-time dimension. The coefficients α_i $(i = 0, \cdots, 5)$, β_j $(j = 1, 2, 3)$ and Γ_k $(k = 4, 5)$ are given by (4.46)

$$\alpha_0 = 0, \quad \alpha_1 = 0, \quad \alpha_2 = \frac{M_0^2}{48}, \quad \alpha_3 = -\frac{M_0^2}{16}, \quad \alpha_4 = \frac{7}{24}, \quad \alpha_5 = -\frac{7}{16},$$

$$\beta_1 = 0, \quad \beta_2 = -\frac{9}{128}, \quad \beta_3 = 0, \quad \Gamma_4 = \frac{1}{8}, \quad \Gamma_5 = \frac{3}{8}.$$

Eventually, the PCB terms are absorbed by decomposing the $\overline{\text{MS}}$-renormalized LECs in the $O(p^2)$ Lagrangian via

$$h_i^r(\mu) = \tilde{h}_i + \frac{\delta_i}{16\pi^2 F_0^2} M_0^2\,, \tag{5.53}$$

with the coefficient δ_i $(i = 0, \cdots, 5)$ defined by

$$\begin{aligned} &\delta_0 = \delta_1 = 0\,,\ \delta_2 = -\frac{1}{72} + \frac{1}{48}\log\frac{M_0^2}{\mu^2}\,,\ \delta_3 = \frac{1}{24} - \frac{1}{16}\log\frac{M_0^2}{\mu^2}\,, \\ &\delta_4 = -\frac{35}{72M_0^2} + \frac{7}{24M_0^2}\log\frac{M_0^2}{\mu^2}\,,\ \delta_5 = \frac{35}{48M_0^2} - \frac{7}{16M_0^2}\log\frac{M_0^2}{\mu^2}. \end{aligned} \tag{5.54}$$

They can be read off from Eq. (4.69) by setting $N = 3$. The other LECs such as $g_j^r(\mu)$ and $L_k^r(\mu)$ are untouched when performing the finite EOMS subtraction. The PCB part of the LECs (5.54) is equivalent to replacing the loop functions $\mathcal{F}_{ab}^{(cd)}(s,t)$ in Eq. (5.46) by $\mathcal{F}_{ab}^{(cd)}(s,t)^{\text{PCB}}$ in the amplitudes and then performing the chiral expansion with respect to the chiral quantities. The power counting breaking term of $\mathcal{F}_{ab}^{(cd)}(s,t)$ is of $O(p^2)$ and its explicit form reads

$$\begin{aligned} \mathcal{F}_{ab}^{(cd)}(s,t)^{\text{PCB}} = \frac{1}{16\pi^2}\Bigg\{ &2(s-M_a^2)(s-M_c^2)\left[\frac{1}{2}\log\frac{M_c^2}{\mu^2} - 1\right] - (s-M_a^2)^2\left[\frac{8}{9} - \frac{1}{3}\log\frac{M_c^2}{\mu^2}\right] \\ &-(s-M_c)^2\left[1 - \log\frac{M_c^2}{\mu^2}\right] + 2(t-2M_b^2)M_c^2\left[\frac{1}{9} - \frac{1}{6}\log\frac{M_c^2}{\mu^2}\right]\Bigg\}\,. \end{aligned} \tag{5.55}$$

As a consequence, one can simply obtain the amplitudes both free of UV divergences and PCB by

replacing the functions $\mathcal{F}_{ab}^{(cd)}(s,t)$ by $\mathcal{F}_{ab}^{(cd)}(s,t) - \mathcal{F}_{ab}^{(cd)}(s,t)^{\rm PCB}$ and ignoring the UV divergence, i.e. terms proportial to R, in loop functions. After the two steps described above, we have obtained the full renormalized amplitudes. For the sake of easy practical usage, the chiral-limit D meson mass M_0 and the chiral-limit decay constant F_0 should be further related to the corresponding physical quantities according to the following expressions:

$$M_D^2 = {M_0}^2 + 2\,(h_0 + h_1)M_\pi^2 + 4\,h_0\,M_K^2\,, \tag{5.56}$$

$$M_{D_s}^2 = {M_0}^2 + 2\,(h_0 - h_1)M_\pi^2 + 4\,(h_0 + h_1)M_K^2\,, \tag{5.57}$$

$$F_\pi = F_0 + \frac{1}{2F_0}\,(2\bar{I}_\pi^r + \bar{I}_K^r) + \frac{4M_\pi^2}{F_0}\,(L_4^r + L_5^r) + \frac{8M_K^2}{F_0}L_4^r\,. \tag{5.58}$$

Here, we rewrite F_0 in terms of F_π rather than F_K and F_η. This is the convention to be used throughout. Alternatively, one can also rewrite it in terms of F_K or F_η, and the difference is of higher order. The loop functions and LECs with a superscript r stand for their finite parts, namely, the contributions proportional to the UV divergence R are removed.

5.2.4 Unitarization

To study the nonperturbative effect, we unitarize the obtained amplitudes Eq. (5.49). Phenomenologically, it is now well-known that the unitarized amplitudes can well describe the scattering data for the pion and kaon systems up to 1.2 GeV, see e.g. Refs. [131, 132]. The unitarization is equivalent to a resumation of the s-channel potentials, and can extend the applicable energy range of the perturbative amplitudes. We thus expect that these amplitudes allow for a description of the lattice data at pion masses higher than the conventional ChPT. Yet, there is no rigorous proof a priori. For varying the quark masses (or equivalently the masses of the Goldstone bosons), it provides a way to performing the chiral extrapolation of lattice simulation results or studying the quark mass dependence of physical quantities.

Before unitarization, the partial wave projection to S-wave is performed

$$\mathcal{A}_\ell^{(S,I)}(s)_{D_1\phi_1\to D_2\phi_2} = \frac{1}{2}\int_{-1}^{1} \mathrm{d}\cos\theta\, P_\ell(\cos\theta)\,\mathcal{A}^{(S,I)}_{D_1\phi_1\to D_2\phi_2}(s, t(s,\cos\theta))\,, \tag{5.59}$$

with $\ell = 0$. Here, the Mandelstam variable t is expressed in terms of s and the scattering angle θ, i.e. Eq. (5.4). From Eq. (5.4), one sees that at each of the thresholds of $D_1\phi_1$ and $D_2\phi_2$, i.e. when s takes one of the following two values

$$s_1 = (M_{D_1} + M_{\phi_1})^2\,, \qquad s_2 = (M_{D_2} + M_{\phi_2})^2\,, \tag{5.60}$$

t is independent of $\cos\theta$. Taking $s = s_1$ for instance, the S-wave amplitude becomes

$$\mathcal{A}^{(S,I)}_{\ell=0}(s_1)_{D_1\phi_1\to D_2\phi_2} = \mathcal{A}^{(S,I)}_{D_1\phi_1\to D_2\phi_2}(s_1, t(s_1))\,. \tag{5.61}$$

This means that the S-wave amplitude at threshold can be obtained directly from the full amplitude by setting the energy squared at its threshold value. However, note that this simple recipe can only be used for the single channel case. For coupled channels, it is necessary to perform the partial wave projection using Eq. (5.59). Before unitarization, it is helpful to use matrix notation to denote the partial wave amplitudes with definite strangeness S and isospin I. In the matrix notation, the subscript $D_1\phi_1 \to D_2\phi_2$ is redundant. For single channels, this is apparent since the process is specified uniquely by (S, I). For coupled channels, taking $(S, I) = (1, 1)$ for example, there are four processes: $D_s\pi \to D_s\pi$, $DK \to DK$,

$DK \to D_s\pi$ and its time reversal process. Using time reversal invariance, one can write

$$\mathcal{A}_\ell^{(1,1)}(s) = \begin{pmatrix} \mathcal{A}_\ell^{(1,1)}(s)_{D_s\pi\to D_s\pi} & \mathcal{A}_\ell^{(1,1)}(s)_{DK\to D_s\pi} \\ \mathcal{A}_\ell^{(1,1)}(s)_{DK\to D_s\pi} & \mathcal{A}_\ell^{(1,1)}(s)_{DK\to DK} \end{pmatrix}. \tag{5.62}$$

Later on, we will refer to the amplitudes for a given process in the isospin basis by $\mathcal{A}_\ell^{(S,I)}(s)_{ij}$, with i and j being channel indices. Unitarization of the scattering amplitudes will be discussed in the matrix notation in the following.

In the present work, we will consider two different versions of unitarization for the sake of comparison and for quantifying the inherent model-dependence of such approaches. For the sake of simplicity and generality, all the quantum number indices of the amplitudes such as S, I and ℓ will be suppressed in this section. That is to say T, $\mathcal{A}$, and N, which will appear later on, are $T_\ell^{(S,I)}$, $\mathcal{A}_\ell^{(S,I)}$ and $N_\ell^{(S,I)}$, respectively, for our case.

The first approach we will use is the one proposed in Ref. [90], which is denoted by UChPT throughout this paper. The unitarized two-body scattering amplitude has the form [90]

$$T(s) = [1 - N(s)\cdot G(s)]^{-1}\cdot N(s), \tag{5.63}$$

where the function $G(s)$ encodes the two-body right-hand cut and is given by the two-point loop function

$$G(s)_i = i\int \frac{\mathrm{d}^4 q}{(2\pi)^4}\frac{1}{(q^2 - M_{D_i}^2 + i\epsilon)((P-q)^2 - M_{\phi_i}^2 + i\epsilon)}\,, \qquad s \equiv P^2\,. \tag{5.64}$$

Note that $G(s)_i$ is counted as $O(p)$ and its explicit expression is

$$\begin{aligned} G(s)_i = \frac{1}{16\pi^2}\Bigg\{ & a(\mu) + \ln\frac{M_{D_i}^2}{\mu^2} + \frac{s - M_{D_i}^2 + M_{\phi_i}^2}{2s}\ln\frac{M_{\phi_i}^2}{M_{D_i}^2} \\ & + \frac{\sigma_i}{2s}\Big[\ln\Big(s - M_{\phi_i}^2 + M_{D_i}^2 + \sigma_i\Big) - \ln\Big(-s + M_{\phi_i}^2 - M_{D_i}^2 + \sigma_i\Big) \\ & + \ln\Big(s + M_{\phi_i}^2 - M_{D_i}^2 + \sigma_i\Big) - \ln\Big(-s - M_{\phi_i}^2 + M_{D_i}^2 + \sigma_i\Big)\Big]\Bigg\}, \end{aligned} \tag{5.65}$$

with $\sigma_i = \{[s - (M_{\phi_i} + M_{D_i})^2][s - (M_{\phi_i} - M_{D_i})^2]\}^{1/2}$ and μ the renormalization scale. One can define a μ-independent parameter $\tilde{a} \equiv a(\mu) + \ln\Big(M_{D_i}^2/\mu^2\Big)$, since a change of μ in the logarithm can be compensated by $a(\mu)$. Notice that the parameter $\tilde{a}$ in $G(s)$ of Eq. (5.65) cannot be absorbed by redefining the LECs. It is introduced through the dispersion integral along the right-hand cut, and is a free parameter in principle. The only constraint here is from the requirement of a proper power counting: while all other terms in Eq. (5.65) are of order $O(p)$, $\tilde{a}$ should be much smaller than 1 so that its presence will not cause a breaking of the power counting if we expand the resumed amplitude to a certain order, i.e. $\tilde{a} = O(p)$.

While the right-hand cut effect is collected in the $G(s)$ function, the $N(s)$ function is free of any two-body right-hand cut. It, however, may include the left-hand cuts due to the crossed channels. Up to NNLO, i.e. leading one-loop order, the amplitudes Eq. (5.49) contains right-hand cuts which come from s-channel loops, thus can not serve as the kernel $N(s)$. The kernel $N(s)$ can be obtained perturbatively by matching to the standard ChPT amplitudes order by order. It is easy to find

$$N(s) = \mathcal{A}^{(1)}(s) + \mathcal{A}^{(2)}(s) + \mathcal{A}^{(3)}(s) - \mathcal{A}^{(1)}(s)\cdot G(s)\cdot\mathcal{A}^{(1)}(s), \tag{5.66}$$

where $\mathcal{A}^{(n)}(s)$ stand for the partial wave amplitudes from the perturbative calculation with the superscript n denoting the chiral order. Notice that the right hand cut from the NNLO amplitude is subtracted in the last term in order to avoid double counting in the unitarization.

The second approach to unitarize amplitudes is the inverse amplitde method (IAM) [81, 132, 133], or see Sec. 3.3. In our case, the IAM unitarized amplitude has the form

$$T(s) = \tilde{T}^{(1)}(s) \cdot [\tilde{T}^{(1)}(s) - \tilde{T}^{(2)}(s)]^{-1} \cdot \tilde{T}^{(1)}(s), \tag{5.67}$$

where

$$\tilde{T}^{(1)}(s) \equiv \mathcal{A}^{(1)}(s)\,, \quad \tilde{T}^{(2)}(s) \equiv \mathcal{A}^{(2)}(s) + \mathcal{A}^{(3)}(s)\,. \tag{5.68}$$

The above assignments guarantee that the unitarized amplitudes exactly obey unitarity when the perturbatively unitary equations are employed, i.e.,

$$\mathrm{Im}\,\mathcal{A}^{(1)}(s) = 0\,, \quad \mathrm{Im}\,\mathcal{A}^{(2)}(s) = 0\,, \quad \mathrm{Im}\,\mathcal{A}^{(3)}(s) = \mathcal{A}^{(1)}(s)\,\tilde{\rho}(s)\,\mathcal{A}^{(1)}(s)^{\dagger}\,, \tag{5.69}$$

with $\tilde{\rho}(s) = \mathrm{diag}\{\tilde{\rho}(s)_i\}$, $\tilde{\rho}(s)_i = -q_i/(8\pi\sqrt{s})$ and q_i is the magnitude of the c.m. three-momentum in the i^{th} channel.

5.3 Numerical analysis

5.3.1 Scattering lengths and pion mass dependence

Given definite strangeness S and isospin I, the S-wave scattering lengths of the i^{th} channel are related to the diagonal elements of the T-matrix, [4]

$$a_i^{(S,I)} = -\frac{1}{8\pi(M_{D_i} + M_{\phi_i})} T_{\ell=0}^{(S,I)}(s_{\text{th}})_{ii}\,, \qquad s_{\text{th}} = (M_{D_i} + M_{\phi_i})^2\,. \tag{5.70}$$

Here, M_{D_i} and M_{ϕ_i} denote the masses of the charmed meson and Goldstone boson ϕ in the channel i, respectively, and $T_{\ell=0}^{(S,I)}(s_{\text{th}})$ stands for the S-wave unitarized amplitude at threshold using either UChPT given by Eq. (5.63) or IAM given by Eq. (5.67).

Due to the short lifetime of the charmed meson, there are no experimental data for D-ϕ scattering lengths. Nevertheless, lattice QCD calculations in the last a few years provide very valuable information on the interaction between the charmed mesons and light pseudoscalar mesons [29, 98–100]. Since the lattice calculations were performed at several unphysical pion masses, in order to describe these lattice data, one should know the pion mass dependence of the scattering lengths. This is achieved by replacing all the quantities in the expressions by the pion mass dependent ones. For the involved meson masses, we have

$$M_K = \sqrt{\mathring{M}_K^2 + M_\pi^2/2}\,, \quad M_D = \mathring{M}_D + (h_1 + 2h_0)\frac{M_\pi^2}{\mathring{M}_D}\,, \quad M_{D_s} = \mathring{M}_{D_s} + 2h_0\frac{M_\pi^2}{\mathring{M}_{D_s}}\,. \tag{5.71}$$

Note that all the formulae shown above are of NLO for the pion mass dependence. [5] Here the LEC h_1

[4] We are using the sign convention such that the scattering length for a repulsive interaction is negative.

[5] In Eq. (5.71), although the formula we used for the kaon mass is a LO expression in $SU(3)$ ChPT, it contains two parts: the part $\sim \mathring{M}_K^2$ proportional to $B_0 m_s$ remains in the $SU(2)$ chiral limit and is regarded as a LO contribution of the pion mass

can be fixed by the mass difference between D and D_s. Using these two equations, one has [28]

$$h_1 = \frac{M_{D_s}^2 - M_D^2}{4(M_K^2 - M_\pi^2)} = 0.4266\,, \tag{5.72}$$

where the physical values for the meson masses are used, i.e., $M_\pi = 138$ MeV, $M_K = 496$ MeV, $M_D = 1867$ MeV and $M_{D_s} = 1968$ MeV.[6] The pion decay constant should also be substituted by [16]

$$F_\pi = F_0\left\{1 - 2\mu_\pi - \mu_K + \frac{4M_\pi^2}{F_0^2}\left[L_4^r(\mu) + L_5^r(\mu)\right] + \frac{8M_K^2}{F_0^2}L_4^r(\mu)\right\}\,, \tag{5.73}$$

where M_K is understood as the one in Eq. (5.71), and μ_ϕ is a scale dependent function for the Goldstone boson ϕ

$$\mu_\phi = \frac{M_\phi^2}{32\pi^2 F_0^2}\ln\frac{M_\phi^2}{\mu^2}. \tag{5.74}$$

So far, except for h_1, the LECs L_4^r, L_5^r and h_0 and the chiral limit quantities $\mathring{M}_K$, $\mathring{M}_D$, $\mathring{M}_{D_s}$ and F_0 are all unknown. Since we will fit to the lattice results on the scattering lengths calculated in Ref. [29], we choose to fix the above mentioned quantities from fitting to the lattice data calculated using the same gauge configurations. In addition, the kaon decay constant F_K data are also included to have a bigger data set for fixing F_0 and $L_{4,5}^r$. The pion mass dependence of F_K is given by [16]

$$F_K = F_0\left\{1 - \frac{3}{4}\left(\mu_\pi + 2\mu_K + \mu_\eta\right) + \frac{4M_\pi^2}{F_0^2}L_4^r(\mu) + \frac{4M_K^2}{F_0^2}\left[2L_4^r(\mu) + L_5^r(\mu)\right]\right\}, \tag{5.75}$$

with $M_\eta^2 = (4M_K^2 - M_\pi^2)/3$ and M_K given by Eq. (5.71).

The lattice data for M_K, M_D and M_{D_s} are taken from Ref. [29]. There are four data sets for each quantity, corresponding to the four ensembles (labelled by M007, M010, M020 and M030) with pion mass approximately 301.1 MeV, 363.8 MeV, 511.0 MeV and 617.0 MeV, in order. Since the same ensembles are employed in Ref. [134], we take the data for f_π and f_K from Ref. [134], where $f_\pi = \sqrt{2}F_\pi$ and $f_K = \sqrt{2}F_K$. Those lattice data are well described as shown in Fig. 5.5 [7] when the parameters take the values given in Table 5.3. Our fitting values for $L_{4,5}^r$ are consistent with the determinations given in Refs. [135, 136]. Therein, the values are obtained at $\mu = M_\eta$, and the corresponding values transformed to $\mu = M_\rho$ can be found in Ref. [137].

5.3.2 Fits to lattice data on the scattering lengths

Introduction to the fitting procedure

Since all the necessary preparations are completed, we proceed to the description of the lattice QCD data of the S-wave scattering lengths. There are two points to be discussed before carrying out the fits.

dependence, while the part related to $B_0 m_{u/d} \sim M_\pi^2/2$ vanishes in the $SU(2)$ chiral limit and is thus a NLO contribution. In this sense, we spelled out the pion mass dependence for all of the masses and decay constants consistently up to the order M_π^2.

[6] The mass of the η is always expressed in terms of M_π and M_K through the Gell-Mann–Okubo mass relation, $3M_\eta^2 = 4M_K^2 - M_\pi^2$.

[7] We have neglected the subtleties due to the use of mixed action gauge configurations in the lattice calculations, which in principle requires to use the partially quenched ChPT instead of the standard one for the chiral extrapolation, and the effect of finite lattice spacing, see Ref. [134].

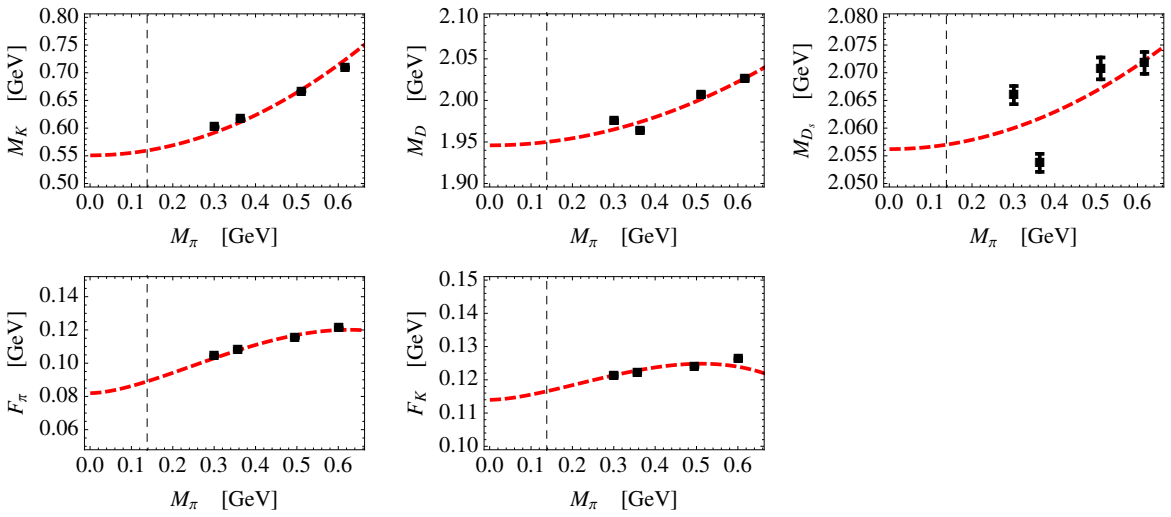

Figure 5.5: Chiral extrapolation of masses and decay constants. All the lattice data are obtained from the same ensembles, namely M007-M030. Data for M_K, M_D and M_{D_s} is taken from Ref. [29] and the one for F_π and F_K from Ref. [134]. Except for M_{D_s}, the data errors are so tiny that we do not show them explicitly in the plots. The vertical dashed line corresponds to the physical pion mass.

Table 5.3: Parameters for chiral extrapolation. L_4^r and L_5^r are obtained at $\mu = M_\rho$ (= 775.5 MeV). The masses and decay constant in the chiral limit are in units of MeV. h_0 and h_1 and dimensionless. The asterisk marks an input value.

$\mathring{M}_K$	$\mathring{M}_D$	$\mathring{M}_{D_s}$	h_0	h_1	F_0	$10^3 \cdot L_4^r$	$10^3 \cdot L_5^r$
560.41	1940.4	2061.2	0.0172	0.4266*	73.31	0.0095	1.3264

The first one is related to the lattice data. From Ref. [29], 20 data for 5 channels are available. Amongst the five channels, the $D_s\pi$ with $(S, I) = (1, 1)$ can actually couple the isovector DK channel while the other four are single channels. Although in Ref. [29] only the $D_s\pi$ interpolating operator was constructed and used, the propagation of all the quarks should know about the presence of the coupled DK channel with $(S, I) = (1, 1)$ because the channel-coupling in this case does not require disconnected Wick contractions which were not included in Ref. [29]. Thus, we will describe the $D_s\pi$ data using a coupled-channel unitarized amplitude.

In addition, lattice QCD results were published in the last two years for two more channels: $D\pi$ with $(S, I) = (0, 1/2)$ [99] and DK with $(S, I) = (1, 0)$ [100]. These channels are more difficult since both of them involve disconnected Wick contractions, [8] but they are also more interesting as they can provide valuable information for the lightest scalar charmed mesons in the corresponding channels. The calculation for the $D\pi$ scattering was performed using $N_f = 2$ gauge configurations, and the DK calculation has results from both $N_f = 2$ and $N_f = 2 + 1$ gauge configurations. Because the amplitudes derived here are based on $SU(3)$ ChPT, we will only include in the fits the new result with $N_f = 2 + 1$, i.e. $a^{(1,0)}_{DK\to DK} = -1.33(20)$ fm obtained at $M_\pi = 156$ MeV, and the unitarized amplitude used in the fits

[8] It is shown in Ref. [138] that as long as the singly disconnected Wick contractions contribute, which is the case for the isoscalar DK channel, they are of LO in both the $1/N_c$ and chiral expansion. Therefore, they cannot be neglected.

is obtained including the $D_s\eta$ coupled channel. Notice that these new lattice calculations use gauge configurations and actions different from those in Ref. [29], the chiral-limit masses for the kaon and charmed mesons should take different values from those given in Table 5.3. Because the physical masses of the involved ground state mesons such as the kaon and charmed mesons were reproduced rather well with the lattice setup used in Ref. [100] (for details, see Ref. [101]), the chiral-limit values of the involved meson masses and F_0 are determined by requiring them to coincide with the corresponding phyiscal values at the physical pion mass, namely, $\mathring{M}_K = 486.3$ MeV, $\mathring{M}_D = 1862.3$ MeV, $\mathring{M}_{D_s} = 1967.7$ MeV and $F_0 = 76.23$ MeV. The values for the LECs in the extrapolating expressions of these quantities are the same as those listed in Table 5.3.

The other point concerns the LECs to be determined. There are 7 unknown LECs in total: h_2, h_3, h_4, h_5, g_1, g_2 and g_3. As mentioned in Ref. [29], h_2 (h_3) and h_4 (h_5) are largely correlated. Therefore, redefinitions of the LECs are employed to reduce these correlations, which are

$$h_{24} = h_2 + h_4' \,, \quad h_{35} = h_3 + 2\,h_5' \,, \quad h_4' = h_4 \bar{M}_D^2 \,, \quad h_5' = h_5 \bar{M}_D^2. \tag{5.76}$$

The new parameters h_{24}, h_{35}, h_4' and h_5' will be determined in our fits. The average of the physical masses of the charmed D and D_s mesons, $\bar{M}_D = (M_D^{\rm phy} + M_{D_s}^{\rm phy})/2$, is introduced to make the four new parameters dimensionless. Similarly, for the LECs from the NNLO contact terms, g_2 and g_3 are largely correlated with each other, and it is better to redefine these LECs as

$$g_{23} = g_2' - 2g_3' \,, \quad g_1' = g_1 \bar{M}_D \,, \quad g_2' = g_2 \bar{M}_D \,, \quad g_3' = g_3 \bar{M}_D^3. \tag{5.77}$$

The parameters g_1', g_{23} and g_3' have a dimension of inverse mass and will be fixed from fitting to the lattice data. One can fix g_1' and g_{23} separately only when the coupled-channel unitarized amplitudes are used, i.e. from fitting to the lattice results of the $D_s\pi$ and the isoscalar DK scattering lengths. The single-channel unitarized amplitudes is only sensitive to the combination $g_{123} = g_{23} - g_1'$, instead of g_1' and g_{23} separately, and g_3'.

Results

We will try different fit procedures. In the fit UChPT-6(a), all of the 20 data points for 5 channels, with pion masses from 301 MeV up to 617 MeV, in Ref. [29] as well as the $N_f = 2 + 1$ datum for the isoscalar DK channel, with an almost physical pion mass of 156 MeV, in Ref. [100] are taken into consideration. We notice that there are two possibilities for a scattering length to be negative in our sign convention: a repulsive interaction, and an attractive interaction with a bound state pole below the threshold. In the $(S, I) = (1, 0)$ channel, there is the well-known state $D_{s0}^*(2317)$ below the DK threshold which was not included as an explicit degree of freedom in our theory. Because the number of data is small but the number of parameters is large, a direct fit to these lattice data might result in solutions which are not physically acceptable. For instance, within the range of the parameters of a direct fit, the $(S, I) = (1, 0)$ DK channel could even be repulsive which is reflected by the fact that the kernel of the unitarized amplitude takes a positive value at the threshold. Given that the LO interaction in the corresponding DK channel is the most attractive one among all the charmed meson–Goldstone boson scattering processes, see Table II in Ref. [29] for instance, we regard such a situation as unacceptable. Therefore, we put a constraint by hand requiring that when all the particles take their physical values there is a bound state pole in the $(S, I) = (1, 0)$ channel at 2317 MeV. Following Ref. [29], this is done by adjusting the subtraction constant $\tilde{a}$ in the loop function $G(s)$ in the unitarized amplitude, Eq. (5.63), to produce the pole at the right position. The resulting values of the LECs from the fit are shown in Table 6.3.

However, a pion mass larger than 600 MeV is definitely too large for the chiral extrapolation using

Table 5.4: Values of the LECs from the 6-channel fits using the method of UChPT. The h_i's are dimensionless, and the g_1', g_{23} and g_3' are in GeV^{-1}.

	UChPT-6(a) no prior	UChPT-6(b) no prior	UChPT-6(a') with prior	UChPT-6(b') with prior
h_{24}	$0.79^{+0.10}_{-0.09}$	$0.76^{+0.10}_{-0.09}$	$0.83^{+0.11}_{-0.10}$	$0.80^{+0.10}_{-0.10}$
h_{35}	$0.73^{+0.50}_{-0.38}$	$0.81^{+0.95}_{-0.62}$	$0.43^{+0.23}_{-0.23}$	$0.40^{+0.33}_{-0.29}$
h_4'	$-1.49^{+0.55}_{-0.57}$	$-1.56^{+0.61}_{-0.65}$	$-1.33^{+0.60}_{-0.60}$	$-1.72^{+0.64}_{-0.63}$
h_5'	$-11.47^{+2.24}_{-2.79}$	$-15.38^{+4.81}_{-7.20}$	$-4.25^{+0.65}_{-0.66}$	$-2.60^{+0.84}_{-0.87}$
g_1'	$-1.66^{+0.31}_{-1.59}$	$-2.44^{+0.57}_{-0.64}$	$-1.10^{+0.18}_{-0.23}$	$-1.90^{+0.58}_{-0.35}$
g_{23}	$-1.24^{+0.28}_{-1.51}$	$-2.00^{+0.52}_{-0.51}$	$-0.70^{+0.19}_{-0.24}$	$-1.48^{+0.61}_{-0.37}$
g_3'	$2.12^{+0.55}_{-0.45}$	$2.85^{+1.41}_{-0.96}$	$0.98^{+0.15}_{-0.14}$	$0.58^{+0.20}_{-0.19}$
χ^2/d.o.f.	$\frac{31.52}{21-7} = 2.25$	$\frac{13.43}{16-7} = 1.49$	$\frac{77.72-23.34}{21-7} = 3.88$	$\frac{51.71-16.60}{16-7} = 3.90$

the standard ChPT. The unitarized approach arguably has a larger convergence range than the standard ChPT. But the range is not known a priori. Therefore, for the sake of comparison, we perform another fit, denoted as UChPT-6(b), using the same method but excluding the lattice data at $M_\pi = 617$ MeV. The fit results are shown in the third column of Table 6.3. One can see that the values of all the LECs from these two fits are similar, but those from UChPT-6(b) have larger uncertainties as a result of being less constrained. The fit results from both fits are plotted in Fig. 5.6. The bands represent the variation of the scattering lengths with respect to the LECs within 1-σ standard deviation. As we can see, both fits describe the lattice data reasonably well with the exception that the isoscalar DK scattering length around $M_\pi = 156$ MeV is too large in comparison with the lattice result. However, both fits are consistent with the $N_f = 2$ lattice result for DK at a pion mass around 266 MeV which was not included in the fits. We notice that the lattice ensemble for the $M_\pi = 156$ MeV datum has a rather small volume with $M_\pi L \approx 2.3$. It is a bit too small for Lüscher's finite volume formalism to be strictly applicable, and thus this datum might bear a large systematic uncertainty. The isospin-3/2 $D\pi \to D\pi$ scattering length vanishes at the chiral limit as required by chiral symmetry. Lattice discretization often breaks chiral symmetry. However, due to the use of the domain-wall action for the valence quarks in the lattice calculation of the pionic channels, the chiral behavior is protected in our case. For related discussions in mixed-action ChPT, we refer to Refs. [139–142].

In both fits, the values of all the LECs except for h_5' turn out to be of a natural size. However, the absolute value of the dimensionless LEC h_5' is too large to be natural. This means that the absolute value of h_5' is so large that this single term would give a contribution larger than the LO amplitude. It would spoil the convergence, and thus the perturbative expansion, at least for some quantities (although for some other quantities, due to fine-tuned cancellation the sum of the NLO contribution could still be much smaller than the LO one). Therefore, we try to constrain all the LECs to natural values following Ref. [143] which discusses the use of the Bayesian method in effective field theories. Following that paper, the so-called augmented chi-squared can be defined by [9]

$$\chi^2_{\rm aug} = \chi^2 + \chi^2_{\rm prior}\,, \tag{5.78}$$

[9] The method in Ref. [143] was only derived for the case that the dependence on the parameters to be fitted is linear. Although our case is non-linear and thus the augmented χ^2 lacks a strict statistical meaning, we still try this method as the χ^2 defined in this way comprises a "naturalness prior" so as to favor natural values for the LECs.

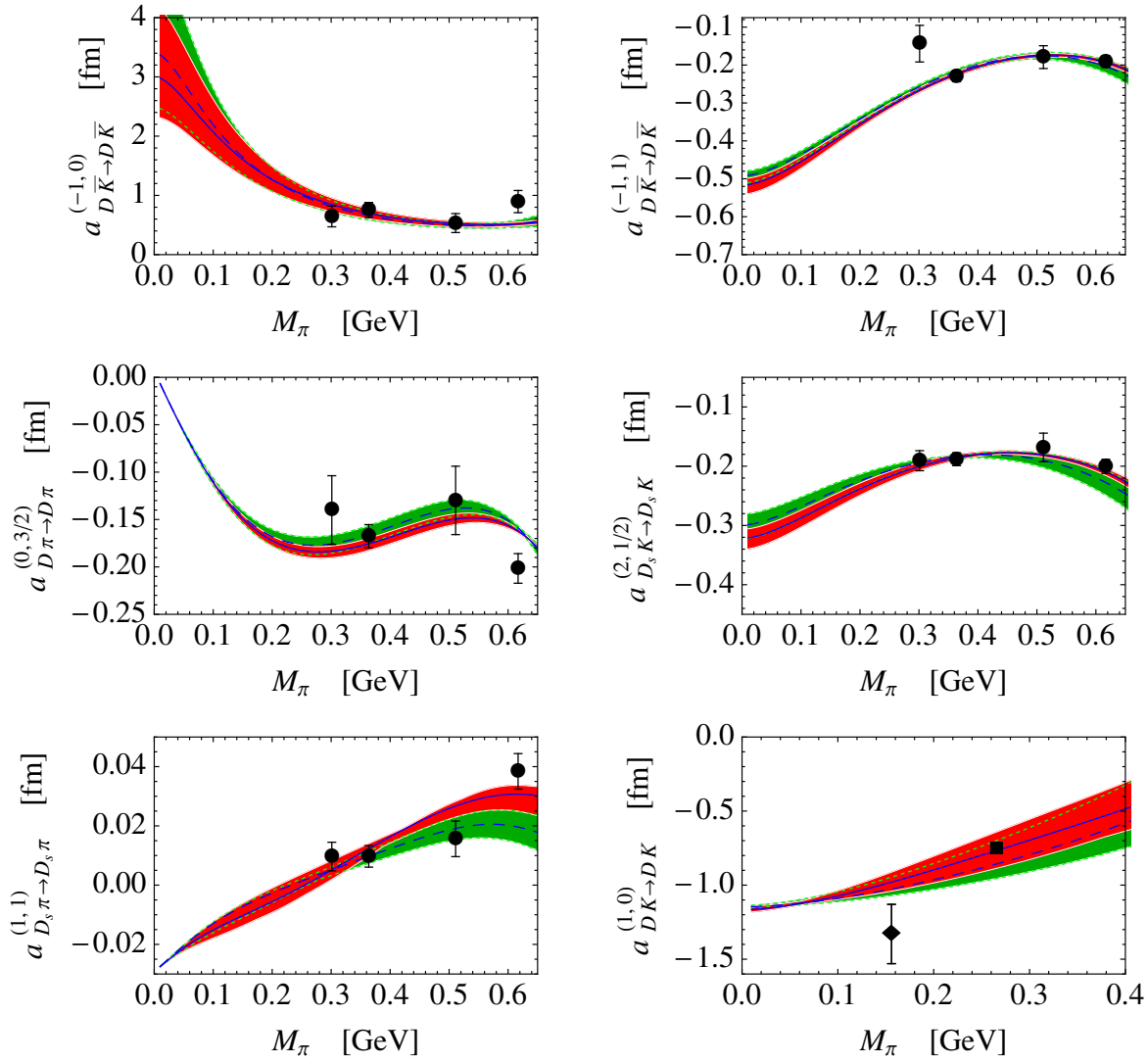

Figure 5.6: Comparison of the results of the 6-channel fits (without a prior χ^2) to the lattice data of the scattering lengths. UχPT-6(a): solid blue line with red band, UχPT-6(b): dashed blue line with green band. The filled circles are lattice results in Ref. [29], and the filled square (not included in the fits) and diamond are taken from Ref. [100].

where χ^2 is the usual chi-squared used in the standard least chi-squared fit and $\chi^2_{\rm prior}$ is a prior chi-squared encoding the naturalness requirement of the fit parameters. In our specific case, the $\chi^2_{\rm prior}$ is set to be the sum of squares of the fit LECs. This means that we require the dimensionless LECs $h_i^{(\prime)}$'s to be $O(1)$ and g_i''s to be $O(1\ \text{GeV}^{-1})$. The results by minimizing the augmented chi-squared are listed in the last two columns in Table 6.3, denoted as UChPT-6(a') and UChPT-6(b'), where the values for χ^2 are given with $\chi^2_{\rm prior}$ subtracted. One sees that the value of h_5' gets more natural at the price of a larger χ^2. A comparison of the scattering lengths with the lattice data in various channels is given in Fig. 5.7, and one can see that the lattice data in all six channels can still be described reasonably well.

It turns out that in all of these fits $|h_5'| > |h_4'|$, which is consistent with the N_c counting $|h_4'| = O(|h_5'|/N_c)$ [29]. The values of the h_i's are different from those obtained in Ref. [29]. The reason may

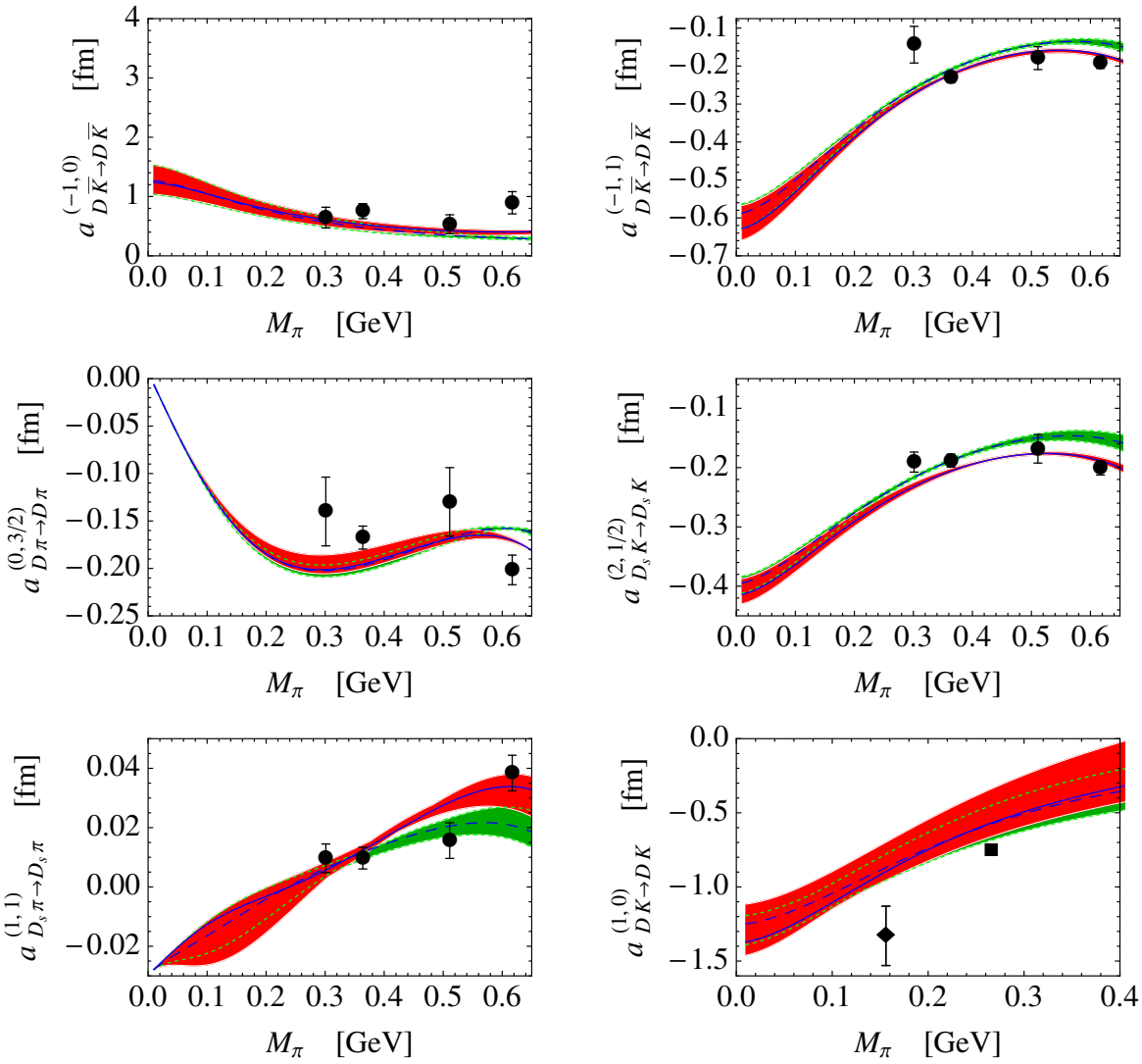

Figure 5.7: Comparison of the results of the 6-channel fits (with a prior χ^2) to the lattice data of the scattering lengths. UχPT-6(a): solid blue line with red band, UχPT-6(b): dashed blue line with green band. The filled circles are lattice results in Ref. [29], and the filled square (not included in the fits) and diamond are taken from Ref. [100].

be attributed to the use of the EOMS scheme in this work, and all of $h_{2,3,4,5}$ absorb a power counting breaking contribution, see Eq. (5.53). For the case of the $D_s\pi$, the scattering length does not vanish at the limit of a vanishing pion mass. This is due to the presence of the DK-loop in the coupled-channel amplitude which has a nonvanishing contribution in the $SU(2)$ chiral limit. We have checked that the elastic contribution tends to zero as M_π approaches zero as required by chiral symmetry.

Table 5.5: Values of the LECs from the 4-channel fits using both the methods of UChPT and IAM. The h_i's are dimensionless, and the $g_{123} = g_{23} - g'$ and g'_3 are in GeV^{-1}.

	UChPT-4	IAM-4
h_{24}	$0.50^{+0.09}_{-0.10}$	$0.53^{+0.07}_{-0.07}$
h_{35}	$-0.89^{+0.93}_{-0.91}$	$-0.59^{+1.04}_{-1.11}$
h'_4	$1.23^{+1.03}_{-1.08}$	$0.64^{+0.66}_{-0.66}$
h'_5	$-3.09^{+4.69}_{-4.72}$	$-6.08^{+6.05}_{-5.99}$
g_{123}	$0.18^{+0.18}_{-0.18}$	$0.23^{+0.21}_{-0.22}$
g'_3	$1.01^{+0.87}_{-0.86}$	$1.42^{+1.08}_{-1.10}$
χ^2/d.o.f.	$\frac{13.59}{16-6} = 1.36$	$\frac{13.97}{16-6} = 1.40$

For comparison, we also perform fits with just the four single-channel data, i.e. the $D_s\pi$ and isoscalar DK data are excluded. For this case, we use two different unitarization methods: UChPT, to be denoted as UChPT-4, and IAM, to be denoted as IAM-4. We did not use the IAM approach in the 6-channel fits because this approach is not suitable to unitarize a perturbative amplitude with a zero LO contribution. As can be seen from Eq. (5.67), if the LO amplitude vanishes the unitarized one will vanish as well. This happens to the case of the $D_s\pi$. The UChPT approach is free of this problem. The results of these two fits are compiled in Table 5.5. Notice that in this case g'_1 and g_{23} cannot be determined separately, and the effective combined parameter is $g_{123} = g_{23} - g'_1$. One sees that the values of LECs from the fits using different unitarization methods are consistent with each other, [10] but are only marginally consistent with those in the 6-channel fits. In addition, the uncertainties are quite large. More lattice simulations are apparently necessary to pin down the LEC values. A comparison of the results of the 4-channel fits to the lattice data in these channels are plotted in Fig. 5.8.

For reference, the values for the scattering lengths extrapolated to the physical pion mass are presented in Table 5.6. The chiral limit values in Table 5.3 are adopted for all the 16 channels when performing the chiral extrapolation . Here we only show the results using the 6-channel fits to the data with the pion mass up to 511 MeV, i.e. UChPT-6(b) and UChPT-6(b'). We notice that the numerical results of the scattering lengths extrapolated to the physical pion masses in some channels differ from those obtained in Ref. [29]. This could indicate that the uncertainties are underestimated as the $SU(3)$ formalism for UChPT was applied to pion masses higher than 500 MeV. We expect that the situation will improve when lattice results at lower pion masses are availble.

[10] However, not all of the LECs in these different unitarization methods ought to take the same values. One can see this by expanding the IAM resummed amplitude up to $O(p^3)$. Considering the single channel case for simplicity, one has $T_{\rm IAM}(s) = \mathcal{A}^{(1)}(s) + \mathcal{A}^{(2)}(s) + \mathcal{A}^{(3)}(s) + [\mathcal{A}^{(2)}(s)]^2/\mathcal{A}^{(1)}(s) + O(p^4)$. It is different from that of UChPT, $T_{\rm UChPT}(s) = \mathcal{A}^{(1)}(s) + \mathcal{A}^{(2)}(s) + \mathcal{A}^{(3)}(s) + O(p^4)$. Thus, the LECs in the $O(p^3)$ Lagrangian could take different values.

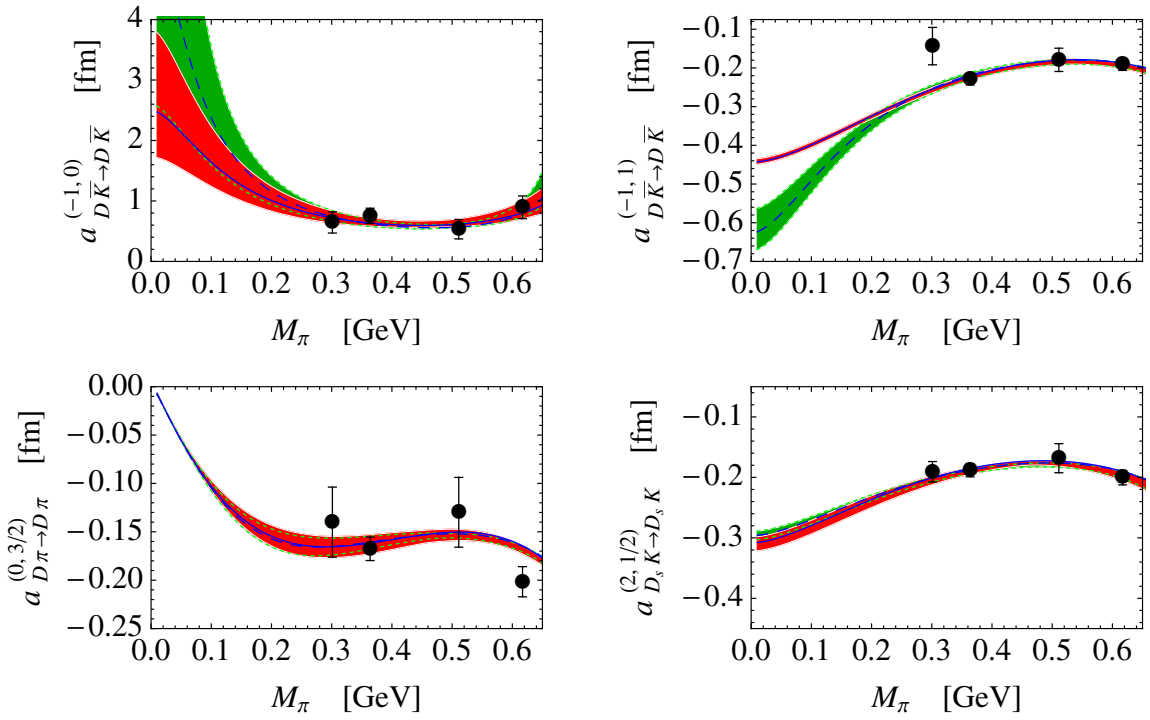

Figure 5.8: Comparison of the results of the 4-channel fits to the lattice data of the scattering lengths. UχPT-4: solid red line with blue band, IAM-4: dashed red line with green band. The lattice data are taken from Ref. [29].

Table 5.6: Predictions of the scattering lengths at physical pion mass using the LECs determined in the 6-channel fits UChPT-6(b) and UChPT-6(b') in units of fm.

$a^{(S,I)}_{ii}$	UChPT-6(b)	UChPT-6(b')
$a^{(-1,0)}_{D\bar{K}\to D\bar{K}}$	$1.76^{+0.39}_{-0.31}$	$0.93^{+0.15}_{-0.15}$
$a^{(-1,1)}_{D\bar{K}\to D\bar{K}}$	$-0.40^{+0.01}_{-0.01}$	$-0.45^{+0.01}_{-0.02}$
$a^{(0,\frac{1}{2})}_{D\pi\to D\pi}$	$0.65^{+0.11}_{-0.09}$	$0.42^{+0.04}_{-0.05}$
$a^{(0,\frac{1}{2})}_{D\eta\to D\eta}$	$-0.18^{+0.04}_{-0.04}+i\,0.00^{+0.01}_{-0.00}$	$-0.21^{+0.05}_{-0.04}+i\,0.01^{+0.01}_{-0.01}$
$a^{(0,\frac{1}{2})}_{D_s\bar{K}\to D_s\bar{K}}$	$-1.37^{+0.21}_{-0.04}+i\,0.61^{+0.45}_{-0.02}$	$-0.47^{+0.06}_{-0.07}+i\,0.50^{+0.18}_{-0.16}$
$a^{(0,\frac{3}{2})}_{D\pi\to D\pi}$	$-0.14^{+0.01}_{-0.01}$	$-0.15^{+0.01}_{-0.01}$
$a^{(1,0)}_{DK\to DK}$	$-1.04^{+0.06}_{-0.03}$	$-1.50^{+0.13}_{-0.26}$
$a^{(1,0)}_{D_s\eta\to D_s\eta}$	$-0.62^{+0.02}_{-0.03}+i\,0.01^{+0.01}_{-0.00}$	$-0.76^{+0.05}_{-0.05}+i\,0.05^{+0.00}_{-0.01}$
$a^{(1,1)}_{D_s\pi\to D_s\pi}$	$-0.01^{+0.01}_{-0.01}$	$-0.01^{+0.01}_{-0.01}$
$a^{(1,1)}_{DK\to DK}$	$-1.11^{+0.23}_{-0.09}+i\,0.77^{+0.27}_{-0.04}$	$-0.82^{+0.59}_{-0.38}+i\,1.64^{+0.01}_{-0.11}$
$a^{(2,\frac{1}{2})}_{D_sK\to D_sK}$	$-0.25^{+0.01}_{-0.02}$	$-0.32^{+0.01}_{-0.01}$

5.4 Dynamically generated resonances

The unitary S-matrix could have poles in the complex energy ($\sqrt{s}$) plane in the region not far from the relevant thresholds. Bound states and resonances are poles located on the physical and unphysical Riemann sheets, respectively. Different Riemann sheets are characterized by the sign of the imaginary part of the loop function on the right branch cuts. Each loop function $G_i(s)$ has two sheets: the physical/first Riemann sheet and the unphysical/second Riemann sheet, denoted as $G_I^i(s)$ and $G_{II}^i(s)$, respectively. The expression in Eq. (5.65) defines the physical Riemann sheet, while the expression on the second sheet is given by analytic continuation via [131]

$$G_{II}^i(s+i\epsilon) = G_I^i(s+i\epsilon) - 2i\,\mathrm{Im}\,G_I^i(s+i\epsilon). \tag{5.79}$$

For the n-channel case, there exist 2^n Riemann sheets in total. Different sheets can be accessed by properly choosing the loop functions $G_{I/II}^i(s)$. We use the sign of the imaginary part of $G^i(s)$ above threshold to indicate the $G_{I/II}^i(s)$. In this convention, for the coupled-channel case, the first Riemann sheet is labelled as $(+,+,+,\ldots)$, while $(-,+,+,\ldots)$, $(-,-,+,\ldots)$, $(-,-,-,\ldots)$ and so on correspond to the second, third, fourth, ... sheets, respectively. Normally, at a given energy s, only the sheet which can be reached from the physical one by crossing the branch cut from $s+i\epsilon$ to $s-i\epsilon$ between the thresholds thr_{n-1} and thr_n, has a significant impact on physical observables.

The physical meson masses and decay constant are employed in the pole searching, and the obtained poles are listed in Table. 5.7. For the $(S,I)=(1,0)$ coupled-channel system, in addition to the pole at $\sqrt{s}=2.317$ GeV on the physical sheet, which corresponds to $D_{s0}^*(2317)$ and was used as a condition to constrain the parameters, using the central values of the parameters we also found a pair of poles with a small but nonvanishing imaginary part on the second Riemann sheet, $\sqrt{s}=(2.439\pm i0.01)$ GeV. The only work which reported an analogous pole is Ref. [115], where a virtual state at $\sqrt{s}=2.356$ GeV below DK threshold on the second Riemann sheet was reported in an NLO calculation including $DK, D_s\eta$ and $D_s\eta'$ channels. We check whether such a pole exists using the parameters from the NLO fits in Ref. [29], and found that only part of the allowed parameter space allows for the pole on the unphysical Riemann sheet. Moreover, the effect of this virtual state pole located at $\sqrt{s}=2.356$ GeV on the physical amplitude is negligible in the NLO calculation, as can be seen from the left column of Fig. 5.9. However, the pole on the second Riemann sheet in the NNLO calculation can have a non-negligible effect on specific physical amplitudes, as shown in the right column of Fig. 5.9. These different behaviors are mainly due to different locations of the poles. Nevertheless, we see that the lattice data on the scattering lengths are insufficient to constrain the parameters, and as a result, calculations at different orders may even have a sizeable discrepancy in amplitudes not far from thresholds. More lattice data on $D\phi$ scattering observables are needed to better pin down the LECs.

In addition, we also found a pair of poles $\sqrt{s}=(2.534\pm i0.097)$ GeV on the second Riemann sheet which are not included in Table 5.7. They have a negligible effect on physical amplitudes and would disappear if the u- and t-channels are turned off. Likewise, we do not include the following poles in Table 5.7 since they are located far from the physical region and have little effect: poles at $\sqrt{s}=(2.448\pm i0.049)$ GeV and $(2.267\pm i0.099)$ GeV on the third Riemann sheet for $(S,I)=(1,0)$ and $(1,1)$, respectively; poles at $(2.257\pm i0.018)$ GeV on the second Riemann sheet in the $(-1,0)$ $D\bar{K}\to D\bar{K}$ channel.

It is well-known that the unitarization approach, relying on right-hand unitarity and the on-shell approximation, has the problem of violation of unitarity when the left-hand cut occurs in the on-shell potential. For instance, the left-hand cut in the $K\bar{K}\to K\bar{K}$ amplitude leads a violation of unitarity for the

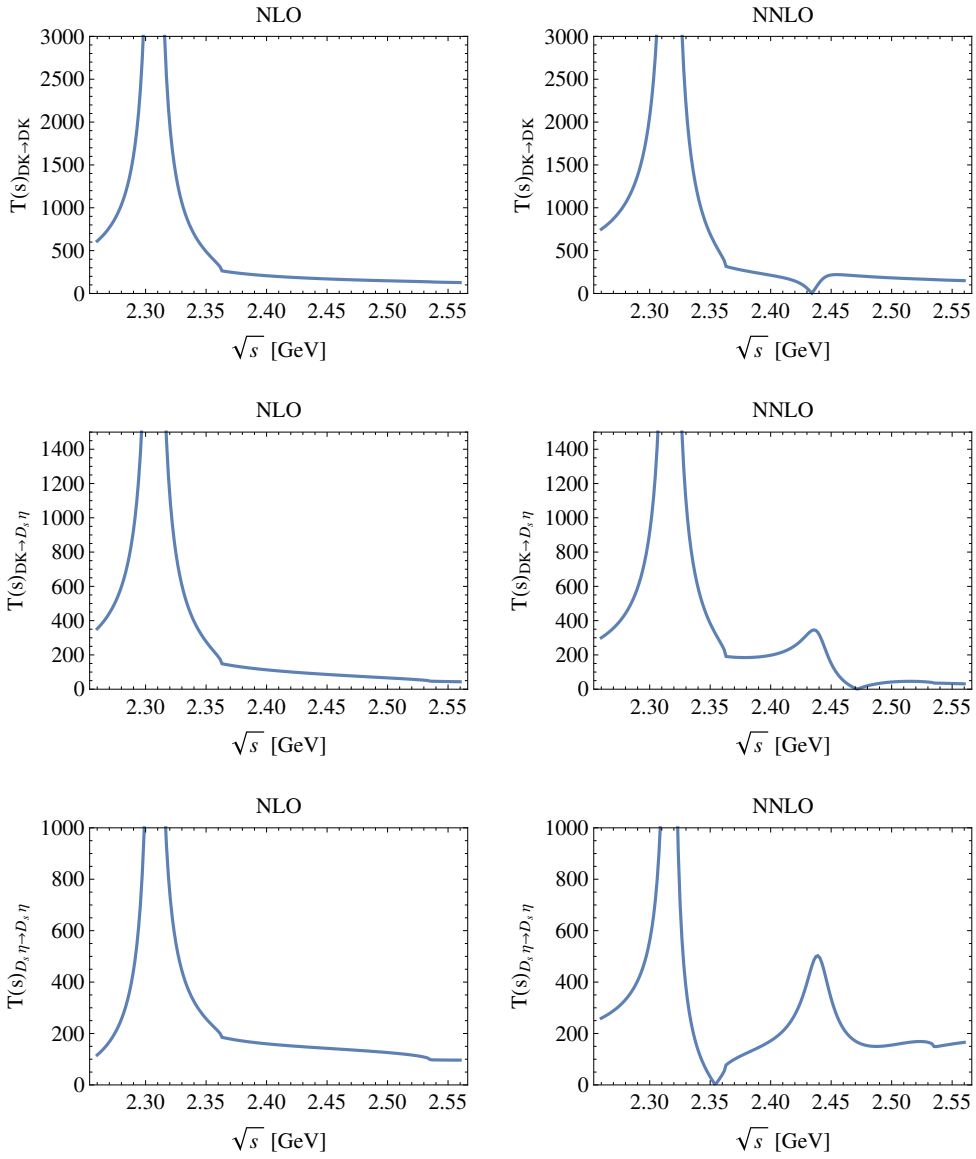

Figure 5.9: Absolute values of amplitudes for $(S, I) = (1, 0)$ in NLO and NNLO calculations, respectively.

Table 5.7: Poles in the coupled-channel amplitudes based on UChPT-6(b) in Table 4 of Ref. [65]. Physical masses and decay constants are used to obtain the poles. The Riemann sheets on which the poles are located are indicated in the last column.

(S,I)	Channel	Thr(MeV)	Re(MeV)	Im(MeV)	RS
$(1,0)$	$DK \to DK$	2363	2317	0	I
	$D_s\eta \to D_s\eta$	2535	2439	± 10	II
$(1,1)$	$D_s\pi \to D_s\pi$	2106	2378	± 19	II
	$DK \to DK$	2363			

Table 5.8: Poles in the single-channel amplitudes based on UChPT-6(b) in Table 4 of Ref. [65]. Physical masses are used to obtain the poles. The Riemann sheets on which the poles are located are indicated in the last column.

(S,I)	Channel	Thr(MeV)	Re(MeV)	Im(MeV)	RS
$(1,0)$	$DK \to DK$	2363	2277	0	I
			2436	± 15	II
$(0,1/2)$	$D\pi \to D\pi$	2005	2107	± 82	II

$\pi\pi$ scattering in the $\pi\pi$–$K\bar{K}$ coupled-channel system [144, 145]. [11] The same unitarity violation happens to the $D\phi$ scattering with $(S,I) = (0,1/2)$, which has three coupled channels: $D\pi$, $D\eta$ and $D_s\bar{K}$. One of the left-hand cuts from the inelastic channel $D_s\bar{K} \to D\eta$ amplitude, from $(1.488\ \text{GeV})^2$ to $(2.318\ \text{GeV})^2$, overlaps with the right-hand cut starting from the $D\pi$ threshold, which can be verified by the discontinuity across the real axis below the $D\pi$ threshold. Although this left-hand cut is not numerically important, its presence together with other left-hand cuts and right-hand cuts make the whole real axis nonanalytic. Since Eq. (5.63) was derived using the N/D method neglecting the left-hand cuts, its continuation to the complex plane near the left-hand cut is untrustworthy. As a result, the coupled-channel amplitudes obtained from Eq. (5.63) do not have the correct analytic properties even in the relevant energy region. Consequently, a pair of pole at $(2.046 \pm i0.050)$ GeV are found on the first Riemann sheet for the coupled-channel $(S,I) = (0,1/2)$ amplitude. As we know, poles on the first Riemann sheet can only be located on the real axis below the lowest threshold, which are associated with bound states. A pole on the first sheet with a nonvanishing imaginary part or above the lowest threshold is inconsistent with causality. The appearance of the pole on the first sheet in the coupled-channel $(S,I) = (0,1/2)$ is due to the existence of the coupled-channel cut. The left-hand cuts stem from the one-loop potentials, and are absent in the NLO cases.

If we consider only the single-channel $D\pi$ for $(S,I) = (0,1/2)$, there is no such a problem as it comes from the left-hand cut of the inelastic channels. We searched for poles in the single-channel amplitude, and found a pair of poles in the second Riemann sheet given in Table 5.8,[12] corresponding to the lower pole at $(2.105 - i0.102)$ GeV of the two-pole structure of $D_0^*(2400)$ advocated in Ref. [123].

In addition, we also investigated the pole movements with varying pion masses. The pion mass dependence trajectories of the poles can provide us with useful information about the properties of

[11] As pointed out by Refs [144, 146], the unitarity violation is numerically small in the $\pi\pi$–$K\bar{K}$ case, hence no serious problem was caused there.

[12] Notice that the poles found in both the single-channel and coupled-channel unitarized NLO amplitudes are similar to each other in Ref. [28].

the different states, as discussed, e.g., in Ref. [147]. The M_π trajectory for the pole corresponding to $D_{s0}^*(2317)$ is plotted in Fig. 5.10. The pole positions on the first Riemann sheet, which are identified as the pole mass, are shown as the solid line. The dotted line stands for the trajectory of the DK threshold. From Fig. 5.10, one can see that the $D_{s0}^*(2317)$ always stays below the corresponding DK threshold as a bound state for a wide range of M_π. The trajectory of $D_{s0}^*(2317)$ is quite similar to the NLO fit result, as shown in Ref. [115].

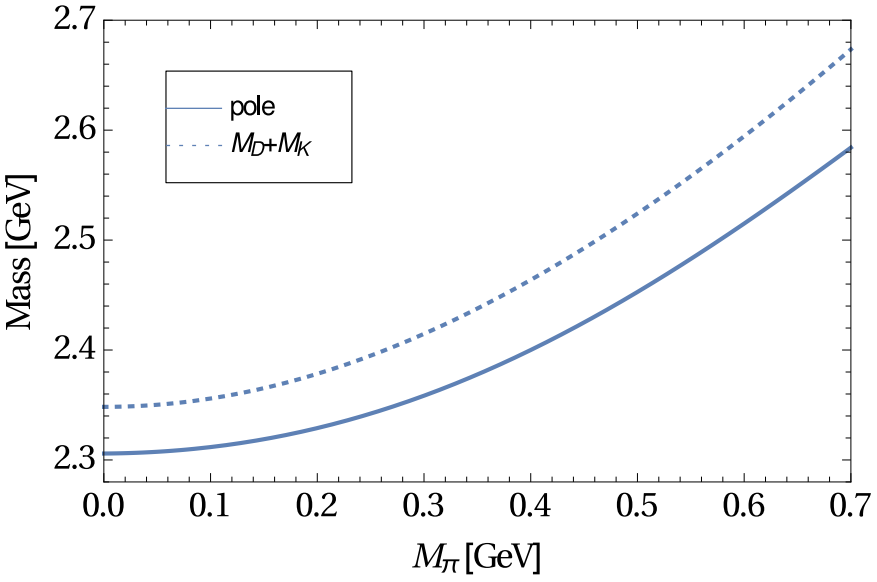

Figure 5.10: The trajectory of the pole $D_{s0}^*(2317)$ with varying M_π.

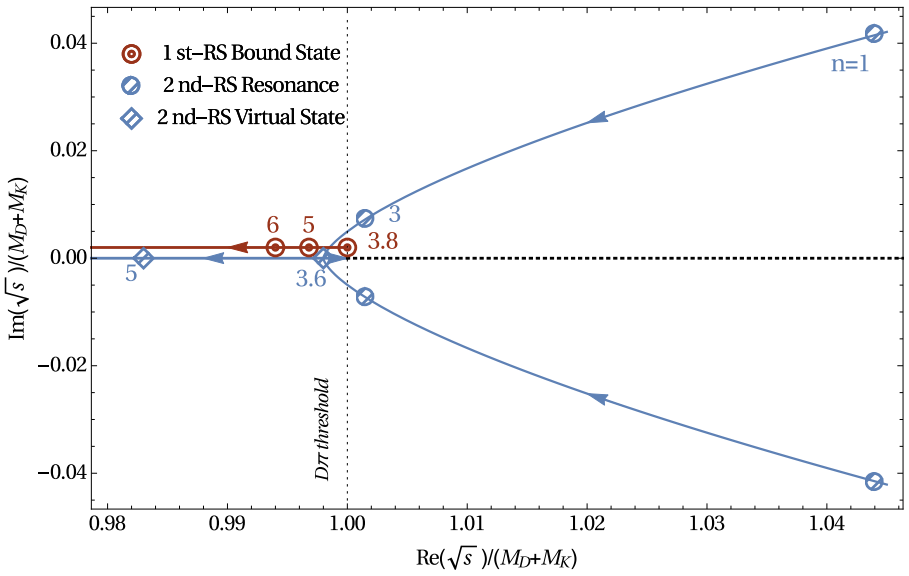

Figure 5.11: The trajectory of the pole around 2.1 GeV for the single-channel $(S, I) = (0, 1/2)$ with varying M_π.

On the contrary, the pion mass dependence trajectory of the pole around 2.1 GeV on the second

Riemann sheet for the single-channel $(S, I) = (0, 1/2)$ in Table 5.8 is quite complicated, as shown in Fig. 5.11. As the value of M_π increases from $M_\pi^{\rm Phy}$, both the real and imaginary parts of the pole tend to decrease on the second Riemann sheet. At some point around $3.2M_\pi^{\rm Phy}$, the real part of the pole becomes lower than the corresponding $D\pi$ threshold. When M_π increases to around $3.6M_\pi^{\rm Phy}$, the pair of poles hits the real axis below the threshold and these become two virtual states on the second Riemann sheet. If we further increase the pion mass, one of the virtual poles would move along the real axis away from the threshold, while the other one moves towards the threshold and becomes a bound state of the first Riemann sheet at $3.8M_\pi^{\rm Phy}$. If we keep increasing M_π, both the virtual state and bound state move away from the threshold along the real axis. The behavior of the pole is similar to the corresponding ones in Refs. [28, 115] as well as the pion mass dependence of the $f_0(500)$ in Ref. [148]. It is a general phenomenon for S-wave states.

CHAPTER 6

Including vector charmed mesons

Heavy quark effective theory (HQEF), see Refs. [44–49] or Sec. 2.1.4, provides a successful way to investigating physics of hadrons containing a single-heavy quark (c, d quark for instance). For the heavy mesons, heavy quark spin symmetry implies that the pseudoscalar and vector mesons can be assigned to the same multiplet. The $D\phi$ interaction is of great importance in understanding the heavy-light meson spectrum on one hand, and serves as a nice playground to combine heavy quark symmetry and chiral symmetry on the other hand. The $D\phi$ interaction can give guidance for $D^*\phi$, $B\phi$ and $B^*\phi$ interactions, since similarities among them exist due to heavy quark spin and flavor symmetries [111–113]. Heavy quark symmetries relate the pseudoscalar D mesons to the vector D^* as well as to the bottom analogues.

The aim of this chapter is to present a full calculation of $D\phi$ scattering using the EOMS scheme within a manifestly Lorentz invariant chiral effective theory with explicit vector charmed mesons, to be denoted as D^*, up to NNLO, i.e. the leading one-loop order. In Chapter 5, the $D\phi$ scattering amplitudes are presented up to NNLO in the absence of the D^*. A systematic calculation including the D^* mesons is given for the first time here. In order to judge the importance of the D^*, a selection of all the diagrams which survives in the limit of heavy quark is used to fit to the lattice data. Then a complete calculation including the D^* mesons is then considered. It is important to check whether the full finite c-quark mass effects, corresponding to including the D^* which are degenerate with the D mesons in the heavy quark limit, are sizeable.

6.1 Theoretical framework

6.1.1 Effective Lagrangian

To set up the effective Lagrangian, we first specify the corresponding power counting rules including the charmed vector mesons D^*, which serve as spin-1 matter fields. They transform under the chiral symmetry same to spinless matter fields (2.143),

$$D_\mu^{*\dagger} \to h(x) D_\mu^{*\dagger}, \quad D_\mu^* \to D_\mu^* h(x)^{-1}. \tag{6.1}$$

At low energies, the counting rules for the Goldstone bosons are same to that without D^*. The nonvanishing masses of the D and D^* in the chiral limit introduce new scales M_0 and M_0^*, both counted as $O(1)$. As a consequence, at low energies, the temporal components of the momenta of the D and D^* are counted as $O(1)$, while the spatial components are counted as $O(p)$. Therefore, the virtuality $q^2 - M_0^{(*)2}$ in the propagators scales as $O(p)$, and thus the heavy meson propagators scale as $O(p^{-1})$. The

Goldstone boson propagators are counted as $O(p^{-2})$ as usual. Based on the counting rules for the vertices and propagators, one can assign a chiral order for a given Feynman diagram, and hence for any physical quantities. As discussed in Sec. 2.5, the presence of the matter fields lead to the notable PCB issue. The EOMS scheme can be extended to ChPT for multi-matter fields.

Given the chiral transformation and the power counting discussed above, one can construct the effective Lagrangian relevant to D-ϕ scattering amplitudes up to NNLO,

$$\mathcal{L}_{\text{eff}} = \sum_{i=1}^{2} \mathcal{L}_{\phi\phi}^{(2i)} + \sum_{j=1}^{3} \mathcal{L}_{D\phi}^{(j)} + \sum_{k=1}^{3} \mathcal{L}_{D^*\phi}^{(k)} + \sum_{l=1}^{3} \mathcal{L}_{D^*D\phi}^{(l)} \tag{6.2}$$

with the superscripts specifying the chiral dimensions. Here $D_\mu^* = (D^{*0}, D^{*+}, D_s^{*+})_\mu$ denotes the D^* meson fields. The part for the Goldstone and spinless matter sector $\sum_{i=1}^{2} \mathcal{L}_{\phi\phi}^{(2i)} + \sum_{j=1}^{3} \mathcal{L}_{D\phi}^{(j)}$ is same to that without D^*, i.e. Eqs. (2.87, 2.97, 2.105 and 2.147). The relevant terms for the interaction between the D^* and the Goldstone bosons are [111–113][1]

$$\begin{aligned} \mathcal{L}_{D^*\phi}^{(1)} &= -\frac{1}{2}\mathcal{F}^{\mu\nu}\mathcal{F}_{\mu\nu}^{\dagger} + M_0^{*2} D^{*\nu} D_\nu^{*\dagger} , \\ \mathcal{L}_{D^*\phi}^{(2)} &= D_\mu^* \left[\tilde{h}_0 \langle \chi_+ \rangle + \tilde{h}_1 \chi_+\right] D^{\mu *\dagger} , \end{aligned} \tag{6.3}$$

with $\tilde{h}_{0,1}$ analogous to $h_{0,1}$ and $\mathcal{F}_{\mu\nu} = (\mathcal{D}_\mu D_\nu^* - \mathcal{D}_\nu D_\mu^*)$.

Finally, the LO axial coupling has the form

$$\mathcal{L}_{D^*D\phi}^{(1)} = i\, g_0 \left(D_\mu^* u^\mu D^\dagger - D\, u^\mu D_\mu^{*\dagger}\right) . \tag{6.4}$$

As pointed out in Refs. [24, 149], the resonance-exchange contributions of $O(p^2)$ and $O(p^3)$ can be taken into account by shifting the coupling in the LO resonance-exchange contribution and the LECs in the contact terms. This also holds true for our case. Thus, we do not need the $O(p^2)$ and $O(p^3)$ terms for the $D^*D\phi$ coupling.

6.1.2 Chiral potentials up to leading one-loop order

Up to NNLO, the Feynman diagrams needed for our calculation are displayed in Fig. 6.1. Accordingly, the chiral potential for the process $D_1(p_1)\phi_1(p_2) \to D_2(p_3)\phi_2(p_4)$ can be written as

$$\mathcal{V}_{D_1\phi_1 \to D_2\phi_2}(s,t) = \mathcal{V}_{\text{LO}}^{(\text{WT})} + \mathcal{V}_{\text{LO}}^{(\text{EX})} + \mathcal{V}_{\text{NLO}}^{(\text{CT})} + \mathcal{V}_{\text{NNLO}}^{(\text{CT})} + \mathcal{V}_{\text{NNLO}}^{(\text{Loop})} . \tag{6.5}$$

As usual, the Mandelstam variables are defined by $s = (p_1 + p_2)^2$ and $t = (p_1 - p_3)^2$, while u can be obtained via $u = \sum_{i=1}^{2}(M_{D_i}^2 + M_{\phi_i}^2) - s - t$. The potentials at tree-level are given by

$$\mathcal{V}_{\text{LO}}^{(\text{WT})}(s,t) = C_{\text{LO}} \frac{s-u}{4F_0^2} , \tag{6.6}$$

$$\mathcal{V}_{\text{LO}}^{(\text{EX})}(s,t) = C_S \frac{g_0^2}{F_0^2}\mathcal{F}_S(s,t) + C_U \frac{g_0^2}{F_0^2}\mathcal{F}_U(s,t) , \tag{6.7}$$

[1] The other terms in NLO and NNLO Lagrangians do not contribute to the NNLO $D\phi$ scattering and therefore are not explicitly shown here.[125]

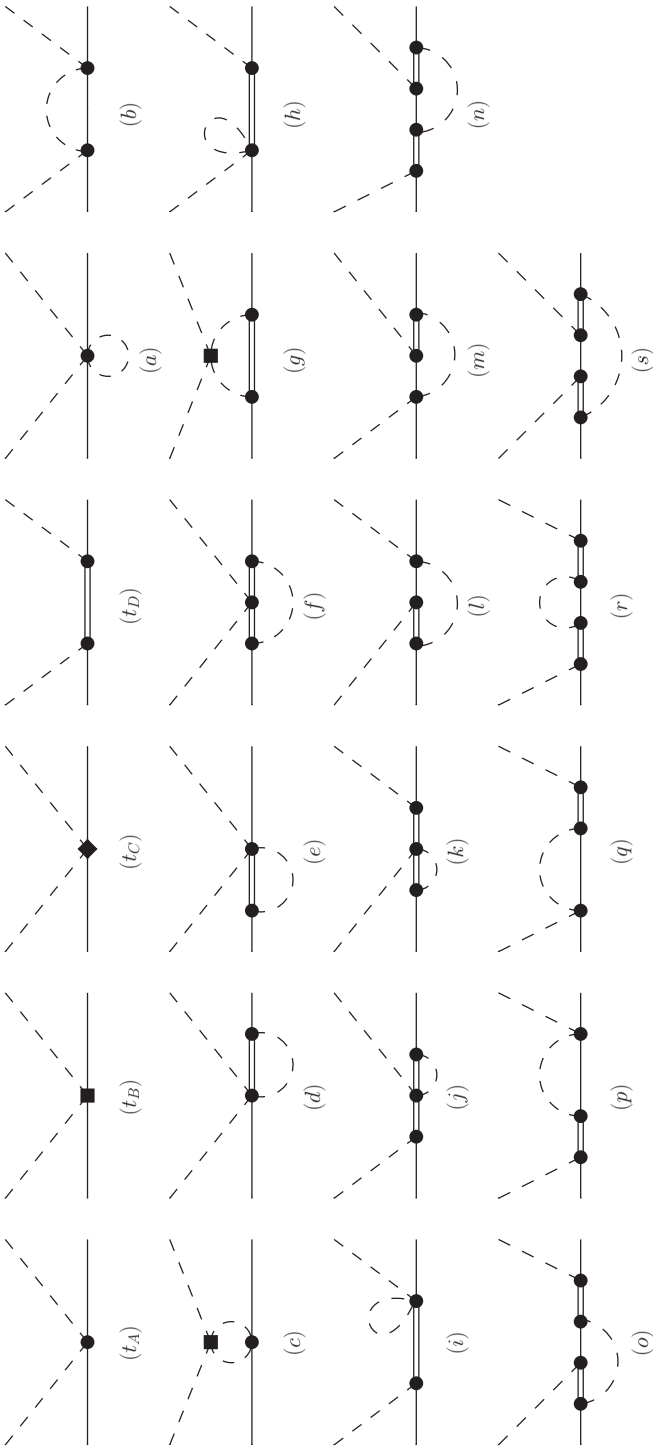

Figure 6.1: Feynman diagrams contributing to $D\phi$ scattering up to NNLO with explicit D^* mesons. The dashed, solid and double-solid lines stand for Goldstone bosons ϕ, pseudo-scalar D mesons and vector D^* mesons, respectively. The dot, square and diamond represent vertices coming from Lagrangians of $O(p^1)$, $O(p^2)$ and $O(p^3)$, in order.

$$\mathcal{V}^{(\mathrm{CT})}_{\mathrm{NLO}}(s,t) = \frac{1}{F_0^2}\Big[-4h_0 C_0^{(2)} + 2h_1 C_1^{(2)} - 2C_{24}^{(2)}\mathcal{H}_{24}(s,t) + 2C_{35}^{(2)}\mathcal{H}_{35}(s,t)\Big]\,, \tag{6.8}$$

$$\mathcal{V}^{(\mathrm{CT})}_{\mathrm{NNLO}}(s,t) = \frac{4g_1}{F_0^2}\Big[C_{1a}^{(3)}(p_1+p_3)\cdot(p_2+p_4) + C_{1b}^{(3)}(p_1+p_3)\cdot p_2\Big] + \frac{4C_{23}^{(3)}\mathcal{G}_{23}(s,t)}{F_0^2}, \tag{6.9}$$

where the involved coefficients corresponding to various scattering processes are shown in Table 6.1. The functions in the D^*-exchange potentials read

$$\mathcal{F}_S(s,t) = \frac{(p_1+p_2)\cdot p_4 (p_1+p_2)\cdot p_2 - M_0^{*2} p_2\cdot p_4}{M_0^{*2}(s-M_0^{*2})}\,, \tag{6.10}$$

$$\mathcal{F}_U(s,t) = \frac{(p_1-p_4)\cdot p_2 (p_1-p_4)\cdot p_4 - M_0^{*2} p_2\cdot p_4}{M_0^{*2}(u-M_0^{*2})}\,. \tag{6.11}$$

The functions in the NLO potentials read

$$\mathcal{H}_{24}(s,t,u) = 2h_2\, p_2\cdot p_4 + h_4\,(p_1\cdot p_2 p_3\cdot p_4 + p_1\cdot p_4 p_2\cdot p_3)\,, \tag{6.12}$$

$$\mathcal{H}_{35}(s,t,u) = h_3\, p_2\cdot p_4 + h_5\,(p_1\cdot p_2 p_3\cdot p_4 + p_1\cdot p_4 p_2\cdot p_3)\,, \tag{6.13}$$

while the one in the NNLO potentials is

$$\begin{aligned}\mathcal{G}_{23}(s,t,u) = &-g_2\, p_2\cdot p_4 (p_1+p_3)\cdot(p_2+p_4)\\ &+2g_3\left[(p_1\cdot p_2)(p_1\cdot p_4)p_1\cdot(p_2+p_4) + (p_1\to p_3)\right]\,.\end{aligned} \tag{6.14}$$

As for the one-loop potentials at NNLO, the parts without explicit D^* mesons can be found in the last chapter and the ones involving explicit D^* states are too lengthy to be shown here. Note that $\mathcal{V}^{(\mathrm{Loop})}_{\mathrm{NNLO}}$ in Eq. (6.5) contains the contribution from wave function renormalization as well. We performed renormalization of the one-loop potentials using the so-called EOMS scheme. In this scheme, the UV divergence are absorbed by the counterterms when the bare LECs are expressed in terms of the renormalized ones via

$$\begin{aligned} M_0^2 &= M_0^{r2}(\mu) + \beta_{M_0^2}\frac{R}{16\pi^2 F_0^2}\,,\\ M_0^{*2} &= M_0^{*r2}(\mu) + \beta_{M_0^{*2}}\frac{R}{16\pi^2 F_0^2}\,,\\ h_i &= h_i^r(\mu) + \beta_{h_i}\frac{R}{16\pi^2 F_0^2}\,, \quad (i=0,1,\cdots,5)\\ g_j &= g_j^r(\mu) + \beta_{g_j}\frac{R}{16\pi^2 F_0^2}\,, \quad (j=0,1,2,3). \end{aligned} \tag{6.15}$$

Here, μ is the scale introduced in dimensional regularization. Then additional subtractions are performed by splitting the UV-renormalized LECs via

$$h_i^r(\mu) = \bar{h}_i + \frac{\bar{\beta}_{h_i}}{16\pi^2 F_0^2}\,, \qquad (i=1,2,\cdots,5)\,, \tag{6.16}$$

Table 6.1: The coefficients in the D^* exchanging tree-level amplitudes of the 10 relevant physical processes.

	Physical processes	$C_{\rm LO}$	C_S	C_U	$C_0^{(2)}$	$C_1^{(2)}$	$C_{24}^{(2)}$	$C_{35}^{(2)}$	$C_{1a}^{(3)}$	$C_{1b}^{(3)}$	$C_{23}^{(3)}$
1	$D^0K^- \to D^0K^-$	1	0	2	M_K^2	$-M_K^2$	1	1	M_K^2	0	1
2	$D^+K^+ \to D^+K^+$	0	0	0	M_K^2	0	1	0	0	0	0
3	$D^+\pi^+ \to D^+\pi^+$	1	0	2	M_π^2	$-M_\pi^2$	1	1	M_π^2	0	1
4	$D^+\eta \to D^+\eta$	0	$\frac{1}{3}$	$\frac{1}{3}$	M_η^2	$-\frac{1}{3}M_\pi^2$	1	$\frac{1}{3}$	0	0	0
5	$D_s^+K^+ \to D_s^+K^+$	1	0	2	M_K^2	$-M_K^2$	1	1	M_K^2	0	1
6	$D_s^+\eta \to D_s^+\eta$	0	$\frac{4}{3}$	$\frac{4}{3}$	M_η^2	$\frac{4}{3}(M_\pi^2 - 2M_K^2)$	1	$\frac{4}{3}$	0	0	0
7	$D_s^+\pi^0 \to D_s^+\pi^0$	0	0	0	M_π^2	0	1	0	0	0	0
8	$D^0\eta \to D^0\pi^0$	0	$\frac{1}{\sqrt{3}}$	$\frac{1}{\sqrt{3}}$	0	$-\frac{1}{\sqrt{3}}M_\pi^2$	0	$\frac{1}{\sqrt{3}}$	0	0	0
9	$D_s^+K^- \to D^0\pi^0$	$-\frac{1}{\sqrt{2}}$	$\sqrt{2}$	0	0	$-\frac{1}{2\sqrt{2}}(M_K^2 + M_\pi^2)$	0	$\frac{1}{\sqrt{2}}$	$-\frac{1}{\sqrt{2}}M_K^2$	$\frac{1}{\sqrt{2}}(M_K^2 - M_\pi^2)$	$-\frac{1}{\sqrt{2}}$
10	$D_s^+K^- \to D^0\eta$	$-\sqrt{\frac{3}{2}}$	$\sqrt{\frac{2}{3}}$	$-\sqrt{\frac{8}{3}}$	0	$\frac{1}{2\sqrt{6}}(5M_K^2 - 3M_\pi^2)$	0	$-\frac{1}{\sqrt{6}}$	$-\sqrt{\frac{3}{2}}M_K^2$	$\frac{1}{\sqrt{6}}(M_\pi^2 - M_K^2)$	$-\sqrt{\frac{3}{2}}$

$$g_0^r(\mu) = \bar{g}_0 + \frac{\bar{\beta}_{g_0}}{16\pi^2 F_0^2}\,, \tag{6.17}$$

such that the PCB terms from the one-loop potentials are canceled. The remaining LECs g_1, g_2 and g_3 are untouched at the chiral order we are working. The β-functions and the coefficients $\bar{\beta}_{h_i}$ and $\bar{\beta}_{g_0}$ are given in Appendix B.

Having the amplitudes in Eq. (6.5), one needs to unitarize it. In this section, we employ the first unitarization discussed in last chapter. The $N(s)$ function is modified to

$$N(s) = \mathcal{V}_{\rm LO}^{\rm (WT+EX)}(s) + \mathcal{V}_{\rm NLO}^{\rm (CT)}(s) + \mathcal{V}_{\rm NNLO}^{\rm (CT+Loop)}(s) - \mathcal{V}_{\rm LO}^{\rm (WT+EX)}(s)\cdot G(s)\cdot \mathcal{V}_{\rm LO}^{\rm (WT+EX)}(s). \tag{6.18}$$

6.2 Numerical analysis

The LECs in Lagrangian Eq. (6.2) can be determined by fitting the scattering lengths to Lattice data. However, due to the poverty of the available data, in order to reduce the number of free parameters, a set of LECs are determined by symmetries, e.g. one has $\tilde{h}_1 = h_1$ and $\tilde{h}_0 = h_0$.[2] [3] Then the pion mass dependence of the masses of the vector mesons reads, consistent with the general expression derived in Ref. [150],

$$M_{D^*} = \mathring{M}_{D^*} + (\tilde{h}_1 + 2\tilde{h}_0)\frac{M_\pi^2}{\mathring{M}_{D^*}}, \quad M_{D_s^*} = \mathring{M}_{D_s^*} + 2\tilde{h}_0\frac{M_\pi^2}{\mathring{M}_{D_s^*}}. \tag{6.19}$$

Here, $\mathring{M}_{D^*}$ and $\mathring{M}_{D_s^*}$ denote the corresponding two-flavor chiral limit masses, which can be estimated by the relations

$$\mathring{M}_{D^*} - \mathring{M}_D \simeq M_{D^*}^{\rm Phy} - M_D^{\rm Phy}, \quad \mathring{M}_{D_s^*} - \mathring{M}_{D_s} \simeq M_{D_s^*}^{\rm Phy} - M_{D_s}^{\rm Phy}, \tag{6.20}$$

with $M_{D^*}^{\rm Phy}$ and $M_{D_s^*}^{\rm Phy}$ denoting the corresponding physical masses, 2.008 GeV and 2.112 GeV, respectively. The $DD^*\pi$ axial coupling constant g_0 is fixed by the decay width $\Gamma_{D^{*+}\to D^0\pi^+}$. To one-loop order, the axial coupling is corrected by a one-loop part, $g^r = g_0 + g_{\text{one-loop}}$. The axial relation between the axial coupling g defined here and the coupling g which is employed usually in the heavy meson ChPT [111–113, 151] is $g^r = \sqrt{M_D M_{D^*}}\,g$. Following Ref. [152], we take $g = 0.570 \pm 0.006$, determined by calculating the decay width of the process $D^{*+} \to D^0\pi^+$, and then one gets $g^r \simeq (1103.3 \pm 11.6)$ MeV.

6.2.1 Contribution of vector charmed mesons in heavy quark limit

In this section, contributions from vector charmed mesons will be included explicitly in order to quantify their influences on the S-wave scattering lengths. The diagrams that survive in the heavy quark limit, see also Ref. [125], are taken into account and shown in Fig. 6.2. Those diagrams vanishing in the heavy quark limit are suppressed by $1/m_c$ and therefore are neglected.

To compare with the result of the case without D^* explicitly included, we utilize the same fit procedures. In parallel to the four kinds of 6-channel fits in the previous section, we refit the S-wave scattering lengths and the results are shown in Table 6.2. In each case, the LECs as well as the chi-squared are

[2] Analogous to Eq. (5.72), it is easy to see that $\tilde{h}_1 = (M_{D_s^*}^2 - M_{D^*}^2)/[4(M_K^2 - M_\pi^2)] = 0.472$, which is close to h_1 numerically.

[3] As discussed in Ref. [122], the beraking of heavy quark spin symmetry is only about 3%. Therefore, to a good approximation, we impose these two heavy-quark limit relations.

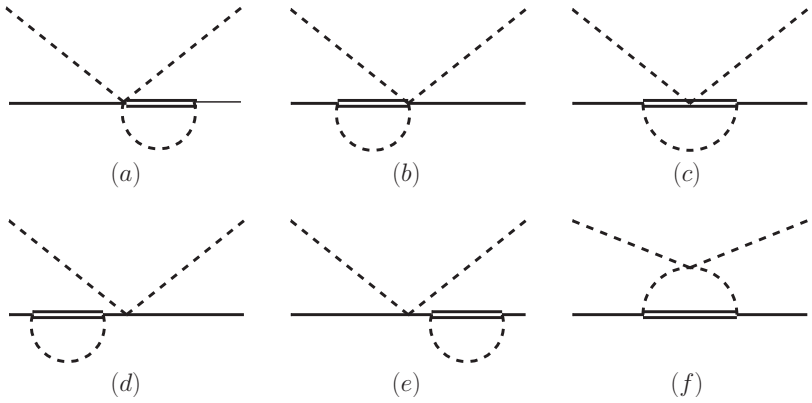

Figure 6.2: Feynman diagrams (including the vector charmed mesons) that survive in the heavy quark limit.

almost same as before. This implies that the influence of D^* to the S-wave scattering lengths is marginal and it is a good approximation to exclude them in the calculation.

Table 6.2: Values of the LECs from the 6-channel fits (including explicit D^*) using the method of UChPT. The h_i's are dimensionless, and the g_1', g_{23} and g_3' are in GeV^{-1}.

	UChPT-6(a) no prior	UChPT-6(b) no prior	UChPT-6(a') with prior	UChPT-6(b') with prior
h_{24}	$0.80^{+0.08}_{-0.08}$	$0.80^{+0.10}_{-0.09}$	$0.85^{+0.10}_{-0.10}$	$0.85^{+0.10}_{-0.10}$
h_{35}	$0.82^{+0.60}_{-0.48}$	$0.98^{+0.97}_{-0.64}$	$0.50^{+0.23}_{-0.23}$	$0.59^{+0.30}_{-0.29}$
h_4'	$-1.27^{+0.52}_{-0.51}$	$-1.40^{+0.59}_{-0.62}$	$-1.22^{+0.58}_{-0.57}$	$-1.59^{+0.62}_{-0.61}$
h_5'	$-11.61^{+2.53}_{-3.07}$	$-15.06^{+4.86}_{-7.31}$	$-3.87^{+0.67}_{-0.69}$	$-2.48^{+0.84}_{-0.83}$
g_1'	$-2.94^{+0.99}_{-0.36}$	$-2.69^{+0.51}_{-0.61}$	$-1.45^{+0.20}_{-0.30}$	$-1.90^{+0.39}_{-0.43}$
g_{23}	$-2.56^{+0.99}_{-0.31}$	$-2.28^{+0.46}_{-0.48}$	$-1.10^{+0.21}_{-0.31}$	$-1.51^{+0.40}_{-0.45}$
g_3'	$2.15^{+0.60}_{-0.49}$	$2.80^{+1.42}_{-0.96}$	$0.91^{+0.15}_{-0.15}$	$0.56^{+0.19}_{-0.19}$
χ^2/d.o.f.	$\frac{29.36}{21-7} = 2.10$	$\frac{13.75}{16-7} = 1.53$	$\frac{74.22-21.56}{21-7} = 3.76$	$\frac{50.06-15.96}{16-7} = 3.79$

6.2.2 Complete contribution of vector charmed mesons

In this section, a complete contribution of vector charmed mesons to the $D\phi$ scattering is considered, i.e. including the one-loop diagrams that vanish in the heavy quark limit. It will give us a hint on the importance of the finite mass effect of c-quark in charm sector.

Compared to the NLO fits [28, 115], the NNLO fits have larger χ^2 values, even though three more LECs g_i ($i = 1, 2, 3$) are included in the fits. This could be because the unitarization method we use works better for the tree-level potentials than one-loop ones. On the one hand, the left-hand cuts, stemming from the t- and u- channels, appear in the one-loop potentials, which would cause the problem of violation of right-hand unitarity in the region where the left- and right- cuts overlap, see more discussions in the next section. On the other hand, the off-shell effects are partially included in the unitarized amplitudes if the one-loop potentials are employed. Both of the above-mentioned effects have non-trivial analytical structures and could make the NNLO unitarization much more cumbersome than the NLO one. Related

to this is the fact that the scattering length $a^{(1,1)}_{D_s\pi\to D_s\pi}$ remains sizeable in the $SU(2)$ chiral limit of $M_\pi \to 0$, as shown in Figs. 6.3 and 6.4. This was also the case in Ref. [65].[4]

Table 6.3: Values of the LECs from the 6-channel fits using the method of UChPT. The h_i's are dimensionless, and the g_1', g_{23} and g_3' are in GeV^{-1}.

	UChPT-6(a) no prior	UChPT-6(b) no prior	UChPT-6(a') with prior	UChPT-6(b') with prior
h_{24}	$0.44^{+0.07}_{-0.07}$	$0.49^{+0.08}_{-0.08}$	$0.52^{+0.09}_{-0.09}$	$0.61^{+0.10}_{-0.10}$
h_{35}	$0.49^{+0.68}_{-0.57}$	$1.03^{+1.20}_{-0.91}$	$-0.19^{+0.23}_{-0.22}$	$0.27^{+0.27}_{-0.26}$
h_4'	$-0.06^{+0.48}_{-0.46}$	$-0.66^{+0.54}_{-0.54}$	$-0.31^{+0.55}_{-0.53}$	$-1.07^{+0.60}_{-0.60}$
h_5'	$-20.23^{+3.04}_{-3.53}$	$-23.91^{+6.83}_{-8.98}$	$-6.33^{+0.66}_{-0.67}$	$-3.68^{+0.75}_{-0.76}$
g_1'	$-2.17^{+0.27}_{-0.32}$	$-2.79^{+0.55}_{-2.53}$	$-1.56^{+0.12}_{-0.14}$	$-1.74^{+0.16}_{-0.20}$
g_{23}	$-1.83^{+0.21}_{-0.25}$	$-2.33^{+0.44}_{-0.49}$	$-1.28^{+0.14}_{-0.15}$	$-1.38^{+0.17}_{-0.21}$
g_3'	$3.20^{+0.67}_{-0.57}$	$3.83^{+1.71}_{-1.31}$	$0.92^{+0.14}_{-0.14}$	$0.19^{+0.18}_{-0.18}$
χ^2/d.o.f.	$\frac{43.81}{21-7} = 3.13$	$\frac{14.26}{16-7} = 1.58$	$\frac{143.78-45.36}{21-7} = 7.03$	$\frac{69.95-20.08}{16-7} = 5.54$

Among various fits, UChPT-6(b) has the smallest χ^2, which is also true for the previous fits without D^* [65]. In addition, the fits with and without dynamical D^* have similar values of the chi-squared and the LECs, which indicates that the influence of the D^* on the quantities in question is small. This conffirms the conclusion in the previous subsection.

[4] It is due to the nonvanishing $\mathring{M}_K$ in loops contributing to the $D_s\pi \to D_s\pi$ potential in the $SU(2)$ chiral limit. Near the $D_s\pi$ threshold, the u- and t-channel loops dominate in the $SU(2)$ chiral limit, which indicates that the left-hand cuts are non-negligible. In the NLO case, the scattering length $a^{(1,1)}_{D_s\pi\to D_s\pi}$ is negligible in the $SU(2)$ chiral limit [29, 115].

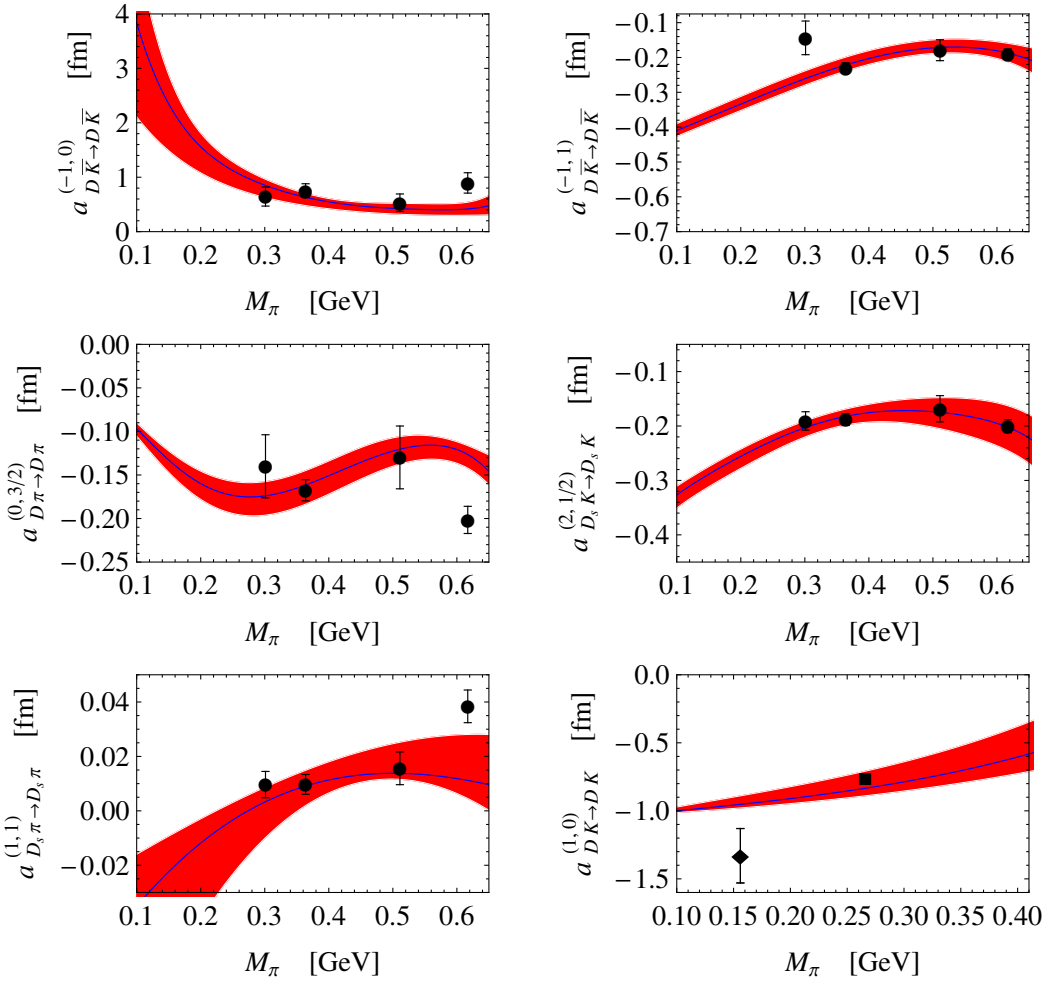

Figure 6.3: The results of the UChPT-6(b) fits to the lattice data of the scattering lengths. The filled circles are lattice results in Ref. [29], and the filled square (not included in the fits because it refers to $N_f = 2$) and diamond are taken from Ref. [100].

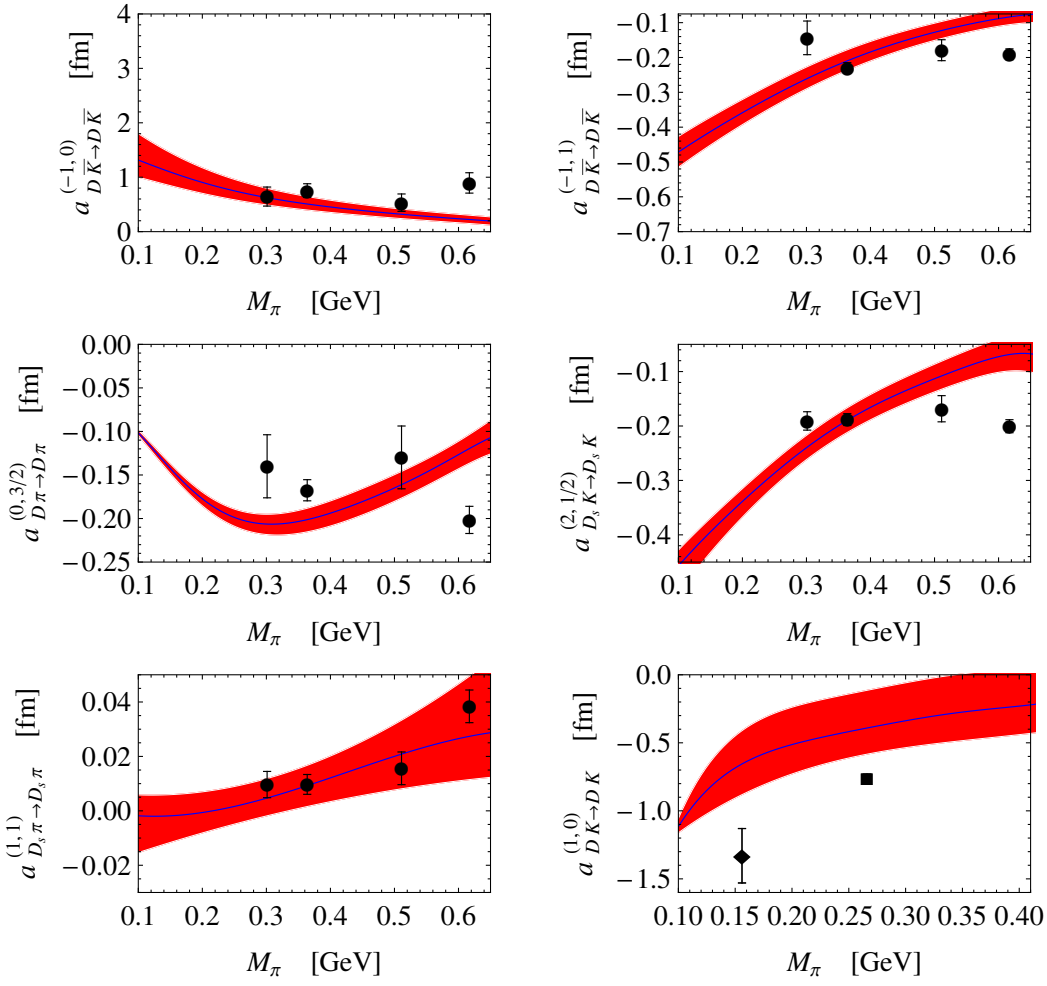

Figure 6.4: The results of the UChPT-6(b') fits to the lattice data of the scattering lengths. The filled circles are lattice results in Ref. [29], and the filled square (not included in the fits because it refers to $N_f = 2$) and diamond are taken from Ref. [100].

CHAPTER 7

Aspects of the low-energy constants in the chiral Lagrangian for charmed mesons

Ideally, the low-energy constants (LECs) should be pinned down by comparing with (or performing fits to) experimental or lattice QCD data of selected observables in certain processes, as done in the last two chapters. Since these values of LECs should be universal, consequently, predictions for other processes or physical quantities can be made. For instance, the LECs of the fundamental πN interaction [23, 24, 153–156], which are fixed by fitting to experimental πN scattering data, are employed to make predictions in $\pi\pi N$ physics, see e.g.Ref. [157] and NN physics, see Ref. [158] for a review. However, things become cumbersome when there are not sufficiently many data or, even worse, no good data for fixing the LECs. Furthermore, even if the LECs have been extracted or estimated using some procedure, the reliability of these values still needs to be further analyzed.

A phenomenological approach to estimate the LECs was discussed in detail in Refs. [159–161], and is traditionally referred to as the resonance saturation. Therein, phenomenological Lagrangians respecting chiral symmetry including explicit meson resonances are constructed and then the resonance fields are integrated out to generate contributions to the LECs in the mesonic ChPT Lagrangian at tree level in terms of the resonance couplings and masses. It was found that whenever the vector and axial vector mesons contribute, they almost saturate the empirical values of the LECs, which is a modern version of the vector meson dominance hypothesis. Similarly, the resonance exchange model also provides a fairly good phenomenological description of the LECs in the chiral Lagrangian for the pion-nucleon interactions, c.f. Ref. [162], where it is found that the Δ resonance provides the dominant contribution to some of the LECs, i.e., c_3 and c_4.[1] In view of the success achieved in both the purely mesonic ChPT and baryon ChPT, the resonance exchange method will be discussed in this paper to estimate the LECs related to the interactions between charmed D mesons and Goldstone bosons (ϕ), which are badly known because no experimental data for t $D\phi$ scattering are available and almost all the existing extractions result from fitting to lattice results of scattering lengths for certain channels. The scarcity of data and the model dependence of the unitarization method cause discrepancies among the extracted values for some of the LECs.

Furthermore, in this chapter we will investigate model-independent positivity constraints on the $D\phi$ interaction as well. Similar to the case for the $\pi\pi$ [163–167] and πN [168, 169] scattering, these constraints will be derived in the upper part of the Mandelstam triangle (with $t > 0$) based on axiomatic principles of the S-matrix theory such as analyticity, unitarity and crossing symmetry. After applying the obtained constraints to the chiral perturbative and EOMS-renormalized amplitudes, e.g., given in Chapter 5, one

[1] Note that there is also an important contribution from the ρ-meson to c_4.

obtains restrictions on the involved LECs at a certain given order. These axiomatic constraints will be confronted with the numerical values of the LECs determined through various phenomenological fits to lattice data.

7.1 Low-energy constants and resonance exchanges

As mentioned in last chapter, the pseudoscalar and vector charmed mesons are related to each other via heavy-quark spin symmetry. One can construct ChPT for heavy mesons by treating the pseudoscalars and the vectors simultaneously in a spin multiplet. The scattering processes of the Goldstone bosons off the pseudoscalar and vector charmed mesons can thus be described by the same chiral Lagrangian at low energies. So far, most of the available information for LECs was obtained from fitting to the lattice data of the S-wave scattering lengths for the $D\phi$ systems. It has been shown by explicit calculations that the D^* contribution is negligible in these quantities [65, 114]. Hence, we can focus on the Lagrangian without the D^*, and keep in mind that such a theory is basically equivalent to the one with the D^* explicitly included when discussing the S-wave $D\phi$ scattering.

In this section, the LO chiral Lagrangians for various resonances are discussed and constructed. Then making use of the approach of resonance exchange to analyze the resonance contributions to the LECs of $D\phi$ Lagrangian. The corresponding numerical results are given subsequently.

7.1.1 Chiral resonance Lagrangians

The saturation of LECs by the contributions from resonances is based on scale separation such that the low-energy effective Lagrangian contains only the low-lying degrees of freedom and the resonances at the hard scale are considered to be integrated out. The local operators in the Lagrangian are constructed in terms of the effective degrees of freedom, while the high-energy contribution including the effects from resonances enter the LECs, which are coefficients of the operators. In principle, the LECs can be calculated in the full theory by a matching procedure. In the case of the chiral Lagrangian, since we cannot solve the nonperturbative QCD analytically, we may match the chiral Lagrangian containing only the low-lying degrees of freedom to the one with resonances, which is applicable in a larger energy range phenomenologically despite the more complicated renormalization and power counting issues related to the large masses and instability of the resonances. For such a matching, one expects that the resonances with relatively low masses contribute dominantly to the LECs.

To analyze the resonance contributions to the chiral LECs, the chiral resonance Lagrangians are necessary. We will first introduce the Lagrangians related to excited charmed mesons, with the orbital angular momentum between the charmed quark and light quark $\ell \leq 1$, then the ones concerning the light-flavor mesonic excitations will be discussed.

The excited charmed mesons with $\ell \leq 1$ include D_0^* with $J^P = 0^+$, D_1' and D_1 with $J^P = 1^+$, and D_2^* with $J^P = 2^+$.[2] Though more and more candidates for states with $\ell \geq 2$ were discovered experimentally [170–172], their classifications in the charmed spectra still need to be investigated or confirmed. Furthermore, their contributions should be smaller than those with $\ell \leq 1$ because of higher masses as mentioned above. Hence we do not include them in our analysis.

For the scalar D_0^* SU(3) triplet, $D_0^* = (D_0^{*0}, D_0^{*+}, D_{s0}^{*+})$, the corresponding Lagrangian is

$$\mathcal{L}_{D_0^* D\phi} = g_0 \left(D_0^* u^\mu \mathcal{D}_\mu D^\dagger + \mathcal{D}_\mu D u^\mu D_0^{*\dagger} \right) . \tag{7.1}$$

[2] Note that the D^* vector mesons with $J^P = 1^-$ are treated as the spin partner of the D as discussed at the beginning of this section.

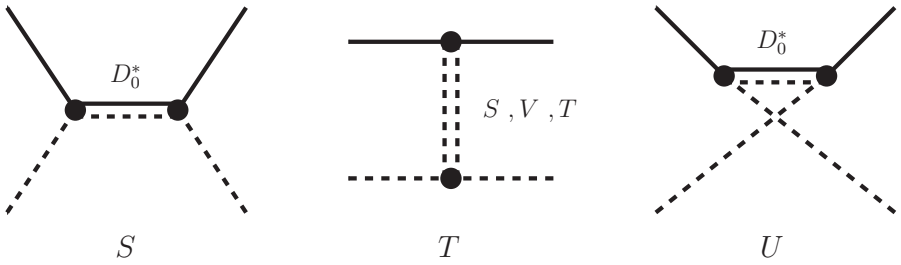

Figure 7.1: Diagrams for the resonance-exchange contribution to $D\phi$ scattering.

The coupling g_0 will be determined via the LO calculation of the decay $D_0^* \to D^+\pi^-$.

As for the tensor D_2^* triplet, $D_2^* = (D_2^{*0}, D_2^{*+}, D_{s2}^{*+})$, the lowest-order Lagrangian for the $D_2^* D\Phi$ interaction

$$\mathcal{L}_{D_2^* D\Phi} \propto D^*_{2,\mu\nu}\{\mathcal{D}^\mu, u^\nu\}D^\dagger + h.c., \tag{7.2}$$

is of second chiral order. Physically, the coupling of a tensor charmed meson to a pseudoscalar charmed meson and a light pseudoscalar is in a D-wave, and starts from $O(p^2)$. Thus, the exchange of tensor charmed mesons will not contribute to the LECs in the $O(p^2)$ and $O(p^3)$ Lagrangians, and its contribution starts from $O(p^4)$ in the chiral expansion.

The axial vector charmed mesons D_1 and D_1' do not contribute to the LECs in the chiral Lagrangian for the $D\phi$ interactions since there is no $D_1^{(\prime)}D\phi$ coupling due to parity conservation. Yet, they will contribute to those in the $D^*\phi$ Lagrangian. At leading order of the heavy quark expansion, such contributions are equal to those of the D_0^* and D_2^* to the $D\phi$ Lagrangian.

Therefore, among the excited charmed mesons, we only need to take into account the exchange of the scalar ones for our purpose of estimating resonance contributions to the $O(p^2)$ and $O(p^3)$ LECs. With the above Lagrangians, we can then calculate the $D\phi$ scattering amplitudes by exchanging the D_0^* whose Feynman diagrams are shown in Fig. 7.1 (see the first and third diagrams). It is evident that they contribute to $D\phi$ scattering in both the s- and u-channels.

For the light-flavor mesonic resonances, the low-lying vector, scalar and tensor states will be considered. They contribute to $D\phi$ scattering in t-channel, see the second Feynman diagram in Fig. 7.1. For the vector resonance, the involved interactions read [159, 160]

$$\begin{aligned}
\mathcal{L}_{V\phi\phi} &= \frac{i\,g_V}{\sqrt{2}}\langle \hat{V}_{\mu\nu} u^\mu u^\nu \rangle\,, \qquad (\hat{V}_{\mu\nu} \equiv \partial_\mu V_\nu - \partial_\nu V_\mu)\,, \\
\mathcal{L}_{DDV} &= i\,g_{DDV}\left\{D\,V^\mu(\partial_\mu D^\dagger) - (\partial_\mu D)\,V^\mu D^\dagger\right\}\,,
\end{aligned} \tag{7.3}$$

where V_μ denotes the vector meson multiplet of interest with its explicit form given by

$$V_\mu = \begin{pmatrix} \frac{\rho^0}{\sqrt{2}} + \frac{\omega}{\sqrt{2}} & \rho^+ & K^{*+} \\ \rho^- & -\frac{\rho^0}{\sqrt{2}} + \frac{\omega}{\sqrt{2}} & K^{*0} \\ K^{*-} & \bar{K}^{*0} & \tilde{\phi} \end{pmatrix}_\mu\,. \tag{7.4}$$

Here, the ideal mixing scheme between ω_1 and ω_8, i.e., $\omega_1 = \sqrt{2/3}\omega + \sqrt{1/3}\tilde{\phi}$ and $\omega_8 = \sqrt{1/3}\omega - \sqrt{2/3}\tilde{\phi}$, is employed to construct the physical ω and $\tilde{\phi}$. Note that we have denoted the physical $\phi(1020)$ by the symbol $\tilde{\phi}$ in order to avoid possible confusion with the notation for the matrix of Goldstone bosons.

The Lagrangians concerning the scalar resonance exchange take the following form [159, 160]

$$\begin{aligned}\mathcal{L}_{S\phi\phi} &= c_d\langle S\, u_\mu u^\mu\rangle + c_m\langle S\chi_+\rangle + \tilde{c}_d\, S_1\langle u_\mu u^\mu\rangle + \tilde{c}_m\, S_1\langle\chi_+\rangle\,,\\ \mathcal{L}_{DDS} &= g_{DDS}\, D\, S\, D^\dagger + \tilde{g}_{DDS}\, DD^\dagger S_1\,,\end{aligned} \tag{7.5}$$

with S_1 and S denoting the scalar singlet and octet, respectively. In Eqs. (7.3) and (7.5), the Lagrangians for the coupling of the light-flavor resonances to the Goldstone bosons are taken from Refs. [159, 160].

Finally, we also consider the light-flavor tensor resonances with quantum numbers 2^{++}, denoted by $T^{\mu\nu}$. We construct the Lagrangian for the DDT coupling as

$$\mathcal{L}_{DDT} = g_{DDT}\mathcal{D}_\mu D T^{\mu\nu}\mathcal{D}_\nu D^\dagger. \tag{7.6}$$

The 2^{++} mesons are described by the symmetric hermitian fields [173]

$$T_{\mu\nu} = T^0_{\mu\nu}\frac{\lambda_0}{\sqrt{2}} + \frac{1}{\sqrt{2}}\sum_{i=1}^{8}\lambda_i T^i_{\mu\nu},\quad T_{\mu\nu} = T_{\nu\mu}\,, \tag{7.7}$$

where the singlet and octet components are

$$T^0 = f_2^0,\quad \text{and}\quad \frac{1}{\sqrt{2}}\sum_{i=1}^{8}\lambda_i T^i = \begin{pmatrix} \frac{a_2^0}{\sqrt{2}} + \frac{f_2^8}{\sqrt{6}} & a_2^+ & K_2^{*+} \\ a_2^- & -\frac{a_2^0}{\sqrt{2}} + \frac{f_2^8}{\sqrt{6}} & K_2^{*0} \\ K_2^{*-} & \bar{K}_2^{*0} & -\frac{2f_2^8}{\sqrt{6}} \end{pmatrix}, \tag{7.8}$$

respectively.

To estimate the contribution of 2^{++} mesons to LECs of $D\phi$ Lagrangian, the coupling of the tensor meson to the Goldstone bosons is needed as well, which can be constructed as [173]

$$\mathcal{L} = -\frac{1}{2}\langle T_{\mu\nu}D_T^{\mu\nu,\rho\sigma}T_{\rho\sigma}\rangle + \langle T_{\mu\nu}J_T^{\mu\nu}\rangle,\qquad J_T^{\mu\nu} \equiv g_T\{u^\mu, u^\nu\}\,, \tag{7.9}$$

where $J_T^{\mu\nu}$ is the tensor current and

$$\begin{aligned} D_T^{\mu\nu,\rho\sigma} &= (\mathcal{D}^2 + M_T^2)\left[\frac{1}{2}(g^{\mu\rho}g^{\nu\sigma} + g^{\mu\sigma}g^{\nu\rho}) - g^{\mu\nu}g^{\rho\sigma}\right] \\ &\quad + g^{\rho\sigma}\mathcal{D}^\mu\mathcal{D}^\nu + g^{\mu\nu}\mathcal{D}^\rho\mathcal{D}^\sigma - \frac{1}{2}(g^{\nu\sigma}\mathcal{D}^\mu\mathcal{D}^\rho + g^{\rho\nu}\mathcal{D}^\mu\mathcal{D}^\sigma + g^{\mu\sigma}\mathcal{D}^\rho\mathcal{D}^\nu + g^{\rho\mu}\mathcal{D}^\sigma\mathcal{D}^\nu). \end{aligned} \tag{7.10}$$

7.1.2 Integrating out resonances

In essence, the contribution of a resonance to LECs is the coefficients of a local expansion of the effective nonlocal generating potential obtained by integrating out the resonance. Usually it can be achieved by two different ways. The first one is to integrate out the resonance using the path integral and then make an expansion (chiral expansion for our case). The second method is to calculate certain physical processes with and without the resonances respectively, and then match the two results to fix the contribution of the resonances to LECs, usually associated with a local expansion.

To see it more clearly, we evaluate the contribution of the tensor mesons with 2^{++} to $D\phi$ LECs by

integrating out the tensor mesons at tree level, see also Eq. (2.3). From the Lagrangian (7.9) one obtains the equation of motion for the tensor mesons

$$T_{\rho\sigma} = (D_T^{\mu\nu,\rho\sigma})^{-1} J_T^{\mu\nu}. \tag{7.11}$$

At tree level, integrating out a field is equivalent to replacing the field by its classical solution of motion. Inserting the EoM for the tensor mesons, i.e. Eq. (7.11), into $\mathcal{L}_{DDT}$, we get

$$\begin{aligned} \mathcal{L}_{DDT} &= \mathcal{L}_{DDT}^{(2)} + O(p^4), \\ \mathcal{L}_{DDT}^{(2)} &= \frac{g_{DDT}}{M_T^2} \mathcal{D}_\mu D J_T^{\mu\nu} \mathcal{D}_\nu D^\dagger = \frac{g_{DDT} g_T}{M_T^2} \mathcal{D}_\mu D \{u^\mu, u^\nu\} \mathcal{D}_\nu D^\dagger. \end{aligned} \tag{7.12}$$

Here we have employed the chiral expansion by regarding the momenta of the tensor is of order $O(p)$ since it couples to $g_T\{u^\mu, u^\nu\}$. It is then easy to see that the light-tensor mesons contribute to the LECs and only contribute to h_5 up to $O(p^2)$. The contribution is

$$h_5^T = \frac{g_{DDT} g_T}{M_T^2}. \tag{7.13}$$

Since the pesudoscalar charmed mesons D and vector charmed mesons D^* can be assigned into a doublet in the heavy quark limit as discussed in the last chaper, one may wonder about the contribution of the D^* to the LECs of $D\phi$ Lagrangian. In what follows we investigate the contribution of D^* by integrating out the D^*. The relevant Lagrangian can be written as

$$\mathcal{L}_{DD^*\phi} = D_\mu^* \mathcal{D}^{\mu\nu} D_\nu^* + i g_0 (D_\mu^* u^\mu D^\dagger - D u^\mu D_\mu^{*\dagger}), \tag{7.14}$$

where

$$\mathcal{D}^{\mu\nu} = (\mathcal{D}^2 - M_{D^*}^2) g^{\mu\nu} - \mathcal{D}^\nu \mathcal{D}^\mu. \tag{7.15}$$

The effective generating functional at tree-level is

$$\begin{aligned} e^{iZ_{\text{eff}}[D,\phi]} &= \int [dD^* dD^{*\dagger}] e^{i\mathcal{L}_{DD^*\phi}} \\ &= N \exp\left(i (i g_0)^2 \int d^4x d^4y D(x) u^\mu(x) D_F^{\mu\nu}(x-y) u^\nu(y) D^\dagger(y) \right), \end{aligned} \tag{7.16}$$

where N is an irrelevant normalization constants and

$$D_F^{\mu\nu}(x-y) = \int \frac{d^4p}{(2\pi)^4} e^{-ip(x-y)} \frac{-1}{p^2 - M_{D^*}^2} (g^{\mu\nu} - \frac{p^\mu p^\nu}{M_{D^*}^2}) \tag{7.17}$$

is the D^* propagator. To make the chiral quantities more explicit, we define $l = p - p_0$ with $p_0^2 = M_D^2$. Then

$$Z_{\text{eff}} = (i g_0)^2 \int d^4x d^4y \frac{d^4l}{(2\pi)^4} D(x) u_\mu(x) u_\nu(y) D^\dagger(y) \frac{1}{l^2 + 2l \cdot p_0 - \Delta^2} (g^{\mu\nu} - \frac{p^\mu p^\nu}{M_{D^*}^2}) e^{-ip(x-y)} \tag{7.18}$$

with $\Delta = M_{D^*}^2 - M_D^2$. In ChPT, the momenta of D and D^* are treated as large. The theory works in the

low energy region where $l \ll p$, and thus l is regarded as a chiral quantity. In this convention, we have the match

$$p_\mu u^\nu D^\dagger \to -i\partial_\mu (u^\nu D^\dagger), \qquad p_{0\mu} u^\nu D^\dagger \to -i u^\nu \partial_\mu D^\dagger. \tag{7.19}$$

In other words, it is equivalent to imposing D on-shell and at the same time operator product expanding $u^\nu(y)D^\dagger(y)$ as:

$$\begin{aligned} u^\nu(y)D^\dagger(y) = u^\nu(x)D^\dagger(x) + (y-x)_\alpha \partial_\alpha \Big(u^\nu(x)D^\dagger(x)\Big) \\ + \frac{1}{2}(y-x)_\alpha (y-x)_\beta \partial_\alpha \partial_\beta \Big(u^\nu(x)D^\dagger(x)\Big) + \cdots . \end{aligned} \tag{7.20}$$

Here, ∂_μ indicates a small momentum l_μ, which means that it only acts on the Goldstone fields, and $\cdots$ denotes the higher order contributions.

The first term of Eq. (7.18), i.e. the term proportional to $g_{\mu\nu}$, is evaluated as:

$$\begin{aligned} \mathcal{L}_{\text{eff}}^{g_{\mu\nu}} &= (ig_0)^2 D u^\mu u_\mu D^\dagger \int d^4y \frac{d^4l}{(2\pi)^2} e^{-il(x-y)} \frac{-1}{l^2 + 2l\cdot p_0 - \Delta^2} \\ &\quad + (ig_0)^2 D u^\mu (\partial_\alpha u_\mu) D^\dagger \int d^4y \frac{d^4l}{(2\pi)^2} e^{-il(x-y)} \frac{-1}{l^2 + 2l\cdot p_0 - \Delta^2} (y-x)^\alpha \\ &\quad + \frac{1}{2}(ig_0)^2 D u^\mu (\partial_\alpha \partial_\beta u_\mu) D^\dagger \int d^4y \frac{d^4l}{(2\pi)^2} e^{-il(x-y)} \frac{-1}{l^2 + 2l\cdot p_0 - \Delta^2} (y-x)^\alpha (y-x)^\beta + \dots \\ &= g_0^2 D u^\mu u_\mu D^\dagger \frac{1}{-\Delta^2} g_0^2 D u^\mu (\partial_\alpha u_\mu) D^\dagger \int d^4l \frac{\partial}{i\partial l_\alpha} \delta^4(l) \frac{1}{l^2 + 2l\cdot p_0 - \Delta^2} \\ &\quad + \frac{1}{2} g_0^2 D u^\mu (\partial_\alpha \partial_\beta u_\mu) D^\dagger \int d^4l \frac{\partial^2}{i^2 \partial l_\beta \partial l_\alpha} \delta^4(l) \frac{1}{l^2 + 2l\cdot p_0 - \Delta^2} + \dots \\ &= -D u^\mu u_\mu D^\dagger \frac{g_0^2}{\Delta^2} D u^\mu (\partial_\alpha u^\mu) \partial^\alpha D^\dagger \frac{2g_0^2}{\Delta^4} \\ &\quad + D u^\mu (\partial_\alpha \partial^\alpha u_\mu) D^\dagger \frac{g_0^2}{\Delta^4} - D u^\mu (\partial_\alpha \partial_\beta u_\mu) \partial^\alpha \partial^\beta D^\dagger \frac{4g_0^2}{\Delta^6} + \dots , \end{aligned} \tag{7.21}$$

where $\Delta^2 = M_{D^*}^2 - M_D^2$. Similarly, the second term of Eq. (7.18) can be evaluated as:

$$\begin{aligned} \mathcal{L}_{\text{eff}}^{p_\mu p_\nu} &= (ig_0)^2 D u_\mu(x) u_\nu D^\dagger(y) \int d^4y \frac{d^4l}{(2\pi)^2} e^{-il(x-y)} \frac{-1}{l^2 + 2l\cdot p_0 - \Delta^2} \Big(-\frac{p^\mu p^\nu}{M_{D^*}^2}\Big) + \dots \\ &= \frac{\tilde{g}^2}{M_{D^*}^2} D u^\mu(x) \partial_\mu \partial_\nu (u^\nu D^\dagger(y)) \int d^4y \frac{d^4l}{(2\pi)^2} e^{-il(x-y)} \frac{1}{l^2 + 2l\cdot p_0 - \Delta^2} + \dots \\ &= -\frac{g_0^2}{M_{D^*}^2} \Big(\frac{D u^\mu \partial_\mu \partial_\nu (u^\nu D^\dagger)}{\Delta^2} - \frac{2 D u^\mu \partial_\mu \partial_\nu ((\partial_\alpha u^\nu) \partial^\alpha D^\dagger)}{\Delta^4} - \frac{D u^\mu \partial_\mu \partial_\nu ((\partial_\alpha \partial^\alpha u^\nu) D^\dagger)}{\Delta^4} \\ &\quad + \frac{4 D u^\mu \partial_\mu \partial_\nu ((\partial_\alpha \partial_\beta u^\nu) \partial^\alpha \partial^\beta D^\dagger)}{\Delta^6} \Big) + \dots \end{aligned} \tag{7.22}$$

Making use of integration by parts, it can be simplified as

$$\begin{aligned}\mathcal{L}_{\text{eff}}^{p_\mu p_\nu} = -\frac{g_0^2}{M_{D^*}^2}\Big(&\frac{Du^\mu u^\nu \partial_\mu\partial_\nu D^\dagger}{\Delta^2} + \frac{Du^\mu(\partial_\nu u^\nu)\partial_\mu D^\dagger}{\Delta^2} + \frac{Du^\mu(\partial_\mu u^\nu)\partial_\nu D^\dagger}{\Delta^2} + \frac{Du^\mu(\partial_\mu\partial_\nu u^\nu)D^\dagger}{\Delta^2}\\ &-\frac{2Du^\mu(\partial_\alpha u^\nu)\partial_\mu\partial_\nu\partial^\alpha D^\dagger}{\Delta^4} - \frac{2Du^\mu(\partial_\nu\partial_\alpha u^\nu)\partial_\mu\partial^\alpha D^\dagger}{\Delta^4} - \frac{2Du^\mu(\partial_\mu\partial_\alpha u^\nu)\partial_\nu\partial^\alpha D^\dagger}{\Delta^4}\\ &-\frac{Du^\mu(\partial_\alpha\partial^\alpha u^\nu)\partial_\mu\partial_\nu D^\dagger}{\Delta^4} + \frac{4Du^\mu(\partial_\alpha\partial_\beta u^\nu)\partial_\mu\partial_\nu\partial^\alpha\partial^\beta D^\dagger}{\Delta^6}\Big) + \ldots,\end{aligned} \tag{7.23}$$

where $\Sigma^2 = M_{D^*}^2 + M_D^2$ and we used the integration by parts in the last step. Putting $\mathcal{L}^{g_{\mu\nu}}$ and $\mathcal{L}^{p_\mu p_\nu}$ together, up to $O(p^3)$ we have

$$\begin{aligned}\mathcal{L}_{\text{eff}} = &-Du^\mu u_\mu D^\dagger\frac{g_0^2}{\Delta^2} + \frac{g_0^2}{\Delta^2(\Sigma^2+\Delta^2)}\mathcal{D}_\mu D\{u^\mu, u^\nu\}\mathcal{D}_\nu D^\dagger\\ &+\frac{g_0^2\Sigma^2}{4\Delta^4(\Sigma^2+\Delta^2)}D\Big([u_\mu,[\mathcal{D}_\nu,u^\mu]]+[u_\mu,[\mathcal{D}^\mu,u_\nu]]\Big)\mathcal{D}^\nu D^\dagger + \frac{1}{4\Delta^4}D\,[u_\mu,[\mathcal{D}_\nu,u_\rho]]\mathcal{D}^{\mu\nu\rho}D^\dagger + \text{h.c.}\end{aligned} \tag{7.24}$$

By comparing Eq. (7.24) with Eq. (2.147) one obtains the contribution of D^* to the LECs

$$\begin{aligned}h_3^{D^*} &= -h_5^{D^*}(\Delta+\Sigma) = \frac{g_0^2}{\Delta},\\ g_1^{D^*} &= g_2^{D^*}\frac{\Delta^2}{\Sigma^2} = g_3^{D^*}\Delta^2 = \frac{g_0^2}{4(\Delta^2+\Sigma^2)\Delta^2}.\end{aligned} \tag{7.25}$$

From the above calculations, one may notice that the contribution of D^* is arranged in a chiral expansion whose coefficients is proportional to $\frac{p_\chi}{\Delta}$. In contrast to $\frac{p_\chi}{\Lambda_\chi}$, the expansion with $\frac{p_\chi}{\Delta}$ has a bad convergence property. It implies that the first terms can not be treated as a good approximation of the contribution of D^*. A numerical analysis shows the contribution of D^* to LECs, i.e. Eq. (7.25), is large and thus implies that its contribution to $D\phi$ scattering is nonnegligible. However a more detailed analysis shows that the contribution of D^* to $D\phi$ scattering at different orders would compensate with each other significantly, which leads to a negligible contribution in total. It is in agreement with the conclusion that the local chiral expansion of the effective potential is not well defined and makes the obtained LECs untrustworthy. Furthermore, in the limit of heavy quark, D and D^* are treated as a spin multiplet. The Lagrangian describing the interaction of $D\phi$ and $D^*\phi$ shares the same form and LECs. Hence in the following sections, we focus on the contribution of resonances to the LECs of the Lagrangian describing the interaction between the multiplet and Goldstone bosons.

7.1.3 Resonance contributions to the LECs

Alternatively, one can evaluate the contribution of resonances to LECs by mathching the amplitudes between with and without resonances explicitly. The resonance-exchange amplitudes, corresponding to the Feynman diagrams in Fig. 7.1, are calculated and their explicit expressions are given for completeness. For a given amplitude, we use capital subscripts, S, T and U, to label the channels and superscripts, D_0^*, V (vector) and S (scalar), to mark which resonance is exchanged. The coefficients appearing in the

amplitudes are listed in Table 7.1.

- D_0^* exchange: ($m = \mathring{M}_{D_0^*}$)

$$\begin{aligned} \mathcal{A}_S^{D_0^*}(s,t,u) &= C_S^{D_0^*} \frac{g_0^2}{F_0^2} \frac{p_1 \cdot p_2 \, p_3 \cdot p_4}{s - m^2} , \\ \mathcal{A}_U^{D_0^*}(s,t,u) &= C_U^{D_0^*} \frac{g_0^2}{F_0^2} \frac{p_1 \cdot p_4 \, p_2 \cdot p_3}{u - m^2} . \end{aligned} \tag{7.26}$$

- Light-flavor vector meson exchange:

$$\mathcal{A}_T^V(s,t,u) = C_T^V \frac{g_{DDV} g_V}{F_0^2} \left\{ \frac{(p_1 - p_3) \cdot p_2 \, (p_1 + p_3) \cdot p_4}{M_V^2 - t} - (p_2 \leftrightarrow p_4) \right\} . \tag{7.27}$$

- Light-flavor scalar meson exchange:

$$\mathcal{A}_T^S(s,t,u) = \frac{2 g_{DDS} \left\{ C_{T,m}^{S8} - C_{T,d}^{S8} \, p_2 \cdot p_4 \right\}}{3 F_0^2 (M_{S8}^2 - t)} + \frac{4 \tilde{g}_{DDS} \left\{ C_{T,m}^{S1} - C_{T,d}^{S1} \, p_2 \cdot p_4 \right\}}{F_0^2 (M_{S1}^2 - t)} . \tag{7.28}$$

Table 7.1: Coefficients for the resonance-exchange amplitudes.

Physical Processes	$C_S^{D_0^*}$	$C_U^{D_0^*}$	C_T^V	$C_{T,m}^{S8}$	$C_{T,d}^{S8}$	$C_{T,m}^{S1}$	$C_{T,d}^{S1}$
$D^0 K^- \to D^0 K^-$	0	2	$\sqrt{2}$	M_K^2	1	M_K^2	1
$D^+ K^+ \to D^+ K^+$	0	0	0	$-2M_K^2$	-2	M_K^2	1
$D^+ \pi^+ \to D^+ \pi^+$	0	2	$\sqrt{2}$	M_π^2	1	M_π^2	1
$D^+ \eta \to D^+ \eta$	$\frac{1}{3}$	$\frac{1}{3}$	0	$\frac{1}{3}(5M_\pi^2 - 8M_K^2)$	-1	M_η^2	1
$D_s^+ K^+ \to D_s^+ K^+$	0	2	$\sqrt{2}$	M_K^2	1	M_K^2	1
$D_s^+ \eta \to D_s^+ \eta$	$\frac{4}{3}$	$\frac{4}{3}$	0	$\frac{2}{3}(8M_K^2 - 5M_\pi^2)$	2	M_η^2	1
$D_s^+ \pi \to D_s^+ \pi$	0	0	0	$-2M_\pi^2$	-2	M_π^2	1
$D^0 \eta \to D^0 \pi^0$	$\sqrt{\frac{1}{3}}$	$\sqrt{\frac{1}{3}}$	0	$\sqrt{3} M_\pi^2$	$\sqrt{3}$	0	0
$D_s^+ K^- \to D^0 \pi^0$	$\sqrt{2}$	0	-1	$\frac{3}{2\sqrt{2}}(M_K^2 + M_\pi^2)$	$\frac{3}{\sqrt{2}}$	0	0
$D_s^+ K^- \to D^0 \eta$	$\sqrt{\frac{2}{3}}$	$-2\sqrt{\frac{2}{3}}$	$-\sqrt{3}$	$\sqrt{\frac{3}{8}}(3M_\pi^2 - 5M_K^2)$	$-\sqrt{\frac{3}{2}}$	0	0

In order to calculate the tree-level resonance-exchange contribution to the LECs, these Born-term amplitudes are expanded in powers of $s - M_0^2$, M_ϕ^2 and t and then compared with the contact term contributions given in Eqs. (5.38) and (5.41). Consequently, the D_0^*-exchange contributions to the LECs

are

$$\begin{aligned} h_5^{D_0^*} &= -\frac{g_0^2}{2\Delta_0^2}\,, \\ g_1^{D_0^*} &= g_2^{D_0^*} = g_3^{D_0^*}\,\Delta_0^2 = -\frac{g_0^2}{8\Delta_0^2}\,, \end{aligned} \tag{7.29}$$

with the difference of the squared masses, $\Delta_0^2 \equiv \overset{\circ}{M}{}_0^{*2} - \overset{\circ}{M}{}_0^2$, where $\overset{\circ}{M}{}_0^*$ is the chiral limit mass of the D_0^*.

The light vector mesons contribute to g_1 and g_2 as follows

$$g_1^V = g_2^V = -\frac{g_{DDV}\,g_V}{2\sqrt{2}\,M_V^2}\,. \tag{7.30}$$

From the above equations, we note that light vector-meson exchange does not contribute to any LEC in the $O(p^2)$ Lagrangian, which is different from the pion-nucleon case in Ref. [162]. This is due to the fact that the Lorentz index of the vector is contracted with the Gamma matrices in the nucleon case, but in our case with those of the derivatives of the D mesons. For a t-channel exchange, this partial derivative contributes as $O(p^1)$. Together with the $O(p^2)$ $V\phi\phi$ vertex the t-channel vector-meson exchange thus starts to contribute at $O(p^3)$.

The light-flavor scalar mesons contribute as

$$\begin{aligned} h_0^S &= -\frac{\tilde{g}_{DDS}\,\tilde{c}_m}{M_{S1}^2} + \frac{g_{DDS}\,c_m}{3M_{S8}^2}\,, \quad h_1^S = -\frac{g_{DDS}\,c_m}{M_{S8}^2}\,, \\ h_2^S &= \frac{\tilde{g}_{DDS}\,\tilde{c}_d}{M_{S1}^2} - \frac{g_{DDS}\,c_d}{3M_{S8}^2}\,, \quad h_3^S = -\frac{g_{DDS}\,c_d}{M_{S8}^2}\,. \end{aligned} \tag{7.31}$$

Here, M_{S1} and M_{S8} denote the masses of singlet and octet scalars, respectively. Without entering the discussion about which values should be used for the light scalar multiplets, we make use of large N_c and set $M_S = M_{S_1} = M_{S_8}$, as done in Ref. [162]. Furthermore, the singlet couplings can be expressed in terms of the octet ones through the relations: $\tilde{c}_{m,d} = c_{m,d}/\sqrt{3}$ and $\tilde{g}_{DDS} = g_{DDS}/\sqrt{3}$. By imposing these large-N_c relations, the above expressions in Eqs. (7.31) are reduced to

$$h_0^S = 0\,, \quad h_1^S = -\frac{g_{DDS}\,c_m}{M_S^2}\,, \quad h_2^S = 0\,, \quad h_3^S = -\frac{g_{DDS}\,c_d}{M_S^2}\,. \tag{7.32}$$

One sees that the LECs h_0 and h_2 receive no contribution from the light scalar mesons in the large-N_c limit. In fact, these two LECs, together with h_4, are of one order higher in the $1/N_c$ expansion in comparison with $h_i (i = 1, 3, 5)$ [107, 108].

As shown in last section, the exchange of light tensor mesons with $J^{PC} = 2^{++}$ contributes only to h_5, which is of the form

$$h_5^T = \frac{g_{DDT} g_T}{M_T^2}\,, \tag{7.33}$$

with g_{DDT} and g_T the coupling constants for D-D-tensor and π-π-tensor vertices, respectively, see Eqs. (7.6) and (7.9).

7.1.4 Numerical results

To obtain numerical estimates for the LECs, we need to know the resonance couplings. However, not all of the involved couplings are really known. Thus, for the measurable ones ($\tilde{g}, g_0, g_V, c_d, c_m$ and g_T), we will extract the values from experimental data, and for the ones in the vertices where not all three particles can on go shell simultaneously (g_{DDV}, g_{DDS} and g_{DDT}), we will take model values for an estimate.

The numerical value of the resonance coupling g_0 can be obtained by calculating the decay width $\Gamma(D_0^* \to D^+\pi^-)$. At LO, we have

$$\Gamma(D_0^* \to D^+\pi^-) = \frac{1}{4\pi}\frac{|g_0^2|}{F_0^2}\frac{\left(m_{D_0^*}\sqrt{M_\pi^2 + |\vec{q}_\pi|^2} - M_\pi^2\right)^2}{m_{D_0^*}^2}, \tag{7.34}$$

with $\vec{q}_\pi$ the pion momentum in the rest frame of the initial particle. Comparing with the empirical value taken from the Particle Data Group [174], we get

$$|g_0| = 0.68 \pm 0.05\,. \tag{7.35}$$

The couplings of the light-flavor resonances to the Goldstone bosons, g_V and $c_{m,d}$, have been used in many studies of the chiral resonance Lagrangian, and we take the updated determinations in Ref. [175]

$$\begin{aligned} |g_V| &= 0.0846 \pm 0.0008\,, \\ |c_m| &= (80 \pm 21)\ \text{MeV}\,, \\ |c_d| &= (26 \pm 7)\ \text{MeV}\,. \end{aligned} \tag{7.36}$$

From the decay width of the $f_2(1270) \to \pi\pi$ [174], we get $|g_T| = 28$ MeV. Note that, as discussed in Ref. [162], if the πN LEC c_1 is completely saturated by scalar exchange, a positive c_m is demanded. Together with the constraint $4c_m c_d = F_0^2$, see e.g. Ref. [176], we will set $c_{m,d} > 0$ in the following.

For the troublesome couplings, we take the following values:

$$\begin{aligned} g_{DDV} &= 1.46\,, \\ g_{DDS} &= 5058\ \text{MeV}\,, \\ g_{DDT} &= 3.9 \times 10^{-3}\ \text{MeV}^{-1}\,, \end{aligned} \tag{7.37}$$

The value of g_{DDV} is taken from the analysis of the DDV vertex using light-cone QCD sum rules [177]. For the g_{DDS}, we have utilized the large-N_c relation $g_{DDS} = \sqrt{3}\tilde{g}_{DDS}$, and take the value $g_{DD\sigma}$ used in Ref. [178], which was extracted from the parity doubling model of Ref. [179], for $\tilde{g}_{DDS}$. There is no available modeling of g_{DDT}, and we thus estimate it using QCD sum rules in Appendix C. The problem is that it is hard to quantify the uncertainty of these parameters. Yet, there is evidence that these model values are of the right order: the dimensionless values for g_{DDV}, $g_{DDS}/\Lambda_{\text{had}} \sim 5$ and $g_{DDT}\Lambda_{\text{had}} \sim 4$, where $\Lambda_{\text{had}} = O(1\ \text{GeV})$ is a typical hadronic scale, have more or less natural sizes of $O(1)$.

For the masses involved in our numerical estimate, we take

$$\begin{aligned} \overset{\circ}{M} &\cong \overline{M}_D = \frac{1}{2}(M_D^{\text{phy.}} + M_{D_s}^{\text{phy.}}) = 1918\ \text{MeV}\,, \\ \overset{\circ}{M}_0^* &\cong \overline{M}_{D_0^*} = \frac{1}{2}(M_{D_0^*}^{\text{phy.}} + M_{D_{s0}^*}^{\text{phy.}}) = 2318\ \text{MeV}\,, \\ M_V &= 764\ \text{MeV}\,, \quad M_S = 980\ \text{MeV}\,, \quad M_T = 1270\ \text{MeV}\,, \end{aligned} \tag{7.38}$$

Table 7.2: Estimates of the resonance contributions to the LECs. Here $h_{0,2,4}$, which vanish in the large-N_c limit, are not shown. The columns starting with D_0^*, V, S and T list the contributions from the exchange of the scalar charmed mesons, light-flavor vector, scalar and tensor mesons, respectively. The last column sums over all these contributions.

LEC	D_0^*	V	S	T	Total
h_1	0	0	0.4	0	0.4
h_3	0	0	0.1	0	2.3
h_5 [GeV^{-2}]	-0.1	0	0	± 0.1	$[-0.5, -0.3]$
g_1 [GeV^{-2}]	-0.03	∓ 0.07	0	0	$[-0.04, 0.1]$
g_2 [GeV^{-2}]	-0.03	∓ 0.07	0	0	$[-0.04, 0.1]$
g_3 [GeV^{-4}]	0.02	0	0	0	0.02

where the chiral limit masses are identified with the corresponding averaged physical masses, which is acceptable given the accuracy we are aiming at. To be consistent with using the values of g_V and $c_{m,d}$ given above, the values for M_V and M_S are also taken from Ref. [175]. The mass for the tensor multiplet is chosen to be the mass of $f_2(1270)$ following Ref. [173].

With the resonance couplings and masses specified above, we are now in the position to estimate the resonance contributions to the LECs based on the analytical expressions, Eqs. (7.29-7.33). The numerical results are shown in Table 7.2 and the sum of various contributions is given in the last column. Because of the poor knowledge on the values of the off-shell couplings $g_{DDV,DDS,DDT}$, no reasonable error estimate can be made here. Furthermore, the signs of $g_{V,T}$ are not fixed, hence contributions from the t-channel exchanges of the light-flavor vector and tensor mesons might be either positive or negative as listed in Table 7.2, and they also take two possible values in the last column of the table due to interference with the contribution from the scalar charmed mesons.

7.1.5 Comparison with results from unitarized ChPT (UChPT)

We compare the estimates of the LECs with those from fits to the lattice data on of scattering lengths of some selected channels at the NLO and NNLO in the framework of UChPT [90] (and references therein) in Table 7.3 and Table 7.4, respectively, where the definitions of the combinations of the LECs are given in Eq. (5.76 and 5.77).[3] The following observations can be made:

(i) Provided that a positive value of c_m is chosen, h_1 is saturated by the light scalar exchange, which is similar to the LEC c_1 in the πN case [162]. The value of h_1 is fixed through the mass difference between strange and nonstrange charmed mesons, which is then adopted in these fits. One sees that

[3] The notations of the LECs adopted in Ref. [122] are connected to ours by $h_0 = 2c_0$, $h_1 = -2c_1$,

$$h_{24} = 2\left[c_{24} + 2c_4(1 - \frac{\bar{M}_D^2}{m_P^2})\right] \text{ , } h_{35} = -2\left[c_{35} + 2c_5(1 - \frac{\bar{M}_D^2}{m_P^2})\right] \text{ , } h_4' = -4c_4\frac{\bar{M}_D^2}{m_P^2} \text{ , } h_5' = 2c_5\frac{\bar{M}_D^2}{m_P^2} \text{ ,}$$

with $m_P = 1.9721$ GeV specified in Ref. [122] and $\bar{M}_D = (M_D^{\rm phy} + M_{D_s}^{\rm phy})/2$.

Table 7.3: Comparison of the values of the LECs from the estimate using resonances with those from fits to lattice data in various formulations of unitarized ChPT at NLO. The LECs in this table are dimensionless.

LEC	Table V [29]	Table VIII [29]	HQS [122]	χ-SU(3) [122]	Resonance
h_0	0.01	0.01	0.03	0.03	0
h_1	0.42	0.42	0.43	0.43	0.4
h_{24}	$-0.10^{+0.05}_{-0.06}$	$0.10^{+0.05}_{-0.06}$	-0.12 ± 0.05	-0.14 ± 0.04	0
h_{35}	$0.25^{+0.13}_{-0.13}$	$0.26^{+0.09}_{-0.10}$	0.23 ± 0.09	0.12 ± 0.08	$[-1.4, 0.1]$
h'_4	$-0.32^{+0.35}_{-0.34}$	$-0.30^{+0.31}_{-0.28}$	-0.20 ± 0.31	-0.83 ± 0.30	0
h'_5	$-1.88^{+0.63}_{-0.61}$	$-1.94^{+0.46}_{-0.38}$	-1.82 ± 0.57	-1.00 ± 0.40	$[-0.7, 0]$

the estimate here is in a good agreement with the empirical value. The agreement in turn might indicate that the model estimate for g_{DDS} is reasonable.

(ii) Because we only have the absolute values for g_V and g_T, one sees that the estimates from exchanging resonances are roughly consistent with those determined from the various NLO UChPT fits, while there are tensions when comparing with those from the NNLO UChPT fits in Ref. [65]. While there are quite a few fit parameters at NNLO, not many lattice data exist. On the one hand, more lattice calculations on observables for the scattering processes between heavy mesons and light mesons would be welcome to better pin down the LECs at NNLO. On the other hand, as pointed out in Ref. [159], the values of the LECs, which are scale-dependent in general, are dominated by the resonances only when the renormalization scale μ is not too far away from the resonance region. The NLO fit results are obtained with $\mu = 1$ GeV, i.e. the scale appearing in the subtraction constant $a(\mu)$, which is around the masses of the light vector and scalar resonances. However, the NNLO fit results in Ref. [65] are obtained by setting $\mu = \bar{M}_D = 1.92$ GeV for convenience. Note that the scale-dependence of the NNLO LECs stems both from the renormalization of the one-loop amplitude using EOMS scheme and the unitarization procedure accompanied by the subtraction constant $a(\mu)$.

7.2 Positivity constraints on the $D\phi$ interactions

In this section, positivity constraints on the $D\phi$ interactions will be derived by using basic axiomatic principles of S-Matrix theory, such as unitarity, analyticity and crossing symmetry. Such constraints are important in the sense that model-independent information for the $D\phi$ interactions is provided. When employed in ChPT, they are translated into a much more practical form, i.e. positivity bounds on the LECs. In general, these involved LECs are unknown and not fixed by chiral symmetry. Furthermore, the number of the LECs increases when going to higher orders. Therefore, such bounds are of great use, especially for those which can not be measured directly in experiments such as the $D\phi$ interactions

Table 7.4: Comparison of the values of the LECs from the estimate using resonances with those from various fits to lattice data in unitarized ChPT at NNLO.

LEC	UχPT-6a [65]	UχPT-6b [65]	UχPT-6a' [65]	UχPT-6b' [65]	Resonance
h_0	0.02	0.02	0.02	0.02	0
h_1	0.43	0.43	0.43	0.43	0.4
h_{24}	$0.79^{+0.10}_{-0.09}$	$0.76^{+0.10}_{-0.09}$	$0.83^{+0.11}_{-0.10}$	$0.80^{+0.10}_{-0.10}$	0
h_{35}	$0.73^{+0.50}_{-0.38}$	$0.81^{+0.95}_{-0.62}$	$0.43^{+0.23}_{-0.23}$	$0.40^{+0.33}_{-0.29}$	$[-1.4, 0.1]$
h'_4	$-1.49^{+0.55}_{-0.57}$	$-1.56^{+0.61}_{-0.65}$	$-1.33^{+0.60}_{-0.60}$	$-1.72^{+0.64}_{-0.63}$	0
h'_5	$-11.47^{+2.24}_{-2.79}$	$-15.38^{+4.81}_{-7.20}$	$-4.25^{+0.65}_{-0.66}$	$-2.60^{+0.84}_{-0.87}$	$[-0.7, 0]$
g'_1 [GeV^{-1}]	$-1.66^{+0.31}_{-1.59}$	$-2.44^{+0.57}_{-0.64}$	$-1.10^{+0.18}_{-0.23}$	$-1.90^{+0.58}_{-0.35}$	$[-0.2, -0.1]$
g_{23} [GeV^{-1}]	$-1.24^{+0.28}_{-1.51}$	$-2.00^{+0.52}_{-0.51}$	$-0.70^{+0.19}_{-0.24}$	$-1.48^{+0.61}_{-0.37}$	$[-0.5, -0.2]$
g'_3 [GeV^{-1}]	$2.12^{+0.55}_{-0.45}$	$2.85^{+1.41}_{-0.96}$	$0.98^{+0.15}_{-0.14}$	$0.58^{+0.20}_{-0.19}$	0.14

under consideration. In what follows, details on the derivation of these constraints as well as practical applications of the bounds on the $D\phi$ interactions will be presented.

7.2.1 Positivity constraints implied by dispersion relations

For elastic $D\phi$ scattering, the Mandelstam triangle is the region bounded by $s = (M_D + M_\phi)^2$, $u = (M_D + M_\phi)^2$ and $t = 4M_\phi^2$ in the Mandelstam plane as displayed in Fig. 5.1. Inside the Mandelstam triangle, the scattering amplitude is analytic and real, see e.g. Ref. [180] for an early application in the context baryon ChPT. Following Refs. [165, 169], we restrict ourselves to the upper part of the Mandelstam triangle with $t \geq 0$. Using unitarity, analyticity and crossing symmetry, an n-time subtracted fixed-t dispersion relation for the elastic $D\phi$ scattering amplitude with definite (S, I) can be written as

$$\frac{\mathrm{d}^n}{\mathrm{d}s^n}\mathcal{M}^{(S,I)}_{D\phi\to D\phi}(s,t) = \frac{n!}{\pi}\int_{(M_D+M_\phi)^2}^{+\infty}\mathrm{d}x'\left[\delta^{II'}\frac{\mathrm{Im}\,\mathcal{M}^{(S,I')}_{D\phi\to D\phi}(x'+i\epsilon,t)}{(x'-s)^{n+1}} + (-1)^n C^{II'}_{us}\frac{\mathrm{Im}\,\mathcal{M}^{(S,I')}_{D\bar{\phi}\to D\bar{\phi}}(x'+i\epsilon,t)}{(x'-u)^{n+1}}\right], \tag{7.39}$$

where $\bar{\phi}$ denotes the antiparticle of ϕ, and $C^{II'}_{us}$ represents the u-s crossing matrix which is defined as

$$\mathcal{A}^I(u,t,s) = C^{II'}_{us}\mathcal{A}^{I'}(s,t,u), \tag{7.40}$$

where we have written explicitly all of the three Mandelstam variables so as to make the u-s crossing explicit, and C_{su} is defined by exchanging the s- and u-channel amplitudes in the above equation. The matrices satisfy $C^{II'}_{us}C^{I'J}_{su} = \delta^{IJ}$. We want to mention that the imaginary part of $\mathcal{M}$ is positive definite

above threshold.[4] Besides, we have assumed that all the processes involved in the dispersion relation are single-channel interactions such that the integration starts at the corresponding thresholds. The case with multi-channel interactions will be discussed later. Both imaginary parts in the brackets in Eq. (7.39) are positive definite when x' is above threshold, i.e. $x' > (M_D + M_\phi)^2$.[5] In addition, the s-channel coefficient $\delta^{II'}$ is always non-negative. However, the u-channel one $(-1)^n C_{us}^{II'}$ is sometimes not. The aim is therefore to construct certain combinations of the $D\phi$ amplitudes with different isospins such that

$$\frac{\mathrm{d}^n}{\mathrm{d}s^n}\left[\alpha^I \mathcal{M}^{(S,I)}_{D\phi\to D\phi}(s,t)\right] \geq 0\,. \tag{7.41}$$

where summation over I is assumed. In combination with Eq. (7.39), a sufficient condition for the above positivity condition to hold is given by

$$\alpha^I \delta^{II'} \geq 0\,, \quad \alpha^I C_{us}^{II'} \geq 0 \text{ (for even } n)\,. \tag{7.42}$$

For the multi-channel case, all the cuts from the coupled channels need to be taken into account, and the integration should start from the lowest threshold. Taking the process $DK \to DK$ as an example, the integration in the $(S,I) = (1,1)$ channel will start at the $D_s\pi$ threshold rather than its physical DK threshold. Since the imaginary part $\mathrm{Im}\, T^{(1,1)}_{DK\to DK}(x' + i\epsilon, t)$ could be negative in the region $x' \in \left[(M_{D_s} + M_\pi)^2, (M_D + M_K)^2\right]$, the positivity condition in Eq. (7.41) is not applicable any more. However, as discussed in Ref. [166], in the multi-channel case, the positivity conditions hold for processes of the type $a + b \to a + b$ such that $m_a + m_b$ is the lightest threshold for both the s- and u-channels. This statement is obtained from the condition that the dispersion relation in Eq. (7.39) is true and that $t \geq 0$ which ensures the positivity of the Legendre polynomials for all partial waves. For details we refer to Section IV in Ref. [166]. With this statement, amongst all the $D\phi$ scattering channels, only $D\pi \to D\pi$ and $D_s\pi \to D_s\pi$ survive.

In order to derive positivity constraints on the $D\pi \to D\pi$ and $D_s\pi \to D_s\pi$ scattering amplitudes, we need to know the explicit forms of the u-s crossing matrices for these two processes, which are

$$C_{us} = \begin{pmatrix} -\frac{1}{3} & \frac{4}{3} \\ \frac{2}{3} & \frac{1}{3} \end{pmatrix}\,, \quad \text{for } D\pi \to D\pi\,, \quad \text{and} \quad C_{us} = 1\,, \quad \text{for } D_s\pi \to D_s\pi\,. \tag{7.43}$$

For the $D\pi$ case, the matrix is arranged such that the first channel refers to $I = 1/2$ and the second to $I = 3/2$. From now on, we will focus on the $n = 2$ case, which is the minimal number of subtractions in the dispersion integral required by the Froissart bound [181].

For $D\pi \to D\pi$, the upper-part of the Mandelstam triangle is $\mathcal{R}_{D\pi} = \{(s,t)|s \leq (M_D + M_\pi)^2, s + t \geq (M_D - M_\pi)^2, 0 \leq t \leq 4M_\pi^2\}$. When $(s,t) \in \mathcal{R}_{D\pi}$, a sufficient condition for $\frac{\mathrm{d}^2}{\mathrm{d}s^2}\left\{\alpha^I \mathcal{M}^I_{D\pi\to D\pi}(s,t)\right\} \geq 0$ is given by $2\alpha^{3/2} \geq \alpha^{1/2} \geq 0$. We choose the following three combinations of $\alpha^{1/2}$ and $\alpha^{3/2}$ to get bounds on three physical scattering amplitudes:

$$\begin{cases} \alpha^{1/2} = 0\,, \alpha^{3/2} = 1 \;: & -\frac{\mathrm{d}^2}{\mathrm{d}s^2}\mathcal{A}_{D^+\pi^+\to D^+\pi^+}(s,t) \geq 0\,, \\ \alpha^{1/2} = \frac{2}{3}\,, \alpha^{3/2} = \frac{1}{3} \;: & -\frac{\mathrm{d}^2}{\mathrm{d}s^2}\mathcal{A}_{D^0\pi^+\to D^0\pi^+}(s,t) \geq 0\,, \\ \alpha^{1/2} = \frac{1}{3}\,, \alpha^{3/2} = \frac{2}{3} \;: & -\frac{\mathrm{d}^2}{\mathrm{d}s^2}\mathcal{A}_{D^+\pi^0\to D^+\pi^0}(s,t) \geq 0\,, \end{cases} \tag{7.44}$$

[4] Here, we follow the convention $S = \mathbf{1} + i(2\pi)^4\delta^{(4)}(\sum_i p_i - \sum_f p_f)\mathcal{M}$, to define the scattering amplitude $\mathcal{M}(s,t)$.

[5] Since for each partial wave ℓ, $\mathrm{Im}\,\mathcal{M}_\ell(s) = \frac{2|\vec{k}|}{\sqrt{s}}|\mathcal{M}_\ell(s)|^2 \geq 0$ above threshold and the Legendre polynomials $P_\ell(\cos\theta) \geq 0$ for $t \geq 0$ (or equivalently $\cos\theta \geq 1$), one has $\mathrm{Im}\,\mathcal{M}^{(S,I)}(s,t) = \sum_{\ell=0}^{\infty}(2\ell+1)\,P_\ell(t)\,\mathrm{Im}\mathcal{M}^{(S,I)}_\ell(s) \geq 0$.

with $\mathcal{A} = -\mathcal{M}$.

For $D_s\pi \to D_s\pi$, the upper-part of the Mandelstam triangle is $\mathcal{R}_{D_s\pi} = \{(s,t)|s \leq (M_{D_s} + M_\pi)^2, s + t \geq (M_{D_s} - M_\pi)^2, 0 \leq t \leq 4M_\pi^2\}$. When $(s,t) \in \mathcal{R}_{D_s\pi}$, a sufficient condition for $\frac{\mathrm{d}^2}{\mathrm{d}s^2}\left\{\alpha^I \mathcal{M}^I_{D_s\pi\to D_s\pi}(s,t)\right\} \geq 0$ is $\alpha^1 \geq 0$. Choosing $\alpha^1 = 1$, one has

$$-\frac{\mathrm{d}^2}{\mathrm{d}s^2}\mathcal{A}_{D_s^+\pi^+\to D_s^+\pi^+}(s,t) \geq 0\,. \tag{7.45}$$

In the above, we have written the constraints in terms of the scattering amplitudes which are either explicitly given in Chapter 5 or easily obtainable by using crossing symmetry and isospin symmetry. Hence their analytical expressions up to NNLO are all known and can be inserted into the above inequalities to obtain bounds on the LECs, which will be discussed in the next section.

7.2.2 Positivity bounds on the LECs

The representation of the $D\phi$ scattering amplitudes in the manifestly Lorentz covariant framework obtained in Chapter 5 is suitable to obtain reliable bounds on the LECs, since it possesses the correct analytic behavior inside the Mandelstam triangle. In the covariant formalism for the $SU(3)$ case, the NLO (tree-level) $D\phi$ amplitudes were first given by Ref. [28] and then followed by Refs. [29, 121, 122]. These amplitudes can be employed to derive positivity bounds on the LECs with the help of the inequalities given in Eq. (7.44) and Eq. (7.45). Note that, throughout this work, we follow the notations of Ref. [29], and the results from other works with different notations can be easily adopted to ours.

Bounds up to $O(p^2)$

Inserting the amplitudes up to NLO into Eqs. (7.44) and (7.45), the constraints on the scattering amplitudes turn into bounds on the LECs h_4 and h_5. Each inequality leads to one bound on the LECs. The intersection of all of the obtained bounds has a simple form

$$\begin{cases} h_4 - h_5 \geq 0 \\ h_4 \geq 0 \end{cases}, \qquad \text{or equivalently} \qquad \begin{cases} h_4' - h_5' \geq 0 \\ h_4' \geq 0 \end{cases}. \tag{7.46}$$

Here, the parameters h_4 and h_5 are in units of GeV^{-2}, while h_4' and h_5' are dimensionless. The region restricted by the bounds on h_4' and h_5' in Eq. (7.46) is depicted as the light yellow area in Fig. 7.2. Two different sets of fitting values from Refs. [29, 122] which resum the NLO scattering amplitudes in different ways are shown for comparison:[6]

(i) The first set is taken from Ref. [29]. There are two different fits: one with 5 parameters which are four LECs and one subtraction constant used to regularize the loop integral (cf. Table V therein), and the other with 4 parameters with the subtraction constant fixed from reproducing the $D_{s0}^*(2317)$ mass in the $(S,I) = (1,0)$ channel (cf. Table VIII therein). The 1-σ regions, with the parameter correlations in the fits taken into account, from these two fits for the values for h_4' and h_5' are shown by the regions surrounded by the green dot-dashed line (for the 5-parameters fit) and by magenta dashed line (for the 4-parameter fit).

[6] The results in Ref. [121] are not taken into consideration, since the preliminary lattice data [98], which are different from the final ones in Ref. [29], are used to perform fits there.

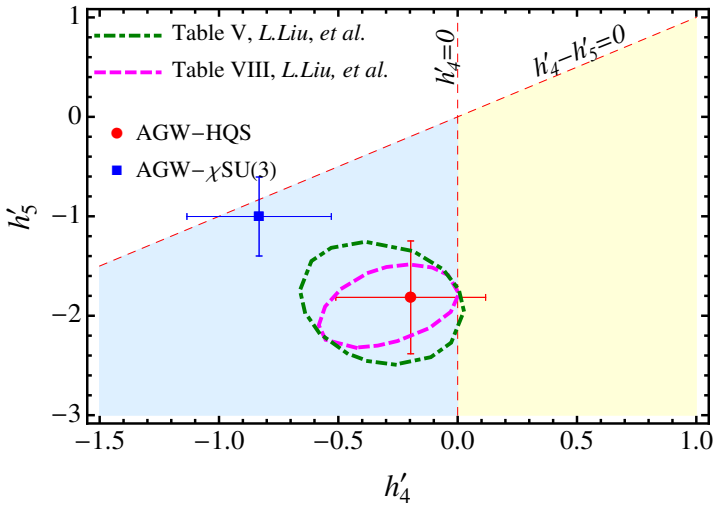

Figure 7.2: Comparison of the NLO positivity bounds for h_4' and h_5' with their values obtained from fitting to the lattice data using unitarized ChPT at NLO. The positivity-bound region is depicted in light yellow bounded by the lines $h_4' = 0$ and $h_4' - h_5' = 0$. The area in light blue denotes the region where the bound $h_4' - h_5' \geq 0$ is respected while $h_4' \geq 0$ is violated. The green dot-dashed and magenta dashed ellipses represent the 1-σ regions for h_4' and h_5' from the 5- and 4-parameter fits in Ref. [29], respectively. The red dot and blue square with error bars, denoted by AGW-HQS and AGW-χSU(3), respectively, are taken from Ref. [122].

(ii) The second set is taken from Ref. [122]. In that work, a special renormalization scheme is proposed to deal with the so-called power counting breaking terms appearing in the loop functions. In Fig. 7.2, the blue square and red dot represent the fit values taken from χ-SU(3) fit and HQS fit, which correspond to different regularizations of the scalar two-point scalar loop integral, in Ref. [122], respectively.

As can be seen from Fig. 7.2, the fit values from Ref. [29] are only marginally consistent with the region allowed by the bounds. The LEC values from the HQS fit in Ref. [122] has a small overlap with the positivity bound, while the ones from the χ-SU(3) fit are completely outside the region derived from positivity.

Bounds up to $O(p^3)$

Inserting the $D\phi$ amplitudes up to NNLO into the positivity constraints in Eqs. (7.44) and (7.45), one gets bounds on the LECs at the NNLO level, which are

$$\begin{cases} h_4 - h_5 - 24M_D\,\nu_D\,g_3 \geq f^{(2)}_{D^+\pi^+\to D^+\pi^+}(s,t), & (s,t)\in\mathcal{R}_{D\pi}\,, \\ h_4 - h_5 + 24M_D\,\nu_D\,g_3 \geq f^{(2)}_{D^0\pi^+\to D^0\pi^+}(s,t), & (s,t)\in\mathcal{R}_{D\pi}\,, \\ h_4 - h_5 \geq f^{(2)}_{D^+\pi^0\to D^+\pi^0}(s,t), & (s,t)\in\mathcal{R}_{D\pi}\,, \\ h_4 \geq f^{(2)}_{D_s^+\pi^+\to D_s^+\pi^+}(s,t), & (s,t)\in\mathcal{R}_{D_s\pi}\,, \end{cases} \tag{7.47}$$

where

$$\nu_D \equiv \frac{s-u}{4M_D}, \qquad \text{and} \quad f^{(2)}_{\text{process}}(s,t) \equiv \frac{F_\pi^2}{2}\frac{d^2}{ds^2}\mathcal{A}^{\text{loop}}_{\text{process}}(s,t).$$

Each bound would become more stringent if one always sets $f^{(2)}_{\text{process}}(s,t)$ at its maximum inside $\mathcal{R}_{D\pi}$ (or $\mathcal{R}_{D_s\pi}$). Numerically, we find

$$\begin{aligned}&\max\{f^{(2)}_{D^+\pi^+\to D^+\pi^+}(s,t)\} = \max\{f^{(2)}_{D^0\pi^+\to D^0\pi^+}(s,t)\} = 0.34,\\ &\max\{f^{(2)}_{D^+\pi^0\to D^+\pi^0}(s,t)\} = 0.28\end{aligned} \tag{7.48}$$

in the region $(s,t)\in\mathcal{R}_{D\pi}$, and

$$\max\{f^{(2)}_{D_s^+\pi^+\to D_s^+\pi^+}(s,t)\} = 0.15 \tag{7.49}$$

in the region $(s,t)\in\mathcal{R}_{D_s\pi}$. By further using the condition $|\nu_D| \le \nu_D^{\text{th}}(t) = M_\pi + t/(4M_D) \le M_\pi + M_\pi^2/M_D$, one finally obtains the following bounds

$$\begin{cases} h_4' - h_5' - 24|g_3'|(M_D+M_\pi)M_\pi/\bar{M}_D \ge 1.25\,, \\ h_4' \ge 0.55\,, \end{cases} \tag{7.50}$$

which are expressed in terms of h_4', h_5' and g_3'. Comparing with the $O(p^2)$ bounds given in Eq. (7.46), the $O(p^3)$ bounds are much more stringent.

In order to compare the values of h_4' and h_5' from the fits to the lattice data using unitarized ChPT at NNLO with these bounds, we choose to fix g_3' at three typical values: the central and the two extremes within the 1-σ region of each fit. For convenience, we define a function of g_3', $g(g_3') \equiv 1.25 + 24|g_3'|(M_D+M_\pi)M_\pi/\bar{M}_D$, and rewrite the bounds in Eq. (7.50) as

$$\begin{cases} h_4' - h_5' \ge g(g_3')\,, \\ h_4' \ge 0.55\,. \end{cases} \tag{7.51}$$

Notice that the bounds depend on the renormalization scale μ since the loop contributions $f^{(2)}_{\text{process}}(s,t)$ are involved. The NNLO bounds in Eq. (7.50) and Eq. (7.51) are obtained by setting $\mu = \bar{M}_D$ in accordance with Ref. [65]. The comparison is shown in Fig. 7.3. The bounds displayed in the graphs in the first, second and third column correspond to taking the central, the lowest and the largest value in each fit for g_3', respectively. As seen from the plots, no fit completely obeys the bounds. For UChPT-6(a) and UChPT-6(b), the fit values are consistent with the first bound in Eq. (7.50) while they violate the second one, i.e., the one restricting h_4' only. Both bounds are violated in the fits for UChPT-6(a') and UChPT-6(b'), which are the ones with a prior, which requires all of the LECs (made dimensionless) to be take natural values of order $O(1)$.

These comparisons, however, have to be interpreted with caution. The positivity bounds in Eq. (7.46) and (7.50) were derived using the perturbative scattering amplitudes, while the fits in Ref. [29, 65, 122] were performed using resummed amplitudes with perturbative kernels. The resummed amplitudes using various unitarization approaches in the literature break the crossing symmetry, which, however, is one of the main components in deriving the positivity bounds through dispersion relations. It is thus not surprising that the LECs determined in the UChPT fits do not respect the positivity bounds. Nevertheless, we notice that all of these fits prefer a negative value for h_4 while the positivity bound requires it to be positive.

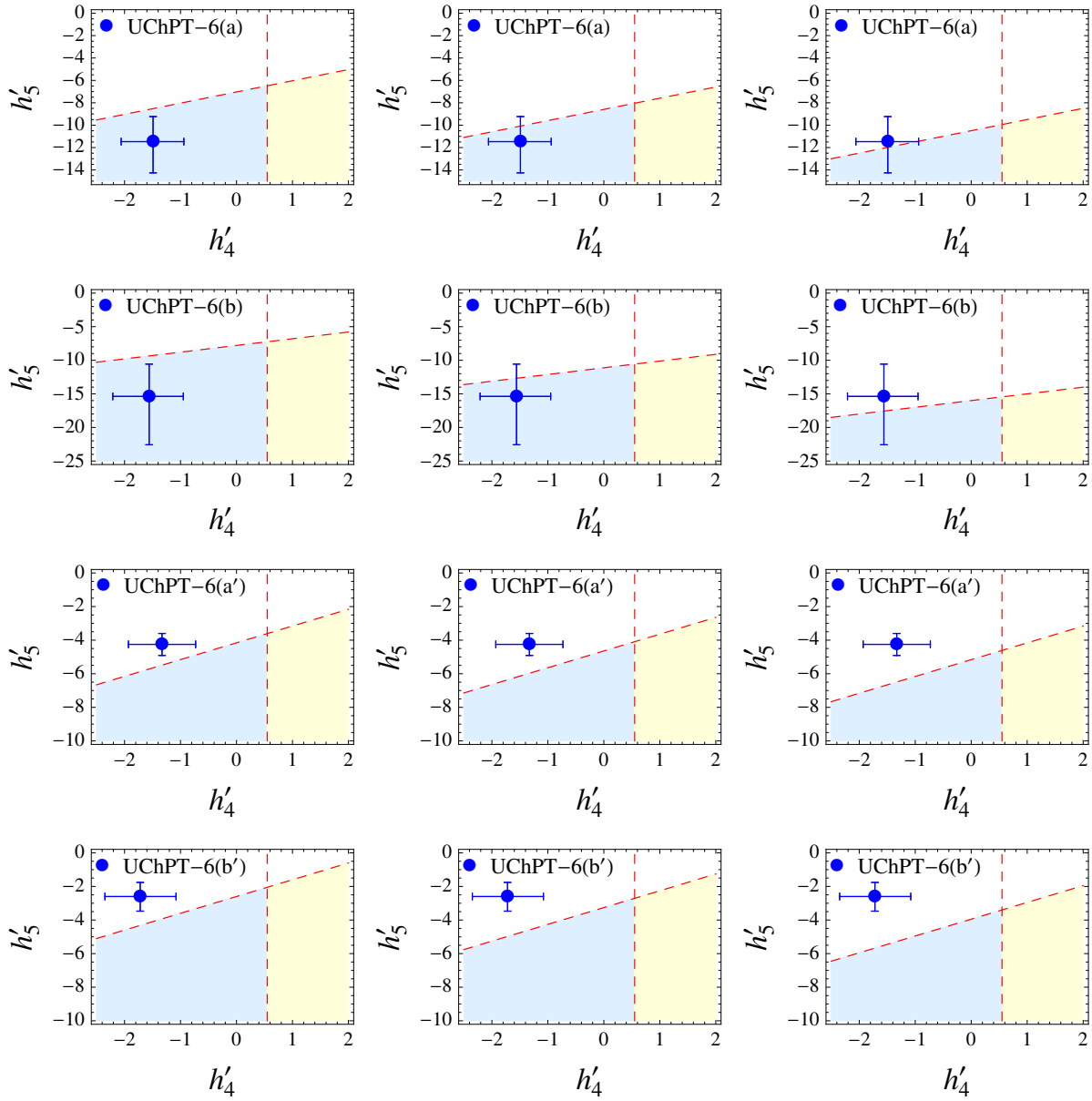

Figure 7.3: Comparison of the positivity bounds for h_4' and h_5' with their 6-channel NNLO fit values. The graphs in the first, second and third column correspond to the case that g_3' is fixed at its lowest, central and largest value, respectively. The blue dots with error bars represent the fitting values of h_4' and h_5' from different fits: UChPT-6(a), UChPT-6(b), UChPT-6(a') and UChPT-6(b'), see Ref. [65]. The NNLO positivity-bound region is in light yellow bounded by the lines $h_4' = 0.55$ and $h_4' - h_5' = g(g_3')$. The area in light blue denotes the region where the bound $h_4' - h_5' \geq g(g_3')$ is respected while $h_4' \geq 0.55$ is violated.

CHAPTER 8

Summary

In this thesis we have investigated the interactions between charmed pseudoscalar mesons D and Goldstone bosons ϕ within the framework of chiral perturbation theory (ChPT) to third chiral order in a manifestly Lorentz-invariant form.

After constructing the chiral Lagrangian for spinless matter fields living in a fundamental $SU(N)$ representation, we have given the explicit generating functional for Green functions of at most four external fields up to $O(p^3)$, i.e. the leading one-loop order, in Chapter 4. The associated loops bring ultraviolet (UV) divergences to the theory, which need to be renormalized. To remove the UV divergences we have employed the heat kernel techniques to extract the terms with a pole at $d = 4$, which correspond to the UV divergences in dimensional regularization. Then those UV divergences are absorbed by the counter terms, i.e. the low-energy constants (LECs), in both the $O(p^2)$ and $O(p^3)$ Lagrangians. Besides the UV divergences, the loops also lead to the existence of the so-called power counting breaking (PCB) terms due to the inclusion of the new scale, the nonvanishing mass of the matter fields. We have derived the PCB terms in the one-loop effective generating functional in the extended-on-mass-shell (EOMS) scheme at the Lagrangian level. They are absorbed into a redefinition of the $O(p^2)$ LECs. After removing the UV divergences and PCB terms, we have obtained a covariant chiral effective generating functional free of UV divergences and PCB terms up to the next-to-next leading order (NNLO). The framework can be used for any theories with spontaneous symmetry breaking of $SU(N)_L \times SU(R)_R$ to $SU(N)_V$ with spinless matter fields in the fundamental representation. Examples in QCD of the matter fields are ground state pseudoscalar mesons except for the pions such as kaons[1] and heavy mesons.

In Chapter 5 we have investigated the D-ϕ scattering with the amplitudes obtained in Chapter 4 by setting $N = 3$ and treating the charmed pseudoscalar mesons as the matter fields. The complete analytical expressions for the amplitudes and the redefinition of LECs to remove UV divergences and PCB terms are given explicitly. In order to describe the S-wave scattering lengths at unphysically high pion masses and to study the possible dynamically generated resonances that are absent in the Lagrangian, e.g. the $D_{s0}^*(2317)$, at relatively high energies, which is a nonperturbative effect, two different unitarization procedures are employed. Since the lattice simulations are performed with fixed charm and strange quark masses with varying up and down quark masses, we have derived the corresponding pion mass dependences of the scattering lengths by extrapolation of the involved masses and the pion decay constant. In order to determine the LECs, we have performed fits to scattering lengths in a few channels computed in lattice QCD at various unphysical pion masses. We tried different fitting procedures with and without a naturalness constraint. It turns out that the absolute value of h_5' could be quite large if the naturalness constraint is not enforced. We want to stress that more lattice simulations in different channels are

[1] If this is fixed at its physical value.

necessary for a better determination of the involved LECs and a better understanding of the scalar and axial-vector charmed mesons. When the LECs are well constrained, we can make reliable predictions in the channels which have not been calculated on the lattice and in the bottom sector utilizing heavy quark flavor or spin symmetry.

In addition, we also investigated possible dynamically generated resonances using the unitarized scattering amplitudes by analytic continuation. It is worth noticing that a pair of poles with nonvanishing imaginary parts are found on the physical Riemann sheet in the coupled-channel $(S, I) = (0, 1/2)$ amplitude, which are at odds with causality. The issue is caused by the coupled-channel left-hand cut, which is not taken into account in the unitarization procedure we used. It may be avoided by using a single-channel potential if we only focus on the region near the $D\pi$ threshold. In the end, we studied the trajectories of the poles corresponding to the $D_{s0}^*(2317)$ and a resonance in the $(S, I) = (0, 1/2)$ channel with varying the pion mass. They exhibit similar behaviors as in the NLO case given by Ref. [115]. To summarize, the LECs are badly determined due to the scarcity of available data. Thus to come to firmer conclusions, more lattice data are required, as also concluded from investigations based on the resonance-exchange model and S-matrix properties in Chapter 7.

In Chapter 6, contributions from vector charmed mesons D^* were included explicitly in order to quantify their influences on the S-wave scattering lengths. We have calculated the potential for the scattering of Goldstone bosons off pseudoscalar charmed mesons including the vector charmed mesons as explicit degrees of freedom up to the NNLO in a framework of covariant ChPT. We have explicitly shown that the UV divergences and PCB terms from one-loop potentials are absorbed by a redefinition of the LECs, collected in Appendix B. For an easy comparison to the previous case without including D^* explicitly, we have used a similar fit procedure as in Chapter 5. In order to access the importance of the contribution of D^*, a selection of the diagrams which survives in the limit of heavy quark is used to fit to the lattice data. It turns out that the influence of D^* to the S-wave scattering lengths is marginal in the heavy quark limit. A complete calculation including the D^* is given subsequently to evaluate the full contribution of D^*. The numerical fit implies that the full influence of D^* is marginal and it is a good approximation to exclude them in the calculation.

Due to the large number of LECs and the scarcity of available data, the reliability of the LECs determined in Chapters 5 and 6 needs to be further analyzed. In Chapter 7 we have estimated the LECs in the NLO and NNLO chiral Lagrangian for the $D\phi$ interaction using resonance saturation. These LECs receive contributions from exchanging the scalar charmed mesons, the light-flavor vector, scalar and tensor mesons. We found that h_1 is entirely saturated by the light scalar-meson exchange. The resulting estimates are consistent with the NLO UChPT fitting results in Refs. [29, 122], while sizeable deviation from the determinations with the NNLO UChPT, see Chapter 5, are found.

In parallel, with the help of axiomatic S-matrix principles, such as unitarity, analyticity and crossing symmetry, we derived positivity constraints on the $D\pi$ and $D_s\pi$ scattering amplitudes in upper parts of Mandelstam triangles, $\mathcal{R}_{D\pi}$ and $\mathcal{R}_{D_s\pi}$, respectively. In combination with the corresponding scattering amplitudes calculated in ChPT using the EOMS scheme, the constraints are then translated into a set of bounds on the LECs. At order $O(p^2)$, the bounds are independent of the Mandelstam variables s, t and hence have unique forms throughout $\mathcal{R}_{D\pi}$ or $\mathcal{R}_{D_s\pi}$. At order $O(p^3)$, the most stringent bounds are obtained by zooming inside the upper part of the Mandelstam triangle such that they can easily be employed and implemented to constrain future analyses. Finally, as a first use of these bounds, the values of LECs in the literature are compared with them. The comparison shows that the bounds, in particular the one constraining h_4 only, are badly violated in all the previous determinations from fitting to lattice data using UChPT. The most probable reason for this is that the UChPT amplitudes violate crossing symmetry which is the basis of deriving the positivity bounds.

For a more reasonable comparison, one needs to derive positivity bounds for the unitarized amplitudes.

One possible attack to the problem could come from using the method proposed in Ref. [182] where the author proposed a crossing-symmetric amplitude for the process $\gamma\pi \to \pi\pi$ combining the inverse amplitude method, which is one of the unitarization approaches, and the Roy equation. In our case, the problem is much more involved due to different masses and coupled channels. Whether such a method can lead to a feasible procedure still needs to be seen.

APPENDIX A

One-loop integrals

In this Appendix we give the definition for the one-loop integrals employed in this work as well as the explicit formulae for derivatives of one-loop integrals, which can be used to extract the regular part of loop integrals.

A.1 Definition of the one-loop integrals

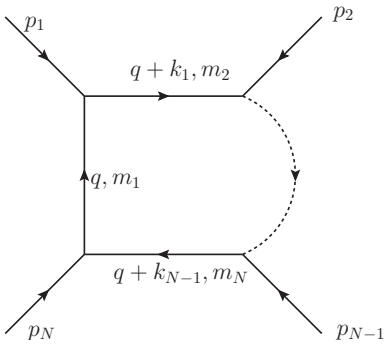

Figure A.1: A general one-loop diagram. The p_i denotes the external momentum, q and $q + k_i$ represent the internal momenta and m_i is the corresponding propagator mass. The dashed line indicates the possible remaining structure of internal propagators associated with external momenta.

Consider a general one-loop diagram Fig. A.1, the N-point one-loop integral contained in this diagram is [183]

$$T^N_{\mu_1,\ldots\mu_p} = \frac{(2\pi\mu)^{4-d}}{i\pi^2}\int d^d k \frac{k_{\mu_1}\cdots k_{\mu_p}}{[k^2 - m_1^2][(k+q_1)^2 - m_2^2]\ldots[(k+q_{N-1})^2 - m_N^2]}, \tag{A.1}$$

where the momenta k_i that appear in the denominators are related to he external momenta p_i as

$$k_i = \sum_{j=1}^{i} p_j. \tag{A.2}$$

The denominator arises from the propagators running in the loop. P, the number of ks in the numerator,

determines the Lorentz tensor structure of the integral, i.e. $P = 0$ denotes a scalar integral, $P = 1$ a vector integral, etc. Following the notation of Ref. [184] we set $T^1 = A$, $T^2 = B$, $T^3 = C$, $T^4 = D$, etc.

A.1.1 Scalar integrals

One-point function

$$A_0(m^2) = \frac{(2\pi\mu)^{4-d}}{i\pi^2}\int d^dk \frac{1}{k^2 - m^2}.$$

Two-point function

$$B_0(p_1^2, m_1^2, m_2^2) = \frac{(2\pi\mu)^{4-d}}{i\pi^2}\int d^dk \frac{1}{[k^2 - m_1^2][(k+p_1)^2 - m_2^2]}.$$

Threee-point function

$$\begin{aligned} &C_0(p_1^2, p_2^2, p_{12}^2, m_1^2, m_2^2, m_3^2) \\ &= \frac{(2\pi\mu)^{4-d}}{i\pi^2}\int d^dk \frac{1}{[k^2 - m_1^2][(k+p_1)^2 - m_2^2][(k+p_1+p_2)^2 - m_3^2]}. \end{aligned}$$

Four-point function

$$\begin{aligned} &D_0(p_1^2, p_2^2, p_3^2, p_4^2, p_{12}^2, p_{23}^2, m_1^2, m_2^2, m_3^2, m_4^2) \\ &= \frac{(2\pi\mu)^{4-d}}{i\pi^2}\int d^dk \frac{1}{[k^2 - m_1^2][(k+p_1)^2 - m_2^2][(k+p_1+p_2)^2 - m_3^2][(k+p_1+p_2+p_3)^2 - m_4^2]}. \end{aligned}$$

Above we have used the abbreviation $p_{ij} = p_i + p_j$.

A.1.2 Tensor decomposition

The integrals with a tensor structure can be reduced to linear combinations of Lorentz covariant tensors constructed from the metric tensor $g_{\mu\nu}$ and a linearly independent set of the momenta [185]. The choice of this basis is not unique. For the integrals up to the four-point function the decomposition reads explicitly

$$\begin{aligned} B_\mu &= k_{1\mu} B_1, \\ B_{\mu\nu} &= g_{\mu\nu} B_{00} + k_{1\mu} k_{1\nu} B_{11}, \\ B_{\mu\nu\rho} &= (g_{\mu\nu} k_{1\rho} + g_{\nu\rho} k_{1\mu} + g_{\mu\rho} k_{1\nu}) B_{001} + k_{1\mu} k_{1\nu} k_{1\rho} B_{111}, \\ C_\mu &= k_{1\mu} C_1 + k_{2\mu} C_2 = \sum_{i=1}^{2} k_{i\mu} C_i, \\ C_{\mu\nu} &= g_{\mu\nu} C_{00} + \sum_{i,j=1}^{2} k_{i\mu} k_{j\nu} C_{ij}, \\ C_{\mu\nu\rho} &= \sum_{i=1}^{2} (g_{\mu\nu} k_{i\rho} + g_{\nu\rho} k_{i\mu} + g_{\mu\rho} k_{i\nu}) C_{00i} + \sum_{i,j,\ell=1}^{2} k_{i\mu} k_{j\nu} k_{\ell\rho} C_{ij\ell}, \end{aligned}$$

$$
\begin{aligned}
D_\mu &= \sum_{i=3}^{3} k_{i\mu} D_i, \\
D_{\mu\nu} &= g_{\mu\nu} D_{00} + \sum_{i,j=1}^{3} k_{i\mu} k_{j\nu} D_{ij}, \\
D_{\mu\nu\rho} &= \sum_{i=1}^{3} (g_{\mu\nu} k_{i\rho} + g_{\nu\rho} k_{i\mu} + g_{\mu\rho} k_{i\nu}) D_{00i} + \sum_{i,j,\ell=1}^{3} k_{i\mu} k_{j\nu} k_{\ell\rho} D_{ij\ell}, \\
D_{\mu\nu\rho\sigma} &= (g_{\mu\nu} g_{\rho\sigma} + g_{\mu\rho} g_{\nu\sigma} + g_{\mu\sigma} g_{\nu\rho}) D_{0000} \\
&\quad + \sum_{i,j=1}^{3} (g_{\mu\nu} k_{i\rho} k_{j\sigma} + g_{\nu\rho} k_{i\mu} k_{j\sigma} + g_{\mu\rho} k_{i\nu} k_{j\sigma} + g_{\mu\sigma} k_{i\nu} k_{j\rho} + g_{\nu\sigma} k_{i\mu} k_{j\rho} + g_{\rho\sigma} k_{i\mu} k_{j\nu}) D_{00ij} \\
&\quad + \sum_{i,j,\ell,m=1}^{3} k_{i\mu} k_{j\nu} k_{\ell\rho} k_{m\sigma} D_{ij\ell m}.
\end{aligned} \tag{A.3}
$$

In terms of these notations, the loop integrals A and B involved in the calculations are given as following:

$$
\begin{aligned}
A_0(m_a^2) &= -m_a^2 \Big(R + \ln \frac{m_a^2}{\mu^2} \Big), \\
B_0(p^2, m_a^2, m_b^2) &= -R + 1 - \ln \frac{m_b^2}{\mu^2} + \frac{\Delta_{ab} + p^2}{2p^2} \ln \frac{m_b^2}{m_a^2} \\
&\quad + \frac{p^2 - (m_a - m_b)^2}{p^2} \rho_{ab}(p^2) \ln \frac{\rho_{ab}(p^2) - 1}{\rho_{ab}(p^2) + 1}, \\
B_1(p^2, m_a^2, m_b^2) &= \frac{1}{2p^2} \Big[A_0(m_a^2) - A_0(m_b^2) - (p^2 + \Delta_{ab}) B_0(p^2, m_a^2, m_b^2) \Big], \\
B_{00}(p^2, m_a^2, m_b^2) &= \frac{1}{12p^2} \Big[(p^2 + \Delta_{ab}) A_0(m_a^2) + (p^2 - \Delta_{ab}) A_0(m_b^2) + (4p^2 m_a^2 - (p^2 + \Delta_{ab})^2) B_0(p^2, m_a^2, m_b^2) \Big] \\
&\quad - \frac{1}{18} (p^2 - 3m_a^2 - 3m_b^2), \\
B_{11}(p^2, m_a^2, m_b^2) &= \frac{1}{3p^4} \Big[(2p^2 + \Delta_{ab}) A_0(m_b^2) - (p^2 + \Delta_{ab}) A_0(m_a^2) - (p^2 m_a^2 - (p^2 + \Delta_{ab})^2) B_0(p^2, m_a^2, m_b^2) \Big] \\
&\quad + \frac{1}{18p^2} (p^2 - 3m_a^2 - 3m_b^2),
\end{aligned} \tag{A.4}
$$

where $\Delta_{ab} = m_a^2 - m_b^2$,

$$
\rho_{ab}(p^2) = \sqrt{\frac{p^2 - (m_a + m_b)^2}{p^2 - (m_a - m_b)^2}} \tag{A.5}
$$

and $R = \dfrac{2}{d-4} + \gamma_E - 1 - \ln 4\pi$, with γ_E the Euler's constant, $\gamma_E = 0.57721\ldots$.

A.2 Derivatives of one-loop integrals

As discussed in Chapter 2, the PCB terms of loop integrals are regular with respect to the chiral quantities. That means one can extract the PCB terms by Taylor expansion with chiral quantities, i.e. by taking derivatives of loop integrals with respect to chiral quantities. In this section, we investigate the PCB terms by calculating the derivatives of loop integrals. We adapt the derivatives of two-, three- and four-point functions calculated by Devaraj and Stuart [186, 187].

A.2.1 Derivatives of the two-point loop function

Performing the usual Feynman parameterization of the two-point loop integral one obtains

$$B_0(p^2, m_1^2, m_2^2) = (-1)^i (4\pi)^{2-d/2}\Gamma(2-\frac{d}{2})\int_0^1 dz[az^2+bz+c]^{\frac{d}{2}-2}, \tag{A.6}$$

where $a=-p^2$, $b=p^2-m_1^2+m_2^2$, $c=m_1^2-i\epsilon$. It follows that

$$\begin{aligned}
\frac{\partial}{\partial p^2}B_0(p^2, m_1^2, m_2^2) &= (-1)^i (4\pi)^{2-d/2}\Gamma(3-\frac{d}{2})\int_0^1 dz\frac{z(z-1)}{(az^2+bz+c)^{3-d/2}},\\
\frac{\partial}{\partial m_1^2}B_0(p^2, m_1^2, m_2^2) &= (-1)^i (4\pi)^{2-d/2}\Gamma(3-\frac{d}{2})\int_0^1 dz\frac{z-1}{(az^2+bz+c)^{3-d/2}}.
\end{aligned} \tag{A.7}$$

The partial derivative with respect to m_2^2 can be easily obtained due to that B_0 is symmetric in its mass arguments. On the other hand, integrating B_0 by parts one finds

$$\begin{aligned}
B_0(p^2, m_1^2, m_2^2) &= (-1)^i (4\pi)^{2-d/2}\Gamma(2-\frac{d}{2})\Big[\int_0^1 d\Big(z(az^2+bz+c)^{d/2-2}\Big) - \int_0^1 dz\frac{z(\frac{d}{2}-2)(2az+b)}{(az^2+bz+c)^{3-d/2}}\Big]\\
&= (-1)^i (4\pi)^{2-d/2}\Gamma(2-\frac{d}{2})\Big[(m_2^2)^{d/2-2} + (2-\frac{d}{2})\int_0^1 dz\frac{z(2az+b)}{(az^2+bz+c)^{3-d/2}}\Big]\\
&= B_0(0, m_2^2, m_2^2) + (-1)^i (4\pi)^{2-d/2}\Gamma(3-\frac{d}{2})\int_0^1 dz\frac{z(2az+b)}{(az^2+bz+c)^{3-d/2}}.
\end{aligned} \tag{A.8}$$

Therefore, one has

$$(-1)^i (4\pi)^{2-d/2}\Gamma(3-\frac{d}{2})\int_0^1 dz\frac{z(2az+b)}{(az^2+bz+c)^{3-d/2}} = B_0(p^2, m_1^2, m_2^2) - B_0(0, m_2^2, m_2^2). \tag{A.9}$$

We write [188]

$$\frac{z(z-1)}{az^2+bz+c} = \alpha_0 + \beta_1\frac{z(2az+b)}{az^2+bz+c} + \beta_0\frac{2az+b}{az^2+bz+c}, \tag{A.10}$$

in which

$$\alpha_0 = -\frac{b}{a}\frac{2a+b}{b^2-4ac}, \quad \beta_1 = \frac{1}{a}\frac{b^2-2ac+ab}{b^2-4ac}, \quad \beta_0 = \frac{c}{a}\frac{2a+b}{b^2-4ac}. \tag{A.11}$$

The integral of last term of Eq. (A.11) can be evaluated as:

$$\begin{aligned}
&(-1)^i(4\pi)^{2-d/2}\Gamma(3-\frac{d}{2})\int_0^1 dz\frac{2az+b}{(az^2+bz+c)^{3-d/2}}\\
&=(-1)^i(4\pi)^{2-d/2}\Gamma(3-\frac{d}{2})\int_0^1 \frac{d(az^2+bz+c)}{(az^2+bz+c)^{3-d/2}}\\
&=(-1)^i(4\pi)^{2-d/2}\Gamma(2-\frac{d}{2})[c^{d/2-2}-(a+b+c)^{d/2-2}]\\
&=B_0(0,m_1^2,m_1^2)-B_0(0,m_2^2,m_2^2).
\end{aligned} \tag{A.12}$$

Inserting Eqs. (A.9) and (A.12) into Eq. (A.7) one obtains the derivative of B_0 function with respect to p^2. The derivatives with respect to masses can be obtained in a similar way. Following the notation of Ref. [186], the derivatives of the two-point functions read

$$\begin{aligned}
\frac{\partial}{\partial p^2}B_0(p^2,m_1^2,m_2^2) &= \frac{1}{p^2D}\Big[B_0(0,m_1^2,m_1^2)(-p^2+m_1^2-m_2^2)m_1^2\\
&\quad -(p^2+m_1^2-m_2^2)(p^2-m_1^2+m_2^2+m_2^2B_0(0,m_2^2,m_2^2)\\
&\quad +B_0(p^2,m_1^2,m_2^2)(-m_1^4+(p^2+2m_2^2)m_1^2-m_2^4+p^2m_2)\Big]\\
&= \frac{1}{D}\Big[(-p^2+m_1^2+m_2^2)p^2-A_0(m_2^2)(p^2+m_1^2-m_2^2)\\
&\quad -A_0(m_1^2)(p^2-m_1^2+m_2^2)+B_0(p^2,m_1^2,m_2^2)(p^2(m_1^2+m_2^2)-(m_1^2-m_2^2)^2)\Big],
\end{aligned} \tag{A.13}$$

$$\begin{aligned}
\frac{\partial}{\partial m_1^2}B_0(p^2,m_1^2,m_2^2) &= \frac{1}{m_1^2D}\Big[-A_0(m_1^2)(-p^2+m_1^2+m_2^2)\\
&\quad +m_1^2\Big(2A_0(m_2^2)-(p^2-m_1^2+m_2^2)(B_0(p^2,m_1^2,m_2^2)-1)\Big)\Big],
\end{aligned} \tag{A.14}$$

where

$$D=(m_1^4-2(p^2+m_2^2)m_1^2+(p^2-m_2^2)^2). \tag{A.15}$$

After some calculations, some special cases read

$$\begin{aligned}
\frac{\partial}{\partial p^2}B_0(p^2,m^2,0)\Big|_{p^2=m^2} &= -\frac{m^2+A_0(m^2)}{2m^4},\\
\frac{\partial}{\partial M^2}B_0(m^2,m^2,M^2)\Big|_{M^2=0} &= \frac{3m^2-A_0(m^2)}{2m^4},
\end{aligned} \tag{A.16}$$

where we have used the symmetry of the loop functions under permutation of its mass arguments and

$$\begin{aligned}
B_0(0,m^2,m^2) &= \frac{d/2-2}{m^2}A_0(m^2),\\
B_0(m^2,m^2,0) &= \frac{d/2-1}{m^2(d-3)}A_0(m^2).
\end{aligned} \tag{A.17}$$

As a consequence, the regular part of a two-point function $B_0(s, m^2, M^2)$ with m the mass of matter field and M the Goldstone boson mass reads

$$\begin{aligned} B_0^{\text{reg.}}(s, m^2, M^2) = & B_0(m^2, m^2, 0) \\ & + (s - m^2) \frac{\partial}{\partial s} B_0(s, m^2, 0)\Big|_{s=m^2} \\ & + M^2 \frac{\partial}{\partial M^2} B_0(m^2, m^2, M^2)\Big|_{M^2=0} + \cdots \\ = & \left(1 - \ln \frac{m^2}{\mu^2}\right) - \frac{s - m^2}{2m^2}\left(1 - \ln \frac{m^2}{\mu^2}\right) + \frac{M^2}{2m^2}\left(3 + \ln \frac{m^2}{\mu^2}\right) + \cdots , \end{aligned} \tag{A.18}$$

which is identical to Eq. (C.3) in Ref. [65].

A.2.2 Derivatives of the three-point loop function

The derivatives of the three-point function can be expressed as a sum of the scalar three-point function and mass-derivatives of the two-point function. To see this one writes

$$\begin{aligned} \frac{\partial}{\partial m_1^2} B_0(p^2, m_1^2, m_2^2) &= -\int_0^1 dx \frac{1 - x}{p^2 x^2 + (m_2^2 - m_1^2 - p^2)x + m_1^2}, \\ \frac{\partial}{\partial m_2^2} B_0(p^2, m_1^2, m_2^2) &= -\int_0^1 dx \frac{x}{p^2 x^2 + (m_2^2 - m_1^2 - p^2)x + m_1^2}. \end{aligned} \tag{A.19}$$

The Feynman parameter representation of the scalar three-point function reads

$$\begin{aligned} C_0(p_1^2, p_2^2, p_{12}^2, m_1^2, m_2^2, m_3^2) &= \int_0^1 dx \int_0^x dy \frac{1}{(ax^2 + by^2 + cxy + dx + ey + f)^{3-d/2}} \\ &= \int_0^1 dx \int_0^x dy \frac{1}{D_c^{3-d/2}}, \end{aligned} \tag{A.20}$$

where

$$\begin{aligned} a = -p_1^2, \quad & b = -p_2^2, \quad & c = p_1^2 + p_2^2 - p_{12}^2, \\ d = p_1^2 + m_1^2 - m_2^2, \quad & e = p_{12}^2 - p_1^2 + m_2^2 - m_3^2, \quad & f = -m_1^2. \end{aligned} \tag{A.21}$$

The derivatives of C_0 with respect to any argument can be written as

$$C_0' = (3 - \frac{d}{2}) \int_0^1 dx \int_0^x dy \frac{\alpha_{x^2} x^2 + \alpha_{y^2} y^2 \alpha_{xy} xy + \alpha_x x + \alpha_y y + \alpha_1}{D_c^{4-d/2}}, \tag{A.22}$$

where the coefficients α_i are summarized in Table. A.1. They can be expressed as linear combinations of

C_0' w.r.t.	α_{x^2}	α_{y^2}	α_{xy}	α_x	α_y	α_1
p_1^2	1	0	-1	-1	1	0
p_2^2	0	1	-1	0	0	0
p_{12}^2	0	0	1	0	-1	0
m_1^2	0	0	0	-1	0	1
m_2^2	0	0	0	1	-1	0
m_3^2	0	0	0	0	1	0

Table A.1: Coefficients α_i in Eq. (A.22) for derivatives of C_0.

C_0 and mass-derivatives of B_0. The basis can be constructed as [186]

$$
\begin{aligned}
I_1 &= (3-\frac{d}{2})\int_0^1 dx\int_0^x dy \frac{y(2by+cx+e)}{D_c^{4-d/2}},\\
I_2 &= (3-\frac{d}{2})\int_0^1 dx\int_0^x dy \frac{y(2ax+cy+d)}{D_c^{4-d/2}},\\
I_3 &= (3-\frac{d}{2})\int_0^1 dx\int_0^x dy \frac{x(2by+cx+e)}{D_c^{4-d/2}},\\
I_4 &= (3-\frac{d}{2})\int_0^1 dx\int_0^x dy \frac{2ax+cy+d}{D_c^{4-d/2}},\\
I_5 &= (3-\frac{d}{2})\int_0^1 dx\int_0^x dy \frac{2by+cx+e}{D_c^{4-d/2}},\\
I_6 &= (3-\frac{d}{2})\int_0^1 dx\int_0^x dy \frac{dx+ey+2f}{D_c^{4-d/2}}.
\end{aligned}
$$

Using partial integration and the Feynman parametrization of Eqs. (A.19) and (A.22) one can show that

$$
\begin{aligned}
I_1 &= C_0 - \frac{\partial}{\partial m_3^2}B_0(p_{12}^2,m_1^2,m_3^2),\\
I_2 &= -\frac{\partial}{\partial m_3^2}B_0(p_2^2,m_2^2,m_3^2) + \frac{\partial}{\partial m_3^2}B_0(p_{12}^2,m_1^2,m_3^2),\\
I_3 &= -\frac{\partial}{\partial m_3^2}B_0(p_{12}^2,m_1^2,m_3^2) + \frac{\partial}{\partial m_2^2}B_0(p_1^2,m_1^2,m_2^2),\\
I_4 &= \Big(\frac{\partial}{\partial m_1^2}+\frac{\partial}{\partial m_3^2}\Big)B_0(p_{12}^2,m_1^2,m_3^2) - \Big(\frac{\partial}{\partial m_2^2}+\frac{\partial}{\partial m_3^2}\Big)B_0(p_2^2,m_2^2,m_3^2),\\
I_5 &= \Big(\frac{\partial}{\partial m_1^2}+\frac{\partial}{\partial m_2^2}\Big)B_0(p_1^2,m_1^2,m_2^2) - \Big(\frac{\partial}{\partial m_1^2}+\frac{\partial}{\partial m_3^2}\Big)B_0(p_{12}^2,m_1^2,m_3^2),\\
I_6 &= \Big(\frac{\partial}{\partial m_2^2}+\frac{\partial}{\partial m_3^2}\Big)B_0(p_2^2,m_2^2,m_3^2).
\end{aligned}
\tag{A.23}
$$

One can perform the decomposition of C_0' in terms of the above basis

$$C_0' = \sum_{i=1}^{6} \beta_i I_i. \tag{A.24}$$

By comparison of coefficients we get a set of linear equations

$$\begin{pmatrix} 0 & 0 & c & 0 & 0 & 0 \\ 2b & c & 0 & 0 & 0 & 0 \\ c & 2a & 2b & 0 & 0 & 0 \\ 0 & 0 & e & 2a & c & d \\ e & d & 0 & c & 2b & e \\ 0 & 0 & 0 & d & e & 2f \end{pmatrix} \begin{pmatrix} \beta_1 \\ \beta_2 \\ \beta_3 \\ \beta_4 \\ \beta_5 \\ \beta_6 \end{pmatrix} = \begin{pmatrix} \alpha_{x^2} \\ \alpha_{y^2} \\ \alpha_{xy} \\ \alpha_x \\ \alpha_y \\ \alpha_1 \end{pmatrix}. \tag{A.25}$$

From the equations Eq. (A.25) one can solve for the β_i and thus express C_0' as a sum over C_0 and massive-derivatives of B_0.

A.2.3 Derivative of the four-point loop function

The derivatives of the four-point loop functions can be obtained in analogy to that of the three-point functions. The scalar four-point function in terms of Feynman parameters is given by

$$D_0(p_1^2, p_2^2, p_3^2, p_4^2, p_{12}^2, p_{23}^2, m_1^2, m_2^2, m_3^2, m_4^2) = \int_0^1 dx \int_0^x dy \int_0^y dz \frac{1}{D_d^{4-d/2}}, \tag{A.26}$$

where $D_d = ax^2 + by^2 + cz^2 + dxy + exz + fyz + gx + hy + iz + j$ with

$$\begin{aligned} a &= -p_1^2, & b &= -p_2^2, & c &= -p_3^2, \\ d &= p_1^2 + p_2^2 - p_{12}^2, & e &= p_{12}^2 + p_{23}^2 - p_2^2 - p_4^2, & f &= p_2^2 + p_3^2 - p_{23}^2, \\ g &= p_1^2 + m_1^2 - m_2^2, & h &= p_{12}^2 - p_1^2 + m_2^2 - m_3^2, & i &= p_4^2 - p_{12}^2 + m_3^2 - m_4^2, \\ j &= -m_1^2. \end{aligned} \tag{A.27}$$

We can choose a set of basis integrals as follows,

$$\begin{aligned} I_1 &= \int_0^1 dx \int_0^x dy \int_0^y dz z \frac{\partial}{\partial z} \frac{1}{D_d^{4-d/2}}, \\ I_2 &= \int_0^1 dx \int_0^x dy \int_0^y dz x \frac{\partial}{\partial z} \frac{1}{D_d^{4-d/2}}, \\ I_3 &= \int_0^1 dx \int_0^x dy \int_0^y dz y \frac{\partial}{\partial z} \frac{1}{D_d^{4-d/2}}, \\ I_4 &= \int_0^1 dx \int_0^x dy \int_0^y dz z \frac{\partial}{\partial y} \frac{1}{D_d^{4-d/2}}, \\ I_5 &= \int_0^1 dx \int_0^x dy \int_0^y dz x \frac{\partial}{\partial y} \frac{1}{D_d^{4-d/2}}, \end{aligned}$$

$$
\begin{aligned}
I_6 &= \int_0^1 dx \int_0^x dy \int_0^y dz \frac{\partial}{\partial y} \frac{y}{D_d^{4-d/2}}, \\
I_7 &= \int_0^1 dx \int_0^x dy \int_0^y dz \frac{\partial}{\partial y} \frac{1}{D_d^{4-d/2}}, \\
I_8 &= \int_0^1 dx \int_0^x dy \int_0^y dz z \frac{\partial}{\partial x} \frac{1}{D_d^{4-d/2}}, \\
I_9 &= \int_0^1 dx \int_0^x dy \int_0^y dz \frac{\partial}{\partial x} \frac{x}{D_d^{4-d/2}}, \\
I_{10} &= \int_0^1 dx \int_0^x dy \int_0^y dz \frac{\partial}{\partial z} \frac{z}{D_d^{4-d/2}}.
\end{aligned} \tag{A.28}
$$

After some calculations, e.g. see Ref. [187], one finds

$$
\begin{aligned}
I_1 &= \frac{\partial}{\partial m_4^2} C_0(1,2,4) - D_0, \\
I_2 &= \frac{\partial}{\partial m_2^2} C_0(1,2,4) + \frac{\partial}{\partial m_4^2} C_0(1,2,4) - \frac{\partial}{\partial m_2^2} C_0(1,2,3) - \frac{\partial}{\partial m_3^2} C_0(1,2,3), \\
I_3 &= \frac{\partial}{\partial m_4^2} C_0(1,2,4) - \frac{\partial}{\partial m_3^2} C_0(1,2,3), \\
I_4 &= \frac{\partial}{\partial m_4^2} C_0(1,3,4) - \frac{\partial}{\partial m_4^2} C_0(1,2,4), \\
I_5 &= \frac{\partial}{\partial m_3^2} C_0(1,3,4) + \frac{\partial}{\partial m_4^2} C_0(1,3,4) - \frac{\partial}{\partial m_2^2} C_0(1,2,4) - \frac{\partial}{\partial m_4^2} C_0(1,2,4), \\
I_6 &= \frac{\partial}{\partial m_3^2} C_0(1,3,4) + \frac{\partial}{\partial m_4^2} C_0(1,3,4) - \frac{\partial}{\partial m_4^2} C_0(1,2,4), \\
I_7 &= \frac{\partial}{\partial m_1^2} C_0(1,3,4) + \frac{\partial}{\partial m_3^2} C_0(1,3,4) + \frac{\partial}{\partial m_4^2} C_0(1,3,4) \\
&\quad - \frac{\partial}{\partial m_1^2} C_0(1,2,4) - \frac{\partial}{\partial m_2^2} C_0(1,2,4) - \frac{\partial}{\partial m_4^2} C_0(1,2,4), \\
I_8 &= \frac{\partial}{\partial m_4^2} C_0(2,3,4) - \frac{\partial}{\partial m_4^2} C_0(1,3,4), \\
I_9 &= \frac{\partial}{\partial m_2^2} C_0(2,3,4) + \frac{\partial}{\partial m_3^2} C_0(2,3,4) + \frac{\partial}{\partial m_4^2} C_0(2,3,4) \\
&\quad - \frac{\partial}{\partial m_3^2} C_0(1,3,4) - \frac{\partial}{\partial m_4^2} C_0(1,3,4), \\
I_{10} &= \frac{\partial}{\partial m_4^2} C_0(1,2,4).
\end{aligned} \tag{A.29}
$$

Here the arguments of C_0 indicate the propagators, labelled according to their appearance in D_0, e.g. $C_0(1,2,4)$ represents D_0 with the fourth propagator omitted $C_0(1,2,4) = C_0(p_1^2, p_{23}^2, p_4^2, m_1^2, m_2^2, m_4^2)$.

D_0' w.r.t.	α_{z^2}	α_{y^2}	α_{x^2}	α_{xy}	α_{xz}	α_{zy}	α_z	α_y	α_x	α_1
p_1^2	0	0	1	-1	0	0	0	1	-1	0
p_2^2	0	1	0	-1	1	-1	0	0	0	0
p_3^2	1	0	0	0	0	-1	0	0	0	0
p_4^2	0	0	0	0	1	0	-1	0	0	0
p_{12}^2	0	0	0	0	1	-1	0	1	-1	0
p_{23}^2	0	0	0	0	-1	1	0	0	0	0
m_1^2	0	0	0	0	0	0	0	0	-1	1
m_2^2	0	0	0	0	0	0	0	-1	1	0
m_3^2	0	0	0	0	0	0	-1	1	0	0
m_4^2	0	0	0	0	0	0	1	0	0	0

Table A.2: Coefficients α_i in Eq. (A.30) for derivatives of D_0.

Using the Feynman parameter representation for D_0 any derivative of D_0 can be written as

$$D_0' = (4 - \frac{d}{2}) \int_0^1 dx \int_0^x dy \int_0^y dz \\ \frac{\alpha_{x^2} x^2 + \alpha_{y^2} y^2 + \alpha_{z^2} z^2 + \alpha_{xy} xy \alpha_{xz} zx + \alpha_{yz} yz + \alpha_x x + \alpha_y y + \alpha_z z + \alpha_1}{D_d^{5-d/2}}, \tag{A.30}$$

where the coefficients α_i are given in Table A.2.

On the other hand the derivatives of D_0 can be decomposed into a sum over the basis integrals I_i of Eq. (A.28)

$$D_0' = \sum_{i=1}^{10} \beta_i I_i, \tag{A.31}$$

where the coefficients β_i can be solved by a set of linear equations

$$\begin{pmatrix} -4c & 0 & 0 & -2f & 0 & c & 0 & -2e & c & -3c \\ 0 & 0 & -2f & 0 & 0 & -3b & 0 & 0 & b & b \\ 0 & -2e & 0 & 0 & -2d & a & 0 & 0 & -3a & a \\ 0 & -2f & -2e & 0 & -4b & -d & 0 & 0 & -d & d \\ -2e & -4c & 0 & -2d & -2f & e & 0 & -4a & -e & -e \\ -2f & 0 & -4c & -4b & 0 & -f & 0 & -2d & f & -f \\ -2i & 0 & 0 & -2h & 0 & i & -2f & -2g & i & -i \\ 0 & 0 & -2i & 0 & 0 & -h & -4b & 0 & h & h \\ 0 & -2i & 0 & 0 & -2h & g & -2d & 0 & -g & g \\ 0 & 0 & 0 & 0 & 0 & j & -2h & 0 & j & j \end{pmatrix} \begin{pmatrix} \beta_1 \\ \beta_2 \\ \beta_3 \\ \beta_4 \\ \beta_5 \\ \beta_6 \\ \beta_7 \\ \beta_8 \\ \beta_9 \\ \beta_{10} \end{pmatrix} = 2 \begin{pmatrix} \alpha_{z^2} \\ \alpha_{y^2} \\ \alpha_{x^2} \\ \alpha_{xy} \\ \alpha_{xz} \\ \alpha_{yz} \\ \alpha_z \\ \alpha_y \\ \alpha_x \\ \alpha_1 \end{pmatrix}. \tag{A.32}$$

APPENDIX B

Renormalization of LECs within EOMS scheme

B.0.1 β-functions

The β-functions in Eq. (6.15) read

$$
\begin{aligned}
\beta_{M_0^2} &= -\frac{4g_0^2(3m_D^2 - m_{D^*}^2)}{9}\,, \\
\beta_{M_0^{*2}} &= \frac{4g_0^2 m_D^2(3m_{D^*}^2 - m_D^2)}{3m_{D^*}^2}\,, \\
\beta_{h_0} &= \frac{11\, g_0^2\, m_D^2}{24\, m_{D^*}^2}\,, \\
\beta_{h_1} &= \frac{5\, g_0^2\, m_D^2}{8\, m_{D^*}^2}\,, \\
\beta_{h_2} &= \frac{m_D^2(m_{D^*}^4 - 22\, g_0^2\, m_{D^*}^2 + 4\, g_0^4)}{48\, m_{D^*}^4}\,, \\
\beta_{h_3} &= \frac{-9\, m_D^2 m_{D^*}^4 + 18\, g_0^2(3\, m_D^2 m_{D^*}^2 + 16 m_{D^*}^4) + 4 g_0^4(m_D^2 + 2m_{D^*}^2)}{144\, m_{D^*}^4}\,, \\
\beta_{h_4} &= \frac{1}{24}\left(7 - \frac{10\, g_0^2}{m_{D^*}^2} + \frac{4\, g_0^4}{m_{D^*}^4}\right)\,, \\
\beta_{h_5} &= -\frac{7}{16} + \frac{9\, g_0^2}{8 m_{D^*}^2} - \frac{13\, g_0^4}{18 m_{D^*}^4}\,, \\
\beta_{g_0} &= -g_0\, m_{D^*}^2 + g_0^3\left(\frac{7}{4} - \frac{5\, m_D^2}{4\, m_{D^*}^2}\right)\,, \\
\beta_{g_1} &= \frac{-41\, g_0^2\, m_{D^*}^2 + 30\, g_0^4}{288\, m_{D^*}^4}\,, \\
\beta_{g_2} &= -\frac{9}{128} + \frac{67\, g_0^2}{288\, m_{D^*}^2} - \frac{3\, g_0^4}{16\, m_{D^*}^4}\,, \\
\beta_{g_3} &= 0\,.
\end{aligned}
\tag{B.1}
$$

B.0.2 Coefficients of finite shifts

In this appendix, we express the EOMS subtractions in terms of the standard loop function. The explicit coefficients of the finite shifts in Eq. (6.17) are

$$
\begin{aligned}
\bar{\beta}_{h_2} &= \left[-\frac{m_D^2}{72}-\frac{1}{144}\left(\frac{31m_D^2}{m_{D^*}^2}+3\right)g_0^2+\frac{m_D^2\left(m_{D^*}^2-7m_D^2\right)}{72m_{D^*}^4(m_D-m_{D^*})(m_D+m_{D^*})}g_0^4\right] \\
&+\left[-\frac{1}{48}+\frac{3m_D^2-4m_{D^*}^2}{24m_D^2m_{D^*}^2-24m_{D^*}^4}g_0^2+\frac{-3m_D^4+6m_D^2m_{D^*}^2-4m_{D^*}^4}{12m_{D^*}^4(m_D-m_{D^*})^2(m_D+m_{D^*})^2}g_0^4\right]A_0(m_D^2) \\
&+\left[\frac{-8m_D^4+8m_D^2m_{D^*}^2+m_{D^*}^4}{24m_D^2m_{D^*}^2\left(m_D^2-m_{D^*}^2\right)}g_0^2+\frac{-2m_D^4+5m_D^2m_{D^*}^2-2m_{D^*}^4}{12m_{D^*}^4\left(m_D^2-m_{D^*}^2\right)^2}g_0^4\right]A_0(m_{D^*}^2) \\
&+\left[\frac{1}{24}\left(\frac{8m_D^2}{m_{D^*}^2}+\frac{m_{D^*}^2}{m_D^2}+9\right)g_0^2+\frac{m_D^2+m_{D^*}^2}{6m_{D^*}^4}g_0^4\right]B_0(m_D^2,0,m_{D^*}^2)\,, \qquad \text{(B.2)} \\
\bar{\beta}_{h_3} &= \left[\frac{m_D^2}{24}+\left(\frac{3m_D^2}{4m_{D^*}^2}+\frac{1}{6}\right)g_0^2+\frac{7m_D^4-65m_D^2m_{D^*}^2+112m_{D^*}^4}{216m_{D^*}^4\left(m_{D^*}^2-m_D^2\right)}g_0^4\right] \\
&+\left[\frac{1}{16}+\frac{1}{4m_{D^*}^2}g_0^2+\frac{27m_D^4-46m_D^2m_{D^*}^2+58m_{D^*}^4}{36m_{D^*}^4(m_D-m_{D^*})^2(m_D+m_{D^*})^2}g_0^4\right]A_0(m_D^2) \\
&+\left[\frac{3}{8}\left(\frac{1}{m_{D^*}^2}-\frac{2}{m_D^2}\right)g_0^2-\frac{4m_D^6-2m_D^4m_{D^*}^2+68m_D^2m_{D^*}^4+8m_{D^*}^6}{72m_{D^*}^4\left(m_D^3-m_Dm_{D^*}^2\right)^2}g_0^4\right]A_0(m_{D^*}^2) \\
&+\left[\left(\frac{1}{4}-\frac{m_D^2}{4m_{D^*}^2}\right)g_0^2+\frac{-15m_D^6+29m_D^4m_{D^*}^2-m_D^2m_{D^*}^4+35m_{D^*}^6}{18m_{D^*}^4\left(m_D^2-m_{D^*}^2\right)^2}g_0^4\right]B_0(m_{D^*}^2,0,m_D^2) \\
&+\left[-\frac{3}{8}\left(\frac{m_D^2}{m_{D^*}^2}-\frac{2m_{D^*}^2}{m_D^2}+7\right)g_0^2+\frac{m_D^8-5m_D^6m_{D^*}^2-27m_D^4m_{D^*}^4-19m_D^2m_{D^*}^6+2m_{D^*}^8}{18m_{D^*}^4\left(m_D^3-m_Dm_{D^*}^2\right)^2}g_0^4\right] \\
&\quad B_0(m_D^2,0,m_{D^*}^2) \\
&+\left[\frac{\left(m_D^2+3m_{D^*}^2\right)^2}{3m_{D^*}^2\left(m_{D^*}^2-m_D^2\right)}g_0^4\right]C_0(m_{D^*}^2,0,m_D^2,0,m_D^2,m_{D^*}^2) \qquad \text{(B.3)} \\
\bar{\beta}_{h_4} &= \left[-\frac{35}{72}+\frac{1}{36}\left(\frac{3}{m_D^2}+\frac{1}{m_{D^*}^2}\right)g_0^2+\frac{2m_D^2-8m_{D^*}^2}{9m_D^2m_{D^*}^4-9m_{D^*}^6}g_0^4\right] \\
&+\left[-\frac{7}{24m_D^2}+\frac{2}{3m_D^4-3m_D^2m_{D^*}^2}g_0^2-\frac{2}{3m_D^2(m_D^2-m_{D^*}^2)^2}g_0^4\right]A_0(m_D^2) \\
&+\left[-\frac{5m_D^4+m_D^2m_{D^*}^2+2m_{D^*}^4}{12m_D^6m_{D^*}^2-12m_D^4m_{D^*}^4}g_0^2+\frac{\left(m_D^2+m_{D^*}^2\right)^2}{6m_{D^*}^4\left(m_D^3-m_Dm_{D^*}^2\right)^2}g_0^4\right]A_0(m_{D^*}^2) \\
&+\left[\frac{1}{12}\left(-\frac{2m_{D^*}^2}{m_D^4}-\frac{3}{m_D^2}+\frac{5}{m_{D^*}^2}\right)g_0^2-\frac{m_D^2+m_{D^*}^2}{6m_D^2m_{D^*}^4}g_0^4\right]B_0(m_D^2,0,m_{D^*}^2)\,, \qquad \text{(B.4)}
\end{aligned}
$$

$$
\begin{aligned}
\bar{\beta}_{h_5} &= \left[\frac{35}{48} - \frac{1}{4m_{D^*}^2}g_0^2 - \frac{31m_D^2+3m_{D^*}^2}{54m_D^2m_{D^*}^4}g_0^4\right] + \left[\frac{7}{16m_D^2} - \left(\frac{1}{8m_{D^*}^4} + \frac{1}{m_D^2m_{D^*}^2}\right)g_0^2\right. \\
&\quad \left. + \frac{-23m_D^6+74m_D^4m_{D^*}^2-95m_D^2m_{D^*}^4+20m_{D^*}^6}{36m_D^2m_{D^*}^6(m_D-m_{D^*})^2(m_D+m_{D^*})^2}g_0^4\right]A_0(m_D^2) \\
&\quad + \left[\frac{m_D^6+10m_D^4m_{D^*}^2+17m_D^2m_{D^*}^4-4m_{D^*}^6}{36m_D^4m_{D^*}^4\left(m_D^2-m_{D^*}^2\right)^2}g_0^4\right]A_0(m_{D^*}^2) \\
&\quad + \left[\frac{5m_D^8+17m_D^6m_{D^*}^2+39m_D^4m_{D^*}^4-17m_D^2m_{D^*}^6+4m_{D^*}^8}{36m_D^4m_{D^*}^4\left(m_D^2-m_{D^*}^2\right)^2}g_0^4\right]B_0(m_D^2,0,m_{D^*}^2) \\
&\quad + \left[\frac{m_D^2-m_{D^*}^2}{8m_{D^*}^4}g_0^2 + \frac{23m_D^6-53m_D^4m_{D^*}^2+25m_D^2m_{D^*}^4-43m_{D^*}^6}{36m_{D^*}^6\left(m_D^2-m_{D^*}^2\right)^2}g_0^4\right]B_0(m_{D^*}^2,0,m_D^2) \\
&\quad - \left[\frac{\left(m_D^2+3m_{D^*}^2\right)^2}{6m_{D^*}^4\left(m_{D^*}^2-m_D^2\right)}g_0^4\right]C_0(m_{D^*}^2,0,m_D^2,0,m_D^2,m_{D^*}^2)\,, \qquad \text{(B.5)} \\
\bar{\beta}_{g_0} &= \left[\frac{1}{12}\left(3m_D^2-m_{D^*}^2\right)g_0 + \frac{1}{72}\left(41-\frac{39m_D^2}{m_{D^*}^2}\right)g_0^3\right] \\
&\quad + \left[\frac{m_D^2+m_{D^*}^2}{8m_{D^*}^2}g_0 + \frac{5m_D^4-7m_D^2m_{D^*}^2+9m_{D^*}^4}{12m_D^2m_{D^*}^4-12m_{D^*}^6}g_0^3\right]A_0(m_D^2) \\
&\quad + \left[\frac{3\left(m_D^2+m_{D^*}^2\right)}{8m_D^2}g_0 - \frac{17m_D^4-19m_D^2m_{D^*}^2+9m_{D^*}^4}{12m_D^4m_{D^*}^2-12m_D^2m_{D^*}^4}g_0^3\right]A_0(m_{D^*}^2) \\
&\quad - \left[\frac{3\left(m_D^2-m_{D^*}^2\right)^2}{8m_D^2}g_0 - \frac{15m_D^6-33m_D^4m_{D^*}^2-7m_D^2m_{D^*}^4+9m_{D^*}^6}{12m_D^4m_{D^*}^2-12m_D^2m_{D^*}^4}g_0^3\right]B_0(m_D^2,0,m_{D^*}^2) \\
&\quad - \left[\frac{\left(m_D^2-m_{D^*}^2\right)^2}{8m_{D^*}^2}g_0 + \frac{-5m_D^6+7m_D^4m_{D^*}^2+5m_D^2m_{D^*}^4+9m_{D^*}^6}{12m_{D^*}^4\left(m_{D^*}^2-m_D^2\right)}g_0^3\right]B_0(m_{D^*}^2,0,m_D^2) \\
&\quad - \left[\frac{\left(m_D^2+3m_{D^*}^2\right)^2}{6m_{D^*}^2}g_0^2\right]C_0(m_{D^*}^2,0,m_D^2,0,m_D^2,m_{D^*}^2)\,, \qquad \text{(B.6)} \\
\bar{\beta}_{h_0} &= \frac{11m_D^2}{36m_{D^*}^2}g_0^2 + \frac{11}{24m_{D^*}^2}g_0^2A_0(m_{D^*}^2) - \frac{11\left(m_D^2+m_{D^*}^2\right)}{24m_{D^*}^2}g_0^2B_0(m_D^2,0,m_{D^*}^2)\,, \qquad \text{(B.7)} \\
\bar{\beta}_{h_1} &= \frac{5m_D^2}{12m_{D^*}^2}g_0^2 + \frac{5}{8m_{D^*}^2}g_0^2A_0(m_{D^*}^2) - \frac{5\left(m_D^2+m_{D^*}^2\right)}{8m_{D^*}^2}g_0^2B_0(m_D^2,0,m_{D^*}^2)\,. \qquad \text{(B.8)}
\end{aligned}
$$

Here the involved scalar one-loop integrals stand for their finite parts only, which are obtained from the original ones, defined in Appendix A, by performing the $\overline{MS}-1$ subtraction.

APPENDIX C

Estimate of the coupling constant g_{DDT} via QCD sum rules

In this Appendix, we estimate the unknown off-shell coupling constant g_{DDT} using QCD sum rules, following the procedure in, e.g., Refs. [189, 190]. To be specific, we will calculate the $D^0 D^- a_2^+$ coupling. The standard procedure for computing a coupling constant in the method of QCD sum rules is to consider the three-point correlation function, which in our case is given by

$$\Pi_{\mu\nu}(p', p, q) = i^2 \int d^4x \int d^4y \, e^{i(-p'x+yp)} \langle 0|T\{j^{D^0}(x) j^{D^-}(y) j^{a_2^+}_{\mu\nu}(0)\}|0\rangle, \tag{C.1}$$

where $q = p' - p$ denotes the momentum transfer. The interpolating currents that we use for the D^0, D^- and a_2^+ mesons are

$$\begin{aligned} j^{D^0}(x) &= i\bar{u}(x)\gamma_5 c(x)\,, \\ j^{D^-}(x) &= i\bar{c}(x)\gamma_5 d(x)\,, \\ j^{a_2^+}_{\mu\nu}(x) &= \frac{i}{2}\bar{d}(x)(\gamma_\mu \overleftrightarrow{D}_\nu + \gamma_\nu \overleftrightarrow{D}_\mu)u(x)\,, \end{aligned} \tag{C.2}$$

where $\overleftrightarrow{D}_\mu = (\overrightarrow{D}_\mu - \overleftarrow{D}_\mu)/2$.

One can calculate the correlation function in two different ways. On the one hand, the correlation function in Eq. (C.1) can be computed by inserting a complete sets of appropriate hadronic states with the same quantum numbers as the interpolating currents. Following the usual procedure, we obtain

$$\begin{aligned} \Pi^{had}_{\mu\nu}(p'^2, p^2, q^2) = &\frac{\langle 0|j^{D^0}|D^0(p')\rangle \langle 0|j^{D^-}|D^-(p)\rangle \langle 0|j^{a_2^+}_{\mu\nu}|a_2^+(q,\epsilon)\rangle}{(p'^2 - m_D^2)(p^2 - m_D^2)(q^2 - m_a^2)} \\ &\times \langle D^0(p') a_2^+(q,\epsilon)|D^+(p)\rangle + \dots\,, \end{aligned} \tag{C.3}$$

where the ellipses represent the contributions of the excited states and the continuum. The matrix

elements above are parameterized as follows [190]

$$\begin{aligned}
&\langle 0|j^D|D(p)\rangle = i\frac{m_D^2 f_D}{m_c+m_q},\\
&\langle 0|j^{a_2^+}_{\mu\nu}|a_2^+(q,\epsilon)\rangle = m_a^3 f_a \epsilon^{*(\lambda)}_{\mu\nu},\\
&\langle D^0(p')a_2^+(q,\epsilon)|D^+(p)\rangle = g_{DDa_2}\epsilon^{(\lambda)}_{\alpha\beta}p'_\alpha p_\beta,
\end{aligned} \tag{C.4}$$

where f_D, f_a are the decay constants of $D^0(D^-)$ and a_2^+ mesons, and g_{DDa_2} is the form factor of the DDT coupling under consideration. Substituting the above matrix elements into Eq. (C.3), the correlation function takes the form

$$\begin{aligned}
\Pi^{had}_{\mu\nu}(p'^2,p^2,q^2) = i^2\left(\frac{m_D^2 f_D}{m_c+m_q}\right)^2 \frac{g_{DDa_2} f_a m_a^3}{(p'^2-m_D^2)(p^2-m_D^2)(q^2-m_a^2)}\\
\times\left\{1-\frac{1}{3m_a^2}(p^2+p'^2+2q^2)-\frac{1}{3m_a^4}\left[(p^2-p'^2)^2-(q^2)^2\right]\right\}(p'^\mu p^\nu + p'^\nu p^\mu)+\dots,
\end{aligned} \tag{C.5}$$

where only the Lorentz structure $(p'^\mu p^\nu + p'^\nu p^\mu)$ is kept, and the following relation has been used,

$$\sum_\lambda \epsilon^{(\lambda)}_{\mu\nu}\epsilon^{*(\lambda)}_{\alpha\beta} = \frac{1}{2}T_{\mu\alpha}T_{\nu\beta}+\frac{1}{2}T_{\mu\beta}T_{\nu\alpha}-\frac{1}{3}T_{\mu\nu}T_{\alpha\beta}, \tag{C.6}$$

with $T_{\mu\nu} = -g_{\mu\nu}+q_\mu q_\nu/m_a^2$.

On the other hand, the correlation function can be calculated at the quark-gluon level using the QCD operator product expansion (OPE) method. It is convenient to evaluate it in the fixed-point gauge: $(x-x_0)^\mu A^a_\mu(x)=0$, where x_0 is an arbitrary point in the coordinate space and could be chosen at the origin. Then, in the deep Euclidean region, the potential can be expressed in terms of the field strength tensor $G_{\mu\nu} = \lambda^a G^a_{\mu\nu}/2$ as [191]

$$A_\mu(x) = \frac{1}{2}x^\nu G_{\nu\mu}(0)+\frac{1}{3}x^\alpha x^\nu D_\alpha G_{\nu\mu}(0)+\mathcal{O}(x^3)\,. \tag{C.7}$$

Since we are not aiming at a precise calculation, we will only keep the vacuum condensate of the lowest dimension, that is the quark condensate. Considering only the Lorentz structure $(p'^\mu p^\nu + p'^\nu p^\mu)$ and using the double dispersion relation, we find

$$\Pi_{\mu\nu}(p'^2,p^2,q^2) = \Pi(p'^2,p^2,q^2)(p'^\mu p^\nu + p'^\nu p^\mu)+..., \tag{C.8}$$

$$\Pi(p'^2,p^2,q^2) = \int ds_1 ds_2 \frac{\rho^{\rm pert}(s_1,s_2,q^2)}{(s_1-p'^2)(s_2-p^2)}+\Pi^{qq}(p'^2,p^2,q^2), \tag{C.9}$$

where

$$\begin{aligned}
\rho^{\rm pert}(s_1,s_2,q^2) = -\frac{3}{8\pi^2\lambda^{5/2}}(s_1+s_2-t-2m_c^2)\Big\{(s_1s_2+m_c^4)(\lambda+3t(s_1+s_2-t))\\
-3m_c^2(s_1+s_2-t)\left[(s_1-s_2)^2-t(s_1+s_2)\right]\Big\},
\end{aligned} \tag{C.10}$$

with $\lambda = (s_1 + s_2 - t)^2 - 4s_1 s_2$, and

$$\Pi^{qq}(p'^2, p^2, q^2) = \frac{1}{4} m_c \langle \bar{q}q \rangle \left(\frac{1}{p'^2 - m_c^2} + \frac{1}{p^2 - m_c^2} \right) \frac{1}{q^2} \,. \tag{C.11}$$

In order to suppress the contribution from the excited states, we perform a double Borel transformation in both variables p'^2 and p^2 to the correlation functions in Eqs. (C.5) and (C.9). Using the quark-hadron duality, we obtain

$$\begin{aligned} \Pi(M_B^2, M_B'^2, q^2) &= i^2 \frac{g_{DDa_2} f_a m_a^3}{q^2 - m_a^2} \left(\frac{m_D^2 f_D}{m_c + m_q} \right)^2 \left[1 - \frac{2(q^2 + m_D^2)}{3m_a^2} + \frac{q^4}{3m_a^4} \right] e^{-m_D^2/M_B^2 - m_D^2/M_B'^2} \\ &= \int_{s_{1\min}}^{s_1^0} \int_{s_{2\min}}^{s_2^0} ds_1 ds_2 \rho^{\text{pert}}(s_1, s_2, q^2) e^{-s_1/M_B^2 - s_2/M_B'^2} \,. \end{aligned} \tag{C.12}$$

It is clear that the coupling g_{DDa_2} is in fact given by a form factor as a function of the Euclidean momentum $Q^2 = -q^2$ which will be denoted by $g_{DDa_2}^{(a_2)}(Q^2)$, where the superscript means that the meson a_2^+ is off-shell while the D mesons are on-shell since the correlation function is evaluated in the space-like region $Q^2 > 0$.

We neglect the light quark masses and use the following values for numerical analysis: $m_c = 1.27$ GeV, $m_D = 1.87$ GeV, $m_a = 1.32$ GeV, $\langle \bar{q}q \rangle = (-0.24)^3$ GeV, $f_D = 0.207$ GeV [190], and $f_a = 0.041$ [192]. Furthermore, $s_{1\min} = m_c^2$ and $s_{2\min} = \frac{m_c^2}{m_c^2 - s_1} q^2 + m_c^2$. Since the dependence of the form factor on M_B^2 and $M_B'^2$ is weak, one can use set $M_B'^2 = M_B^2$ [189].

The window for the Borel mass M_B^2 can be determined by requiring both the dominance of the ground state hadronic poles and the convergence of OPE. The quark condensate contribution would disappear if the double Borel transformation is performed in the variables p'^2 and p^2. In order to estimate the lower bound of M_B^2, we choose to perform the double Borel transformation in variables p^2 and q^2, and assume the lower bound is same as that in the double Borel transformation in p'^2 and p^2. The lower limit of M_B^2 is estimated by requiring $|\Pi^{qq}(p'^2, M_B^2, M_B^2)/\Pi^{\text{pert}}(p'^2, M_B^2, M_B^2)|$ to be smaller than 25% for Euclidean momentum p'^2. At the same time, the upper bound of the Borel mass M_B^2 can be estimated by requiring the pole contribution (PC) to be larger than 75% which is defined by

$$\text{PC} = \frac{\int_{s_{1\min}}^{s_1^0} ds_1 \int_{s_{2\min}}^{s_2^0} ds_2 \rho^{\text{pert}}(s_1, s_2, q^2) e^{-s_1/M_B^2 - s_2/M_B^2}}{\int_{s_{1\min}}^{\infty} ds_1 \int_{s_{2\min}}^{\infty} ds_2 \rho^{\text{pert}}(s_1, s_2, q^2) e^{-s_1/M_B^2 - s_2/M_B^2}} \,. \tag{C.13}$$

The parameters s_1^0 and s_2^0 are chosen around the region where the variation of coupling constant $g_{DDa_2}^{(a_2)}(Q^2)$ is minimal. Given a value of Q^2, we obtain a corresponding $g_{DDa_2}^{(a_2)}(Q^2)$. From the above requirements, the Borel window we use here is $M_B^2 \sim [3.2\ \text{GeV}^2, 4.0\ \text{GeV}^2]$. We take $M_B^2 = 3.6\ \text{GeV}^2$ for estimating the form factor $g_{DDa_2}^{(a_2)}(Q^2)$, and the values of s_1^0 and s_2^0 are chosen to increase slightly from around 6.0 GeV^2 to 8.5 GeV^2 as increasing Q^2 from 5 GeV^2 to 12 GeV^2. Since we are only able to calculate the form factor in the deep Euclidean region, we need to extrapolate it to $Q^2 = 0$ to get the coupling constant. The extrapolation is rather model-dependent. To be specific, we simply take the form $g_{DDa_2}^{(a_2)}(Q^2) = A \exp\left(-Q^2/B\right)$ used in Refs. [189, 193] despite that no physical reasoning is behind this parametrization. With this form, we fit to a few points in the Euclidean region, and get $A = 10.1\ \text{GeV}^{-1}$

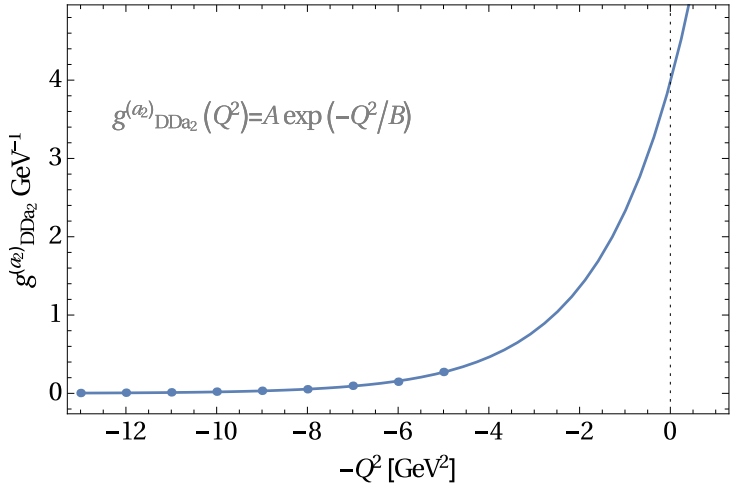

Figure C.1: Momentum dependence of the DDa_2 form factor (for off-shell a_2). The dots give the results from QCD sum rules, and the solid line gives the extrapolation.

and $B = 1.9$ GeV^2. Finally, we get an estimate for the coupling constant as

$$g_{DDT} \approx g_{DDa_2}(0) \approx 3.9 \text{ GeV}^{-1}. \tag{C.14}$$

It should be noted that such an estimate bears a large uncertainty which we do not know how to quantify, and the resulting value can only be regarded as an order-of-magnitude estimate.

Bibliography

[1] C.-N. Yang and R. L. Mills, *Conservation of Isotopic Spin and Isotopic Gauge Invariance*, Phys. Rev. **96** (1954) 191 (cit. on p. 1).

[2] F. Englert and R. Brout, *Broken Symmetry and the Mass of Gauge Vector Mesons*, Phys. Rev. Lett. **13** (1964) 321 (cit. on p. 1).

[3] P. W. Higgs, *Broken Symmetries and the Masses of Gauge Bosons*, Phys. Rev. Lett. **13** (1964) 508 (cit. on p. 1).

[4] G. S. Guralnik, C. R. Hagen and T. W. B. Kibble, *Global Conservation Laws and Massless Particles*, Phys. Rev. Lett. **13** (1964) 585 (cit. on p. 1).

[5] G. Aad et al., *Observation of a new particle in the search for the Standard Model Higgs boson with the ATLAS detector at the LHC*, Phys. Lett. **B716** (2012) 1, arXiv: 1207.7214 [hep-ex] (cit. on p. 1).

[6] S. Chatrchyan et al., *Observation of a new boson at a mass of 125 GeV with the CMS experiment at the LHC*, Phys. Lett. **B716** (2012) 30, arXiv: 1207.7235 [hep-ex] (cit. on p. 1).

[7] G. 't Hooft, *Renormalization of Massless Yang-Mills Fields*, Nucl. Phys. **B33** (1971) 173 (cit. on p. 1).

[8] G. 't Hooft, *Renormalizable Lagrangians for Massive Yang-Mills Fields*, Nucl. Phys. **B35** (1971) 167 (cit. on p. 1).

[9] D. J. Gross and F. Wilczek, *Ultraviolet Behavior of Nonabelian Gauge Theories*, Phys. Rev. Lett. **30** (1973) 1343 (cit. on p. 1).

[10] D. J. Gross and F. Wilczek, *Asymptotically Free Gauge Theories. 1*, Phys. Rev. **D8** (1973) 3633 (cit. on p. 1).

[11] H. D. Politzer, *Reliable Perturbative Results for Strong Interactions?*, Phys. Rev. Lett. **30** (1973) 1346 (cit. on p. 1).

[12] G. 't Hooft, *The Glorious days of physics: Renormalization of gauge theories*, (1998), arXiv: hep-th/9812203 [hep-th] (cit. on p. 1).

[13] S. Weinberg, *The Making of the standard model*, Eur. Phys. J. **C34** (2004) 5, [,99(2005)], arXiv: hep-ph/0401010 [hep-ph] (cit. on p. 1).

[14] S. Weinberg, *Phenomenological Lagrangians*, Physica **A96** (1979) 327 (cit. on pp. 2, 8, 63, 87).

[15] J. Gasser and H. Leutwyler, *Chiral Perturbation Theory to One Loop*, Annals Phys. **158** (1984) 142 (cit. on pp. 2, 25, 68, 72, 73, 87).

[16] J. Gasser and H. Leutwyler, *Chiral Perturbation Theory: Expansions in the Mass of the Strange Quark*, Nucl. Phys. **B250** (1985) 465 (cit. on pp. 2, 73–75, 87, 97).

[17] J. Gasser, M. E. Sainio and A. Švarč, *Nucleons with Chiral Loops*, Nucl. Phys. **B307** (1988) 779 (cit. on pp. 2, 34, 36).

[18] E. E. Jenkins and A. V. Manohar, *Baryon chiral perturbation theory using a heavy fermion Lagrangian*, Phys. Lett. **B255** (1991) 558 (cit. on pp. 2, 35).

[19] V. Bernard et al., *Chiral structure of the nucleon*, Nucl. Phys. **B388** (1992) 315 (cit. on pp. 2, 35–37).

[20] V. Bernard, N. Kaiser and U.-G. Meißner, *Chiral dynamics in nucleons and nuclei*, Int. J. Mod. Phys. **E4** (1995) 193, arXiv: hep-ph/9501384 [hep-ph] (cit. on pp. 2, 35).

[21] T. Becher and H. Leutwyler, *Baryon chiral perturbation theory in manifestly Lorentz invariant form*, Eur. Phys. J. **C9** (1999) 643, arXiv: hep-ph/9901384 [hep-ph] (cit. on pp. 2, 35, 36, 41, 42, 44).

[22] T. Fuchs et al., *Renormalization of relativistic baryon chiral perturbation theory and power counting*, Phys. Rev. **D68** (2003) 056005, arXiv: hep-ph/0302117 [hep-ph] (cit. on pp. 2, 35, 42).

[23] Y.-H. Chen, D.-L. Yao and H. Q. Zheng, *Analyses of pion-nucleon elastic scattering amplitudes up to $O(p^4)$ in extended-on-mass-shell subtraction scheme*, Phys. Rev. **D87** (2013) 054019, arXiv: 1212.1893 [hep-ph] (cit. on pp. 2, 121).

[24] D.-L. Yao et al., *Pion-nucleon scattering in covariant baryon chiral perturbation theory with explicit Delta resonances*, JHEP **05** (2016) 038, arXiv: 1603.03638 [hep-ph] (cit. on pp. 2, 112, 121).

[25] S. Godfrey and K. Moats, *Properties of Excited Charm and Charm-Strange Mesons*, Phys. Rev. **D93** (2016) 034035, arXiv: 1510.08305 [hep-ph] (cit. on p. 2).

[26] K. Chen et al., *Triply heavy tetraquark states with the $QQ\bar{Q}\bar{q}$ configuration*, Eur. Phys. J. **A53** (2017) 5, arXiv: 1609.06117 [hep-ph] (cit. on p. 2).

[27] T. Barnes, F. E. Close and H. J. Lipkin, *Implications of a DK molecule at 2.32-GeV*, Phys. Rev. **D68** (2003) 054006, arXiv: hep-ph/0305025 [hep-ph] (cit. on pp. 3, 79).

[28] F.-K. Guo, C. Hanhart and U.-G. Meißner, *Interactions between heavy mesons and Goldstone bosons from chiral dynamics*, Eur. Phys. J. **A40** (2009) 171, arXiv: 0901.1597 [hep-ph] (cit. on pp. 3, 33, 79, 80, 97, 107, 109, 117, 135).

[29] L. Liu et al., *Interactions of charmed mesons with light pseudoscalar mesons from lattice QCD and implications on the nature of the $D^*_{s0}(2317)$*, Phys. Rev. **D87** (2013) 014508, arXiv: 1208.4535 [hep-lat] (cit. on pp. 3, 79, 80, 96–99, 101–105, 118–120, 132, 135–137, 140).

[30] A. Martínez Torres et al., *Reanalysis of lattice QCD spectra leading to the $D^*_{s0}(2317)$ and $D^*_{s1}(2460)$*, JHEP **05** (2015) 153, arXiv: 1412.1706 [hep-lat] (cit. on p. 3).

[31] H. Georgi, *Weak Interactions and Modern Particle Theory*, 1984, ISBN: 9780805331639 (cit. on p. 5).

[32] A. Pich, "Effective field theory: Course", *Probing the standard model of particle interactions. Proceedings, Summer School in Theoretical Physics, NATO Advanced Study Institute, 68th session, Les Houches, France, July 28-September 5, 1997. Pt. 1, 2*, 1998 949, arXiv: hep-ph/9806303 [hep-ph] (cit. on pp. 5, 9).

[33] A. V. Manohar, *Effective field theories*, Lect. Notes Phys. **479** (1997) 311, arXiv: hep-ph/9606222 [hep-ph] (cit. on pp. 5, 9).

[34] I. Z. Rothstein, "TASI lectures on effective field theories", 2003, arXiv: hep-ph/0308266 [hep-ph] (cit. on p. 5).

[35] J. F. Donoghue, E. Golowich and B. R. Holstein, *Dynamics of the standard model*, Camb. Monogr. Part. Phys. Nucl. Phys. Cosmol. **2** (1992) 1, [Camb. Monogr. Part. Phys. Nucl. Phys. Cosmol.35(2014)] (cit. on pp. 5, 15, 67).

[36] G. Ecker, "Chiral perturbation theory", *Topics on the structure and interaction of hadronic systems. Proceedings, International Workshop on Hadron Physics, Mangaratiba, Brazil, April 15-20, 1996*, 1996 125, arXiv: hep-ph/9608226 [hep-ph] (cit. on pp. 5, 25).

[37] T. Appelquist and J. Carazzone, *Infrared Singularities and Massive Fields*, Phys. Rev. **D11** (1975) 2856 (cit. on p. 6).

[38] B. A. Ovrut and H. J. Schnitzer, *Decoupling Theorems for Effective Field Theories*, Phys. Rev. **D22** (1980) 2518 (cit. on p. 6).

[39] B. A. Ovrut and H. J. Schnitzer, *Decoupling Theorems and Effective Field Theories*, AIP Conf. Proc. **68** (1981) 445 (cit. on p. 9).

[40] S. R. Coleman, J. Wess and B. Zumino, *Structure of phenomenological Lagrangians. 1.*, Phys. Rev. **177** (1969) 2239 (cit. on pp. 10, 18).

[41] C. G. Callan Jr. et al., *Structure of phenomenological Lagrangians. 2.*, Phys. Rev. **177** (1969) 2247 (cit. on pp. 10, 18).

[42] T. Mannel, W. Roberts and Z. Ryzak, *A Derivation of the heavy quark effective Lagrangian from QCD*, Nucl. Phys. **B368** (1992) 204 (cit. on p. 12).

[43] R. Casalbuoni et al., *Phenomenology of heavy meson chiral Lagrangians*, Phys. Rept. **281** (1997) 145, arXiv: hep-ph/9605342 [hep-ph] (cit. on p. 12).

[44] A. V. Manohar and M. B. Wise, *Heavy quark physics*, Camb. Monogr. Part. Phys. Nucl. Phys. Cosmol. **10** (2000) 1 (cit. on pp. 12, 111).

[45] A. G. Grozin, *Introduction to the heavy quark effective theory. part 1*, (1992), arXiv: hep-ph/9908366 [hep-ph] (cit. on pp. 12, 111).

[46] F. Hussain and G. Thompson, "An Introduction to the heavy quark effective theory", *Proceedings, Summer School in High-energy physics and cosmology: Trieste, Italy, June 13-July 29, 1994*, 1994 0045, arXiv: hep-ph/9502241 [hep-ph] (cit. on pp. 12, 111).

[47] H. Georgi, *An Effective Field Theory for Heavy Quarks at Low-energies*, Phys. Lett. **B240** (1990) 447 (cit. on pp. 12, 111).

[48] H. Georgi, "Heavy quark effective field theory", *Theoretical Advanced Study Institute in Elementary Particle Physics (TASI 91): Perspectives in the Standard Model Boulder, Colorado, June 2-28, 1991*, 1991 0589 (cit. on pp. 12, 111).

[49] M. Neubert, *Heavy quark effective theory*, Subnucl. Ser. **34** (1997) 98, arXiv: hep-ph/9610266 [hep-ph] (cit. on pp. 12, 111).

[50] C. Patrignani et al., *Review of Particle Physics*, Chin. Phys. **C40** (2016) 100001 (cit. on pp. 12, 80).

[51] T. Becher, A. Broggio and A. Ferroglia, *Introduction to Soft-Collinear Effective Theory*, Lect. Notes Phys. **896** (2015) pp.1, arXiv: 1410.1892 [hep-ph] (cit. on p. 12).

[52] A. Grozin, "Lectures on Soft-Collinear Effective Theory", *Quantum Field Theory at the Limits: from Strong Fields to Heavy Quarks (HQ 2016) Dubna, Russia, July 18-30, 2016*, 2016, arXiv: 1611.08828 [hep-ph], URL: https://inspirehep.net/record/1500543/files/arXiv:1611.08828.pdf (cit. on p. 12).

[53] O. W. Greenberg, *Spin and Unitary Spin Independence in a Paraquark Model of Baryons and Mesons*, Phys. Rev. Lett. **13** (1964) 598 (cit. on p. 14).

[54] M. Y. Han and Y. Nambu, *Three Triplet Model with Double SU(3) Symmetry*, Phys. Rev. **139** (1965) B1006 (cit. on p. 14).

[55] V. Baluni, *CP Violating Effects in QCD*, Phys. Rev. **D19** (1979) 2227 (cit. on p. 15).

[56] R. J. Crewther et al., *Chiral Estimate of the Electric Dipole Moment of the Neutron in Quantum Chromodynamics*, Phys. Lett. **88B** (1979) 123, [Erratum: Phys. Lett.91B,487(1980)] (cit. on p. 15).

[57] J. M. Pendlebury et al., *Revised experimental upper limit on the electric dipole moment of the neutron*, Phys. Rev. **D92** (2015) 092003, arXiv: 1509.04411 [hep-ex] (cit. on p. 15).

[58] S. Scherer, *Introduction to chiral perturbation theory*, Adv. Nucl. Phys. **27** (2003) 277, arXiv: hep-ph/0210398 [hep-ph] (cit. on pp. 25, 34).

[59] H. W. Fearing and S. Scherer, *Extension of the chiral perturbation theory meson Lagrangian to order p(6)*, Phys. Rev. **D53** (1996) 315, arXiv: hep-ph/9408346 [hep-ph] (cit. on p. 25).

[60] K. Fujikawa, *Path Integral Measure for Gauge Invariant Fermion Theories*, Phys. Rev. Lett. **42** (1979) 1195 (cit. on p. 27).

[61] J. Wess and B. Zumino, *Consequences of anomalous Ward identities*, Phys. Lett. **37B** (1971) 95 (cit. on p. 29).

[62] U.-G. Meißner, *Low-Energy Hadron Physics from Effective Chiral Lagrangians with Vector Mesons*, Phys. Rept. **161** (1988) 213 (cit. on p. 30).

[63] R. Kaiser and H. Leutwyler, *Large N(c) in chiral perturbation theory*, Eur. Phys. J. **C17** (2000) 623, arXiv: hep-ph/0007101 [hep-ph] (cit. on p. 30).

[64] A. Krause, *Baryon Matrix Elements of the Vector Current in Chiral Perturbation Theory*, Helv. Phys. Acta **63** (1990) 3 (cit. on p. 31).

[65] D.-L. Yao et al.,
One-loop analysis of the interactions between charmed mesons and Goldstone bosons,
JHEP **11** (2015) 058, arXiv: 1502.05981 [hep-ph]
(cit. on pp. 33, 64, 71, 77, 80, 107, 118, 122, 132, 133, 137, 138, 148).

[66] M.-L. Du, F.-K. Guo and U.-G. Meißner, *One-loop renormalization of the chiral Lagrangian for spinless matter fields in the SU(N) fundamental representation*, J. Phys. **G44** (2017) 014001, arXiv: 1607.00822 [hep-ph] (cit. on p. 33).

[67] M.-L. Du, F.-K. Guo and U.-G. Meißner, *Subtraction of power counting breaking terms in chiral perturbation theory: spinless matter fields*, JHEP **10** (2016) 122, arXiv: 1609.06134 [hep-ph] (cit. on p. 33).

[68] A. Roessl, *Pion kaon scattering near the threshold in chiral SU(2) perturbation theory*, Nucl. Phys. **B555** (1999) 507, arXiv: hep-ph/9904230 [hep-ph] (cit. on pp. 34, 79).

[69] M. Frink, B. Kubis and U.-G. Meißner, *Analysis of the pion kaon sigma term and related topics*, Eur. Phys. J. **C25** (2002) 259, arXiv: hep-ph/0203193 [hep-ph] (cit. on p. 34).

[70] V. Bernard et al., *Aspects of nucleon Compton scattering*, Z. Phys. **A348** (1994) 317, arXiv: hep-ph/9311354 [hep-ph] (cit. on pp. 35, 37, 80).

[71] H.-B. Tang, *A New approach to chiral perturbation theory for matter fields*, (1996), arXiv: hep-ph/9607436 [hep-ph] (cit. on pp. 35, 37, 38).

[72] P. J. Ellis and H.-B. Tang,
Pion nucleon scattering in a new approach to chiral perturbation theory,
Phys. Rev. **C57** (1998) 3356, arXiv: hep-ph/9709354 [hep-ph] (cit. on pp. 35, 37).

[73] J. Gegelia, G. S. Japaridze and K. S. Turashvili,
Calculation of loop integrals by dimensional counting,
Theor. Math. Phys. **101** (1994) 1313, [Teor. Mat. Fiz.101,225(1994)] (cit. on pp. 35, 42).

[74] D. Lehmann and G. Prezeau, *Effective field theory dimensional regularization*,
Phys. Rev. **D65** (2002) 016001, arXiv: hep-ph/0102161 [hep-ph] (cit. on pp. 39, 43, 44).

[75] V. Bernard, *Chiral Perturbation Theory and Baryon Properties*,
Prog. Part. Nucl. Phys. **60** (2008) 82, arXiv: 0706.0312 [hep-ph] (cit. on p. 39).

[76] J. Gegelia and G. Japaridze, *Matching heavy particle approach to relativistic theory*,
Phys. Rev. **D60** (1999) 114038, arXiv: hep-ph/9908377 [hep-ph] (cit. on p. 42).

[77] M. R. Schindler, J. Gegelia and S. Scherer,
Infrared regularization of baryon chiral perturbation theory reformulated,
Phys. Lett. **B586** (2004) 258, arXiv: hep-ph/0309005 [hep-ph] (cit. on p. 42).

[78] R. G. Newton, *Scattering Theory of Waves and Particles*, 1982 (cit. on p. 52).

[79] J. A. Oller, *Método Quiral No Perturbativo Para El Estudio De La Dinámic Fuerte Mesón-Mesón, Su Espectroscopía y Applicaciones Afines*, 1999 (cit. on p. 53).

[80] J. Nieves and E. Ruiz Arriola, *Bethe-Salpeter approach for unitarized chiral perturbation theory*, Nucl. Phys. **A679** (2000) 57, arXiv: hep-ph/9907469 [hep-ph] (cit. on p. 55).

[81] T. N. Truong, *Chiral Perturbation Theory and Final State Theorem*,
Phys. Rev. Lett. **61** (1988) 2526 (cit. on pp. 56, 96).

[82] T. N. Truong, *Remarks on the unitarization methods*, Phys. Rev. Lett. **67** (1991) 2260
(cit. on p. 56).

[83] A. Dobado and J. R. Pelaez,
A Global fit of pi pi and pi K elastic scattering in ChPT with dispersion relations,
Phys. Rev. **D47** (1993) 4883, arXiv: hep-ph/9301276 [hep-ph] (cit. on p. 56).

[84] A. Dobado and J. R. Pelaez, *The Inverse amplitude method in chiral perturbation theory*,
Phys. Rev. **D56** (1997) 3057, arXiv: hep-ph/9604416 [hep-ph] (cit. on p. 57).

[85] J. A. Oller, E. Oset and J. R. Pelaez,
Nonperturbative approach to effective chiral Lagrangians and meson interactions,
Phys. Rev. Lett. **80** (1998) 3452, arXiv: hep-ph/9803242 [hep-ph] (cit. on p. 57).

[86] G. F. Chew and S. Mandelstam, *Theory of low-energy pion pion interactions*,
Phys. Rev. **119** (1960) 467 (cit. on p. 57).

[87] L. Castillejo, R. H. Dalitz and F. J. Dyson,
Low's scattering equation for the charged and neutral scalar theories,
Phys. Rev. **101** (1956) 453 (cit. on p. 58).

[88] G. F. Chew and S. C. Frautschi, *Potential Scattering as Opposed to Scattering Associated with Independent Particles in the S-Matrix Theory of Strong Interactions*, Phys. Rev. **124** (1961) 264 (cit. on p. 59).

[89] J. A. Oller and E. Oset, *N/D description of two meson amplitudes and chiral symmetry*,
Phys. Rev. **D60** (1999) 074023, arXiv: hep-ph/9809337 [hep-ph] (cit. on p. 60).

[90] J. A. Oller and U.-G. Meißner,
Chiral dynamics in the presence of bound states: Kaon nucleon interactions revisited,
Phys. Lett. **B500** (2001) 263, arXiv: hep-ph/0011146 [hep-ph] (cit. on pp. 60, 80, 95, 131).

[91] G. 't Hooft,
An algorithm for the poles at dimension four in the dimensional regularization procedure,
Nucl. Phys. **B62** (1973) 444 (cit. on pp. 64, 67).

[92] P. Ramond, *Field Theory: A Modern Primer*, Front. Phys. **51** (1981) 1, [Front. Phys.74,1(1989)] (cit. on p. 64).

[93] J. S. Schwinger, *On gauge invariance and vacuum polarization*, Phys. Rev. **82** (1951) 664 (cit. on p. 68).

[94] J. Bijnens and J. Lu, *Technicolor and other QCD-like theories at next-to-next-to-leading order*,
JHEP **11** (2009) 116, arXiv: 0910.5424 [hep-ph] (cit. on p. 72).

[95] R. Unterdorfer and G. Ecker,
Generating functional for strong and nonleptonic weak interactions, JHEP **10** (2005) 017,
arXiv: hep-ph/0507173 [hep-ph] (cit. on p. 74).

[96] M. R. Schindler, J. Gegelia and S. Scherer,
Infrared and extended on mass shell renormalization of two loop diagrams,
Nucl. Phys. **B682** (2004) 367, arXiv: hep-ph/0310207 [hep-ph] (cit. on p. 76).

[97] C. Allton et al.,
Physical Results from 2+1 Flavor Domain Wall QCD and SU(2) Chiral Perturbation Theory,
Phys. Rev. **D78** (2008) 114509, arXiv: 0804.0473 [hep-lat] (cit. on p. 79).

[98] L. Liu, H.-W. Lin and K. Orginos, *Charmed Hadron Interactions*,
PoS **LATTICE2008** (2008) 112, arXiv: 0810.5412 [hep-lat] (cit. on pp. 79, 96, 135).

[99] D. Mohler, S. Prelovsek and R. M. Woloshyn,
$D\pi$ scattering and D meson resonances from lattice QCD, Phys. Rev. **D87** (2013) 034501, arXiv: 1208.4059 [hep-lat] (cit. on pp. 79, 80, 96, 98).

[100] D. Mohler et al., *$D_{s0}^*(2317)$ Meson and D-Meson-Kaon Scattering from Lattice QCD*, Phys. Rev. Lett. **111** (2013) 222001, arXiv: 1308.3175 [hep-lat] (cit. on pp. 79, 80, 96, 98, 99, 101, 102, 119, 120).

[101] C. B. Lang et al., *Ds mesons with DK and D*K scattering near threshold*, Phys. Rev. **D90** (2014) 034510, arXiv: 1403.8103 [hep-lat] (cit. on pp. 79, 80, 99).

[102] E. E. Kolomeitsev and M. F. M. Lutz, *On Heavy light meson resonances and chiral symmetry*, Phys. Lett. **B582** (2004) 39, arXiv: hep-ph/0307133 [hep-ph] (cit. on p. 79).

[103] J. Hofmann and M. F. M. Lutz, *Open charm meson resonances with negative strangeness*, Nucl. Phys. **A733** (2004) 142, arXiv: hep-ph/0308263 [hep-ph] (cit. on p. 79).

[104] F.-K. Guo et al., *Dynamically generated 0+ heavy mesons in a heavy chiral unitary approach*, Phys. Lett. **B641** (2006) 278, arXiv: hep-ph/0603072 [hep-ph] (cit. on p. 79).

[105] D. Gamermann et al., *Dynamically generated open and hidden charm meson systems*, Phys. Rev. **D76** (2007) 074016, arXiv: hep-ph/0612179 [hep-ph] (cit. on p. 79).

[106] A. Faessler et al.,
Strong and radiative decays of the D(s0)(2317) meson in the DK-molecule picture*, Phys. Rev. **D76** (2007) 014005, arXiv: 0705.0254 [hep-ph] (cit. on p. 79).

[107] M. F. M. Lutz and M. Soyeur,
Radiative and isospin-violating decays of D(s)-mesons in the hadrogenesis conjecture, Nucl. Phys. **A813** (2008) 14, arXiv: 0710.1545 [hep-ph] (cit. on pp. 79, 129).

[108] F.-K. Guo et al., *Subleading contributions to the width of the D*(s0)(2317)*, Phys. Lett. **B666** (2008) 251, arXiv: 0806.3374 [hep-ph] (cit. on pp. 79, 129).

[109] B. Aubert et al., *Observation of a narrow meson decaying to $D_s^+\pi^0$ at a mass of 2.32-GeV/c^2*, Phys. Rev. Lett. **90** (2003) 242001, arXiv: hep-ex/0304021 [hep-ex] (cit. on p. 79).

[110] P. Krokovny et al., *Observation of the D(sJ)(2317) and D(sJ)(2457) in B decays*, Phys. Rev. Lett. **91** (2003) 262002, arXiv: hep-ex/0308019 [hep-ex] (cit. on p. 79).

[111] G. Burdman and J. F. Donoghue, *Union of chiral and heavy quark symmetries*, Phys. Lett. **B280** (1992) 287 (cit. on pp. 79, 80, 111, 112, 116).

[112] M. B. Wise, *Chiral perturbation theory for hadrons containing a heavy quark*, Phys. Rev. **D45** (1992) R2188 (cit. on pp. 79, 80, 111, 112, 116).

[113] T.-M. Yan et al., *Heavy quark symmetry and chiral dynamics*, Phys. Rev. **D46** (1992) 1148, [Erratum: Phys. Rev.D55,5851(1997)] (cit. on pp. 79, 80, 111, 112, 116).

[114] M. Cleven et al., *Light meson mass dependence of the positive parity heavy-strange mesons*, Eur. Phys. J. **A47** (2011) 19, arXiv: 1009.3804 [hep-ph] (cit. on pp. 79, 122).

[115] Z.-H. Guo, U.-G. Meißner and D.-L. Yao,
New insights into the $D_{s0}^*(2317)$ and other charm scalar mesons, Phys. Rev. **D92** (2015) 094008, arXiv: 1507.03123 [hep-ph] (cit. on pp. 79, 80, 105, 108, 109, 117, 118, 140).

[116] G. Moir et al., *Excited spectroscopy of charmed mesons from lattice QCD*, JHEP **05** (2013) 021, arXiv: 1301.7670 [hep-ph] (cit. on p. 79).

[117] K. Cichy, M. Kalinowski and M. Wagner, *Mass spectra of mesons containing charm quarks - continuum limit results from twisted mass fermions*, PoS **LATTICE2015** (2015) 093, arXiv: 1510.07862 [hep-lat] (cit. on p. 79).

[118] C. Liu, X. Feng and S. He, *Two particle states in a box and the S-matrix in multi-channel scattering*, Int. J. Mod. Phys. **A21** (2006) 847, arXiv: hep-lat/0508022 [hep-lat] (cit. on p. 79).

[119] M. Lage, U.-G. Meißner and A. Rusetsky, *A Method to measure the antikaon-nucleon scattering length in lattice QCD*, Phys. Lett. **B681** (2009) 439, arXiv: 0905.0069 [hep-lat] (cit. on p. 79).

[120] G. Moir et al., *Coupled-Channel $D\pi$, $D\eta$ and $D_s\bar{K}$ Scattering from Lattice QCD*, JHEP **10** (2016) 011, arXiv: 1607.07093 [hep-lat] (cit. on pp. 79, 80).

[121] P. Wang and X. G. Wang, *Study on 0^+ states with open charm in unitarized heavy meson chiral approach*, Phys. Rev. **D86** (2012) 014030, arXiv: 1204.5553 [hep-ph] (cit. on pp. 80, 135).

[122] M. Altenbuchinger, L.-S. Geng and W. Weise, *Scattering lengths of Nambu-Goldstone bosons off D mesons and dynamically generated heavy-light mesons*, Phys. Rev. **D89** (2014) 014026, arXiv: 1309.4743 [hep-ph] (cit. on pp. 80, 116, 131, 132, 135–137, 140).

[123] M. Albaladejo et al., *Two-pole structure of the $D_0^*(2400)$*, Phys. Lett. **B767** (2017) 465, arXiv: 1610.06727 [hep-ph] (cit. on pp. 80, 107).

[124] Y.-R. Liu, X. Liu and S.-L. Zhu, *Light Pseudoscalar Meson and Heavy Meson Scattering Lengths*, Phys. Rev. **D79** (2009) 094026, arXiv: 0904.1770 [hep-ph] (cit. on p. 80).

[125] L.-S. Geng et al., *Low-energy interactions of Nambu-Goldstone bosons with D mesons in covariant chiral perturbation theory*, Phys. Rev. **D82** (2010) 054022, arXiv: 1008.0383 [hep-ph] (cit. on pp. 80, 112, 116).

[126] T. W. B. Kibble, *Kinematics of General Scattering Processes and the Mandelstam Representation*, Phys. Rev. **117** (1960) 1159 (cit. on p. 81).

[127] G. F. Chew, "The analytic S-Matrix: a theory for strong interactions", *Physique des Hautes Energies: Proceedings, Ecole d'Eté de Physique Théorique, Les Houches, France, 1965*, 1965 187 (cit. on p. 82).

[128] M. J. Moravcsik, *Elementary Particle Theory. A. D. Martin and T. D. Spearman. North-Holland, Amsterdam, and Elsevier, New York, 1970. xvi, 528 pp., illus.* 27.50, Science **170** (1970) 1295, ISSN: 0036-8075, eprint: http://science.sciencemag.org/content/170/3964/1295.1.full.pdf, URL: http://science.sciencemag.org/content/170/3964/1295.1 (cit. on p. 82).

[129] A. M. Badalian et al., *Resonances in Coupled Channels in Nuclear and Particle Physics*, Phys. Rept. **82** (1982) 31 (cit. on p. 82).

[130] P. W. Johnson and R. L. Warnock, *Solution of the unitarity equation with overlapping left and right cuts: a tool for study of the s* and similar systems*, J. Math. Phys. **22** (1981) 385 (cit. on p. 82).

[131] J. A. Oller and E. Oset, *Chiral symmetry amplitudes in the S wave isoscalar and isovector channels and the σ, $f_0(980)$, $a_0(980)$ scalar mesons*, Nucl. Phys. **A620** (1997) 438, [Erratum: Nucl. Phys.A652,407(1999)], arXiv: hep-ph/9702314 [hep-ph] (cit. on pp. 94, 105).

[132] J. A. Oller, E. Oset and J. R. Pelaez, *Meson meson interaction in a nonperturbative chiral approach*, Phys. Rev. **D59** (1999) 074001, [Erratum: Phys. Rev.D75,099903(2007)], arXiv: hep-ph/9804209 [hep-ph] (cit. on pp. 94, 96).

[133] A. Dobado, M. J. Herrero and T. N. Truong, *Unitarized Chiral Perturbation Theory for Elastic Pion-Pion Scattering*, Phys. Lett. **B235** (1990) 134 (cit. on p. 96).

[134] A. Walker-Loud et al., *Light hadron spectroscopy using domain wall valence quarks on an Asqtad sea*, Phys. Rev. **D79** (2009) 054502, arXiv: 0806.4549 [hep-lat] (cit. on pp. 97, 98).

[135] A. Bazavov et al., *MILC results for light pseudoscalars*, PoS **CD09** (2009) 007, arXiv: 0910.2966 [hep-ph] (cit. on p. 97).

[136] R. J. Dowdall et al., *Vus from pi and K decay constants in full lattice QCD with physical u, d, s and c quarks*, Phys. Rev. **D88** (2013) 074504, arXiv: 1303.1670 [hep-lat] (cit. on p. 97).

[137] J. Bijnens and G. Ecker, *Mesonic low-energy constants*, Ann. Rev. Nucl. Part. Sci. **64** (2014) 149, arXiv: 1405.6488 [hep-ph] (cit. on p. 97).

[138] F.-K. Guo et al., *Tetraquarks, hadronic molecules, meson-meson scattering and disconnected contributions in lattice QCD*, Phys. Rev. **D88** (2013) 074506, arXiv: 1308.2545 [hep-lat] (cit. on p. 98).

[139] O. Bär, G. Rupak and N. Shoresh, *Chiral perturbation theory at O(a**2) for lattice QCD*, Phys. Rev. **D70** (2004) 034508, arXiv: hep-lat/0306021 [hep-lat] (cit. on p. 100).

[140] O. Bär et al., *Chiral perturbation theory for staggered sea quarks and Ginsparg-Wilson valence quarks*, Phys. Rev. **D72** (2005) 054502, arXiv: hep-lat/0503009 [hep-lat] (cit. on p. 100).

[141] B. C. Tiburzi, *Baryons with Ginsparg-Wilson quarks in a staggered sea*, Phys. Rev. **D72** (2005) 094501, [Erratum: Phys. Rev.D79,039904(2009)], arXiv: hep-lat/0508019 [hep-lat] (cit. on p. 100).

[142] J.-W. Chen, D. O'Connell and A. Walker-Loud, *Universality of mixed action extrapolation formulae*, JHEP **04** (2009) 090, arXiv: 0706.0035 [hep-lat] (cit. on p. 100).

[143] M. R. Schindler and D. R. Phillips, *Bayesian Methods for Parameter Estimation in Effective Field Theories*, Annals Phys. **324** (2009) 682, [Erratum: Annals Phys.324,2051(2009)], arXiv: 0808.3643 [hep-ph] (cit. on p. 100).

[144] A. Gomez Nicola and J. R. Pelaez, *Meson meson scattering within one loop chiral perturbation theory and its unitarization*, Phys. Rev. **D65** (2002) 054009, arXiv: hep-ph/0109056 [hep-ph] (cit. on p. 107).

[145] L. Y. Dai, X. G. Wang and H. Q. Zheng,
Pole Analysis on Unitarized $SU(3) \times SU(3)$ One Loop χPT Amplitudes,
Commun. Theor. Phys. **57** (2012) 841, arXiv: 1108.1451 [hep-ph] (cit. on p. 107).

[146] F. Guerrero and J. A. Oller, *$K\bar{K}$ scattering amplitude to one loop in chiral perturbation theory, its unitarization and pion form-factors*,
Nucl. Phys. **B537** (1999) 459, [Erratum: Nucl. Phys.B602,641(2001)],
arXiv: hep-ph/9805334 [hep-ph] (cit. on p. 107).

[147] C. Hanhart, J. R. Pelaez and G. Rios, *Remarks on pole trajectories for resonances*,
Phys. Lett. **B739** (2014) 375, arXiv: 1407.7452 [hep-ph] (cit. on p. 108).

[148] C. Hanhart, J. R. Pelaez and G. Rios, *Quark mass dependence of the rho and sigma from dispersion relations and Chiral Perturbation Theory*, Phys. Rev. Lett. **100** (2008) 152001,
arXiv: 0801.2871 [hep-ph] (cit. on p. 109).

[149] H. Krebs, E. Epelbaum and U.-G. Meißner, *Redundancy of the off-shell parameters in chiral effective field theory with explicit spin-3/2 degrees of freedom*, Phys. Lett. **B683** (2010) 222,
arXiv: 0905.2744 [hep-th] (cit. on p. 112).

[150] P. C. Bruns and U.-G. Meißner, *Infrared regularization for spin-1 fields*,
Eur. Phys. J. **C40** (2005) 97, arXiv: hep-ph/0411223 [hep-ph] (cit. on p. 116).

[151] B. Grinstein et al., *Chiral perturbation theory for f D(s) / f D and B B(s) / B B*,
Nucl. Phys. **B380** (1992) 369, arXiv: hep-ph/9204207 [hep-ph] (cit. on p. 116).

[152] M. Albaladejo et al., *Decay widths of the spin-2 partners of the X(3872)*,
Eur. Phys. J. **C75** (2015) 547, arXiv: 1504.00861 [hep-ph] (cit. on p. 116).

[153] N. Fettes, U.-G. Meißner and S. Steininger,
Pion - nucleon scattering in chiral perturbation theory. 1. Isospin symmetric case,
Nucl. Phys. **A640** (1998) 199, arXiv: hep-ph/9803266 [hep-ph] (cit. on p. 121).

[154] N. Fettes and U.-G. Meißner,
Pion nucleon scattering in chiral perturbation theory. 2.: Fourth order calculation,
Nucl. Phys. **A676** (2000) 311, arXiv: hep-ph/0002162 [hep-ph] (cit. on p. 121).

[155] J. M. Alarcón, J. Martin Camalich and J. A. Oller, *Improved description of the πN-scattering phenomenology in covariant baryon chiral perturbation theory*, Annals Phys. **336** (2013) 413,
arXiv: 1210.4450 [hep-ph] (cit. on p. 121).

[156] M. Hoferichter et al.,
Matching pion-nucleon Roy-Steiner equations to chiral perturbation theory,
Phys. Rev. Lett. **115** (2015) 192301, arXiv: 1507.07552 [nucl-th] (cit. on p. 121).

[157] N. Fettes, V. Bernard and U.-G. Meißner, *One loop analysis of the reaction pi N —> pi pi N*,
Nucl. Phys. **A669** (2000) 269, arXiv: hep-ph/9907276 [hep-ph] (cit. on p. 121).

[158] E. Epelbaum, H.-W. Hammer and U.-G. Meißner, *Modern Theory of Nuclear Forces*,
Rev. Mod. Phys. **81** (2009) 1773, arXiv: 0811.1338 [nucl-th] (cit. on p. 121).

[159] G. Ecker et al., *The Role of Resonances in Chiral Perturbation Theory*,
Nucl. Phys. **B321** (1989) 311 (cit. on pp. 121, 123, 124, 132).

[160] G. Ecker et al., *Chiral Lagrangians for Massive Spin 1 Fields*, Phys. Lett. **B223** (1989) 425
(cit. on pp. 121, 123, 124).

[161] J. F. Donoghue, C. Ramirez and G. Valencia,
The Spectrum of QCD and Chiral Lagrangians of the Strong and Weak Interactions,
Phys. Rev. **D39** (1989) 1947 (cit. on p. 121).

[162] V. Bernard, N. Kaiser and U.-G. Meißner, *Aspects of chiral pion - nucleon physics*,
Nucl. Phys. **A615** (1997) 483, arXiv: hep-ph/9611253 [hep-ph] (cit. on pp. 121, 129–131).

[163] B. Ananthanarayan, D. Toublan and G. Wanders,
Consistency of the chiral pion pion scattering amplitudes with axiomatic constraints,
Phys. Rev. **D51** (1995) 1093, arXiv: hep-ph/9410302 [hep-ph] (cit. on p. 121).

[164] P. Dita, *Positivity constraints on chiral perturbation theory pion pion scattering amplitudes*,
Phys. Rev. **D59** (1999) 094007, arXiv: hep-ph/9809568 [hep-ph] (cit. on p. 121).

[165] A. V. Manohar and V. Mateu, *Dispersion Relation Bounds for pi pi Scattering*,
Phys. Rev. **D77** (2008) 094019, arXiv: 0801.3222 [hep-ph] (cit. on pp. 121, 133).

[166] V. Mateu, *Universal Bounds for SU(3) Low Energy Constants*, Phys. Rev. **D77** (2008) 094020,
arXiv: 0801.3627 [hep-ph] (cit. on pp. 121, 134).

[167] Z.-H. Guo, O. Zhang and H. Q. Zheng,
*Positivity constraints on LECs of chi PT lagrangian at O(p**6) level*,
AIP Conf. Proc. **1343** (2011) 259, arXiv: 0911.4447 [hep-ph] (cit. on p. 121).

[168] M. Luo, Y. Wang and G. Zhu, *Unitarity constraints on effective interaction in pi N scattering*,
Phys. Lett. **B649** (2007) 162, arXiv: hep-ph/0611325 [hep-ph] (cit. on p. 121).

[169] J. J. Sanz-Cillero, D.-L. Yao and H.-Q. Zheng,
Positivity constraints on the low-energy constants of the chiral pion-nucleon Lagrangian,
Eur. Phys. J. **C74** (2014) 2763, arXiv: 1312.0664 [hep-ph] (cit. on pp. 121, 133).

[170] B. Aubert et al., *Observation of a New D(s) Meson Decaying to DK at a Mass of 2.86-GeV/c**2*,
Phys. Rev. Lett. **97** (2006) 222001, arXiv: hep-ex/0607082 [hep-ex] (cit. on p. 122).

[171] J. Brodzicka et al., *Observation of a new D(sJ) meson in B+ —> anti-D0 D0 K+ decays*,
Phys. Rev. Lett. **100** (2008) 092001, arXiv: 0707.3491 [hep-ex] (cit. on p. 122).

[172] B. Aubert et al., *Study of D(sJ) decays to D*K in inclusive e+ e- interactions*,
Phys. Rev. **D80** (2009) 092003, arXiv: 0908.0806 [hep-ex] (cit. on p. 122).

[173] G. Ecker and C. Zauner, *Tensor meson exchange at low energies*, Eur. Phys. J. **C52** (2007) 315,
arXiv: 0705.0624 [hep-ph] (cit. on pp. 124, 131).

[174] K. A. Olive et al., *Review of Particle Physics*, Chin. Phys. **C38** (2014) 090001 (cit. on p. 130).

[175] Z.-H. Guo and J. J. Sanz-Cillero, *pi pi-scattering lengths at O(p**6) revisited*,
Phys. Rev. **D79** (2009) 096006, arXiv: 0903.0782 [hep-ph] (cit. on pp. 130, 131).

[176] M. Jamin, J. A. Oller and A. Pich, *Strangeness changing scalar form-factors*,
Nucl. Phys. **B622** (2002) 279, arXiv: hep-ph/0110193 [hep-ph] (cit. on p. 130).

[177] Z.-G. Wang, *Analysis of the vertices DDV and D^*DV with light-cone QCD sum rules*,
Eur. Phys. J. **C52** (2007) 553, arXiv: 0705.3720 [hep-ph] (cit. on p. 130).

[178] G.-J. Ding, *Are Y(4260) and Z+(2) are D(1) D or D(0) D* Hadronic Molecules?*,
Phys. Rev. **D79** (2009) 014001, arXiv: 0809.4818 [hep-ph] (cit. on p. 130).

[179] W. A. Bardeen, E. J. Eichten and C. T. Hill, *Chiral multiplets of heavy - light mesons*,
Phys. Rev. **D68** (2003) 054024, arXiv: hep-ph/0305049 [hep-ph] (cit. on p. 130).

[180] P. Buettiker and U.-G. Meißner, *Pion nucleon scattering inside the Mandelstam triangle*, Nucl. Phys. **A668** (2000) 97, arXiv: hep-ph/9908247 [hep-ph] (cit. on p. 133).

[181] M. Froissart, *Asymptotic behavior and subtractions in the Mandelstam representation*, Phys. Rev. **123** (1961) 1053 (cit. on p. 134).

[182] T. Hannah, *The Anomalous process gamma pi —> pi pi to two loops*, Nucl. Phys. **B593** (2001) 577, arXiv: hep-ph/0102213 [hep-ph] (cit. on p. 141).

[183] A. Denner and S. Dittmaier, *Reduction schemes for one-loop tensor integrals*, Nucl. Phys. **B734** (2006) 62, arXiv: hep-ph/0509141 [hep-ph] (cit. on p. 143).

[184] G. 't Hooft and M. J. G. Veltman, *Scalar One Loop Integrals*, Nucl. Phys. **B153** (1979) 365 (cit. on p. 144).

[185] G. Passarino and M. J. G. Veltman, *One Loop Corrections for e+ e- Annihilation Into mu+ mu- in the Weinberg Model*, Nucl. Phys. **B160** (1979) 151 (cit. on p. 144).

[186] G. Devaraj and R. G. Stuart, *Reduction of one loop tensor form-factors to scalar integrals: A General scheme*, Nucl. Phys. **B519** (1998) 483, arXiv: hep-ph/9704308 [hep-ph] (cit. on pp. 146, 147, 149).

[187] D. Djukanovic, *Virtual Compton scattering in baryon chiral perturbation theory*, PhD thesis: Mainz U., Inst. Kernphys., 2008, URL: http://ubm.opus.hbz-nrw.de/volltexte/2008/1691/ (cit. on pp. 146, 151).

[188] R. G. Stuart, *Algebraic Reduction of One Loop Feynman Diagrams to Scalar Integrals*, Comput. Phys. Commun. **48** (1988) 367 (cit. on p. 146).

[189] M. E. Bracco et al., *Charm couplings and form factors in QCD sum rules*, Prog. Part. Nucl. Phys. **67** (2012) 1019, arXiv: 1104.2864 [hep-ph] (cit. on pp. 157, 159).

[190] K. Azizi, Y. Sarac and H. Sundu, *Analysis of the strong* $D_2^*(2460)^0 \to D^+\pi^-$ *and* $D_{s2}^*(2573)^+ \to D^+K^0$ *transitions via QCD sum rules*, Eur. Phys. J. **C74** (2014) 3106, arXiv: 1402.6887 [hep-ph] (cit. on pp. 157–159).

[191] L. J. Reinders, H. Rubinstein and S. Yazaki, *Hadron Properties from QCD Sum Rules*, Phys. Rept. **127** (1985) 1 (cit. on p. 158).

[192] H.-Y. Cheng, Y. Koike and K.-C. Yang, *Two-parton Light-cone Distribution Amplitudes of Tensor Mesons*, Phys. Rev. **D82** (2010) 054019, arXiv: 1007.3541 [hep-ph] (cit. on p. 159).

[193] G.-L. Yu, Z.-Y. Li and Z.-G. Wang, *Analysis of the strong coupling constant* $G_{D_s^* D_s \phi}$ *and the decay width of* $D_s^* \to D_s\gamma$ *with QCD sum rules*, Eur. Phys. J. **C75** (2015) 243, arXiv: 1502.01698 [hep-ph] (cit. on p. 159).

List of Figures

List of Tables

Acknowledgements

Many people have offered me valuable instructions and help in my studies and life in Bonn. I would like to thank everyone who supported me in the past years.

First and foremost, I would like to express my sincere gratitude to my supervisors, Prof. Dr. Ulf-G. Meißner and Prof. Feng-Kun Guo. Their deep knowledge and thoughtful insights on physics have benefited me enormously. I thank them for giving me the valuable guidance and freedom to explore a broad view on my own. Additional thanks to Prof. Feng-Kun Guo, not only a great supervisor in my studies but also a good friends in my life, for supporting me to visit the Institute of Theoretical Physics in Beijing, where part of this thesis was done. I am grateful to Liu-Fang Bian, Chao-Wei Shen and Prof. Bin-Song Zou for the warm acceptance in Beijing.

Special thanks to Dr. De-Liang Yao for the many useful discussions and great collaborations. He taught me a lot when I have technical problems in the calculation. Without his persistent help, this dissertation would not have been possible.

I thank all members of the theory division of the HISKP for the pleasant and stimulating atmosphere at work. In particular, I thank my office mates Dr. Zhi Yang and Christopher Helmes for their kind help. I thank Dr. Qian Wang, Dr. Zhi-Hui Guo, Prof. Dr. Bastian Kubis, Prof. Dr. Akaki Rusetsky, Dr. Maxim Mai, Dr. Serdar Elhatisari, Dr. Wei Wang, Dr. Liuming Liu, Dr. Jin-Yi Pang, Dr. Li Ma, Christian Jost, Guang-Juan Wang for many interesting discussions and kind help. In addition, I thank my friends Ting Chen, Dechuan Du, Dr. Xiao-Yu Guo, Dr. Jia Liu, Dr. Li-Jia Jiang, Li Sa Schulz, Ann-Kristin Steines, Dr. Xiao-Ping Wang, Dr. Jun-Hui Zheng and Fabian Zink. Without you, my life would be boring and dark. Furthermore, I am very grateful to Barbara Kraus and Christa Börsch for their help.

I wish to express my special thanks to my friends, Dr. Yun-Hua Chen, Suyuan Wang, Naijie Wen, Ronghua Wen and Xuefei Yan, for their patient accompanying when I was in difficulties in my life.

I wish to thank my parents and my sister for their unconditional love and support, which I could always rely on.